Asian Journal of Mycology 9(1): 20–184 (2026) ISSN 2651-1339
www.asianjournalofmycology.org

Article
Doi 10.5943/ajom/9/1/2

AJOM new records and collections of fungi: 201–250

Luangharn T[1], Rathnayaka AR[1,2,3,10], Armand A[1,2], Walker A[1,2], Tennakoon DS[4], Gomdola D[1,2,3], Gonkhom D[1,2], Ren G[8], Gui H[14], Aumentado HDR[1,2], Su H[1,2,6], Shen H[1,2,19], Bera I[1], Senanayake IC[10], Promputtha I[5,12], Ma J[1,9], Liu J[1,2], Zhang J-Y[1,2,9], Lei L[1,2,6], Wu N[1,2,11], Afshari N[1,5], Chaiwan N[5,12], Samaradiwakara NP[1,5,7], de Silva NI[4], Kularathnage ND[1,2,6], Sysouphanthong P[18], Zhao Q[6], Xu N[1,2,13], Jayawardena RS[1,2], Khyaju S[1,2,3], Absalan S[1,5], Tibpromma S[13], Karimi O[1,2], Salichanh T[1,2,3], Du T[20], Yang YY[1,2], Sun Y[1,2,14], Gao Y[1,2,14], Lu Y-Z[9], Yang Y[1,2,9], Hu Y[16], Htet ZH[1,2], Luo Z[19] and Hyde KD[1,17*]

[1]Center of Excellence in Fungal Research, Mae Fah Luang University, Chiang Rai 57100, Thailand
[2]School of Science, Mae Fah Luang University, Muang, Chiang Rai 57100, Thailand
[3]Mushroom Research Foundation, Ban Pa Deng, Pa Pae, Mae Taeng, Chiang Mai 50150, Thailand
[4]Shenzhen Key Laboratory of Microbial Genetic Engineering, College of Life Science and Oceanography, Shenzhen University, Shenzhen 518060, People's Republic of China
[5]Department of Biology, Faculty of Science, Chiang Mai University, Chiang Mai 50200, Thailand
[6]State Key Laboratory of Phytochemistry and Natural Medicines, Kunming Institute of Botany, Chinese Academy of Sciences, Kunming, Yunnan 650201, People's Republic of China
[7]Center of Excellence in Microbial Diversity and Sustainable Utilization, Chiang Mai University, Chiang Mai 50200, Thailand
[8]Guiyang Healthcare Vocational University, Guiyang 550081, Guizhou, People's Republic of China
[9]School of Food and Pharmaceutical Engineering, Guizhou Institute of Technology, Guiyang, Guizhou 550003, People's Republic of China
[10]Yunnan Key Laboratory for Fungal Diversity and Green Development & Yunnan International Joint Laboratory of Fungal Sustainable Utilization in South and Southeast Asia, Germplasm Bank of Wild Species, Kunming Institute of Botany, Chinese Academy of Sciences, Kunming 650201, Yunnan Province, People's Republic of China
[11]School of Life Science and Technology, Center for Informational Biology, University of Electronic Science and Technology of China, Chengdu 611731, People's Republic of China
[12]Office of Research Administration, Chiang Mai University, Chiang Mai 50200, Thailand
[13]Center for Yunnan Plateau Biological Resources Protection and Utilization & Yunnan International Joint Laboratory of Fungal Sustainable Utilization in South and Southeast Asia, College of Biology and Food Engineering, Qujing Normal University, Qujing 655099, People's Republic of China
[14]Department of Plant Pathology, College of Agriculture, Guizhou University, Guiyang, People's Republic of China
[15]Center for Mountain Futures, Kunming Institute of Botany, Chinese Academy of Sciences, Honghe 654400, People's Republic of China
[16]Key Laboratory for Plant Diversity and Biogeography of East Asia, Kunming Institute of Botany, Kunming 650201, Yunnan, People's Republic of China
[17]Department of Botany and Microbiology, College of Science, King Saud University, P.O. Box 22452, Riyadh 11495, Saudi Arabia
[18]Biotechnology and Ecology Institute, Ministry of Agriculture and Environment, km 14, Thangon Road, Xaythany District, Vientiane, Lao PDR
[19]College of Agriculture and Biological Science, Dali University, Dali 671003, Yunnan, People's Republic of China

Submitted 16 May 2025, Accepted 11 December 2025, Published 27 January 2026
Corresponding Author: Kevin D. Hyde – e-mail – kdhyde3@gmail.com

[20] *Yunnan International Joint Laboratory for Digital Conservation and Germplasm Innovation and Application of China-Laos Tea Resources, School of Tea and Coffee, Pu'er University, Pu'er 665000, People's Republic of China*

Luangharn T, Rathnayaka AR, Armand A, Walker A, Tennakoon DS, Gomdola D, Gonkhom D, Bundhun D, Ren G, Gui H, Aumentado HDR, Su H, Shen H, Bera I, Senanayake IC, Promputtha I, Ma J, Liu J, Zhang J-Y, Lei L, Wu N, Afshari N, Chaiwan N, Samaradiwakara NP, de Silva NI, Kularathnage ND, Sysouphanthong P, Zhao Q, Xu R, Jayawardena RS, Khyaju S, Absalan S, Tibpromma S, Karimi O, Salichanh T, Du T, Yang YY, Sun Y, Gao Y, Lu Y-Z, Yang Y, Hu Y, Htet ZH, Luo Z, Hyde KD. 2026 – AJOM new records and collections of fungi: 201–250. Asian Journal of Mycology 9(1), 20–184, Doi 10.5943/ajom/9/1/2

Abstract

This article is the fourth in the Asian Journal of Mycology Notes series, enabling researchers to report 50 new fungal collections, including fungus-host and fungus-taxa. Herewith, we report the distribution of taxa in two phyla (*Ascomycota* and *Basidiomycota*), four classes (*Dothideomycetes*, *Leotiomycetes*, *Sordariomycetes*, and *Agaricomycetes*), 18 orders, and 30 families. The present study provides descriptions and illustrations for six new species (*Amniculicola yunnanensis*, *Melanographium reniforme*, *Mucispora yunnanensis*, *Neomassaria yunnanensis*, *Neoarthrinium bambusae*, and *Tryblidiopsis xizangensis*), 19 new records, 19 new host records, and five new host and geographical records. This article aims to enhance knowledge of novel fungi, their host occurrence, and geography reports. Comprehensive descriptions, illustrations, and multi-gene phylogenetic trees show the placements of the described taxa. Additionally, a platform for disseminating data on fungal collections, including new sequence data, could support future studies. This study aims to expand knowledge on fungal taxa, their host occurrences, and geographical distribution. Detailed descriptions, illustrations, and multi-locus phylogenetic analyses are provided to clarify taxonomic placements.

Keywords – 6 new species – Ascomycota – Basidiomycota – Morphology – Phylogeny

Table of contents

This article presents an updated collection of *Ascomycota* and *Basidiomycota*, following the classification by Wijayawardene et al. (2022a), the class and phyla of the kingdom Fungi, the outline of fungi and fungus-like taxa (Wijayawardene et al. 2022a, Hyde et al. 2024a), notes and outline of brown-spored hyphomycetes (Liu et al. 2024), and outline and divergence times of *Basidiomycota* (He et al. 2019, 2024).

Phylum *Ascomycota*
Class *Dothideomycetes* O.E. Erikss. & Winka
Subclass *Dothideomycetidae* P.M. Kirk et al.
Cladosporiales Abdollahz. & Crous
Cladosporiaceae Chalm. & R.G. Archibald

01. ***Cladosporium ribis*** Y.Q. Yang & Yong Wang, Yang et al., Journal of Fungi 9(250), 13 (2023) (Contributed by Herbert Dustin R. Aumentado and Ruvishika S. Jayawardena)

02. ***Cladosporium tenuissimum*** Cooke, Grevillea 6(40), 140 (1878) (Contributed by Napalai Chaiwan and Itthayakorn Promputtha)

Subclass *Pleosporomycetidae* C.L. Schoch et al.
Hysteriales Lindau.
Hysteriaceae Chevall.

03. ***Rhytidhysteron camporesii*** Ekanayaka & K.D. Hyde, Hyde et al., Fungal Diversity 100, 18 (2020) (Contributed by Tianye Du and Saowaluck Tibpromma)

Pleosporales Luttrell ex M.E. Barr
Amniculicolaceae Y. Zhang ter, C.L. Schoch, J. Fourn., Crous & K.D. Hyde
04. ***Amniculicola yunnanensis*** H.W. Shen & Z.L. Luo, sp. nov. (Contributed by Hongwei Shen and Zonglong Luo)

Didymellaceae Gruyter, Aveskamp & Verkley
05. ***Allophoma tropica*** (R. Schneid. & Boerema) Q. Chen & L. Cai, Chen et al., Studies in Mycology 82, 164 (2015) (Contributed by Nethmini P. Samaradiwakara)

Didymosphaeriaceae Munk
06. ***Neokalmusia aquibrunnea*** J. Yang, Jian K. Liu & K.D. Hyde, Yang et al., Fungal Diversity 119, 37 (2023) (Contributed by Napalai Chaiwan and Itthayakorn Promputtha)

Lophiotremataceae K. Hiray. & Kaz. Tanaka.
07. ***Lophiotrema mucilaginosis*** M. Raza & L. Cai, Phookamsak et al., Fungal Diversity 95, 32 (2019) (Contributed by Guangcong Ren)
08. ***Lophiotrema neoarundinariae*** Y. Zhang ter, Kaz. Tanaka & K.D. Hyde, Zhang et al., Studies in Mycology 64, 97 (2009) (Contributed by Guangcong Ren)

Neohendersoniaceae A. Giraldo & Crous
09. ***Crassiparies quadrisporus*** M. Matsum., K. Hiray. & Kaz. Tanaka, Li et al., Fungal Diversity 78, 63 (2016) (Contributed by Ruifang Xu)

Neomassariaceae H.A. Ariyaw., Jaklitsch & Voglmayr
10. ***Neomassaria yunnanensis*** Y. Gao, H. Gui & K.D. Hyde, sp. nov. (Contributed by Ying Gao and Heng Gui)

Occultibambusaceae D.Q. Dai & K.D. Hyde
11. ***Neooccultibambusa fusispora*** Y.R. Sun, Yong Wang bis & K.D. Hyde, sp. nov. (Contributed by Yaru Sun and Ruvishika S. Jayawardena)

Phaeosphaeriaceae M.E. Barr
12. ***Leptospora macarangae*** Tennakoon, C.H. Kuo & K.D. Hyde, Tennakoon et al., Fungal Diversity 108, 41 (2021) (Contributed by Na Wu)

Pleosporaceae Nitschke
13. ***Parastagonospora macrouniseptata*** Goonas., Camporesi & McKenzie, Goonasekara et al., Asian Journal of Mycology 2(1), 176 (2019) (Contributed by Nuwan D Kularathnage and Indunil C. Senanayake)

Teichosporaceae M.E. Barr
14. ***Magnibotryascoma mali*** Phukhams., Wanas. & K.D. Hyde, Hyde et al., Fungal Diversity 87, 105 (2017) (Contributed by Na Wu)

Paradictyoarthriniaceae Doilom, J.K. Liu & K.D. Hyde

15. ***Paradictyoarthrinium diffractum*** Matsush., Mycological Memoirs 9, 18 (1996) (Contributed by Nimali Indeewari de Silva)

16. ***Paradictyoarthrinium tectonicola*** Doilom & K.D. Hyde, Liu et al., Fungal Diversity 72, 134 (2015) (Contributed by Danushka Sandaruwan)

Dothideomycetes O.E. Erikss. & Winka
Botryosphaeriales C.L. Schoch, Crous & Shoemaker, Mycologia 98, (1050)
Botryosphaeriaceae Theiss. & H. Syd.

17. ***Lasiodiplodia crassispora*** T.I. Burgess & P.A. Barber, Mycologia 98(3), 425 (2006) (Contributed by Achala Roshani Rathnayaka)

18. ***Neofusicoccum parvum*** (Pennycook & Samuels) Crous, Slippers & A.J.L. Phillips, Studies in Mycology 55, 248 (2006) (Contributed by Nimali Indeewari de Silva)

Class *Leotiomycetes* O.E. Erikss. & Winka
Subclass *Leotiomycetidae* P.M. Kirk, P. Cannon, Minter & Stalpers
Marthamycetales P.R. Johnst. & Baral
Marthamycetaceae Baral, Lantz, Hustad & Minter

19. ***Propolis farinosa*** (Pers.) Fr., Summa vegetabilium Scandinaviae 2, 372 (1849) (Contributed by Hongli Su)

Rhytismatales M.E. Barr ex Minter
Rhytismataceae Chevall.

20. ***Tryblidiopsis xizangensis*** H.L. Su, K.D. Hyde & Q. Zhao, sp. nov. (Contributed by Hongli Su)

Class *Sordariomycetes* O.E. Erikss. & Winka
Subclass *Diaporthomycetidae* Senan., Maharachch. & K.D. Hyde
Diaporthales Nannf.

21. ***Diaporthe rosae*** Samarakoon & K.D. Hyde, Wanasinghe et al., Fungal Diversity 89, 185 (2018) (Contributed by Alireza Armand and Ruvishika S. Jayawardena)

Subclass *Hypocreomycetidae* O.E. Erikss. & Winka
Fuscosporellales Jing Yang, Bhat & K.D. Hyde
Fuscosporellacea Jing Yang, Bhat & K.D. Hyde

22. ***Mucispora yunnanensis*** R.J. Xu, L. Lei, K.D. Hyde & Q. Zhao, sp. nov. (Contributed by Lei Lei and Qi Zhao)

Glomerellales Chadef. ex Réblová, W. Gams & Seifert
Glomerellaceae Locq. ex Seifert & W. Gams

23. ***Colletotrichum siamense*** Prihast., L. Cai & K.D. Hyde, Prihastuti et al., Fungal Diversity 39, 98 (2009) (Contributed by Herbert Dustin R. Aumentado and Ruvishika S. Jayawardena)

24. ***Colletotrichum subacidae*** F. Liu, Z.Y. Ma & L. Cai, Liu et al., Studies in Mycology 101, 40 (2022) (Contributed by Alireza Armand and Ruvishika S. Jayawardena)

Pleurotheciales Réblová & Seifert
Pleurotheciaceae Réblová & Seifert

25. ***Phaeoisaria aquatica*** Z.L. Luo, X.J. Su & K.D. Hyde, Luo et al., Mycological Progress 17(5), 514 (2018) (Contributed by Naghmeh Afshari)

Hypocreales Lindau
Bionectriaceae Samuels & Rossman

26. ***Gliomastix polychroma*** (J.F.H. Beyma) Matsushima, Icones Microfungorum a Matsushima Lectorum (Kobe), 77 (1975) (Contributed by Sahar Absalan and Ruvishika S. Jayawardena)

Ophiocordycipitaceae G.H. Sung, J.M. Sung, Hywel-Jones & Spatafora

27. ***Hirsutella minnesotensis*** Sen Y. Chen, Xing Z. Liu & F.J. Chen, Chen et al., Mycologia 92(5), 820 (2000) (Contributed by Jianwei Liu and Thatsanee Luangharn)

Polycephalomycetaceae Y.P. Xiao, Y.B. Wang, T.C. Wen, H. Yu & K.D. Hyde

28. ***Pleurocordyceps yunnanensis*** (Hong Yu bis, Y.B. Wang & Y.D. Dai) Y.H. Wang, S. Ban, W.J. Wang, Yi Li, Ke Wang, P.M. Kirk & Y.J. Yao, Wang et al., Journal of Systematics and Evolution 59(5), 1076 (2021) (Contributed by Yu Yang)

Stachybotryaceae L. Lombard & Crous

29. ***Grandibotrys pseudotheobromae*** L. Lombard & Crous, Lombard et al., Persoonia 36, 189 (2016) (Contributed by Jing-Yi Zhang and Yong-Zhong Lu)

Pleurotheciales Réblová & Seifert
Pleurotheciaceae Réblová & Seifert

30. ***Pleurothecium recurvatum*** (Morgan) Höhn., Centralblatt für Bakteriologie und Parasitenkunde, Abteilung 2(60), 26 (1923) (Contributed by Jian Ma)

Subclass ***Xylariomycetidae*** O.E. Erikss & Winka
Amphisphaeriales D. Hawksw. & O.E. Erikss.
Apiosporaceae K.D. Hyde, J. Fröhl., Joanne E. Taylor & M.E. Barr

31. ***Neoarthrinium bambusae*** J.W. Liu, Senan & K.D. Hyde, sp. nov. (Contributed by Jianwei Liu)

Pestalotiopsidaceae Maharachch. & K.D. Hyde

32. ***Pestalotiopsis chamaeropis*** Maharachch., K.D. Hyde & Crous, Maharachchikumbura et al., Studies in Mycology (2014) (Contributed by Yaru Sun and Ruvishika S. Jayawardena)

Sporocadaceae Corda

33. ***Immersidiscosia eucalypti*** (Pat.) Kaz. Tanaka, Okane & Hosoya, Tanaka et al., Persoonia 26, 94 (2011) (Contributed by Danushka Sandaruwan)

34. ***Neopestalotiopsis perukae*** I.U. Haq, S. Ijaz & N.A. Khan, Pakistan Journal of Agricultural Sciences 58, 1306 (2021) (Contributed by Deecksha Gomdola and Ruvishika S. Jayawardena)

Xylariales Nannf.

35. ***Melanographium reniforme*** Y. Y. Yang, Gomes de Farias & K. D. Hyde, sp. nov. (Contributed by Yanyan Yang)

Xylariaceae Tul. & C. Tul.

36. ***Xylaria grammica*** (Mont.) Mont., Nova Acta Regiae Societatis Scientiarum Upsaliensis 3 1(1), 128 (1851) (Contributed by Omid Karimi)

Phylum ***Basidiomycota*** R.T. Moore
Class ***Agaricomycetes*** Doweld
Agaricales Underw.

Agaricaceae Chevall.

37. ***Coniolepiota spongodes*** (Berk. & Broome) Vellinga, Vellinga et al., Mycologia 103(3), 502 (2011) (Contributed by Phongeun Sysouphanthong)

38. ***Hymenagaricus saisamornae*** J. Kumla & N. Suwannarach, Kumla et al., Chiang Mai Journal of Science 48(3), 83 (2021) (Contributed by Phongeun Sysouphanthong)

39. ***Leucocoprinus cretaceus*** (Bull.) Locq., Bulletin Mensuel de la Société Linnéenne de Lyon 14, 93 (1945) (Contributed by Didsanutda Konkhom)

40. ***Leucocoprinus mucrocystis*** (Pegler) M. Asif, Saba & Vellinga, Asif, Saba & Raz, Mycologia 116(4), 615 (2024) (Contributed by Thaviphone Salichanh and Thatsanee Luangharn)

41. ***Lepiota baiyunensis*** Y.S. Liang & L.H. Qiu, Liang et al., Phytotaxa 606(1), 8 (2023) (Contributed by Arttapon Walker)

42. ***Pseudolepiota zangmui*** Z.W. Ge, Ge & Yang, Phytotaxa 312, 252 (2017) (Contributed by Phongeun Sysouphanthong)

43. ***Xanthagaricus siamensis*** Yuan S. Liu & S. Lumyong, Phytotaxa 437(1), 17 (2020) (Contributed by Phongeun Sysouphanthong)

Polyporales Gäum.

Polyporaceae Fr. ex Corda.

44. ***Ganoderma alpinum*** B.K. Cui, J.H. Xing & Y.F. Sun, Sun et al., Studies in Mycology 101, 348 (2022) (Contributed by Thatsanee Luangharn)

45. ***Ganoderma subellipsoideum*** B.K. Cui, J.H. Xing & Y.F. Sun, Sun et al., Studies in Mycology 101, 348 (2022) (Contributed by Thatsanee Luangharn)

Strophariaceae Singer & A.H. Sm.

46. ***Agrocybe retigera*** (Speg.) Singer, Lilloa 22, 493 (1951) (Contributed by Yuwei Hu)

47. ***Deconica pseudobullacea*** (Petch) Ram. Cruz & Guzmán, Ramírez et al., Sydowia 64(2), 218 (2012) (Contributed by Yuwei Hu)

Steccherinaceae Parmasto

48. ***Trullella yunnanensis*** C.L. Zhao, He, Dong & Zhao, Kew Bull 78(1), 216 (2023) (Contributed by Sabin Khyaju and Thatsanee Luangharn)

Russulales Kreisel ex P.M. Kirk, P.F. Cannon & J.C. David

Russulaceae Lotsy

49. ***Lactarius castaneus*** W.F. Chiu, Lloydia 8(1), 34 (1945) (Contributed by Ishika Bera)

Sebacinales M. Weiss, Selosse, Rexer, A. Urb. & Oberw.

Sebacinaceae K. Wells & Oberw.

50. ***Chaetospermum camelliae*** Agnihothr, Mycopathologia et Mycologia Applicata 16, 115 (1962) (Contributed by Zin Hnin Htet)

Introduction

Fungi are among the most diverse groups of organisms and play a crucial role in maintaining ecosystem stability. They function as decomposers, pathogens, and symbionts, thereby driving nutrient cycling and promoting plant health (Hyde et al. 2023a, Jayawardena et al. 2025). Their diversity encompasses a range of ecological lifestyles, including saprobes, epiphytes, endophytes, pathogens, and mutualistic symbionts, with morphological forms varying from macroscopic mushrooms to unicellular yeasts (Naranjo-Ortiz & Gabaldón 2019). Additionally, fungi have significant applications in the food,

biochemical, and biotechnological industries (Hyde et al. 2024b, c), including their use in fermentation processes, large-scale production of industrial enzymes, and generation of bioactive compounds such as antibiotics. These contributions make fungi essential resources for food production, pharmaceuticals, and various bioprocessing technologies.

The global diversity of fungi ranges from 2.2 to 3.8 million species (Hawksworth & Lücking 2017), with some estimates reaching up to 12 million (Wu et al. 2019). However, fewer than 10% of these species have been described (Hyde et al. 2020c). Currently, fungi are classified into 19 phyla, 83 classes, 1,220 families, 10,685 genera, and approximately 155,000 species (Hyde et al. 2024a, Hibbett et al. 2025). Among these, *Ascomycota* contains the highest number of *incertae sedis* taxa, with approximately 2,680 genera (Hyde et al. 2024a), while *Basidiomycota* comprises 1,928 currently accepted genera (He et al. 2019). Together, these two phyla account for approximately 97% of all known fungal species in the kingdom Fungi (Willis 2018).

The publication of new fungal species and records presents significant challenges. Numerous novel species, new genera, new combinations, new host records, and geographical records of fungi were reported, particularly in *Ascomycota* and *Basidiomycota* (He et al. 2019, Manawasinghe et al. 2024). However, the taxonomic advancements and phylogenetic analyses have been facilitated by dedicated publication series such as Fungal Diversity Notes (Hyde et al. 2017, 2019, Wanasinghe et al. 2018, Jayawardena et al. 2023, Manawasinghe et al. 2024), Fungal Planet (Crous et al. 2013, 2020a, 2022), Mycosphere Notes (Thambugala et al. 2017, Hyde et al. 2021, Manawasinghe et al. 2022), and AJOM Notes (Hyde et al. 2020a, Chethana et al. 2021, 2023).

The AJOM Notes series (Hyde et al. 2020a) has published three volumes (Hyde et al. 2020a, Chethana et al. 2021, 2023), documenting 200 fungal records. This fourth series serves as a crucial platform for publishing novel taxonomic and phylogenetic data, particularly on novel described species, geographical distributions, and host and habitat associations. This study aims to document fungal diversity through integrated morphological and molecular approaches, thereby enhancing species delimitation and clarifying phylogenetic relationships. By expanding the available taxonomic knowledge and providing accurately documented records, this work establishes essential baseline data that will support future taxonomic revisions, biodiversity monitoring, and conservation planning. Details of macro- and micromorphological descriptions and illustrations, DNA sequence data, and phylogenetic analyses were included to support species identification and classification. Furthermore, we anticipate that this report will facilitate the exploration of novel habitats, host shifts, and environmental adaptability, providing valuable insights into fungal evolution. Ultimately, this contributes to the ongoing refinement of fungal taxonomy and enhances our understanding of fungal diversity in an ecological context.

Materials & Methods

Materials and methods follow the previous AJOM Notes (Hyde et al. 2020c, Chethana et al. 2021, 2023). Specimens described in this study were collected from China, India, Laos, and Thailand, across diverse habitats including forests, agricultural fields, grasslands, leaf litter, and decaying wood. The basic information of each note includes classification (genus, family, order, class), accepted species number, type species, life mode, habitat, distribution, and sequence information. Morphological analyses with illustrations of *Ascomycota* were described, followed by Senanayake et al. (2020). Classification of the pathogens is based on the descriptions by Hyde et al. (2024a) and Index Fungorum (2025). In contrast, morphological characteristics of *Basidiomycota* are described, following Lodge et al. (2004), Miettinen & Larsson (2016), and Tulloss (2005), coupled with phylogenetic analyses. Phylogenetic analyses were carried out with 11 loci (ITS, LSU, SSU, *rpb1*, *rpb2*, *tef1-α*, *β-tubulin*, *actin*, *CAL*, *chs-1*, and *gapdh*), depending on the availability of sequence data for each taxon. Maximum likelihood (ML) and Bayesian inference (BI) analysis (Huelsenbeck & Ronquist 2001) were carried out. The posterior probabilities

(PP) were calculated to determine the recombination level within phylogenetically closely related species.

Results

Taxonomy

Phylum *Ascomycota* Caval.-Sm., Biological Reviews 73, 247 (1998)

Class *Dothideomycetes* O.E. Erikss. & Winka, Myconet 1(1), 5 (1997)

Index Fungorum number: IF 501481; Facesoffungi number: FoF 14145

Subclass *Dothideomycetidae* P.M. Kirk, P.F. Cannon, J.C. David & Stalpers ex C.L. Schoch, Spatafora, Crous & Shoemaker, Schoch et al., Mycologia 98(6), 1045 (2007)

Index Fungorum number: IF 90782; Facesoffungi number: FoF 00025

Cladosporiales Abdollahz. & Crous in Abdollahzadeh, Groenewald, Coetzee, Wingfield & Crous, Studies in Mycology 95, 390 (2020)

Index Fungorum number: IF 833140; Facesoffungi number: FoF 07632

Cladosporiaceae Chalm. & R.G. Archibald, Yearbook of Tropical Medicine and Hygiene, 25 (1915)

Index Fungorum number: IF 816548; Facesoffungi number: FoF 06966

Cladosporium Link, Magazin der Gesellschaft naturforschender Freunde zu Berlin 7, 37 (1816) [1815]

Index Fungorum number: IF 7681; Facesoffungi number: FoF 06967

Cladosporium was introduced by Link (1816) and typified by *Cladosporium herbarum. Cladosporium* is a dematiaceous hyphomycetous genus belonging to *Cladosporiaceae* (Schoch et al. 2006). This genus is characterised by coronate conidiogenous loci, intercalary ramoconidia, and conidia in acropetal chains with hila, with a distinctive form in the small conidia, which are commonly formed in branched chains (et al. 2010, 2012). *Cladosporium* species are frequently reported as endophytes, plant pathogens, human pathogens, and hyperparasites of other fungi (Heuchert et al. 2005, Bensch et al. 2015, 2018, Rosado et al. 2019). *Cladosporium* includes more than 559 epithets in the Index Fungorum (2025). However, 230 species are accepted, with 134 species with molecular data (Schubert et al. 2009, Bensch et al. 2010, 2015, 2018, Yang et al. 2023).

Cladosporium is a cosmopolitan fungus that is isolated from soil, food, paint, textiles, and plant pathogenic fungi, and can cause allergies or even plant or animal diseases (Bensch et al. 2012). *Cladosporium* is the most common fungal component isolated from the air and is easily spread through airborne transmission (Farr et al. 1989, Flannigan 2001). The *Cladosporium* species complex comprises three major species complexes: *C. cladosporioides*, *C. herbarum,* and *C. sphaerospermum* (Bensch et al. 2012). *Cladosporium sphaerospermum* complex is mainly characterized by having globose or subglobose, pigmented, almost smooth to verrucose terminal conidia and 0–3-septate, smooth or verruculose ramoconidia (Ellis & Yates 1971, Zalar et al. 2007). *Cladosporium cladosporioides* complex is quite variable, ranging from smooth or almost so to irregularly verruculose-rugose, verrucose, or rough-walled in some species. In contrast, all species in the *C. herbarum* complex possess ornamented conidia with ornamentation ranging from minutely verruculose to verrucose, echinulate, or spiny (Torres-Cortés et al. 2015). In the present study, we introduce new host records belonging to the *Cladosporium cladosporioides* species complex from Thailand. An updated phylogeny for *Cladosporium ribis* and closely related taxa is shown in Fig. 1.

Cladosporium ribis Y.Q. Yang & Yong Wang, Yang et al., Journal of Fungi 9(250), 13 (2023)

Index Fungorum number: IF 662567; Facesoffungi number: FoF 19193 Fig. 2

Pathogenic on *Solanum myriacanthum* leaf. Sexual morph: Undetermined. Asexual morph: Hyphomycetous. On PDA: mycelium is superficial and immersed, with abundant, filiform or narrowly cylindrical, branched, septate hyphae, neither swollen nor constricted, subhyaline or pale olivaceous to brown. *Conidiophores* 8–10.5× 2.5–4 μm ($\overline{x}$ = 45 × 3.5 μm, n = 20), macro- and micronematous, arising

terminally or laterally from ascending hyphae, macronematous *conidiophores* narrowly cylindrical-oblong, often distinctly geniculate, subnodulose, sometimes forming lateral shoulders at or towards the apex, mostly unbranched. *Conidia* 2.45–4.65 × 2–3 µm ($\overline{x}$ = 3.5 × 2.35 µm, n = 30), ellipsoid, aseptate, very pale olivaceous to slightly brown, numerous, apex rounded, ellipsoid or subcylindrical. *Secondary ramoconidia* 4–8.6 × 2.10–3.6 µm ($\overline{x}$ = 5.5 × 2.5 µm, n = 30), ellipsoid, subcylindrical or cylindrical, pale olivaceous or pale to medium olivaceous brown, smooth, occasionally slightly rough-walled, walls unthickened, hila conspicuous, subdenticulate or denticulate.

Culture characteristics – On PDA, colonies are greenish-brown, dark brown to black, with velvety, hairy to feathery, and raised mycelium with an entire (smooth) margin. The reverse side of the colonies is black, with a diameter of 55–70 mm on PDA after incubation at room temperature (28 ± 2°C) for 14 days.

Material examined – Thailand, Chiang Rai Province, Muang, Mae Fah Luang University, a symptomatic leaf of *Solanum myriacanthum*, 13 January 2023, Herbert Dustin Aumentado, MFLU23-0456, living culture MFLUCC 23-0287.

GenBank accession numbers – ITS: OR898232, *tef1-α*: OR900453, *actin*: OR900451.

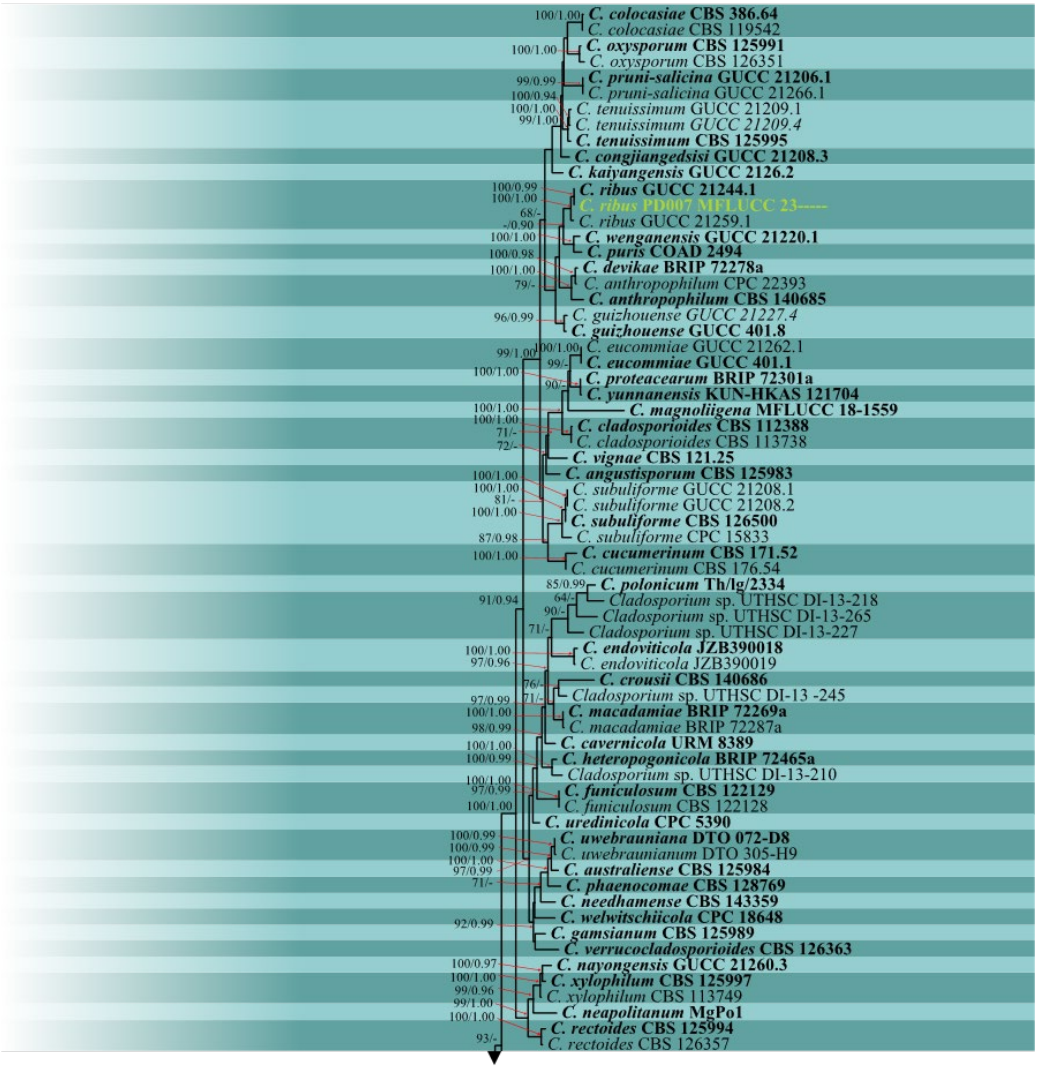

Fig. 1 – Phylogenetic tree obtained from maximum likelihood analyses of a combined ITS, *tef1-α*, and *actin* sequence dataset representing the species of *Cladosporium*. The tree topology of the maximum

likelihood analysis is identical to that of the Bayesian analysis. The best RAxML tree with a final likelihood value of -15754.597 is presented. The evolutionary model GTR+I+G is applied to all genes. One hundred thirty-two (132) strains were included in the combined analyses, which comprised 1105 characters, of which 594 were distinct patterns, 377 were parsimony-informative, 127 were singleton sites, and 601 were constant sites. Bootstrap support values for maximum likelihood (ML) ≥ 60% and Bayesian Posterior Probabilities (PP) ≥ 0.90 are indicated at the nodes as ML/PP. The tree is rooted to *Toxicocladosporium irritans* (CBS 185.58) and *T. protearum* (CBS 126499). The ex-type strains are in bold, and the new isolate of this study is in yellow. Bar = 0.1 represents the estimated number of nucleotide substitutions per site per branch.

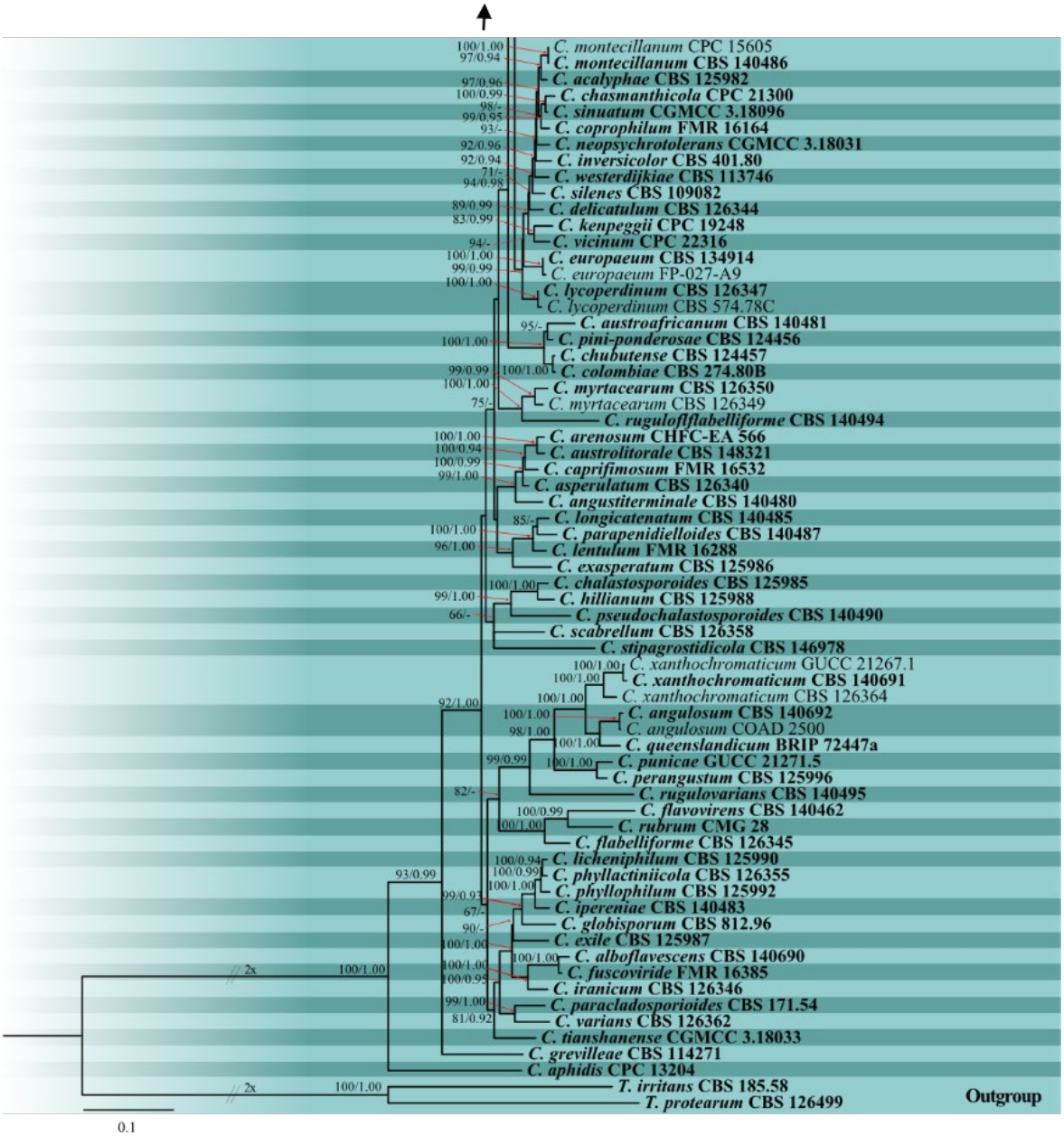

Fig. 1 – Continued.

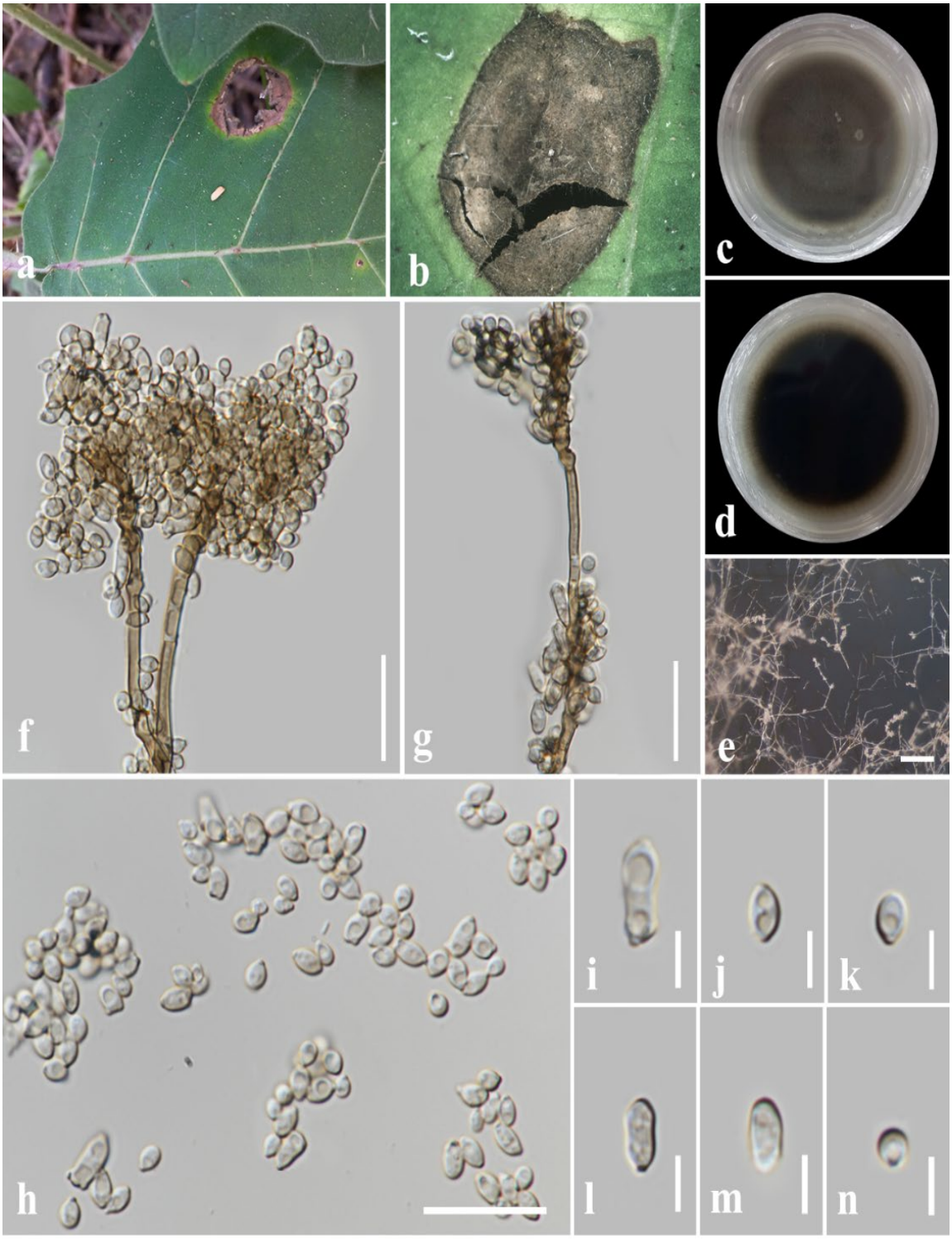

Fig. 2 – *Cladosporium ribis* (MFLU23-0456, **a new host and geographical records**). a, b Leaf spot symptoms on *Solanum myriacanthum*. c, d Colonies on PDA were incubated for 30 days (upper view, bottom view). e Conidial attachment to mycelia on culture. f, g Conidial attachment to conidiophores. h–n Conidia. Scale bars: e = 200 µm, f–h = 20 µm, i–n = 5 µm.

Known distribution – China (Yang et al. 2023), Thailand (this study).
Known hosts – *Ribes burejense* (Yang et al. 2023), *Solanum myriacanthum* (this study).

Notes – *Cladosporium ribis* (MFLUCC 23-0287) clustered with two strains of *C. ribis* (GUCC 2124.1, ex-type culture, and GUCC 21259.1) with 100% ML, 0.99 PP support (Fig. 1). Morphological comparisons with the ex-type strain of *C. ribis* showed closely similar conidia dimensions to *C. ribis* (MFLUCC 23-0287) (2.45–4.65 × 2–3 µm *vs.* 2.5–4.5 × 2–3 µm) with no significant morphological differences between the type strain and our isolate (MFLUCC 23-0287). Pathogenicity testing demonstrated that *C. ribis* (MFLUCC 23-0287) was weakly pathogenic on wounded *Solanum myriacanthum* leaves, inducing lesion symptoms similar to those observed in naturally infected samples. Additionally, a pathogenicity test on *S. myriacanthum* fruits confirmed its ability to infect wounded inoculation sites, leading to fruit splitting and the production of abundant grey mycelium (Fig. 3). The identical fungal isolate was recovered from infected leaf and fruit inoculation sites, thus establishing Koch's postulate. There was no infection observed on non-wounded leaves, fruits, and control samples. This study establishes *S. myriacanthum* as a new host record for *C. ribis*, marking the first report of this fungal pathogen in Thailand.

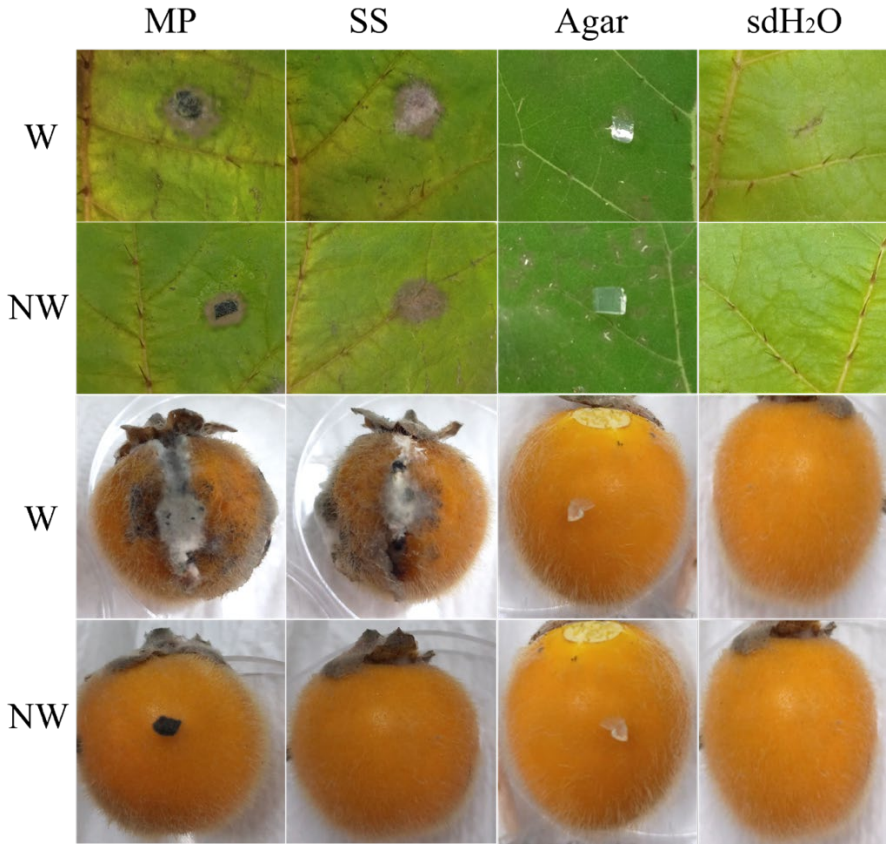

Fig. 3 – Pathogenicity testing of *Cladosporium ribis* on *Solanum myriacanthum* leaves and fruits with symptoms at 14 days post-inoculation. Pathogen inoculations using a mycelial plug (MP) and a spore suspension (SS). W: Wounded, NW: Non-wounded. Control inoculations were done using blank agar and sterile distilled water (sdH_2O).

Cladosporium tenuissimum Cooke, Grevillea 6(40), 140 (1878)

Index Fungorum number: IF145672; Facesoffungi number: FoF 09313 Fig. 4, 5

Saprobic on dead leaves of *Rhododendron* sp. Sexual morph: Undetermined. Asexual morph**:** Colonies on PDA, mycelium superficial and immersed, hyphae loosely branched, septate, and not constricted at septa, hyaline to pale to medium olivaceous-brown, walls thickened, and smooth or

sometimes appearing to be reticulate. *Conidiophores* up to 130 µm long, 2.5–4 µm wide, macronematous, arising laterally or terminally from hyphae, erect, straight to slightly flexuous, filiform to narrowly cylindrical, nodose, with several nodes being quite apart from each other, broad towards the base, branched, pale brown, smooth or sparingly verrucose with darkened and refractive scars. *Conidiogenous cells* 7–35 × 2–4 µm ($\overline{x}$ = 21.5 × 3 µm, n = 10), integrated, terminal and intercalary, geniculate, cylindrical-oblong, nodose with a single node per cell, scars thickened and conspicuous, protuberant. *Conidia* 5–6.5 × 2–3.5 µm ($\overline{x}$ = 5.5 × 2.5 µm, n = 30), solitary or in short, unbranched or branched chains, more or less straight, broadly ellipsoid-subcylindrical to cylindrical, unbranched terminal conidia 0–1. *Cladosporium* septate, dark brown, smooth to loosely verruculose or reticulate, walls unthickened.

Culture characteristics – Conidia germinated on PDA after incubation for 18 hours. Colonies on PDA reaching 50–60 mm diam after incubation at 18°C for 2 weeks, grey to brown, reverse olivaceous-black, velvety, pulvinate to floccose, with a narrow white or grey-olivaceous margin, regular to slightly undulate, aerial mycelium sparse, growth regular, flat to low convex, numerous small but not very conspicuous exudates formed, sporulation profuse.

Material examined – Thailand, Chiang Mai Province, on dead leaves of *Rhododendron* sp., 16 November 2020, N. Chaiwan, Intanon4, living culture MFLUCC 22-0088.

GenBank accession numbers – ITS: OM90893.

Notes – The phylogenetic analysis revealed that our isolates grouped with *Cladosporium tenuissimum*. The morphological characteristics of our strain resembled *C. tenuissimum*. This species was collected from various habitats, including human-associated sources such as thoracentesis fluid (Sandoval-Denis et al. 2016). However, our collection was from dead leaves of *Rhododendron* sp. in Chiang Mai, Thailand. This study represents the first report of *C. tenuissimum* on *Rhododendron* species in Thailand. An updated phylogeny for *C. tenuissimum* and closely related taxa is shown in Fig. 4.

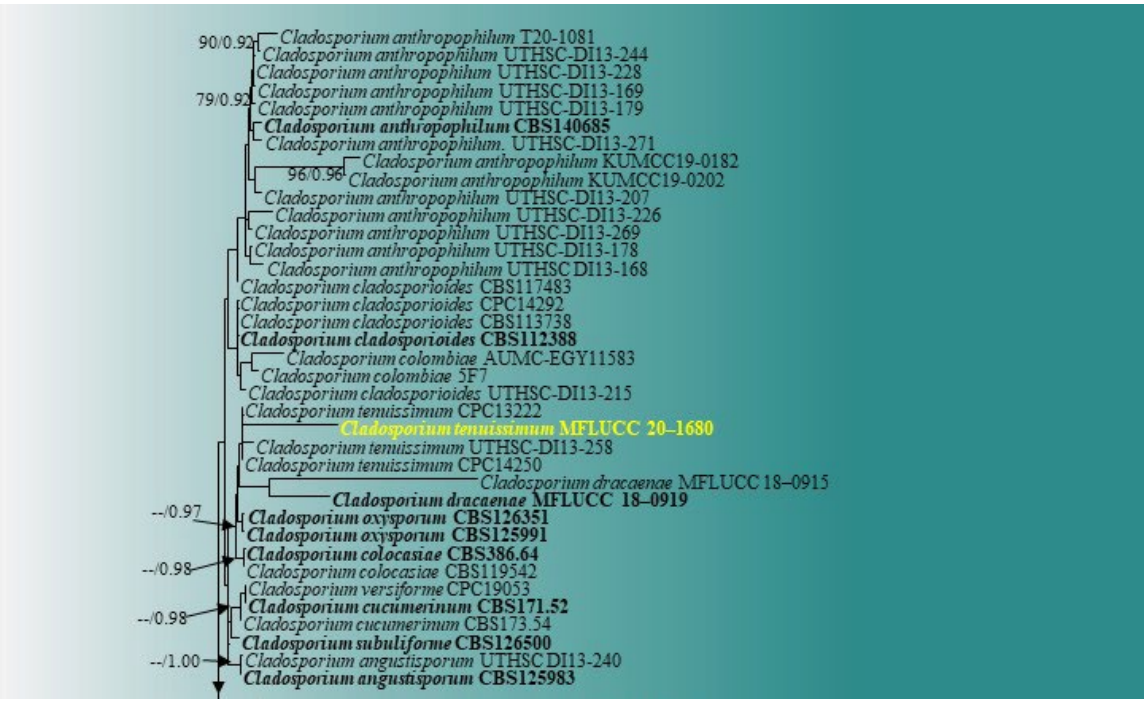

Fig. 4 – Phylogram generated from RAxML analysis based on ITS sequence data of selected *Cladosporiaceae* isolates. Related sequences were obtained from GenBank. One hundred and fourteen taxa are included in the analyses, which comprise 2,745 characters, including gaps. The tree is rooted in *Cladosporium herbarum* (CBS 121621). The best-scoring RAxML tree with a final likelihood value of

−22003.238457 is presented. The matrix contained 1,285 distinct alignment patterns, with 60.03% of the characters being undetermined or gaps. Estimated base frequencies were as follows; A = 0.233071, C = 0.288405, G = 0.248984, T = 0.229540; substitution rates AC = 1.517403, AG = 3.134825, AT = 1.668455, CG = 1.130508, CT = 4.683471, GT = 1.000000; gamma distribution shape parameter α = 0.426819. Maximum-likelihood bootstrap support values ≥ 60% (ML) are shown at the nodes as ML. The scale bar indicates 0.2 changes. The isolates obtained in this study are in yellow, and ex-type taxa are in black bold.

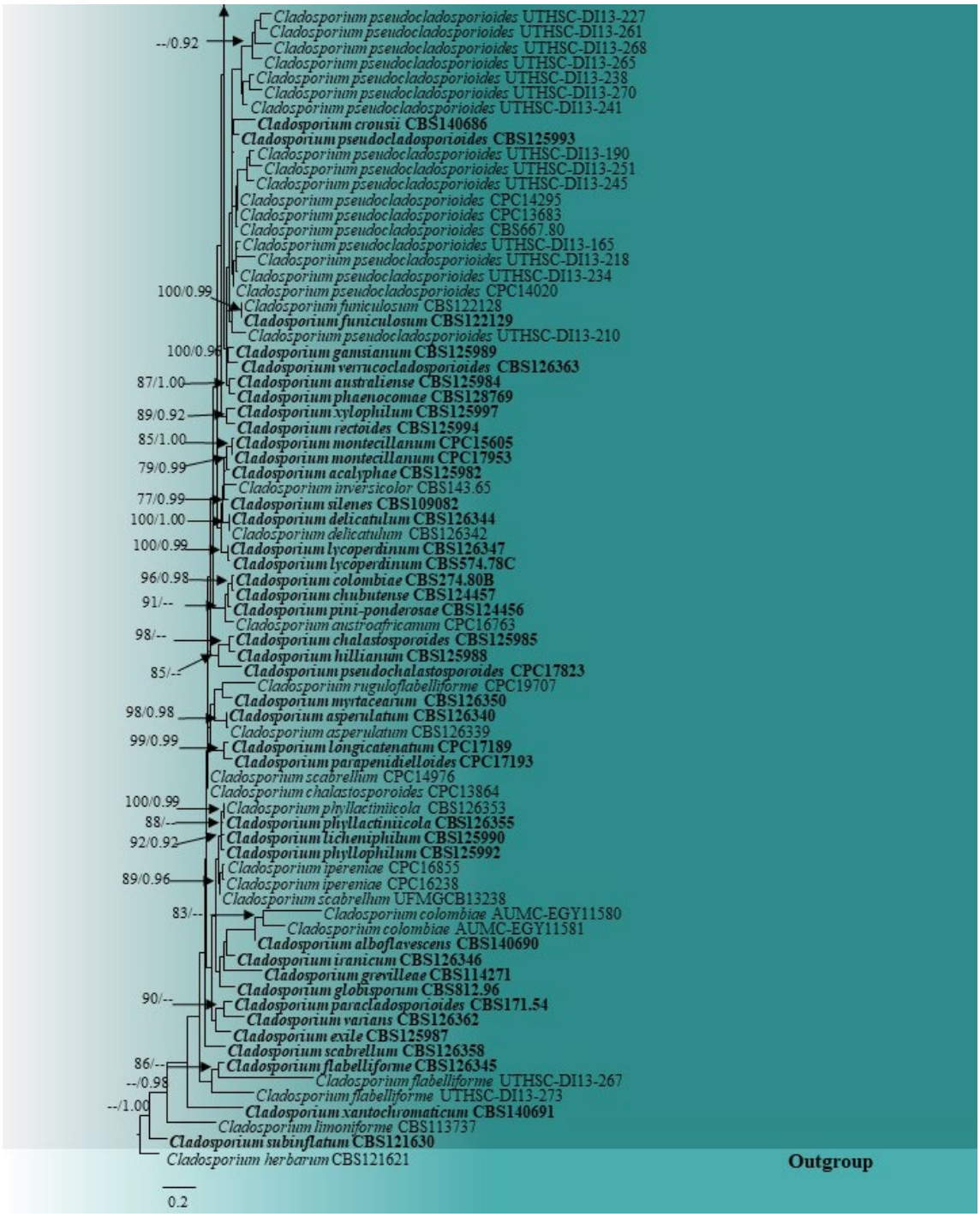

Fig. 4 – Continued.

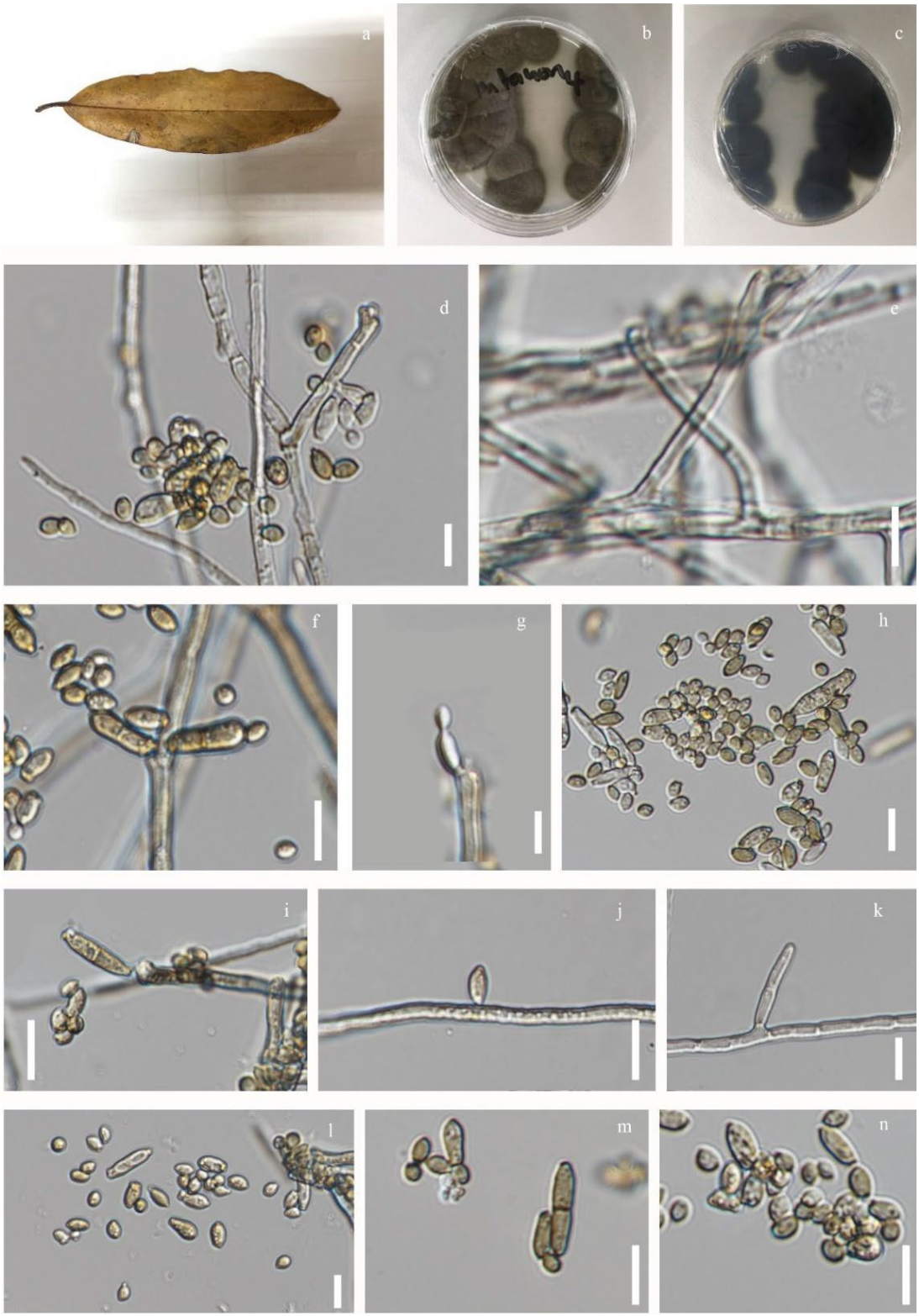

Fig. 5 – *Cladosporium tenuissimum* (MFLU 20-0184, **a new host record**). a Host sample. b, c Culture on PDA. d, f, g, i, j Conidiophore with conidia. e, k Conidiophore. h, l–n Conidia and ramoconidia. Scale bars: d–j, l–n = 10 µm, k = 20 µm.

Hysteriales Lindau (1897)

Index Fungorum number: IF 90549; Facesoffungi number: FoF 07681

Hysteriaceae Chevall (1826)

Index Fungorum number: IF 80901; Facesoffungi number: FoF 01838

Rhytidhysteron Speg. [as '*Rhytidhysterion*'], Anales de la Sociedad Científica Argentina 12(4), 188 (1881)

Index Fungorum number: IF 4740; Facesoffungi number: FoF 08063

Rhytidhysteron was introduced by Spegazzini (1881) to accommodate *R. brasiliense* Speg. and *R. viride* Speg., without designating a type species. Subsequently, Clements & Shear (1931) designated *R. brasiliense* as the type species. Based on molecular data, Boehm et al. (2009) reclassified *Rhytidhysteron*, transferring it from *Patellariaceae* Corda to *Hysteriaceae*. *Rhytidhysteron* is characterized by its sexual morph, which features large ascomata with conspicuous, navicular, gradually opening via a longitudinal sulcus, pigmented ascospores, septate, and muriform (Boehm et al. 2009, Xu et al. 2022, Du et al. 2023), and asexual morph: conidia are classified into two types, "Aposphaeria-like" and "Diplodia-like" (Samuels et al. 1979, Thambugala et al. 2016, Ren et al. 2022). Recently, seven new species have been accepted in *Rhytidhysteron*, viz. *R. ligustrum*, *R. sichuanense*, *R. subrufulum* (Xu et al. 2022), *R. bannaense*, *R. coffeae*, *R. mengziense*, *R. yunnanense* (Du et al. 2023), and *R. juglandis* (Zhao et al. 2025). Currently, 44 records of *Rhytidhysteron* are listed in the Index Fungorum (2025). This study introduces a new host record for *R. camporesii* Ekanayaka & K.D. Hyde, collected from *Wisteria sinensis* (Sims) DC. in China. An updated phylogeny for *Rhytidhysteron* and closely related taxa is shown in Fig. 6.

Subclass *Pleosporomycetidae* C.L. Schoch, Spatafora, Crous & Shoemaker, Mycologia 98, 1048 (2007)

Index Fungorum number: IF 501507; Facesoffungi number: FoF 14163

Rhytidhysteron camporesii Ekanayaka & K.D. Hyde, Hyde et al., Fungal Diversity 100, 18 (2020)

Index Fungorum number: IF 556783; Facesoffungi number: FoF 06459 Fig. 7

Saprobic on the decaying vine of *Wisteria sinensis* (*Fabaceae*). Sexual morph: *Ascomata* 800–1500 µm long × 500–1000 µm wide × 400–700 µm high ($\overline{x}$ = 1113 × 844 × 526 µm, n = 5) apothecial, navicular, solitary, superficial, short stipitate is embedded in the plant tissue, black, smooth, perpendicularly striate, elongate and depressed, compressed at apex, and open an elongated opening through a longitudinal slit, dark reddish-brown at the centre. *Exciple* 40–90 µm wide, composed of thick-walled cells of *textura angularis*, outer layer brown to blackish, inner layer reddish-brown. *Hamathecium* 1.5–3.5 µm wide, dense, hyaline, septate, branched, cellular pseudoparaphyses, forming an orange-red epithecium above asci. *Asci* (147–)160–236 µm × (9–) 10–16 µm ($\overline{x}$ = 195 × 14.5 µm, n = 20), 8-spored, bitunicate, cylindrical, with short and club-shaped pedicel, rounded at the apex, with an ocular chamber. *Ascospores* 31–38(–44) µm × 12–15(–17) µm ($\overline{x}$ = 36 × 14 µm, n = 30), uni-seriate to slightly overlapping, hyaline, 1-septate when immature, becoming brown, 1–3 septate at maturity, ellipsoidal to fusiform, straight or slightly curved, rounded to slightly pointed at both ends, guttulate, rough-walled, without a mucilaginous sheath. Asexual morph: Undetermined.

Culture characteristics – Ascospores germinate on PDA within 24 hours, producing germ tubes from one or both ends. Colonies on PDA reached 6 cm in diameter after one week of incubation at 28°C. The colony was soft, circular, with aerial hyphae raised and a filiform edge, appearing yellow or grey on the forward side and yellowish-brown to dark brown in the bottom view.

Material examined – China, Yunnan Province, Qujing City, Sanjiang Road, Qujing Normal University, on decaying vine of *Wisteria sinensis* (*Fabaceae*), 01 March 2022, T.Y. Du, QJD01 (HKAS 124184, living culture, KUNCC 22-10820).

Known distribution – China (Hyde et al. 2020, Du et al. 2023, this study).

Known hosts – *Cotoneaster franchetii* (Du et al. 2023), *Wisteria sinensis* (this study), and unidentified wood (Hyde et al. 2020).

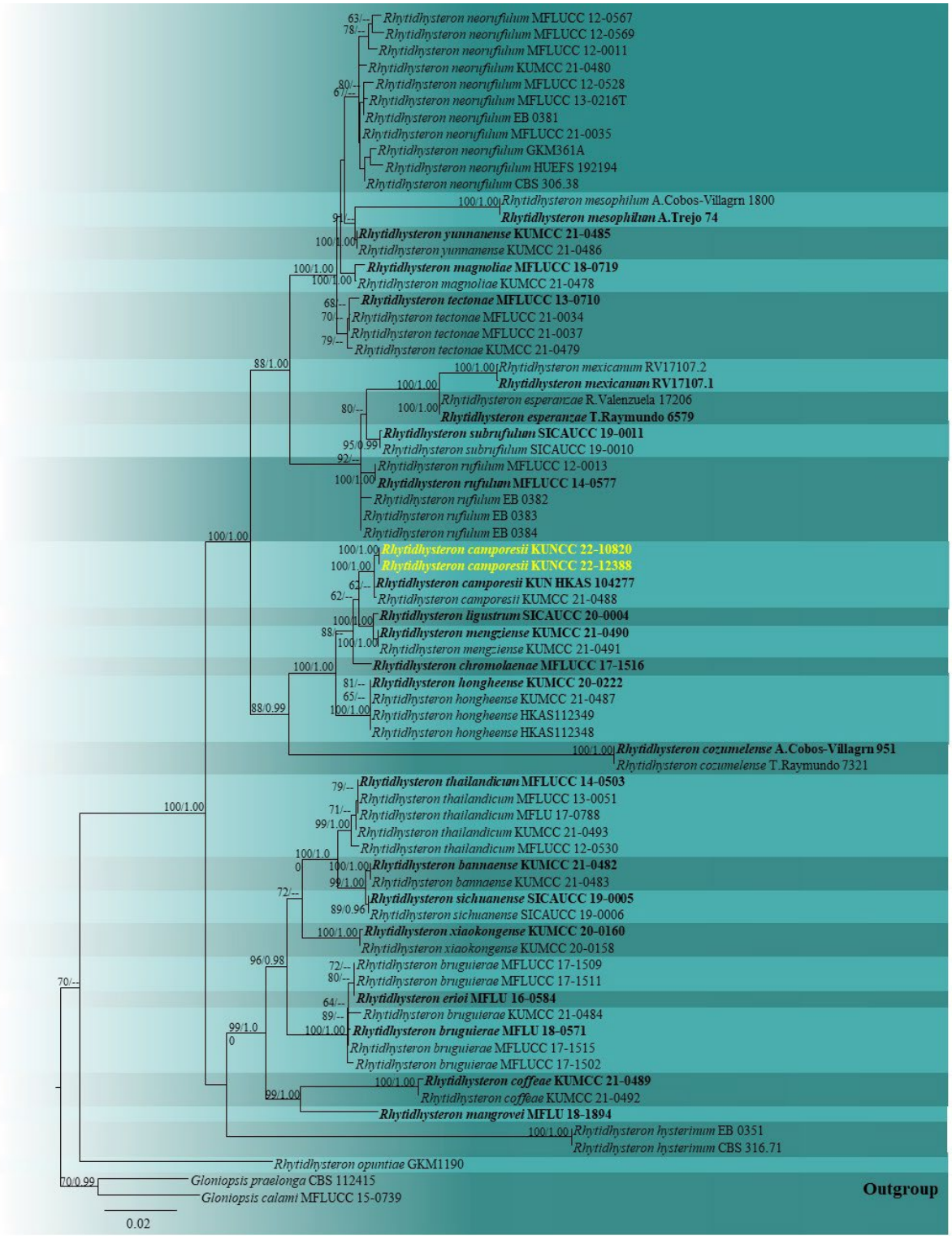

Fig. 6 – Phylogram generated from maximum likelihood analysis based on combined ITS, LSU, SSU, and *tef* sequence data of *Rhytidhysteron*. Seventy-two strains were included in the combined analyses, which comprised 3,406 characters (652 for ITS, 793 for LSU, 1,001 for SSU, and 960 for *tef*). The tree topology of the maximum likelihood analysis is similar to that of the Bayesian analysis. The best RAxML tree with a final likelihood value of -12222.989691 is presented. The matrix contained 767 distinct alignment patterns, with 21.63% of the characters being undetermined or gaps. The evolutionary

model applied to the four loci is GTR+I+G. Bootstrap support values for ML equal to or greater than 60% and Bayesian posterior probabilities equal to or greater than 0.90 are given near nodes, respectively. The tree was rooted with *Gloniopsis calami* S. Konta & K.D. Hyde (MFLUCC 15-0739) and *G. praelonga* (Schwein.) Underw. & Earle (CBS:112415). The newly generated GenBank accession numbers – KUNCC 22-10820: ITS: OR807852, LSU: OR801301, SSU: OR801303, *tef*: PV054485; KUNCC 22-12388: ITS: OR807853, LSU: OR801302, SSU: OR801304, *tef*: PV054486.

Notes – *Rhytidhysteron camporesii* was introduced by Hyde et al. (2020) based on morphology and phylogenetic analyses. The phylogenetic analyses based on a combined multi- gene dataset (LSU, ITS, SSU, and *tef*) placed our collection within *R. camporesii* (KUN-HKAS 104277, KUMCC 21-0488), with relatively strong statistical support (100% ML/1.00 PP).

Fig. 7 – *Rhytidhysteron camporesii* (HKAS 124184, **a new host record**). a, b Appearance of hysterothecia on the host. c, d Vertical section through hysterothecium. e–g Asci. h Epithecium mounted in water. i Pseudoparaphyses. j Exciple. k–m Ascospores. n A germinating ascospore. o, p Colony on PDA medium after incubation for 2 weeks. Scale bars: c, d = 500 μm, e–g = 100 μm, h, i = 10 μm, j = 50 μm, k–n = 20 μm.

In addition, our collection exhibits morphological features similar to those of *R. camporesii*, including black, striated hysterothecia, septate, branched pseudoparaphyses, 8-spored, cylindrical, short-pedicellate asci, and ellipsoidal to fusiform, brown ascospores (Hyde et al. 2020). *Rhytidhysteron camporesii* has been reported only from Kunming, Yunnan Province, China (Hyde et al. 2020, Du et al. 2023). Therefore, we report our collection as a new host record of *R. camporesii* from the decaying vine of *Wisteria sinensis* (*Fabaceae*) in Qujing City, Yunnan Province, China. This is the first record of *R. camporesii* on the *Wisteria sinensis* host.

Pleosporales Luttrell ex M.E. Barr, Prodromus to class *Loculoascomycetes* (Amherst), 67 (1987)

Index Fungorum number: IF 90563; Facesoffungi number: FoF 08715

Amniculicolaceae Y. Zhang ter, C.L. Schoch, J. Fourn., Crous & K.D. Hyde, Zhang et al., Studies in Mycology 64, 95 (2009)

Index Fungorum number: IF 515469; Facesoffungi number: FoF 08153

Amniculicola Y. Zhang & K.D. Hyde, Mycological Research 112(10), 1189 (2008)

Index Fungorum number: IF 511328; Facesoffungi number: FoF 08154

Amniculicola is a freshwater fungal genus introduced by Zhang et al. (2008) to accommodate *A. lignicola* Y. Zhang & K.D. Hyde, which was collected from submerged wood in France. This genus is characterized by ascomata, 1–3-septate ascospores with slit-like ostioles, thin, branching, and anastomosing hamathecia, cylindrical asci, and hyaline (Zhang et al. 2008, 2009a, Hyde et al. 2019). *Amniculicola* is a morphologically distinct genus, with most species producing purple pigmentation on the host substrate during their sexual stages, except for *A. aquatica* and *A. guttulata* (Zhang et al. 2008, 2009a, Hyde et al. 2019, Dong et al. 2020). This genus currently comprises seven species, except *A. longissimi*, with type specimens collected from freshwater habitats (Dong et al. 2020, Magaña-Dueñas et al. 2022). However, most members of *Amniculicola* are known for their sexual morphs; only *A. asexualis* and *A. longissima* have been described based on their asexual morph (Hyde et al. 2019, Magaña-Dueñas et al. 2022). The phylogeny of *Amniculicola* has been extensively studied, and molecular sequence data for all species are available in the NCBI database. The most recent phylogenetic analysis of the genus was conducted by Magaña-Dueñas et al. (2022). An updated phylogeny for *Amniculicola* and closely related taxa is shown in Fig. 8.

Amniculicola yunnanensis H.W. Shen & Z.L. Luo, sp. nov.

Index Fungorum number: IF 572412; Facesoffungi number: FoF 17687 Fig. 9

Etymology – "yunnanensis" refers to the type locality, Yunnan Province, China.

Saprobic on decaying wood on the riverbed. Sexual morph: *Ascomata* 394–537 μm high, 355–464 μm diam., black, solitary, scattered or gregarious, superficial, coriaceous, globose to subglobose, flattened, with ostioles papilla. *Peridium* 61–89 μm thick, comprising several layers, outer layer dark brown, irregularly pigmented, consisting of several thick-walled cells of *textura angularis*; inner layer composed of hyaline, thin-walled cells of *textura angularis*. *Pseudoparaphyses* 1–2 μm diam, dense, trabeculate, filiform, persistent, hyaline, embedded in mucilage, anastomosing between and above the asci. *Asci* 140–170 × 10–12 μm ($\overline{x}$ = 156 × 11 μm, n = 40), 8-spored, bitunicate, fissitunicate, cylindrical to narrowly fusiform, with a twisted, bifurcate, short pedicel, apically rounded or slightly obtuse. *Ascospores* 27–32 × 6–8 μm ($\overline{x}$ = 29 × 7 μm, n = 40), uni-seriate or overlapping, straight or slightly curved, hyaline, fusiform, thin-walled, smooth, 1-septate, deeply constricted at the septa and constricted somewhat at the quarter, the upper cell slightly broader than the lower one, with two prominent big guttules on either side of septa, and 1–4 gradually smaller ones besides, with a thin, hyaline, gelatinous sheath. Asexual morph: Undetermined.

Culture characteristics – Conidia germinate on PDA within 12 hours, and germ tubes are produced at the ends. Colony growth on PDA reached 1.6 cm when incubated at room temperature after 20 days.

Mycelium papillary in the middle, surface rough, fluffy, dense, dry, grey to brown, pale brown to brown from below.

Material examined – China, Yunnan Province, Lijiang City, Ninglang Yi Autonomous County, Lugu Lake, 27°39′40″ N, 100°46′53″ E (2,800 m), on decaying wood, 21 October 2021, L.L. Li, LGH 14-1 (HKAS 125825, holotype), ex-type living cultures (CGMCC3.24261, KUNCC 22–12666).

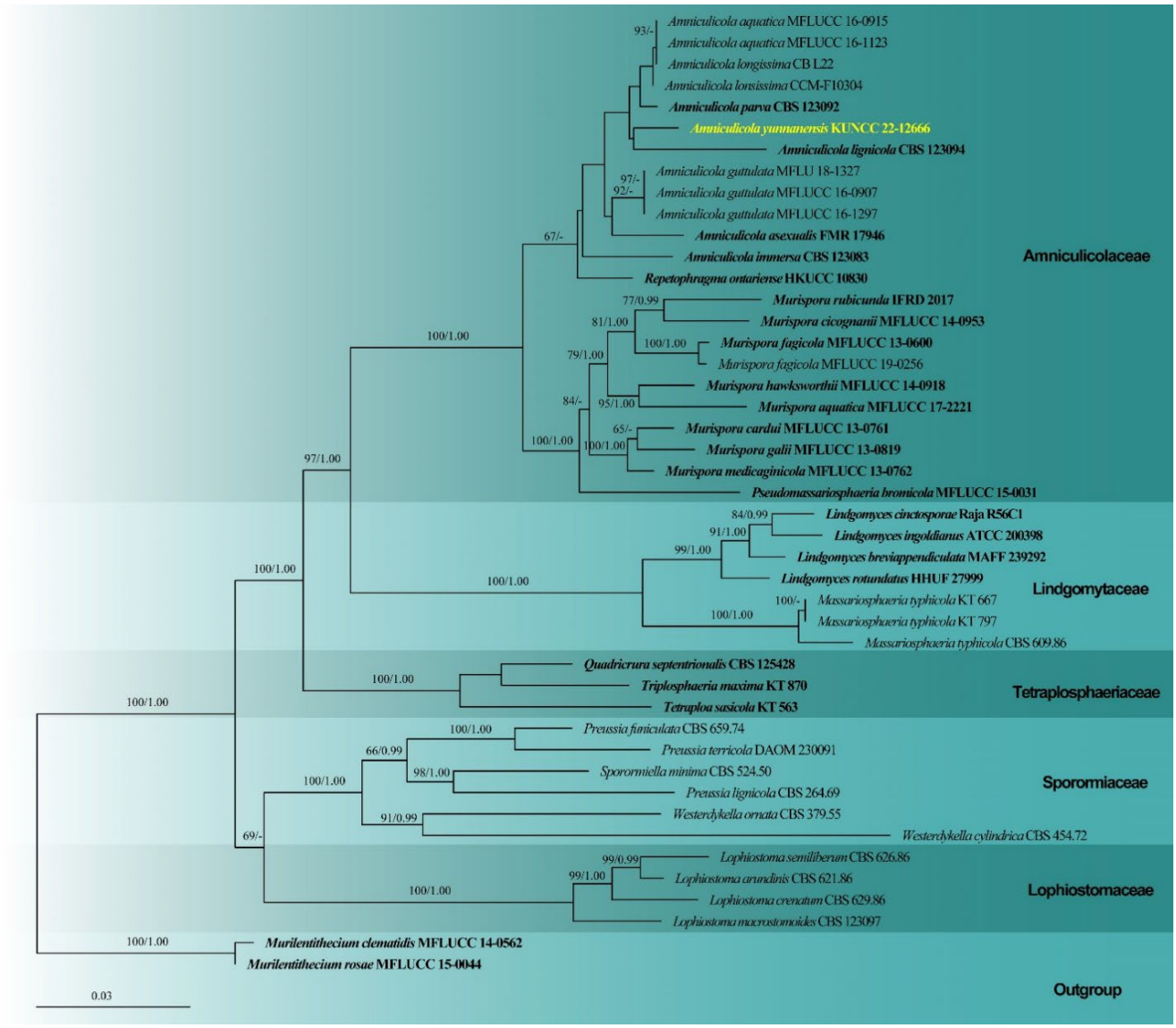

Fig. 8 – Phylogram generated from RAxML analysis based on combined LSU, SSU, ITS, and *tef 1-α* sequence data of the genus *Amniculicolaceae* and related family. One strain is included in the combined analyses, comprising 3,623 characters (1,334 for LSU, 945 for SSU, 497 for ITS, and 847 for *tef1-α*). The tree topology of the maximum likelihood analysis is similar to that of the Bayesian analysis. The best RAxML tree with a final likelihood value of -28476.592376 is presented. The matrix contained 1,027 distinct alignment patterns, with 29.68% of the characters being undetermined or gaps. Evolutionary models applied to ITS and *tef*1-α genes are GTR+I+G, while the LSU gene is modeled as SYM+I+G, and the SSU gene is modeled as HKY+I+G, respectively. Bootstrap support values for ML greater than 75% and Bayesian posterior probabilities greater than 0.97 are given near nodes, respectively. The tree was rooted with *Murilentithecium clematidis* (MFLUCC 14-0562) and *M. rosae* (MFLUCC 15-0044). Ex-type strains are in bold. The newly generated sequences are indicated in yellow.

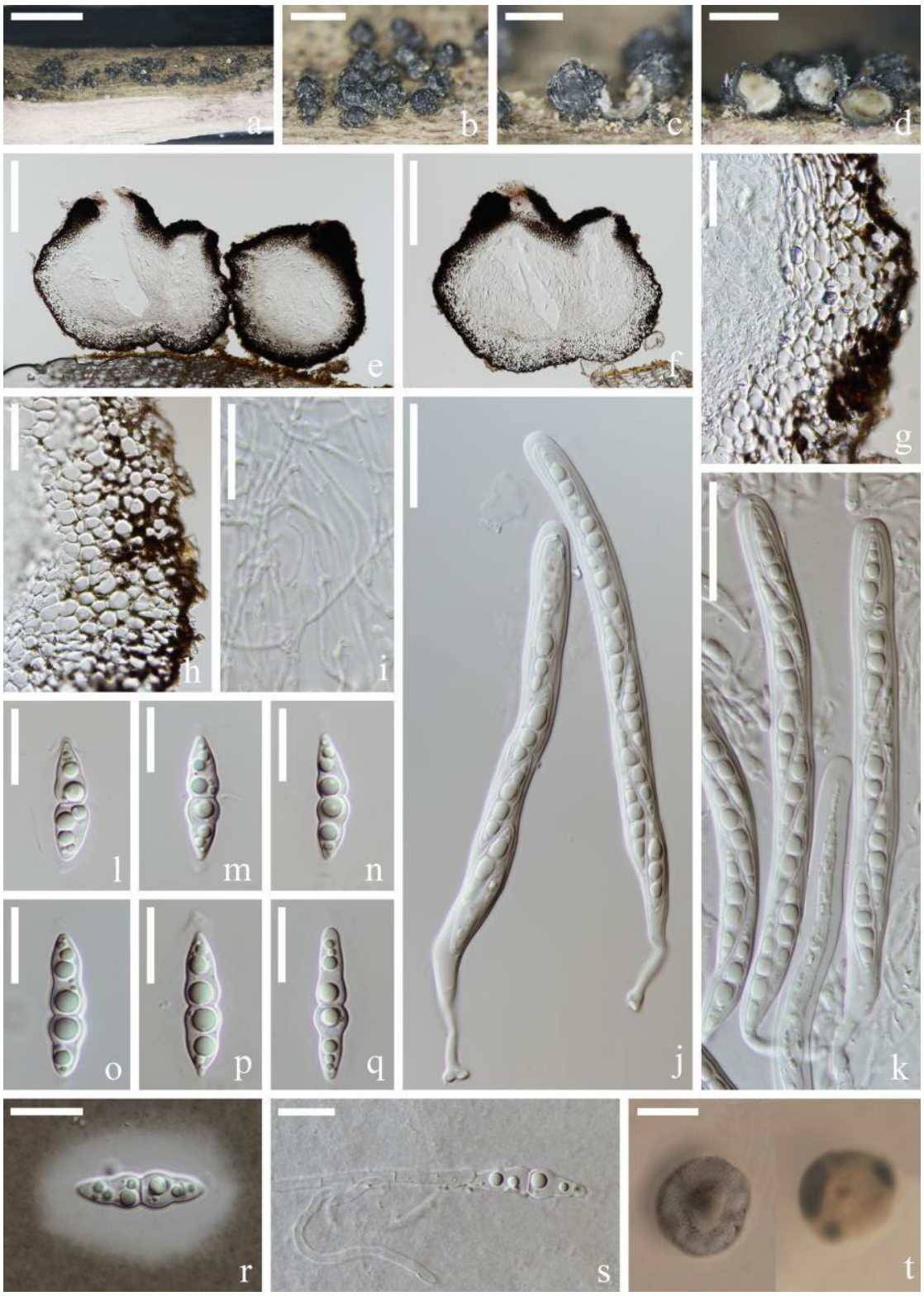

Fig. 9 – ***Amniculicola yunnanensis*** (HKAS 125825, **holotype**). a–d Appearance of ascomata on the host. e, f Sections of ascomata. g, h Section of peridium. i Pseudoparaphyses. j, k Asci. l–r Ascospores. s Germinated conidium. t Colony on PDA. Scale bar: a = 4 mm, b = 1000 μm, c, d = 500 μm, e, f = 200 μm, g–k = 30 μm, i = 20 μm, l–s = 15 μm, t = 1 cm.

GenBank accession number: ITS: OQ874967, LSU: OQ732678, SSU: OQ875037, *tef1-α*: PV220982.

Known distribution – Yunnan Province, China (this study).

Known hosts – Decaying wood of an unknown tree (this study).

Notes – Phylogenetic analysis revealed that the newly identified species, *Amniculicola yunnanensis*, clustered together with other members of *Amniculicola* and formed a sister clade with *A. lignicola* (CBS 123094) with low support (Fig. 8). Sequence comparison of ITS, LSU, SSU, and *tef1-α* regions between *A. yunnanensis* and *A. lignicola* showed nucleotide differences of 11 bp (including 1 gap), 3 bp, and 65 bp. Although *A. yunnanensis* shares morphological similarities with *A. ligncola*, the molecular sequence divergence is quite different. Following the guidelines of Jeewon & Hyde (2016), the comparison of morphological characteristics among accepted sexual species of *Amniculicola* (Table 1) further supports their separation.

Table 1 Morphological comparison of accepted sexual species of *Amniculicola*.

Fungal species	Ascomata	Peridium	Hamathecium	Asci	Ascospores
Amniculicola aquatica	260–330 µm high, 250–320 µm diam., scattered or in small groups, globose to subglobose, superficial	35–50 µm thick	pseudoparaphyses	110–130(–152) × 10–13 µm, cylindrical	24–32 × 6–8 µm, fusiform, hyaline, 1-septate, with a gelatinous sheath
A. guttulata	290–320 µm high, 280–300 µm diam., scattered or in small groups, globose to subglobose, superficial	27–35 µm thick	pseudoparaphyses	113–127 × 9–11 µm, cylindrical	23–27 × 5–7 µm, fusiform, hyaline, 1-septate, with a gelatinous sheath
A. immersa	280–400(–450) µm high, 300–420(–500) µm diam., solitary, scattered or in small groups of 2–3, globose to subglobose, immersed	45–65 µm thick	pseudoparaphyses, 1–1.8 µm wide	150–180 × 13–18 µm, cylindrical to narrowly fusiform	27–31(–36) × 7.5–8.5(–10) µm, broadly fusiform to fusiform, hyaline, 1–3-septate, with a gelatinous sheath
A. lignicola	350–450 µm high, 300–500 µm diam., scattered or in small groups of 2–3, globose to subglobose, immersed to superficial	40–55 µm thick	pseudoparaphyses, <1 µm wide	140–184 × 9–10 µm, cylindrical to narrowly fusiform	(20.5–)28–32 × (6–)8–9(–9) µm, broad fusiform to fusiform, 1-septate, with a gelatinous sheath
A. parva	260–380 µm high, 260–360 µm diam., scattered to gregarious, subglobose, superficial	20–35 µm thick	pseudoparaphyses, 0.8–1.5 µm wide	100–130 × 8–12 µm, cylindrical to narrowly fusiform	(23–)27–32 × 4.5–6.5 µm, narrowly fusiform to fusiform, hyaline, 1(–3)-septate, with a gelatinous sheath

Table 1 Continued.

Fungal species	Ascomata	Peridium	Hamathecium	Asci	Ascospores
A. yunnanensis	394–537 µm high, 355–464 µm diam., scattered or gregarious, globose to subglobose, superficial	61–89 µm thick	pseudoparaphyses, 1–2 µm wide	140–170 × 10–12 µm, cylindrical to narrowly fusiform	27–32 × 6–8 µm, fusiform, hyaline, 1-septate, with a gelatinous sheath

Didymellaceae Gruyter, Aveskamp & Verkley, in Mycological Research 113(4), 516 (2009)

Index Fungorum number: IF 508292; Facesoffungi number: FoF 08216

Allophoma Q. Chen & L. Cai, Studies in Mycology 82, 162 (2015)

Index Fungorum number: IF 814058; Facesoffungi number: FoF 08217

Chen et al. (2015) established *Allophoma* to accommodate phoma-like species distinguished by their variably shaped conidia. The genus comprises phytopathogens and saprobes that inhibit plants, with some species also identified as pathogens of humans and animals (Schneider & Boerema 1975, Valenzuela-Lopez et al. 2017, Yuan et al. 2021). Samaradiwakara et al. (2023) reported the first sexual morph for the genus, derived from its type species, *Allophoma tropica*, which comprises 14 accepted species (Species Fungorum 2025). An updated phylogeny for *Allophoma* and closely related taxa is shown in Fig. 10.

Allophoma tropica (R. Schneid. & Boerema) Q. Chen & L. Cai, Chen et al., Studies in Mycology 82, 164 (2015)

Index Fungorum number: IF 814071; Facesoffungi number: FoF 13240 Fig. 11

Saprobic on leaf litter of *Alzelia xylocarpa.* Sexual morph: Undetermined. Asexual morph: Coelomycetous. *Conidiomata* 200 µm diam, pycnidial, globose to subglobose, mostly solitary, rarely aggregated, or immersed in the agar, with a single ostiole. *Pycnidial wall* 2–5 layered, pseudoparenchymatous. *Conidiophores* are reduced to conidiogenous cells. *Conidiogenous cells* 6–9 × 2–4 µm ($\overline{x}$ = 7–2.5 µm, n = 20), hyaline, smooth, phialidic, ampulliform to doliiform, sometimes flask-shaped or isodiametric. *Conidia* 2–3.5 × 1–2 µm ($\overline{x}$ = 3–1 µm, n = 20), hyaline, smooth, aseptate, thin-walled, shape and size variable, guttulate, ovoid, obovate, and slightly allantoid.

Culture characters – Colonies on PDA reaching 50–75 mm after incubating in the dark at 25°C for 7 days, pale olivaceous grey with pale white to smoke grey powdery spots, aerial mycelia, smooth to slightly waved margin, reverse pale olivaceous grey with pigmentation, and pycnidia visible after 30 days.

Material examined – Thailand, Chiang Rai Province, Mae Fah Luang District, on leaf litter of *Afzelia xylocarpa* (*Fabaceae*), 6 June 2022, N.P. Samaradiwakara AL 12 (MFLU 23-0074).

GenBank accession numbers – ITS: OR711075, LSU: OR711078, *rpb2*: OR724870, *β-tubulin*: OR724871.

Known distribution (based on molecular data) – China (Kularathnage et al. 2023), Germany (Chen et al. 2015), India (Sundararaj et al. 2023), Italy (Gullino et al. 2017), Netherlands (Schneider & Boerema 1975), Thailand (Samaradiwakara et al. 2023).

Known hosts (based on molecular data) – *Canna* sp. (Kularathnage et al. 2023), *Lactuca sativa* (Gullino et al. 2017), *Nayariophyton zizyphifolium* (*Malvaceae*) (Samaradiwakara et al. 2023), *Santalum album* (Sundararaj et al. 2023), *Saintpaulia ionantha* (Chen et al. 2015), and *Syzygium cumini* (Nagarjun et al. 2016).

Notes – Chen et al. (2015) introduced *Allophoma tropica* as a novel combination of *Phoma tropica* (R. Schneid. & Boerema), which was originally described by Boerema & Bollen in 1975. *Allophoma tropica* is the type species of the genus, with its holotype described from *Saintpaulia ionantha* collected in Germany. However, the original description by Chen et al. (2015) lacked detailed morphological characteristics. Subsequently, Kularathnage et al. (2023) identified and described the same species from *Canna* sp. in China, while Samaradiwakara et al. (2023) reported it from *Nayariophyton zizyphifolium*, introducing its sexual morph based on phylogeny analysis and providing detailed morphological characterization. In the present study, the isolate MFLUCC 23-0050 was identified as *A. tropica* (CBS 537.66, CBS 436.75) based on ITS, LSU, *rpb2*, *β-tubulin*, and culture morphology, with 86 ML/0.96 PP support. This isolate was obtained as a saprobe from *Alzelia xylocarpa* leaf litter (MFLUCC 23-0050), representing the first report of *A. tropica* from this host in Thailand.

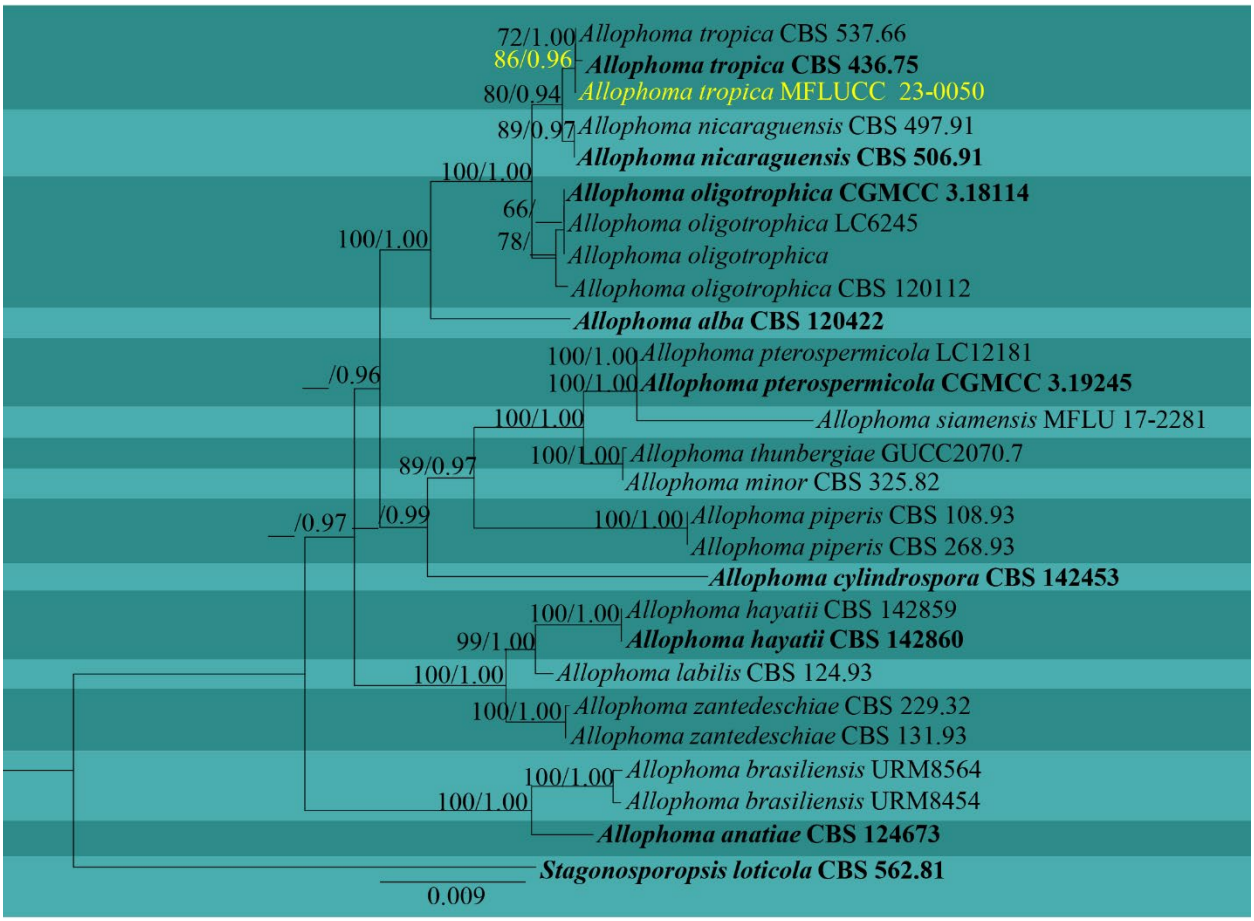

Fig. 10 – Phylogram generated from maximum likelihood analysis based on combined ITS, LSU, *rpb2*, and *β-TUB* sequence data. Twenty-seven strains are included in the combined analyses, which comprise 2,746 characters (482 for ITS, 1,326 for LSU, 596 for *rpb2*, and 333 for *β-tubulin*) after alignment. The tree topology obtained from the maximum likelihood analysis is congruent with that from the Bayesian analysis. The best RAxML tree with a final likelihood value of -6168.328927 is presented. Estimated base frequencies were as follows: A = 0.242107, C = 0.242209, G = 0.274991, T = 0.240693; substitution rates AC = 1.526777, AG = 3.529722, AT = 1.279836, CG = 1.016628, CT = 9.979353, GT = 1.000000; gamma distribution shape parameter α = 0.020000. The evolutionary models applied for the gene regions were TPM2+G for ITS, TIM2+G for LSU, TrNef+G for *rpb2*, and TIM1+G for *β-TUB*. Bootstrap support values for ML greater than 75% and Bayesian posterior probabilities greater than 0.90 are given near nodes, respectively. The tree is

rooted with *Stagonosporopsis loticola* (CBS 562.81). Ex-type strains are in bold. The newly generated sequences are indicated in yellow.

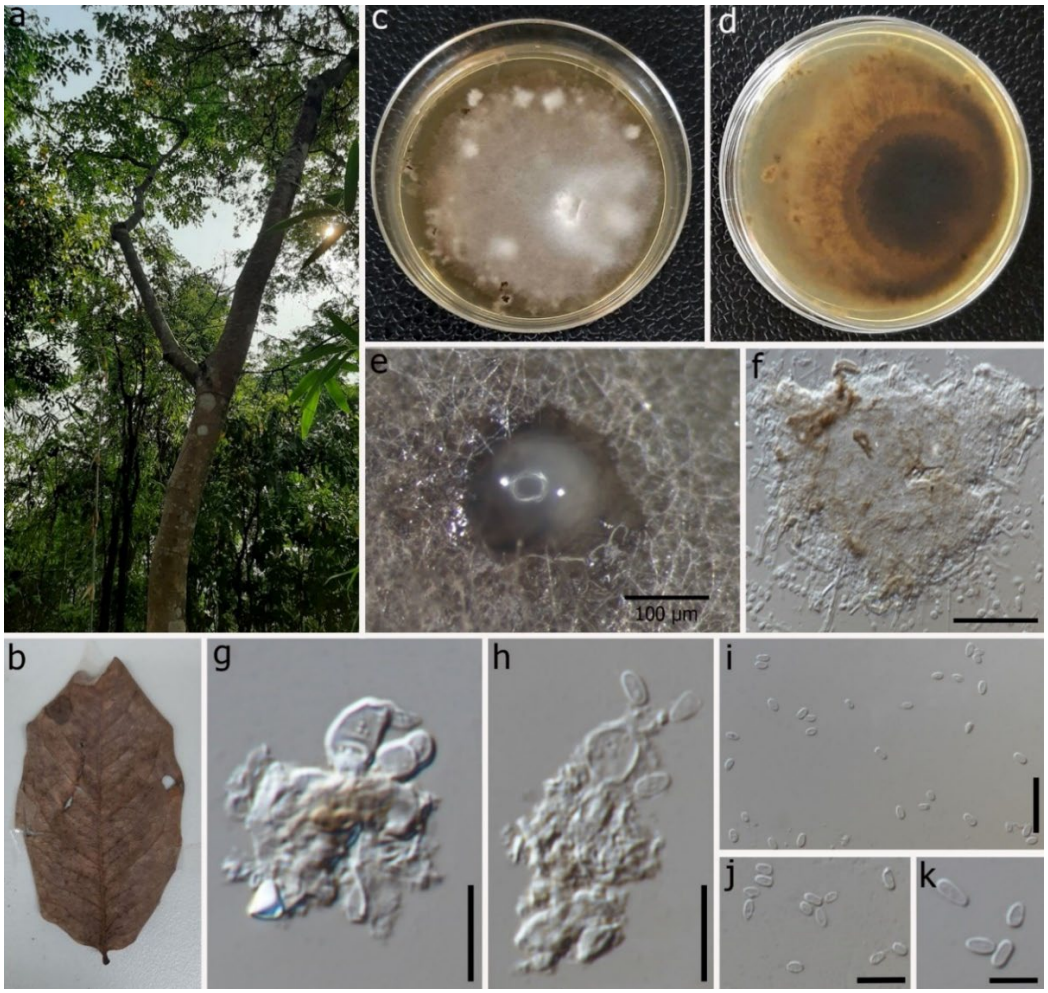

Fig. 11 – *Allophoma tropica* (MFLU 23-0074, a new host and geographical record). a Host *Afzelia xylocarpa*. b Dead leaf of *Afzelia xylocarpa*. c, d Colony on PDA (front and reverse). e Pycnidia forming on PDA. f Section through pycnidium. g, h Conidiogenous cells. i–k Conidia. Scale bars: e = 100 µm, f = 100 µm, g, h = 10 µm, i–k = 2 µm.

Didymosphaeriaceae Munk, Dansk botanisk Arkiv 15(2), 128 (1953)

Index Fungorum number: IF 80702; Facesoffungi number: FoF 00200

Neokalmusia Ariyaw. & K.D. Hyde, in Ariyawansa et al., Fungal Diversity 68, 92 (2014)

Index Fungorum number: IF 550700; Facesoffungi number: FoF 00050

Species of *Neokalmusia* are frequently occur as ascomycetes, with teleomorphs commonly observed in this genus. *Neokalmusia* was established by Ariyawansa et al. (2014) with *N. brevispora* as a type species. Species of *Neokalmusia* reported include sexual morphs, which are widely distributed in different temperature zones worldwide, with records from China, Italy, Japan, and Thailand (Ariyawansa et al. 2014, Tanaka et al. 2015, Wanasinghe & Mortimer 2022). An updated phylogeny for *Neokalmusia* and closely related taxa is shown in Fig. 12.

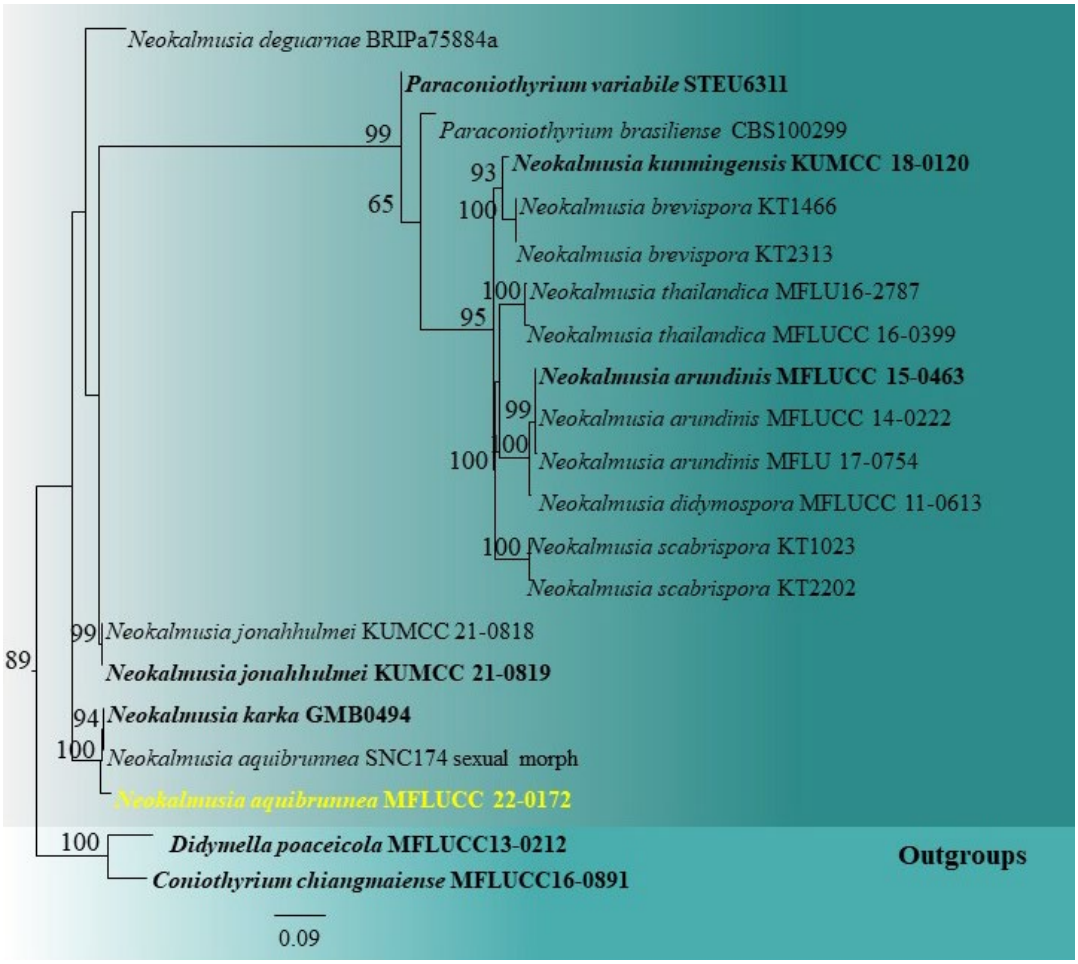

Fig. 12 – Maximum likelihood consensus tree inferred from the combined ITS and LSU multiple sequence alignments. Bootstrap support values for maximum likelihood (ML, first value) of ≥ 80% and Bayesian posterior probabilities of ≥ 0.95 are indicated above the nodes. The scale bar indicates expected changes per site. The tree is rooted to *Coniothyrium chiangmaiense* (MFLUCC 16-0891) and *Didymella poaceicola* (MFLUCC 13-0212). Ex-type strains are in bold. The newly generated sequences are indicated in yellow.

Neokalmusia aquibrunnea J. Yang, Jian K. Liu & K.D. Hyde, in Yang et al., Fungal Diversity 119, 37 (2023)

Index Fungorum number: IF 559449; Facesoffungi number: FoF 12782 Fig. 13

Saprobic on dead stems of *Rhododendron* sp. Sexual morph: *Ascomata* 200–300 µm high ($\bar{x}$ = 250 µm, n = 10), with 350–370 µm diam ($\bar{x}$ = 360 µm, n = 10), scattered or gregarious, erumpent, semi-immersed, perithecial, conical or subglobose, dark brown, ostiolate, clypeus-like at surface view, with a small, papillate, pore-like opening at the center. *Ascomatal wall* coriaceous, 27–50 µm thick, composed of host and fungal tissues, consisting of several layers of dark brown, polygonal, thick-walled cells of *textura angularis*, with uneven thickness, and thickened at the side of the base. *Hamathecium* 1.6–4.3 µm wide, cylindrical, hyaline, septate, branched pseudoparaphyses. *Asci* and *Ascospores* cannot be observed. Asexual morph: The mycelium grows on PDA media, dark brown to black. *Ostioles* absent. *Conidiophores* reduced to conidiogenous cells. *Conidiogenous cells* 3–5 × 5–9 µm ($\bar{x}$ = 4 × 7 µm, n = 30), discrete, phialidic, ampulliform, hyaline to pale brown. *Conidia* 1–3 × 8–10 µm ($\bar{x}$ = 2 × 9 µm, n = 30), mainly 2-celled, formed on phialidic and percurrently proliferating conidiogenous cells, hyaline

when liberated, becoming pale brown, cylindrical to short-cylindrical, rounded at both ends, aseptate or occasionally 1-septate, thin- and smooth-walled, with 2–5 oil guttules.

Culture characteristics – Colonies on PDA reaching 25 mm in diameter after incubating for 7 days, olivaceous-grey-brown to black, reverse olivaceous-grey to leaden-grey or olivaceous-black, irregular, dense, floccose and velvety, slightly raised with fimbriate margin, greenish-grey, and reverse dark grey-brown.

Material examined – Thailand, Chiang Mai Province, on dead stem of *Rhododendron* sp., 16 November 2020, N. Chaiwan, Intanon48 (MFLUCC 22-0172).

GenBank accession numbers – ITS: OM981247.

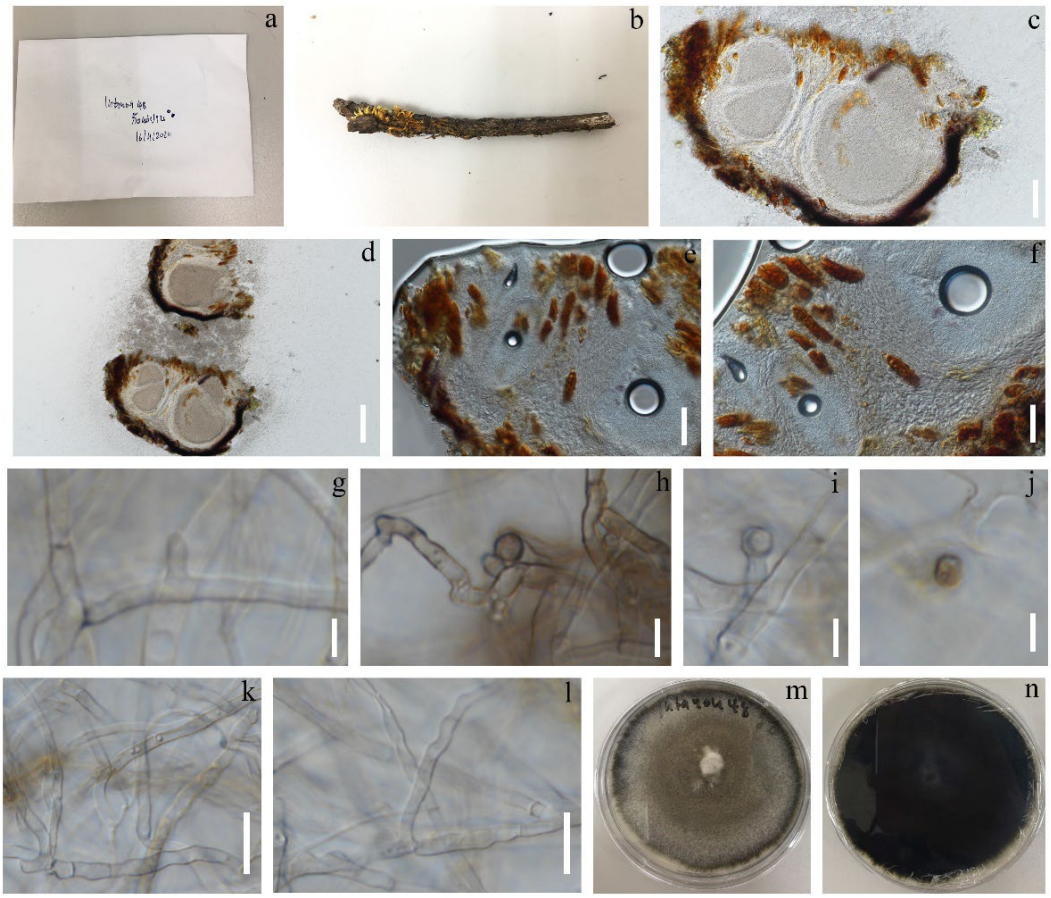

Fig. 13 – *Neokalmusia aquibrunnea* (MFLUCC 22-0172, **a new host record**). a Herbarium in the envelope. b Ascomata on a dead stem host. c–f Section of an ascoma. g Conidiogenous cell. h–j Conidia. k, l Conidiophore. m, n Culture on PDA. Scale bars: c = 50 µm, d = 200 µm, e–f = 20 µm, g–i, k–l = 10 µm, j = 5 µm.

Notes – *Neokalmusia* has been reported as saprobic on bambusicolous hosts across temperate to tropical zones. All species within this genus have been isolated from dead culms of *Bambusoideae* (*Poaceae*). Notable species include *N. scabrispora*, reported on *Phyllostachys* species in Japan (Tanaka et al. 2015), *N. arundinis* from Italy (Thambugala et al. 2017), *N. kunmingensis* and *N. jonahhulmei* from China (Hyde et al. 2020, Wanasinghe & Mortimer 2022), *N. didymospora* and *N. thailandica* from Thailand (Dai et al. 2016, Thambugala et al. 2017). To date, *Neokalmusia* species have been reported only in their sexual state, characterized by immersed, subglobose to oblong ascomata with multiple perithecia, a thin-walled clypeus-like structure, and verrucose ascospores. In this study, we report an

asexual morph of *N. aquibrunnea*, isolated from the *Rhododendron* sp. in Thailand. A BLASTn of the ITS sequence in GenBank revealed a 95.06% similarity to *N. aquibrunnea* (SNC174). Further comparison of the ITS nucleotide sequences of this new species reveals 27/798 (3.38%) nucleotide differences.

Lophiotremataceae K. Hiray. & Kaz. Tanaka, Mycoscience 52(6), 405 (2011)

Index Fungorum number: IF 561063; Facesoffungi number: FoF 00796

Lophiotrema Sacc., Michelia 1(3), 338 (1878)

Index Fungorum number: IF 2934; Facesoffungi number: FoF 08285

Lophiotrema was proposed by Saccardo (1878) and typified by *L. nucula*. This genus was initially classified in the *Lophiostomataceae* family and subsequently transferred to *Lophiotremataceae* (Hirayama & Tanaka 2011). This genus is distinguished by its immersed ascomata with a crest-like ostiolar neck, cylindrical asci, and hyaline, 1-septate ascospores with or without appendages and sheath (Tanaka & Harada 2003, Hashimoto et al. 2017). Species within this genus are predominantly saprobic on various plant species in terrestrial, freshwater, and marine habitats and are distributed worldwide (Wijayawardene et al. 2018, Hongsanan et al. 2020a, b, Boonmee et al. 2021). To date, 17 species have been described in *Lophiotrema*, of which only eight have molecular data available (Boonmee et al. 2021, Wijayawardene et al. 2022b). An updated phylogeny for *Lophiotrem* and closely related taxa is shown in Fig. 14.

Lophiotrema mucilaginosis M. Raza & L. Cai, Fungal Diversity 95, 32 (2019)

Index Fungorum number: IF 555333; Facesoffungi number: FoF 04941 Fig. 15

Saprobic on dead twigs of *Dipterocarpus gracilis* (*Dipterocarpaceae*). Sexual morph: *Ascomata* 190–240 µm high, 150–190 µm diam. ($\overline{x}$ = 221 × 174 µm, n = 5), solitary or gregarious, immersed, subglobose or obpyriform, brown to dark brown, with an ostiole. *Ostiole* 46–60 µm long, 23–30 µm diam., carbonaceous, mostly central, minute papilla, with crest-like opening, filled with hyaline periphysate. *Peridium* 8–13 µm wide, comprises fattened, angular, pseudoparenchymatous, dark brown, thick-walled cells. *Hamathecium* 1.5–2.5 µm wide, filamentous, septate, branched, cellular pseudoparaphyses. *Asci* 70–90 × 8–8.7 µm ($\overline{x}$ = 79 × 8.4 µm, n = 20), 8-spored, bitunicate, fissitunicate, cylindrical, with a short, truncate pedicel, apically rounded, with a minute ocular chamber. *Ascospores* 19–22.5 × 3.5–4.1 µm ($\overline{x}$ = 21 × 3.7 µm, n = 30), 1–2-seriate, fusiform, hyaline, straight or slightly curved, 1(–3)-septate, mostly 3-septate, constricted at the septa, narrower towards both end cells, smooth-walled, guttulate, with an entire mucilaginous sheath. Asexual morph: Undetermined.

Culture characteristics – Ascospores germinate on PDA within 24 hours at room temperature. Germ tubes are produced from the apical or the second cell of the ascospore. Colonies on PDA reaching 25 mm diameter after incubating at 20–25℃ for 2 weeks, mycelia superficial, circular, flat, fimbriate, entire edge, grey with grey-white at the centre; reverse, atrovirens, and pale yellow at the centre.

Material examined – China, Yunnan Province, Baoshan, on dead woody twigs of *Dipterocarpus gracilis* (*Dipterocarpaceae*), 12 July 2020, G.C. Ren, BS16 (HKAS 122873), living culture KUMCC 21-0505.

GenBank accession numbers – ITS: OQ771948, LSU: OQ771954, SSU: OQ771961.

Notes – Phookamsak et al. (2019) introduced *L. mucilaginosis* as a new species collected on dead wood from Yunnan Province, China. Comparatively, the features of our new collections are similar to *L. mucilaginosis* in having immersed ascomata with ostiole; carbonaceous ostiole with crest-like opening, filled with hyaline periphysate; cylindrical asci with an ocular chamber; fusiform, hyaline, 1(–3)-septate ascospores with an entire mucilaginous sheath, but our new collections had smaller asci (81 × 7.5 µm *vs.* 127.5 × 14.5µm) and ascospores (22 × 4 µm *vs.* 39.1 × 8.6 µm) (Phookamsak et al. 2019). Compared to *L. hydei*, our new collections have 1(–3)-septate ascospores with an entire mucilaginous sheath, whereas *L. hydei* has inconspicuously 0–1-septate ascospores without a sheath.

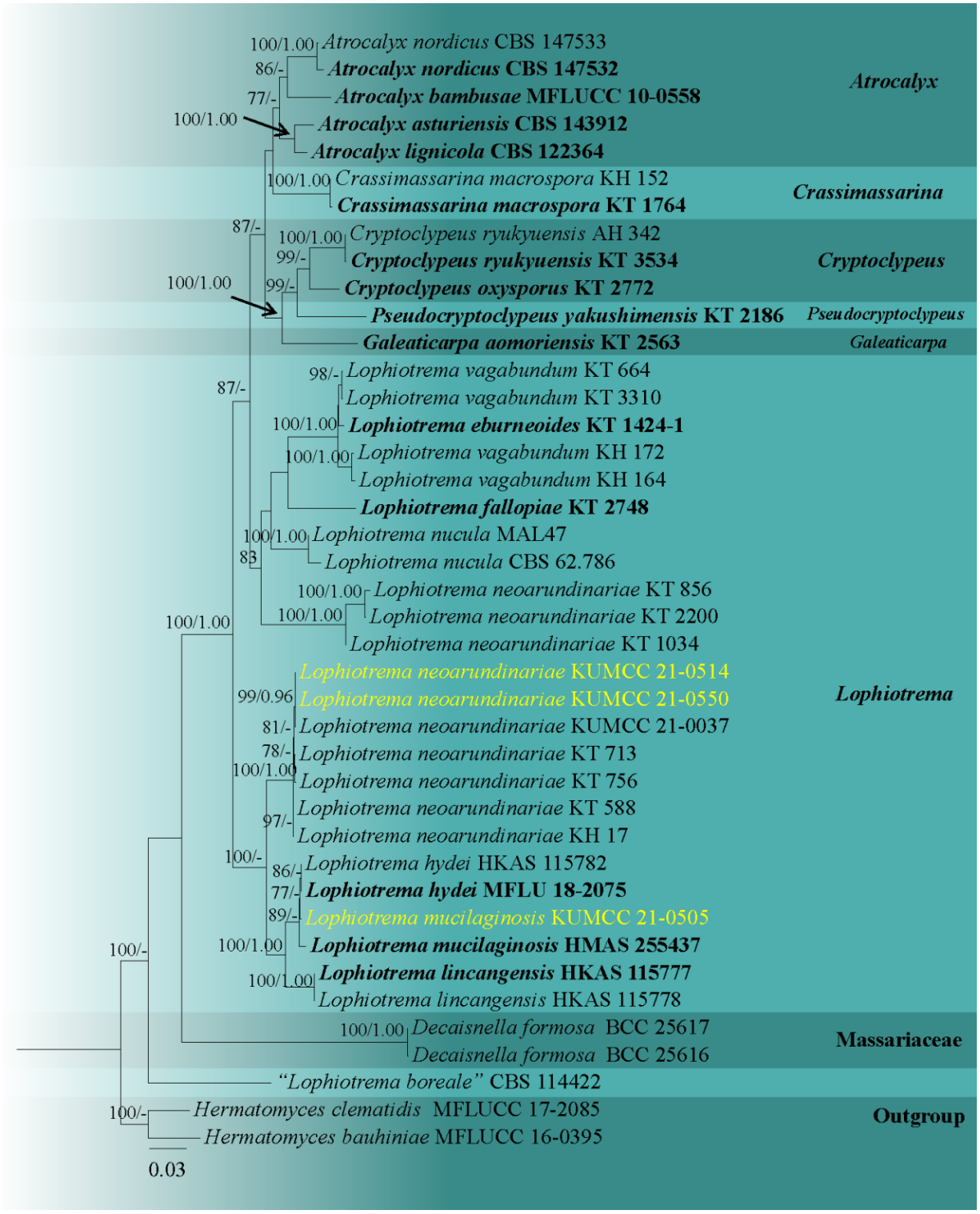

Fig. 14 – Phylogram generated from maximum likelihood analysis based on combined SSU, LSU, ITS, *tef1-α*, and *rpb2* sequence data for *Lophiotremataceae*. Forty-one strains are included in the combined analyses, comprising 4,211 characters (929 characters for SSU, 871 characters for LSU, 510 characters for ITS, 894 characters for *tef1-α*, and 1007 characters for *rpb2*) after alignment. The tree topology of the maximum likelihood analysis is similar to that of the Bayesian analysis. The best RAxML tree with a final likelihood value of -19792.962718 is presented. Estimated base frequencies were as follows:

A = 0.245344, C = 0.262922, G = 0.269151, T = 0.222583; substitution rates AC = 1.704324, AG = 4.372720, AT = 1.430475, CG = 1.274933, CT = 10.117734, GT = 1.000000; gamma distribution shape parameter α = 0.158029. Bootstrap support values for ML and MP greater than 65% and Bayesian posterior probabilities greater than 0.95 are given near the nodes, respectively. The tree is rooted with *Hermatomyces bauhiniae* (MFLUCC 16-0395) and *H. clematidis* (MFLUCC 17-2085). Ex-type strains are in bold. The newly generated sequences are indicated in yellow.

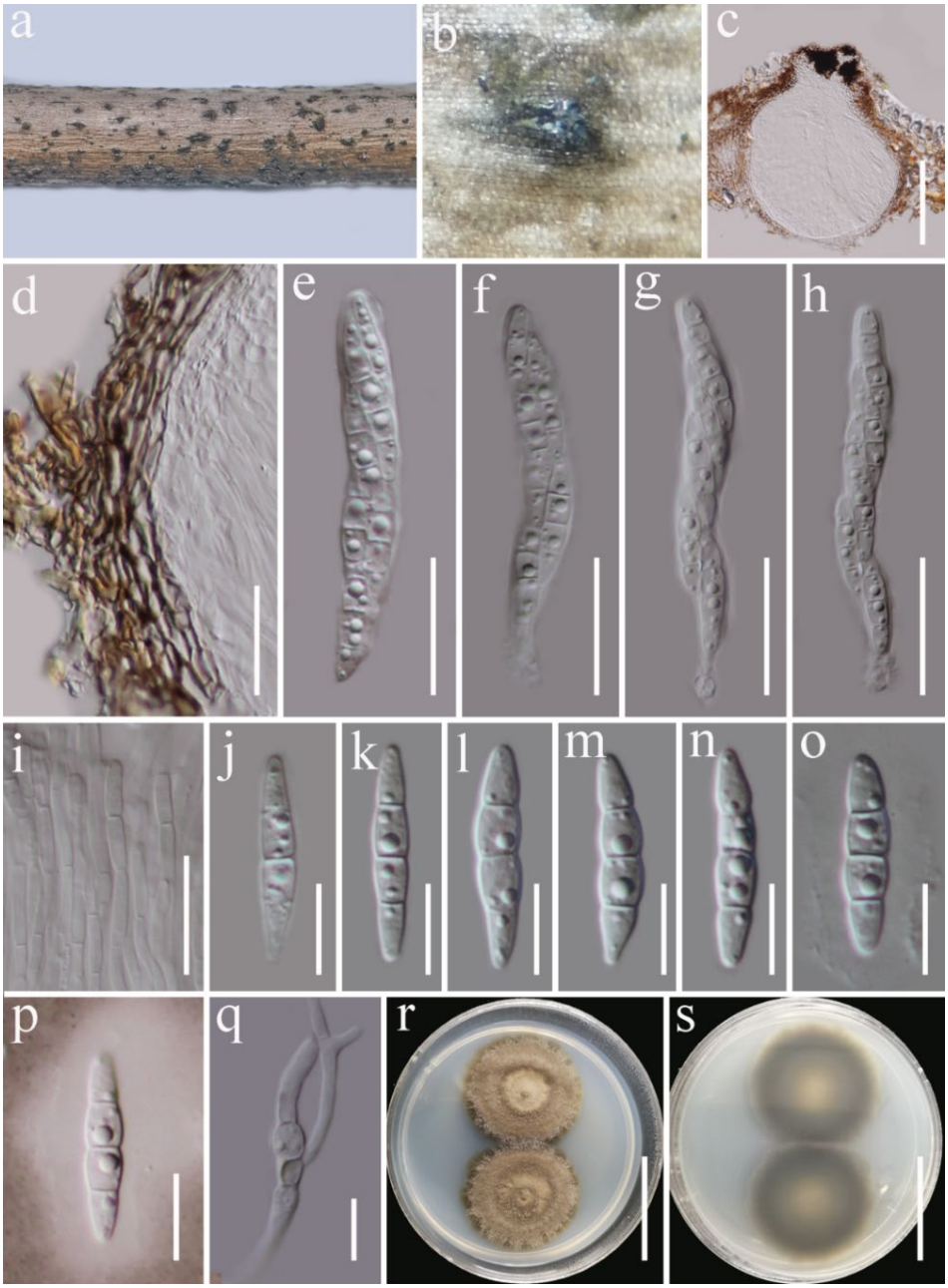

Fig. 15 – *Lophiotrema mucilaginosis* (KUMCC 21-0505, **a new host record**). a, b Appearance of ascomata on host substrate. c Section of ascoma. d Peridium. e–h Asci. i Hamathecium. j–o Ascospores. p Ascospore stained in Indian ink to show the mucilaginous sheath. q Germinated ascospore. r, s Culture characters on PDA (r = upper view, s = bottom view). Scale bars: c = 100 μm, d–i = 20 μm, j–q = 10 μm, r–s = 20 mm.

In our phylogenetic study, the multi-gene phylogenetic analysis based on the combined LSU, ITS, *tef1-α*, and *rpb2* sequences showed that our new strain clustered with *L. hydei* and *L. mucilaginosis* with 89 % ML bootstrap support (Fig. 14). A comparison of LSU and ITS sequence data reveals no significant difference between our new isolates and *L. mucilaginosis*. Therefore, we identify our collection as a new host record of *L. mucilaginosis* on *Dipterocarpus gracilis* from Yunnan Province, China.

Lophiotrema neoarundinariae Y. Zhang ter, Kaz. Tanaka & K.D. Hyde, Zhang et al., Studies in Mycology 64, 97 (2009)

Index Fungorum number: IF 836880; Facesofungi number: FoF 09949 Fig. 16

Saprobic on dead wood of *Dipterocarpus gracilis* (*Dipterocarpaceae*). Sexual morph: *Ascomata* 150–170 μm high, 140–160 μm diam. ($\overline{x}$ = 166 × 150 μm, n = 5), black, scattered, solitary, semi-immersed through host surface, conical, flattened base, uni-loculate, coriaceous, ostioles, papillate. *Ostioles* 40–54 × 22–30 μm ($\overline{x}$ = 46 × 25 μm, n = 5), apically with crest-like papilla, filled with periphyses, carbonaceous, with beak-like opening. *Peridium* 8–17 μm wide, composed of brown, coriaceous, pseudoparenchymatous cells of *textura angularis*, indistinguishable from the host tissues, inner layer comprising hyaline cells of *textura angularis*. *Hamathecium* 1–2 μm wide, hyaline, branched, filamentous, transversely septate, anastomosed pseudoparaphyses, embedded in a gelatinous matrix. *Asci* 70–91 × 7–8 μm ($\overline{x}$ = 81 × 7.5 μm, n = 20), 8-spored, bitunicate, fissitunicate, cylindrical to cylindric-clavate, slightly curved, with a short, truncate pedicel, apically rounded with a well-developed ocular chamber. *Ascospores* 18–23.7 × 3.6–4.4 μm ($\overline{x}$ = 22 × 4 μm, n =30), 1–2-seriate, hyaline, subfusoid to fusiform, with tapering towards rounded ends, straight-to-slightly curved, one-celled when young, 3-septate at maturation, slightly constricted at the septum, smooth-walled, with guttules in each cell. Asexual morph: Undetermined.

Culture characteristics – Ascospores germinate on PDA within 24 hr at room temperature. *Germ tubes* are produced from the apical or the second cell of the ascospore. *Colonies* on PDA, reaching 30 mm diameter after 2 weeks at 20–25°C, mycelia superficial, circular, umbonate at the centre, fimbriate, entire edge, grey-white with granular droplets of oil, black, and glistening; reverse, black, with pale yellow at the centre.

Material examined – China, Yunnan Province, Baoshan, on dead woody twigs of *Dipterocarpus gracilis* (*Dipterocarpaceae*), 12 July 2020, G.C. Ren, BS26 (HKAS 122874), living culture KUMCC 21-0514, living culture KUMCC 21-0550.

Known distribution – Japan, Hong Kong, North America.

Known host – *Arundinaria* sp., *Arundinaria tecta* (on culms), *Bambusa* sp., *Phyllostachys bambusoides*, *Pennisetum purpureum*, *Pennisetum* sp. (Farr & Rossman 2023).

GenBank accession numbers – KUMCC 21-0514: ITS: OQ771949, LSU: OQ771955, SSU: OQ771962, *tef1-α*: OQ784915; KUMCC 21-0550: ITS: OQ771950, LSU: OQ771956, SSU: OQ771963, *tef1-α*: OQ784916.

Notes – *Lophiotrema neoarundinariae* was introduced by Zhang et al. (2009). In this study, a newly collected taxon clustered with *L. neoarundinariae* (KUMCC 21-0037, KT 713, KT 756, KT 588, KH 17) with 99% ML, 1.00 BYPP statistical support (Fig. 14). The features of our new collections are similar to *L. neoarundinariae* (Boonmee et al. 2021). Based on multi-gene phylogenetic analysis and morphology, we reported a new host record on *Dipterocarpus gracilis* from Yunnan, China.

Neohendersoniaceae A. Giraldo & Crous, Mycological Progress 16(4), 343 (2017)

Index Fungorum number: IF 818515; Facesoffungi number: FoF 07373

Crassiparies M. Matsum., K. Hiray. & Kaz. Tanaka, Li et al., Fungal Diversity 78, 63 (2016)

Index Fungorum number: IF 815294; Facesoffungi number: FoF 02024

The genus *Crassiparies* was introduced by Li et al. (2016) with *C. quadrisporus* as the type species. The genus currently comprises three saprobic species: *C. octosporarum*, *C. quadrisporus*, and

C. yunnanensis (Senwanna et al. 2021, Lu et al. 2022). The sexual morph is characterized by hemisphaerical ascomata, cellular, septate pseudoparaphyses, 4-spored, fissitunicate, cylindrical to clavate, pedicellate asci, 1–2-seriate, hyaline, broadly fusiform, straight, with a sub-median septum, 1-septate ascospores (Li et al. 2016). The sexual morph of *Crassiparies* has pycnidial conidiomata with cylindrical to papillate ostiolar necks, phialidic conidiogenous cells, and cylindrical, hyaline, aseptate conidia (Tanaka et al. 2017). An updated phylogeny for the family is provided in Fig. 17.

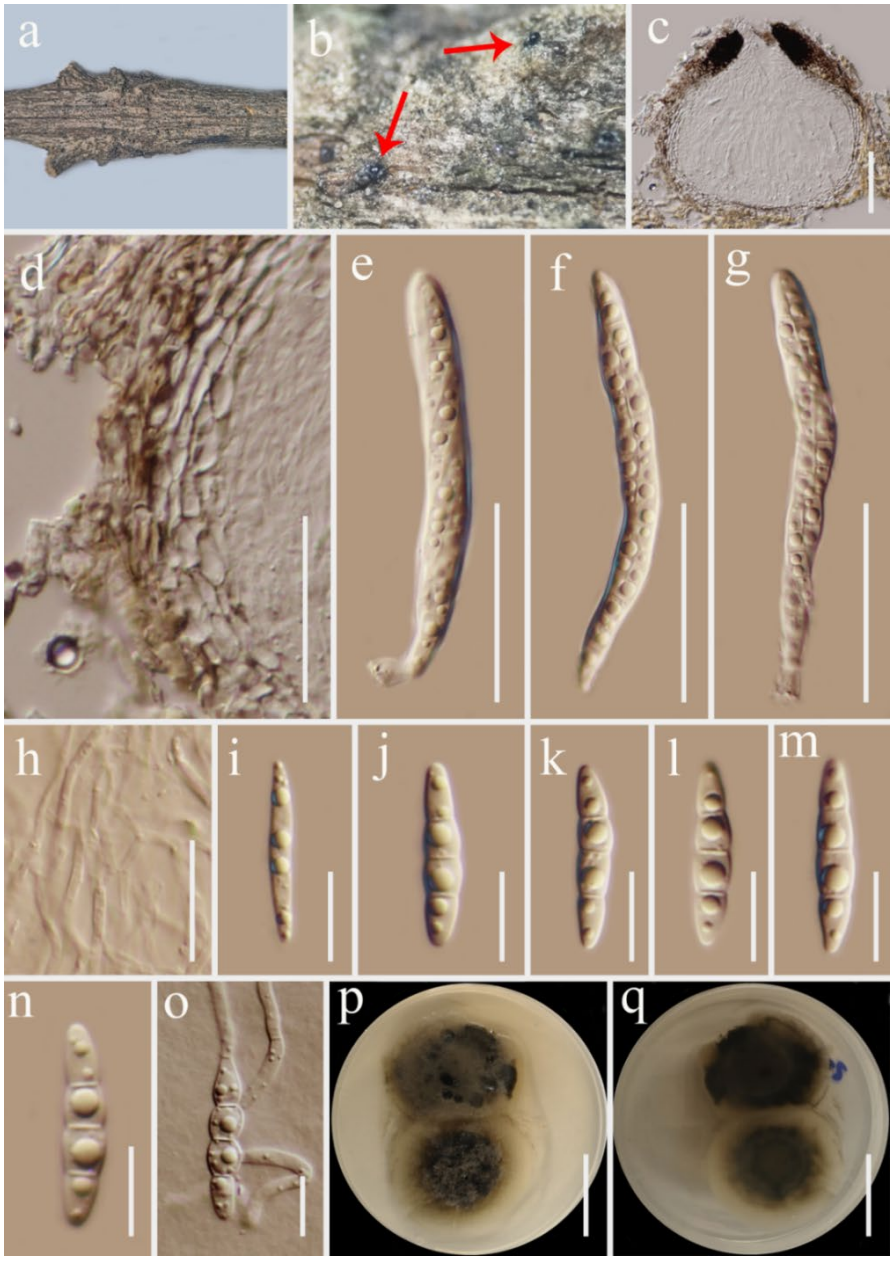

Fig. 16 – *Lophiotrema neoarundinariae* (HKAS 122874, **a new host record**). a Host. b Ascomata on the natural wood surface (arrows). c Section of ascoma. d Peridium. e–g Asci. h Hamathecium. i–n Ascospores. o Germinated ascospore. p, q Culture characters on PDA (p = upper view, q = bottom view). Scale bars: c = 50 µm, d–g = 30 µm, h = 20 µm, i–o = 10 µm, p, q = 3 cm.

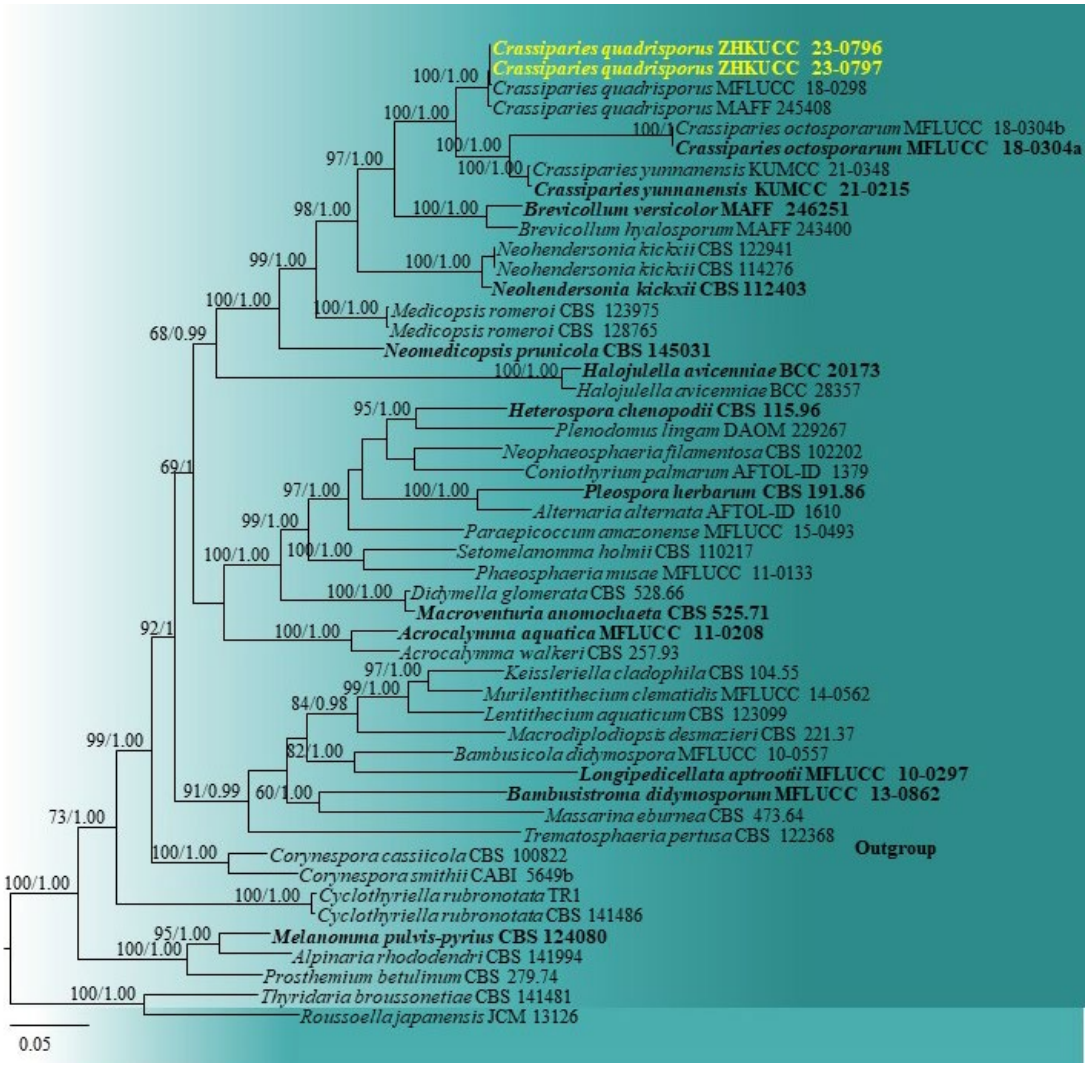

Fig. 17 – Phylogram generated from maximum likelihood analysis based on the combined LSU, SSU, ITS, *rpb2,* and *tef1-α* sequence dataset. Fifty-nine strains are included in the combined analyses, comprising 4,362 characters (879 characters for LSU, 1036 characters for SSU, 544 characters for ITS, 1034 characters for *rpb2,* and 869 characters for *tef1-α*) after alignment. The tree topology of the maximum likelihood analysis is similar to that of the Bayesian analysis. The best RAxML tree with a final likelihood value of -37750.349881 is presented. Estimated base frequencies were as follows: A = 0.246232, C = 0.247486, G = 0.266586, T = 0.239696; substitution rates AC = 1.213871, AG = 3.035704, AT = 1.370400, CG = 1.014097, CT = 5.265263, GT = 1.000000; gamma distribution shape parameter α = 0.206394. Bootstrap support values for ML and MP ≥ 60% and Bayesian posterior probabilities ≥ 0.90 are provided near the nodes, respectively. The tree is rooted with *Roussoella japanensis* (JCM 13126) and *Thyridaria broussonetiae* (CBS 141481). Ex-type strains are in bold. The newly generated sequences are indicated in yellow.

Crassiparies quadrisporus M. Matsum., K. Hiray. & Kaz. Tanaka, Li et al., Fungal Diversity 78, 63 (2016)

Index Fungorum number: IF 815295; Facesoffungi number: FoF 02025 Fig. 18

Saprobic on a twig of *Hevea brasiliensis*. Sexual morph: *Ascomata* 147–362 µm high, 200–318 µm diam ($\overline{x}$ = 273 × 241 µm, n = 10), scattered, immersed, globose to subglobose, with a central ostiole. *Ostioles* 121–190 µm high, 85–142 µm diam. ($\overline{x}$ = 146 × 112 µm, n = 10), brown, papillate. *Peridium*

22.5–56 µm wide ($\bar{x}$ = 34 µm, n = 10), thick at the sides, thin at the base, outer layers dark brown to black, inner layers thin-walled, hyaline, composed of cells of *textura angularis*. *Hamathecium* 2.5–3.5 µm wide ($\bar{x}$ = 3 µm, n = 15), dense, hyaline, septate, branched, filamentous pseudoparaphyses. *Asci* 76–137.5 × 16–23 µm ($\bar{x}$ = 97 × 19 µm, n = 15), 4-spored, bitunicate, fissitunicate, cylindric-clavate or clavate, long pedicellate, apically rounded. *Ascospores* 20–30 × 10–13 µm ($\bar{x}$ = 27 × 11 µm, n = 30), overlapping, hyaline, broadly fusiform, ends rounded, thick-walled, constricted at the septa, 1-septate, 2–3-guttulate, without mucilaginous sheath. Asexual morph: Undetermined.

Culture characteristics – Ascospores germinated on PDA within 24 hours at room temperature. Colonies on PDA irregular, with undulate edges, umbonate, and rough surfaces, and brown to dark brown.

Material examined – China, Yunnan Province, Lincang, on a twig of *Hevea brasiliensis*, 28 July 2022, Rui-Fang Xu, LCR04 (ZHKU 23–0103), living culture ZHKUCC 23–0796.

GenBank accession numbers – ZHKUCC 23–0796: ITS: OR400167, LSU: OR400171, SSU: OR400174, *rpb2*: OR413448, *tef1-α*: OR413446; ZHKUCC 23–0797: ITS: OR400168, LSU: OR400172, SSU: OR400175, *rpb2*: = OR413449, *tef1-α*: = OR413447.

Known distribution – Japan (Li et al. 2016, Tanaka et al. 2017), Thailand (Senwanna et al. 2021), China (this study).

Known hosts – *Acer* sp. (Li et al. 2016), *Hevea brasiliensis* (Senwanna et al. 2021, this study), and *Machilus japonica* (Tanaka et al. 2017).

Notes – Phylogenetic analyses show that the *Crassiparies quadrisporus* strain ZHKUCC 23–0796 and ZHKUCC 23–0797 grouped within the *C. quadrisporus* clade with 100% ML and 1 BYPP bootstrap support (Fig. 17). In a BLASTn search, the closest match of the ITS, LSU, SSU, *rpb2,* and *tef1-α* sequences was with 100% similarity to *C. quadrisporus* (MAFF 245408). Morphological characteristics of our collection (ZHKU 23–0103) are consistent with the holotype described by Li et al. (2016), including immersed, globose to subglobose ascomata, papillate ostioles, *textura angularis* peridium, septate, branched, filamentous pseudoparaphyses, 4-spored, bitunicate, fissitunicate asci, fusiform, constricted at the septa, 1-septate, 2–3-guttulate, without mucilaginous sheath ascospores. Therefore, our isolate is identified as *Crassiparies quadrisporus*. This collection is significant as it represents the first record of *C. quadrisporus* in China and the first report of this species occurring on *Hevea brasiliensis*.

Neomassariaceae H.A. Ariyaw., Jaklitsch & Voglmayr, Cryptogamie, Mycologie 39(3), 367 (2018)

Index Fungorum number: IF 827113; Facesoffungi number: FoF 08315

Neomassaria Mapook, Camporesi & K.D. Hyde, in Hyde et al., Fungal Diversity 80, 74 (2016)

Index Fungorum number: IF 552273; Facesoffungi number: FoF 02437

Neomassaria (*Pleosporales*) was introduced by Hyde et al. (2016) to accommodate *N. fabacearum* and currently contains six species (Yang et al. 2023). Later, *N. fabacearum* was introduced in China as a record (Hu et al. 2022), *N. formosana*, *N. hongheensis*, and *N. khayaewere* from Taiwan, Yunnan, and Guangdong in China, respectively (Ariyawansa et al. 2018a, Yang et al. 2022, 2023), and *N. alstoniae* and *N. thailandica* were reported in Thailand (de Silva et al. 2022). All *Neomassaria* species have been reported as saprobes on dead branches (Hu et al. 2022, Yang et al. 2023). *Neomassaria* is characterised by subglobose to globose, brown to dark brown ascomata, with a central ostiole, 8-spored, bitunicate, pedicellate, oblong to cylindrical, with ocular chamber asci and ellipsoid to fusiform, 1–2 septate, hyaline, with or without guttules, with or without a gelatinous sheath ascospore, but asexual morph has not been observed (Hyde et al. 2016, Ariyawansa et al. 2018a, de Silva et al. 2022, Yang et al. 2022, 2023). An updated phylogeny for *Neomassaria* and closely related taxa is shown in Fig. 19.

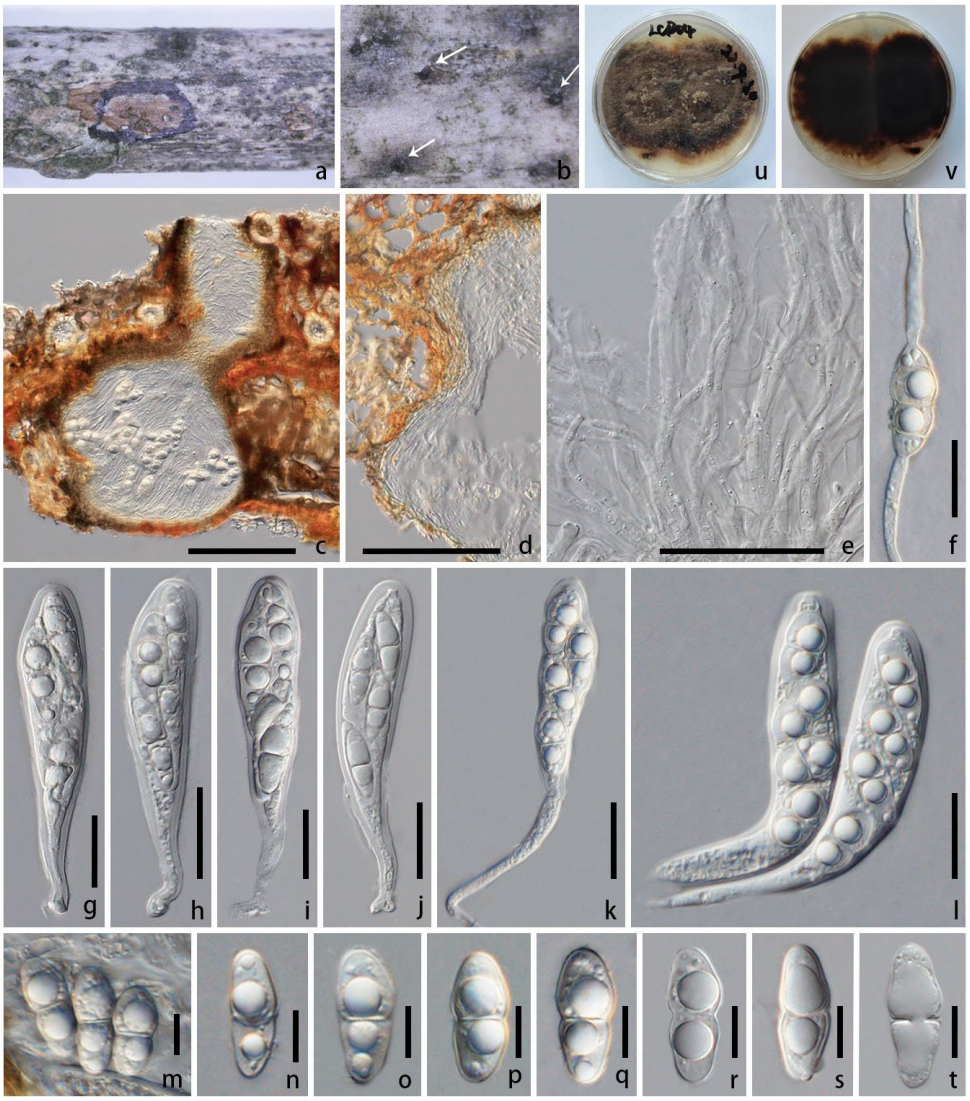

Fig. 18 – *Crassiparies quadrisporus* (ZHKU 23–0103, **a new geographical record**). a Host. b Ascomata on the host surface (the arrow indicates the immersed ascomata). c Section of an ascoma. d Peridium. e Pseudoparaphyses. f Germinated ascospore. g–l Asci. m–t Ascospores. u, v Colonies on PDA after one month. Scale bars: c, d = 100 μm, e = 50 μm, f–l = 20 μm, m–t = 10 μm.

Neomassaria yunnanensis Y. Gao, H. Gui & K.D. Hyde, sp. nov.

MycoBank: MB 849370; Faces of Fungi number: FoF 14378 Fig. 20

Etymology – The specific epithet "yunnanensis" refers to the type locality, Yunnan Province, China.

Saprobic on dead twigs. Sexual morph: *Ascomata* 190–250 × 230–300 μm ($\bar{x}$ = 230 × 260 μm, n = 10), immersed, solitary or gregarious, globose to subglobose, uniloculate, dark brown to black, papillate, with ostiole at the center. *Peridium* 10–20 μm wide ($\bar{x}$ = 15 μm, n = 20), comprising 2–6 layers of brown to dark brown cells of *textura angularis*. *Hamathecium* 1–2 μm wide ($\bar{x}$ = 1.6 μm, n = 25), filiform, hyaline, branched, aseptate. *Asci* (100–)108–130 × (10–)12–15(–17) μm ($\bar{x}$ = 120 × 14 μm, n = 20, SD = 11 × 1.7), eight-spores, bitunicate, fissitunicate or claviform, shortly pedicellate, apically rounded, with an ocular chamber. *Ascospores* (16–)16.5–18(–19) × (5–)5.5–7 μm ($\bar{x}$ = 17.2 × 6.3 μm, n = 25, SD = 0.66 × 0.67), hyaline, 1-septate in the middle, broadly fusiform or ellipsoid, surrounded by a mucilaginous sheath, with 2–4 large guttules. Asexual morph: Undetermined.

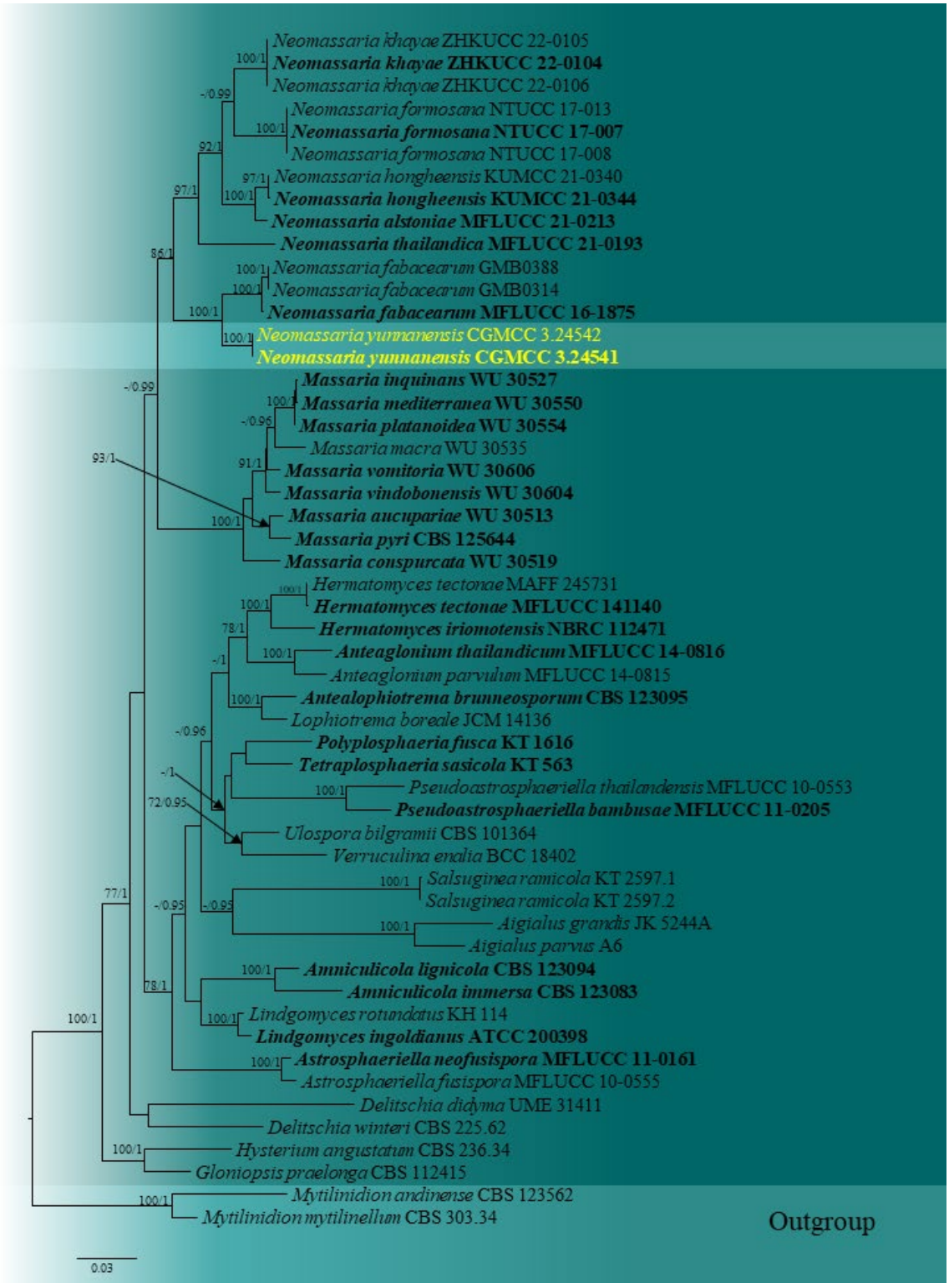

Fig. 19 – Phylogram generated from maximum likelihood analysis based on combined LSU, SSU, and *tef1-α* sequence data. Fifty-three strains were included in the combined analyses, which comprised 2,815 characters (LSU: 1–848, SSU: 849–1,898, *tef1-α*: 1,899–2,815) after alignment. The tree is rooted in *Mytilinidion andinense* (CBS 123562) and *M. mytilinellum* (CBS 303.34). Bootstrap support values for maximum likelihood (ML) ≥ 75% and Bayesian Probability (BYPP) ≥ 0.95 are indicated above the branches. Ex-type strains are in bold, and newly generated sequences are in yellow.

Culture characteristics – Ascospores germinated on PDA within 20 hours, and a germ tube was initially produced from the two ends of the ascospores. Colonies on PDA reach 12 mm in 4 weeks at room temperature (25–27°C), appearing circular and slightly raised. *Cultures* white at the centre, brownish radiating outward appearance (upper view), and yellowish (bottom view).

Material examined – China, Yunnan Province, Kunming City, Kunming Botanical Garden (25°8'19"N, 102°44'25"E), on decaying twigs, 21 March 2021, GY24A (HKAS 126562, holotype), ex-type living culture, CGMCC 3.24541. *ibid*., GY24B (HKAS 128755, paratype), ex-paratype culture, CGMCC 3.24542.

GenBank accession numbers – CGMCC 3.24541: LSU: OR198832, SSU: OR198848, *tef1-α*: OR260540; CGMCC 3.24542: LSU: OR198833, SSU: OR198849, *tef1-α*: OR260541.

Notes – *Neomassaria yunnanensis* is introduced as a new species based on its distinct morphology and phylogenetic analysis of combined LSU, SSU, and *tef1-α* datasets. *Neomassaria yunnanensis* is closely related to *N. fabacearum* with 100% ML and 1.00 BYPP bootstrap support (Fig. 19). The new species differs from *N. fabacearum* in its larger ascomata (230 × 260 µm *vs.* 190 × 130 µm), longer asci (100–130 × 10–17 µm *vs.* 65–85 × 10–15 µm) (Hyde et al. 2016). A pairwise nucleotide comparison showed that *N. yunnanensis* differs from *N. fabacearum* (MFLUCC 16-1875) in 17/839 bp of LSU (2%, without gaps), 54/859 bp of *tef1-α* (6.29%, without gaps). Therefore, based on both morphological and phylogenetic evidence, *N. yunnanensis* is described as a new species.

Occultibambusaceae D.Q. Dai & K.D. Hyde, in Dai et al., Fungal Diversity 82, 25 (2016)

Index Fungorum number: IF 552012; Facesoffungi number: FoF 01973

Neoocculitibambusa Doilom & K.D. Hyde, in Doilom et al., Fungal Diversity 82, 126 (2016)

Index Fungorum number: IF 551981; Facesoffungi number: FoF 01852

Neooccultibambusa was introduced by Doilom et al. (2017) and typified with *N. chiangraiensis*. This genus occurs as a saprobe on several plants in China, Italy, and Thailand (Jayasiri et al. 2016, Doilom et al. 2017, Tibpromma et al. 2018, Yu et al. 2021). The sexual morphs of *Neooccultibambusa* species are characterized by solitary to gregarious, scattered, immersed to semi-immersed, uniloculate, globose to sub-globose ascomata, 8-spored, bitunicate, cylindrical to subcylindrical asci, overlapping biseriate, hyaline to pale brown, fusoid ascospores with 1–3 transverse septa (Doilom et al. 2017). The asexual morphs have macronematous, septate, straight or slightly flexuous, dark brown conidiophores, holoblastic, integrated, terminal, brown, cylindrical conidiogenous cells, and acrogenous, solitary, obclavate, pale to dark brown conidia (Jayasiri et al. 2016, Hyde et al. 2018). Seven species are accepted in *Neooccultibambusa* with descriptions and molecular data (Lu et al. 2025, Index Fungorum 2025). An updated phylogeny for *Neooccultibambusa* and closely related taxa is shown in Fig. 21.

Neooccultibambusa fusispora Y.R. Sun, Yong Wang bis & K.D. Hyde, sp. nov.

Index Fungorum number: IF 903328; Facesoffungi number: FoF 14842 Fig. 22

Etymology – The epithet "*fusispora*" refers to the fusiform ascospores.

Saprobic on dead twigs. Sexual morph: *Ascomata* in vertical section 190–240 µm high, 250–290 µm wide, solitary or scattered, globose, uniloculate, immersed, visible as black dots on the host surface. *Ostiole* central, periphysate. *Peridium* 17–25 µm wide, comprising two layers of pale brown to brown cells of *textura angularis*. *Hamathecium* 1.5–3 µm wide, cellular pseudoparaphyses, anastomosing above asci, embedded in a gelatinous matrix. *Asci* 80–149 × 16–22 µm ($\overline{x}$ = 106 × 18 µm, n = 15), 8-spored, cylindrical to clavate, bitunicate, with a short furcate pedicel, apically rounded, with an ocular chamber. *Ascospores* 31–37 × 5–7.5 µm (x = 34 × 6.5 µm, n = 25), overlapping biseriate, hyaline, fusiform, 1–3-septate, constricted at the center septum, guttulate when young, smooth, surrounded by a gelatinous sheath. Asexual morph: Undetermined.

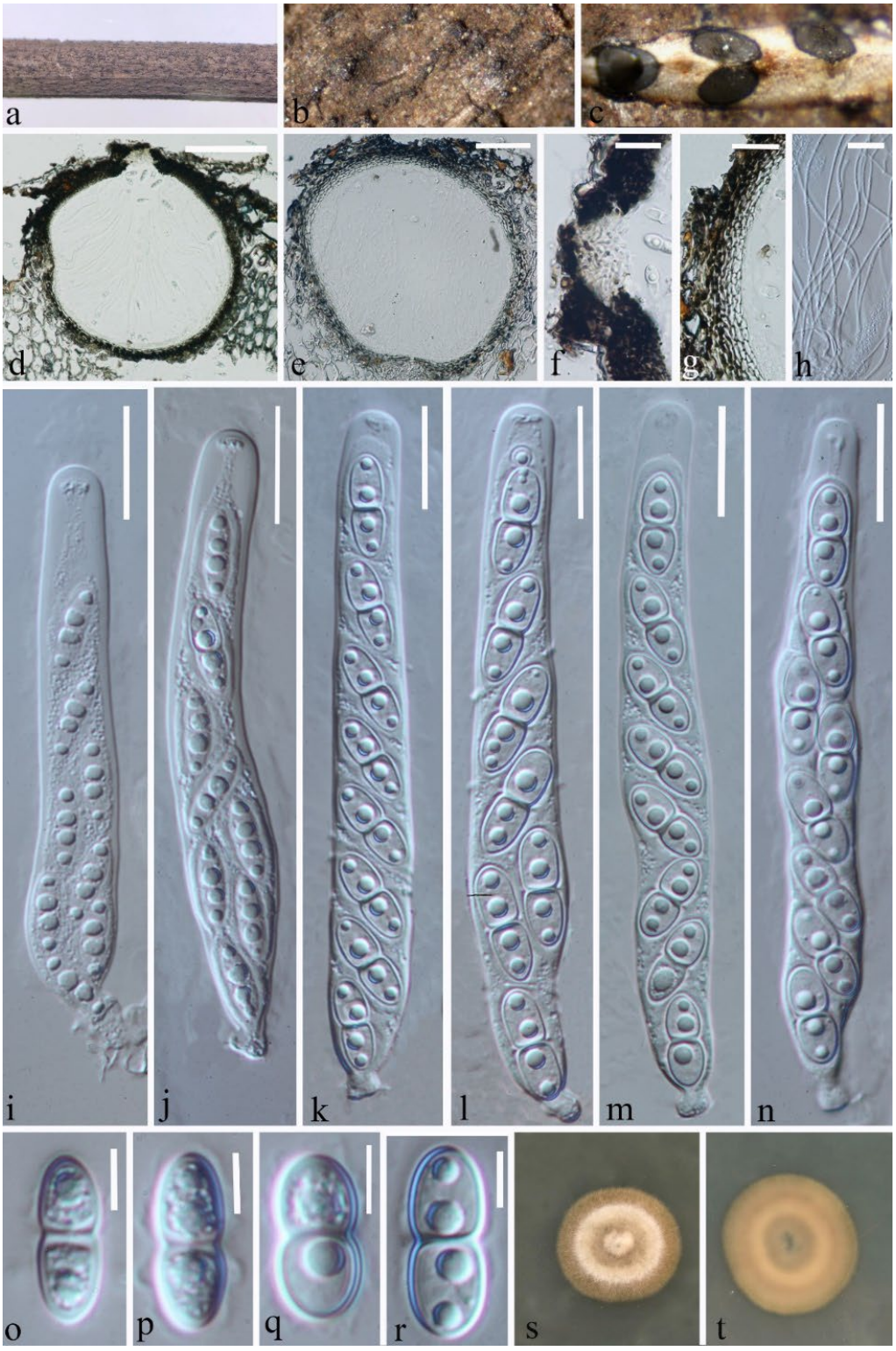

Fig. 20 – ***Neomassaria yunnanensis*** (HKAS 126562, **holotype**). a–c Appearance of ascomata on the substrate. d, e Vertical sections through ascomata. f Ostiole. g Section through the peridium. h Pseudoparaphyses. i–n Asci. o–r Ascospores. s Frontal view of a colony on PDA. t Reverse view of a colony on PDA. Scale bars: d = 100 µm, e = 50 µm, f–g = 20 µm. h = 15 µm, i–n = 20 µm,o–r = 5 µm.

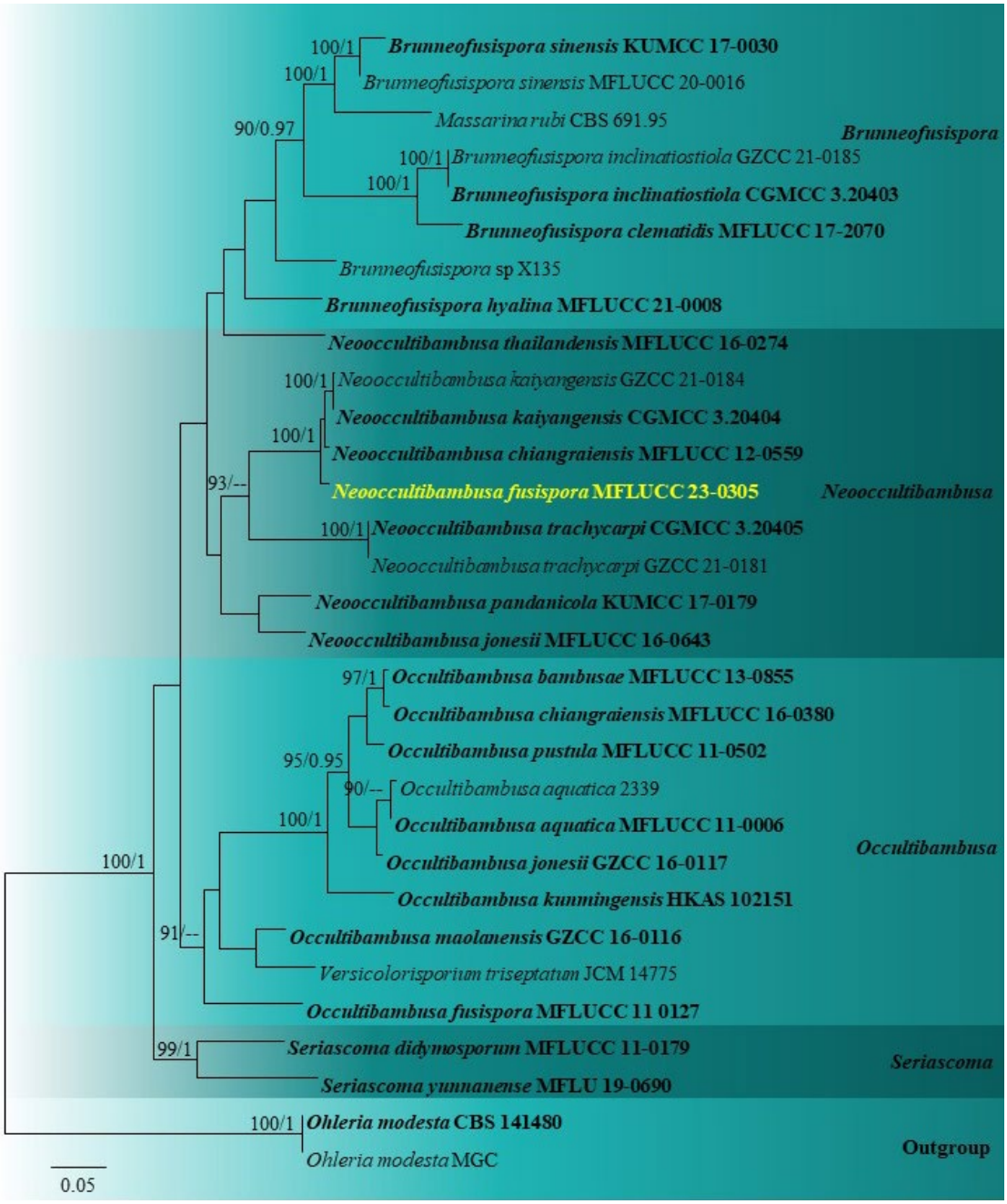

Fig. 21 – Phylogram generated from maximum likelihood analysis based on combined LSU, SSU, ITS, *rpb2,* and *tef1-α* sequence data for *Neoocculitibambusa*. Thirty-one strains are included in the combined analyses, comprising 4,206 characters (803 characters for LSU, 969 characters for SSU, 654 characters for ITS, 887 characters for *rpb2*, and 893 characters for *tef1-α*) after alignment. The tree topology of the maximum likelihood analysis is similar to that of Bayesian analysis. The best RAxML tree with a final likelihood value of -31479.214308 is presented. Estimated base frequencies were as follows: A = 0.087127, C = 0.033474, G = 0.088612, T = 0.058542; substitution rates AC = 0.312229, AG = 2.081526, AT = 3.217693, CG = 0.095403, CT = 0.138768, GT = 1.000000; gamma distribution shape parameter α = 0.161445. Bootstrap support values for ML and MP greater than 75% and Bayesian posterior probabilities greater than 0.95 are given near nodes, respectively. The tree is rooted with *Ohleria modesta* (CBS 141480) and *Ohleria modesta* (MGC). Ex-type strains are in bold. The newly generated sequences are indicated in yellow.

Culture characteristics – Ascospores germinated on PDA within 12 h at 25 °C. Germ tube produced from one end of the ascospore. Colonies on PDA reached 2.5 cm in diameter. after four weeks of incubation, the mycelium pale brown to brown, flossy, circular, with the entire edge, surface rough, olivaceous to brown from above and dark from below.

Material examined – Thailand, Chiang Rai Province, Mae Fah Luang University, Garden of Medicinal Plants, on dead twigs, 23 October 2020, Y.R. Sun, B59 (MFLU 24-0305, holotype), living culture MFLUCC 23–0206, ex-type.

GenBank submissions – ITS: OR470693, LSU: OR470694, SSU: OR470695, *tef1-α*: OR474094.

Notes – The multi-loci phylogenetic analyses of the combined LSU, SSU, ITS, *rpb2,* and *tef1-α* sequences confirmed that our strain belongs to *Neooccultibambusa*, forming a sister clade to *N. chiangraiensis* and *N. kaiyangensis* with maximum bootstrap support (100% ML/1.00 BYPP). Morphologically, *Neooccultibambusa fusispora* differs from *N. chiangraiensis* by its smaller ascomata (250–290 × 190–240 µm *vs.* 345–355 × 245–295 µm) and thinner ascospores (31–37 × 5–7.5 µm *vs.* 36–37 × 8–13 µm) (Doilom et al. 2017). Additionally, *N. fusispora* is also distinguished from *N. kaiyangensis* by its larger asci (80–149 × 16–22 µm *vs.* 70–108 × 7.5–11 µm) and larger ascospores (31–37 × 5–7.5 µm *vs.* 16–23.5 × 3–5.5 µm) (Yu et al. 2021). Thus, based on phylogenetic and morphological evidence, *Neooccultibambusa fusispora* is introduced in this study.

Phaeosphaeriaceae M.E. Barr, Mycologia 71(5), 948 (1979)

Index Fungorum number: IF 81637; Facesoffungi number: FoF 00232

Leptospora Rabenh., Hedwigia 1(18), 116 (1857)

Index Fungorum number: IF 2803; Facesoffungi number: FoF 08334

Rabenhorst (1857) established *Leptospora* to accommodate *Leptospora rubella* as the type species. The genus is characterized by its large, flask-shaped ascomata, cylindrical to cylindrical-clavate asci with short furcate pedicels, and filiform, multi-septate ascospores that taper towards the ends (Hyde et al. 2016, Zhang et al. 2019, Tennakoon et al. 2021). Though more than 42 epithets are listed in Index Fungorum (2025), sequence data are currently available for *L. chromolaenae*, *L. clematidis*, *L. galii*, *L. hydei*, *L. macarangae*, *L. phraeana*, *L. rubella*, and *L. thailandica* in GenBank. The phylogenetic tree (Fig. 23) shows the species arrangement within the genus.

Leptospora macarangae Tennakoon, C.H. Kuo & K.D. Hyde, Tennakoon et al., Fungal Diversity 108, 41 (2021)

Index Fungorum number: IF 555317; Facesoffungi number: FoF 09323 Fig. 24

Saprobic on dead stems of *Vicia* sp., forming conspicuous, rounded, black ascomata. Sexual morph: *Ascomata* 100–210 µm high, 105–166 µm diam., ($\overline{x}$ = 175 × 146 µm, n = 30), immersed to semi-immersed, solitary or aggregated, globose to subglobose, glabrous, coriaceous, with ostioles. *Ostiole* central, papillate, cylindrical, dark brown to light brown. *Peridium* up to 10–23 µm wide, composed of 5–7 layers of *textura angularis*, brown to dark brown. *Hamathecium* 2–4 µm wide, comprises numerous, branched, cellular, hyaline pseudoparaphyses. *Asci* 60–78 × 5–8 µm ($\overline{x}$ = 65 × 7 µm, n = 20), 8-spored, bitunicate, cylindrical to cylindrical-clavate, with short pedicel, ocular chamber visible when immature. *Ascospores* 60–75 × 2–4 µm ($\overline{x}$ = 65 × 3 µm, n = 30), arranged spirally in the ascus, initially hyaline and becoming pale brown at maturity, filiform, tapering towards the ends, straight or curved, ends narrowly rounded, up to 20-septa, not constricted at the septum, with two polar sheaths. Asexual morph: Undetermined.

Material examined – China, Guizhou Province, Maolan Town, on dead stems of *Vicia* sp., 14 April 2019, S.N. Zhang, YW21 (GZAAS 23-0647), living culture GZCC 23-0642.

GenBank accession numbers – ITS: OR229714, LSU: OR229713, *tef1-α*: OR233795.

Known distribution – China (Tennakoon et al. 2021).

Known hosts – *Macaranga tanarius* (Tennakoon et al. 2021).

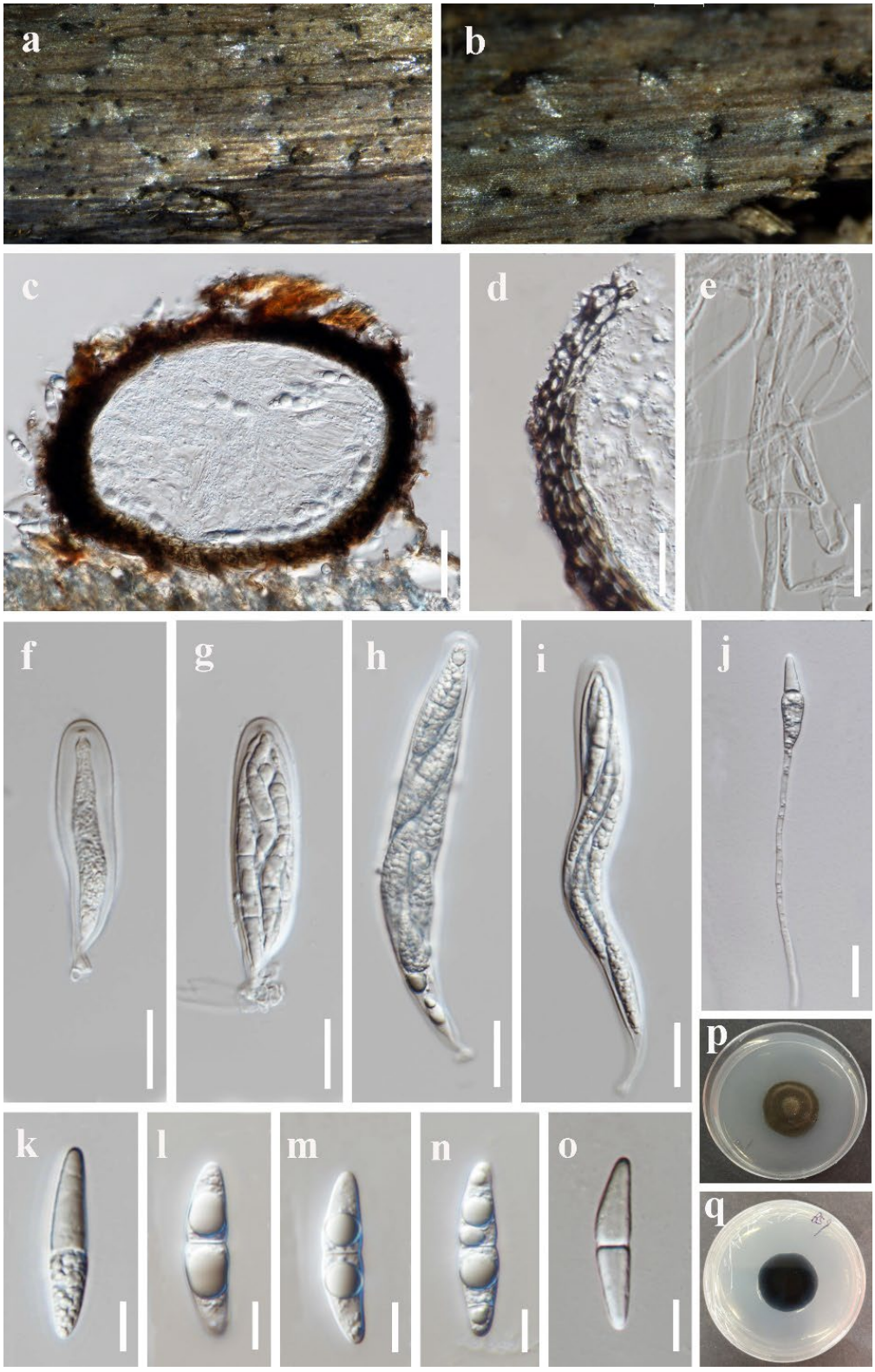

Fig. 22 – ***Neooccultibambusa fusispora*** (MFLU 24-0305, **holotype**). a, b Ascomata on host surface. c Section through ascomata. d Peridium. e Pseudoparaphyses. f–i Asci. j Germinated ascospore. k–o Ascospores. p, q Colonies on PDA (upper view and bottom view). Scale bars: c = 50 µm, d–j = 20 µm, k–o = 10 µm.

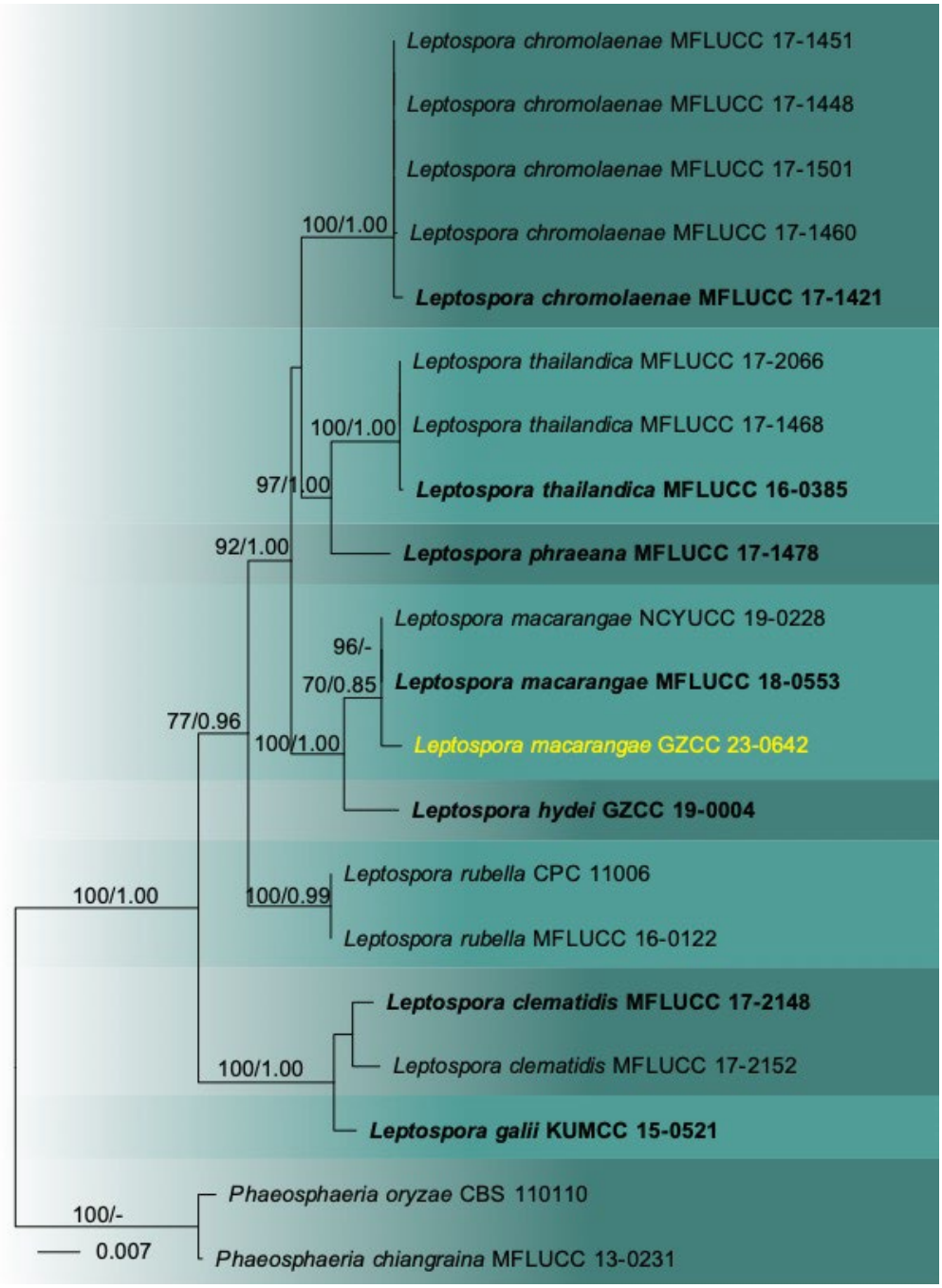

Fig. 23 – Phylogram generated from maximum likelihood analysis based on combined ITS, LSU, and *tef1-α* sequence data. Twenty strains were included in the combined analyses, comprising 2,213 characters (527 for ITS, 818 for *LSU,* and 868 for *tef1-α*) after alignment. The tree topology of the maximum likelihood analysis is similar to that of the Bayesian analysis, and the best RAxML tree, with a final likelihood value of -5086.970709, is presented. Estimated base frequencies were as follows: A = 0.240905, C = 0.247321, G = 0.264937, T = 0.246837; substitution rates AC = 0.745761, AG = 2.939249, AT = 3.980355, CG = 0.386828, CT = 10.863618, GT = 1.000000. The evolutionary model GTR+G was applied to all the gene regions. Bootstrap support values for ML greater than 70% and Bayesian posterior probabilities greater than 0.75 are given near nodes, respectively. The tree is rooted with *Phaeosphaeria chiangraina* (MFLUCC 13-0231) and *P. oryzae* (CBS 110110). Ex-type strains are in bold. The newly generated sequences are indicated in yellow.

Fig. 24 – *Leptospora macarangae* (GZAAS 23-0647, **a new host record**). a, b Ascomata on the host surface. c Vertical section of ascoma. d Vertical section of peridium. e Pseudoparaphyses. f Geminating ascospore. g–i Asci with ascospores. j, k Ascospores. l Colony on PDA (upper view). m Colony on PDA (bottom view). Scale bars: a = 100 μm, b, c = 50 μm, d = 20 μm, e = 10 μm, f–k = 20 μm.

Notes – *Leptospora macarangae* was introduced by Tennakoon et al. (2021) and originally collected from a dead leaf petiole of *Macaranga tanarius* in China (Taiwan Province). The morphology of our collection (GZAAS 23-0647) shares similarities with *L. macarangae* (MFLU 18-0075) in having asci with the same size range (60–78 × 5–8 μm *vs.* 65–78 × 8–9 μm) and filiform, hyaline to pale brown, septate ascospores with two polar sheaths, which are not constricted at the septum (60–75 × 2–4 μm *vs.* 3–75 × 3–3.8 μm) (Tennakoon et al. 2021). Phylogenetic analysis indicates our strain (GZCC 23-0642) clustered together with *L. macarangae* (MFLUCC 18-0553 and NCYUCC 19-0228), with 70% ML, 0.85 BYPP statistical support (Fig. 23). Based on morphological and phylogenetic evidence, we introduce our collection as a new host record of *L. macarangae* from *Vicia* sp. in China.

Pleosporaceae Nitschke, Verh. Naturhistorischen Vereines der Preußischen Rheinlande 26, 74 (1869)

Index Fungorum number: IF 81188; Facesoffungi number: FoF 00500

Parastagonospora Quaedvl., Verkley & Crous, Study in Mycology 75, 362 (2013)

Index Fungorum number: IF 804435; Facesoffungi number: FoF 00260

Parastagonospora was introduced by Quaedvlieg et al. (2013) to accommodate several species previously accommodated in *Leptosphaeria*, *Phaeosphaeria*, *Septoria,* and *Stagonospora*. The sexual morph of this genus is characterized by having immersed ascomata with slightly papillate ostioles, bitunicate, shortly stipitate asci, fusoid, subhyaline to pale brown, septate ascospores, and a 179 coelomycetous asexual morph with hyaline, cylindrical, granular to multi- guttulate, transversely euseptate conidia (Quaedvlieg et al. 2013, Li et al. 2015, Thambugala et al. 2017). *Parastagonospora* species are widespread, occurring mostly on wheat, grasses such as *Dactylis* sp. and *Poa* sp., and other cereal crops (Quaedvlieg et al. 2013, Li et al. 2015, Ghaderi et al. 2017). Apart from *Parastagonospora*, the genera *Neosetophoma, Phaeosphaeria, Phaeosphaeriopsis*, *Setophoma*, *Wojnowicia*, and *Xenoseptoria* in *Phaeosphaeriaceae* have been associated with leaf spots on various hosts (Carson 2005, Quaedvlieg et al. 2013, Phookamsak et al. 2014). An updated phylogeny for *Parastagonospora* and closely related taxa is shown in Fig. 25.

Parastagonospora macrouniseptata Goonas., Camporesi & McKenzie, Goonasekara et al., Asian Journal of Mycology 2(1), 176 (2019)

Index Fungorum number: IF 556607; Facesoffungi number: FoF 06261 Fig. 26

Saprobic on a dead stem of *Zea mays* (Gramineae) appears as black dots on the host surface. Sexual morph: Undetermined. Asexual morph: *Conidiomata* 140–180 μm wide, 115–155 μm high ($\overline{x}$ = 160 × 145 μm, n = 10), dark brown to black, pycnidial, solitary to gregarious, immersed, globose, unilocular, glabrous, ostioles. *Ostiole* central, short papilla. *Conidiomatal wall* 6–14 μm wide ($\overline{x}$ = 12.9 μm, n = 10), composed of thin, dark brown, pseudoparenchymatous cells, gradually merging with hyaline cells of *textura angularis*. *Conidiophores* reduced to conidiogenous cells. *Conidiogenous cells* 3.6–4 × 2.8–3.2 (3.8 × 3 μm, n = 20), hyaline, phialidic, aseptate, smooth, arising from the inner layers of conidioma. *Conidia* 14–18 μm × 1–2.3 μm ($\overline{x}$ = 16.9 × 1.8 μm, n = 20), hyaline, cylindrical, rounded at apex, slightly truncate at base, 1-septate, slightly constricted at the septum, smooth-walled, guttulate.

Material examined – China, Yunnan Province, Lingcang City, 24°26′19″ N, 99°18′15″ E, 670 m, on a stem of *Zea mays*, 29 July 2022, N.D. Kularathnage, NDK 51 (MHZU 22-0148, a new geographical record), living culture ZHKUCC 22-0276.

GenBank accession number – ZHKUCC 22-0276: ITS: PV233905, LSU: PV234053, *tef1-α*: PV294744.

Known distribution – China (this study) and Italy (Goonasekara et al. 2019).

Known hosts – *Dactylis glomerata* (Goonasekara et al. 2019), and *Zea mays* (this study).

Notes – The multi-locus phylogeny of ITS, LSU, and *tef1-α* showed that our isolate (ZHKUCC 22-0276) clusters with *Parastagonospora macrouniseptata* (KUMCC 16-0111) with ML/BI = 99%/0.99 support (Fig. 25). A single-gene comparison of ITS, LSU, and *tef1-α* between our isolate (ZHKUCC 22-

0276) and the type strain of *P. macrouniseptata* (KUMCC 16-0111) revealed base pair differences of 8/568, 2/883, and 2/983, respectively. Morphologically, our specimen closely matches the type collection of *P. macrouniseptata* (KUMCC 16-0111) in all morphological aspects. However, no *Parastagonospora* species have been previously reported from *Zea mays*. This study represents the first record of a *Parastagonospora* species associated with this host genus. Furthermore, *P. macrouniseptata* is newly documented as the first species of this genus reported in the country.

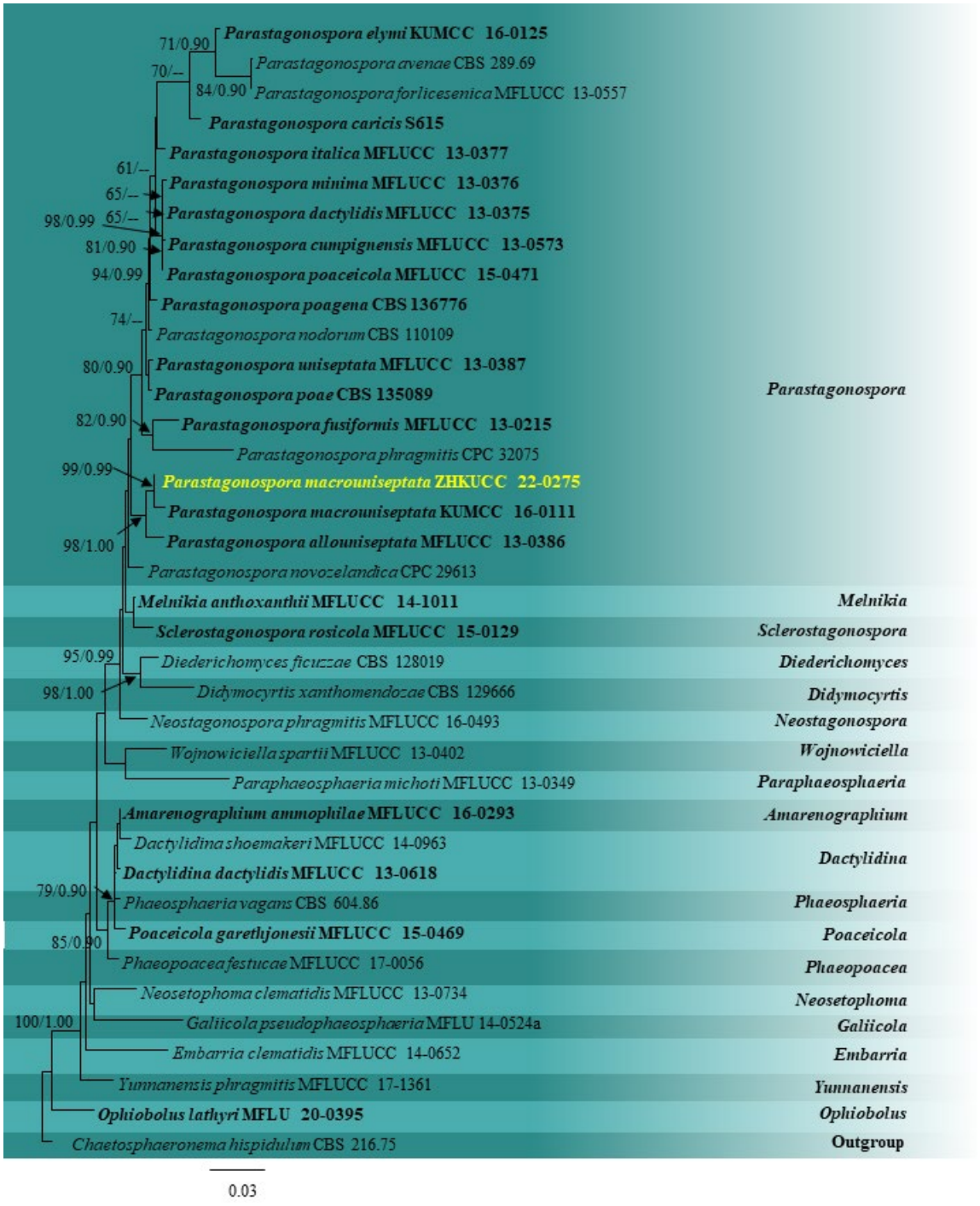

Fig. 25 – Phylogram generated from the maximum likelihood analysis based on the combined ITS, LSU, and *tef1-α* sequence data of the genus *Parastagonospora*. Thirty-eight strains are included in the

combined analyses. The tree topology of the maximum likelihood analysis is similar to that of the Bayesian analysis. The best RAxML tree with a final likelihood value of -4983.29 is presented. The evolutionary model GTR+I+G is applied to all the genes. The matrix contained 285 distinct alignment patterns, with 32.63% of the characters being undetermined or gaps. Bootstrap support values for ML greater than 60% and Bayesian posterior probabilities greater than 0.90 are given near nodes, respectively. The tree was rooted with *Chaetosphaeronema hispidulum* (CBS 216.75). Ex-type strains are in bold. The newly generated sequences are indicated in yellow.

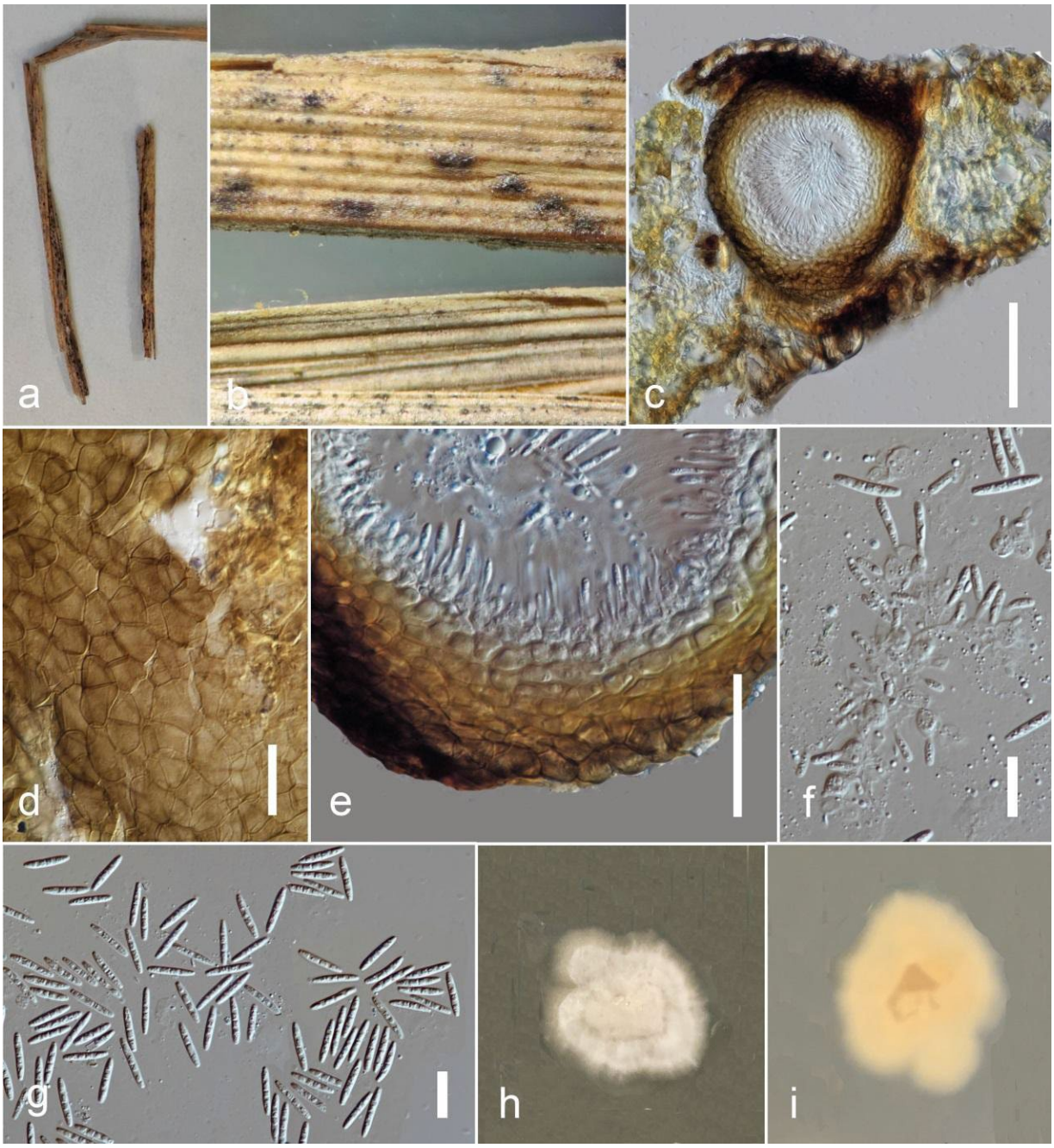

Fig. 26 – *Parastagonospora macrouniseptata* (ZHKUCC 22-0276, **a new geographical record**). a Host. b Appearance of conidiomata on host tissue. c Vertical section of conidiomata. d Cells in peridium. e, f Developing conidia attached to conidiogenous cells. g Conidia. h, i Colonies on PDA (h: upper view, i: bottom view). Scale bars: a, b = 1 mm, c = 200 µm, d, e = 50 µm, f, g = 10 µm.

Teichosporaceae M.E. Barr, Mycotaxon 82, 374 (2002)

Index Fungorum number: IF 82136; Facesoffungi number: FoF 00830

Magnibotryascoma Thambug. & K.D. Hyde, Thambugala et al., Fungal Diversity 74, 249 (2015)

Index Fungorum number: IF 551266; Facesoffungi number: FoF 00835

Magnibotryascoma was introduced by Thambugala et al. (2015) and typified with *M. uniseriata*. The sexual morph of *Magnibotryascoma* is characterized by brown, fusiform to elliptical, 1–3-septate ascospores, while its asexual morph features oval to broad-obovoid, hyaline or reddish brown, aseptate conidia (Thambugala et al. 2015, Jaklitsch et al. 2016, Phukhamsakda et al. 2020, Mortimer et al. 2021). Six *Magnibotryascoma* species are listed in Index Fungorum (accessed in March 2025), *viz. M. acaciae*, *M. kungmingense*, *M. mali*, *M. melanommoides*, *M. rubriostiolata*, and *M. uniseriata* (Hyde et al. 2017, Tennakoon et al. 2021, Crous et al. 2022b). An updated phylogeny for *Neokalmusia* and closely related taxa is shown in Fig. 27.

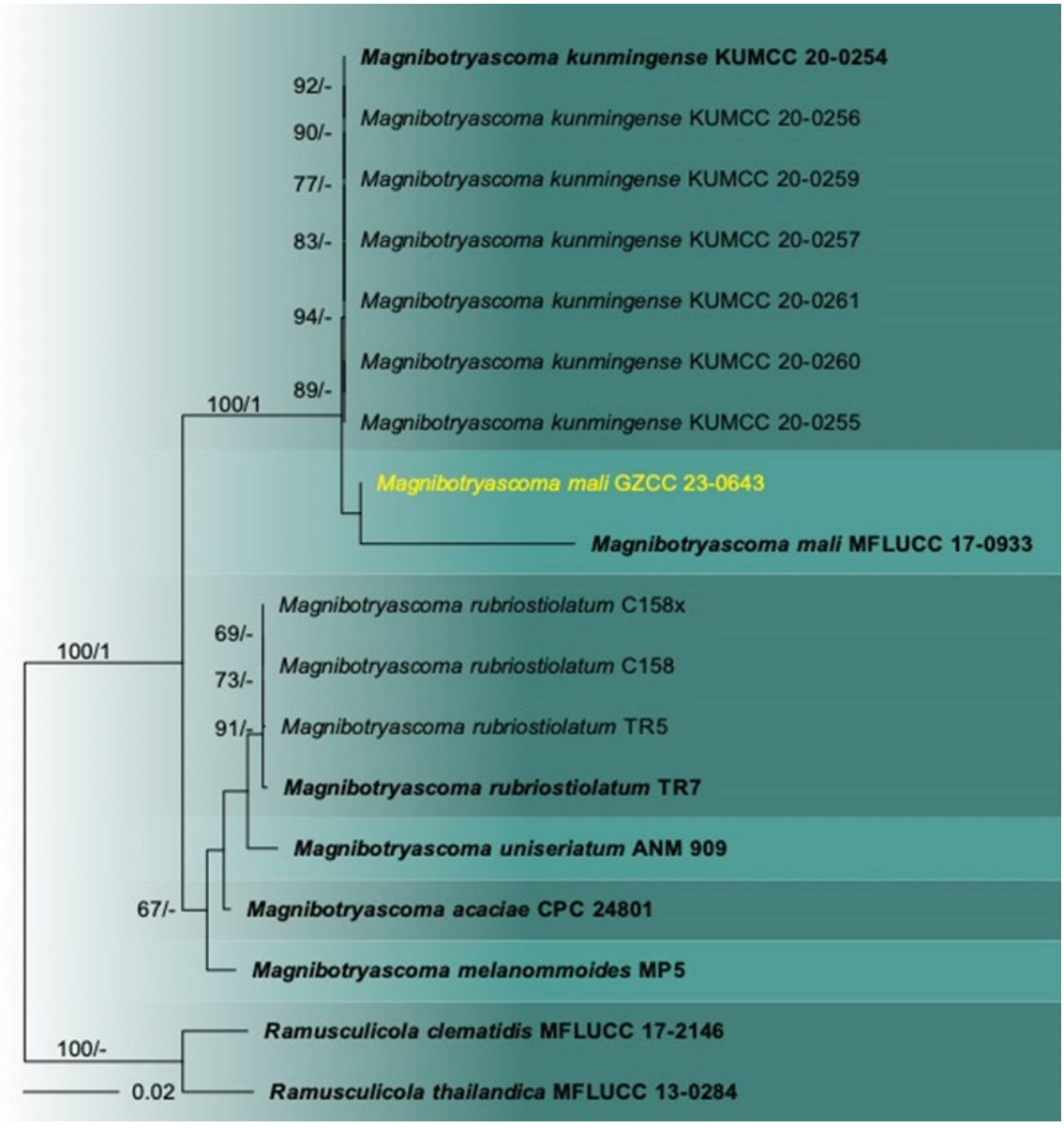

Fig. 27 – Phylogram generated from maximum likelihood analysis based on combined ITS, LSU, SSU, and *tef1-α* sequence data for *Magnibotryascoma.* Eighteen strains were included in the combined

analyses, which comprised 3,319 characters (535 characters for ITS, 844 characters for LSU, 1014 characters for SSU, and 926 characters for *tef1-α*) after alignment. The tree topology of the maximum likelihood analysis is similar to that of the Bayesian analysis. The best RAxML tree with a final likelihood value of -7187.949040 is presented. Estimated base frequencies were as follows: A = 0.235321, C = 0.257226, G = 0.275735, T = 0.231718; substitution rates AC = 1.549943, AG = 2.576608, AT = 1.359571, CG = 1.306546, CT = 8.198721, GT = 1.000000. Bootstrap support values for ML greater than 60% and Bayesian posterior probabilities greater than 0.95 are given near nodes, respectively. The tree was rooted with *Ramusculicola clematidis* (MFLUCC 17-2146) and *R. thailandica* (MFLUCC 13-0284). Ex-type strains are in bold. The newly generated sequences are indicated in yellow.

Magnibotryascoma mali Phukhams., Wanas. & K.D. Hyde, Hyde et al., Fungal Diversity 87, 105 (2017)

Index Fungorum number: IF 553255; Facesoffungi number: FoF 003387 Fig. 28

Saprobic on dead branches of *Manglietia lucida*. Sexual morph: Undetermined. Asexual morph: Coelomycetous, *Conidiomata* 160–240 × 210–230 μm ($\overline{x}$ = 190 × 220 μm, n = 20), immersed to semi-immersed, dark brown to black, solitary, globose to subglobose, unilocular or multi-locular, short-necked, ostioles. *Ostiole* circular, cylindrical, straight or curved, centrally or laterally located. *Peridium* up to 15–25 μm wide, composed of dark brown to black thick-walled *textura globosa*, becoming thin-walled and hyaline towards the inner region. *Paraphyses* absent. *Conidiophores* subcylindrical to ampulliform, reduced to conidiogenous cells. *Conidiogenous cells* 3–8 × 2–4 μm ($\overline{x}$ = 4 × 2 μm, n = 20), hyaline, ampulliform to subcylindrical, smooth-walled, arising from the inner layer of the pycnidium wall. *Conidia* 3–5 × 2–3 μm ($\overline{x}$ = 4 × 2 μm, n = 50), subglobose to oval, guttulate, hyaline when immature, golden brown at maturity, aseptate, with smooth-walled.

Culture characteristics – Conidia germinating on PDA within 12 hours. Colonies slow-growing, reaching 60 mm in diameter after incubation at 20–25°C for 2 weeks, white to brown with age, circular, flattened, dense, slightly cottony, smooth at margins, with a brown reverse.

Material examined – China, Sichuan Province, Chengdu City, Chengdu Botanical Garden, 30°45'59"N, 104°7'19"E, on dead branches of *Manglietia lucida* (*Magnoliaceae*), 15 July 2021, Na Wu, YW345, GZAAS 23-0648, living culture GZCC 23-0643.

GenBank accession numbers: ITS: OR234382, LSU: OR234385, SSU: OR234383, *tef1-α*: OR365760.

Known distribution – China (Hyde et al. 2017, this study), New Zealand (Crous et al. 2022b).

Known hosts – *Malus halliana* (Hyde et al. 2017), *Manglietia lucida* (this study), *Metrosideros* sp. (Crous et al. 2022b), *Osmanthus fragrans* (Chethana et al. 2023).

Notes – Our new collection, obtained from dead branches of *Manglietia lucida* (GZAAS 23-0648) from Chengdu Botanical Garden, China, exhibits morphological features similar to those of the type species, *Magnibotryascoma mali* (MFLU 17-0559). Both species share golden-brown, oval, aseptate, smooth-walled conidia, with comparable conidial dimensions (3–5 × 2–3 μm *vs.* 3–5 × 2.3–3.8 μm) (Hyde et al. 2017). Phylogenetic analysis supports identifying our collection as *M. mali* (Fig. 27). However, the extended branch length of the ex-type strain of *M. mali* (MFLUCC 17-0933) is likely due to an issue with the ITS sequence (Hyde et al. 2017).

Paradictyoarthriniaceae Doilom, J.K. Liu & K.D. Hyde, Liu et al., Fungal Diversity 72, 133 (2015)

Index Fungorum number: IF 550921; Facesoffungi number: FoF 00499

Paradictyoarthrinium Matsush., Matsushima Mycological Memoirs 9, 18 (1996)

Index Fungorum number: IF 27676; Facesoffungi number: FoF 00315

Paradictyoarthrinium was established by Matsushima (1996), with *P. diffractum* as the type species. Currently, the genus comprises five species: *P. diffractum*, *P. aquatica*, *P. hydei*, *P. salsipaludicola*, and *P. tectonicola* (Index Fungorum 2025). Members of this genus are hyphomycetous, saprobic fungi characterized by black, superficial, gregarious, powdery colonies,

macronematous conidiophores, and dark brown, subglobose to ellipsoidal, and muriform conidia (Liu et al. 2018). Phylogenetic analyses of combined LSU, ITS, and *rpb*2 sequence data were used to identify *Paradictyoarthrinium* species (Liu et al. 2018). In this study, we report two new host records of *P. diffractum* and *P. tectonicola* in Thailand. An updated phylogeny for *Paradictyoarthrinium* and closely related taxa is shown in Fig. 29.

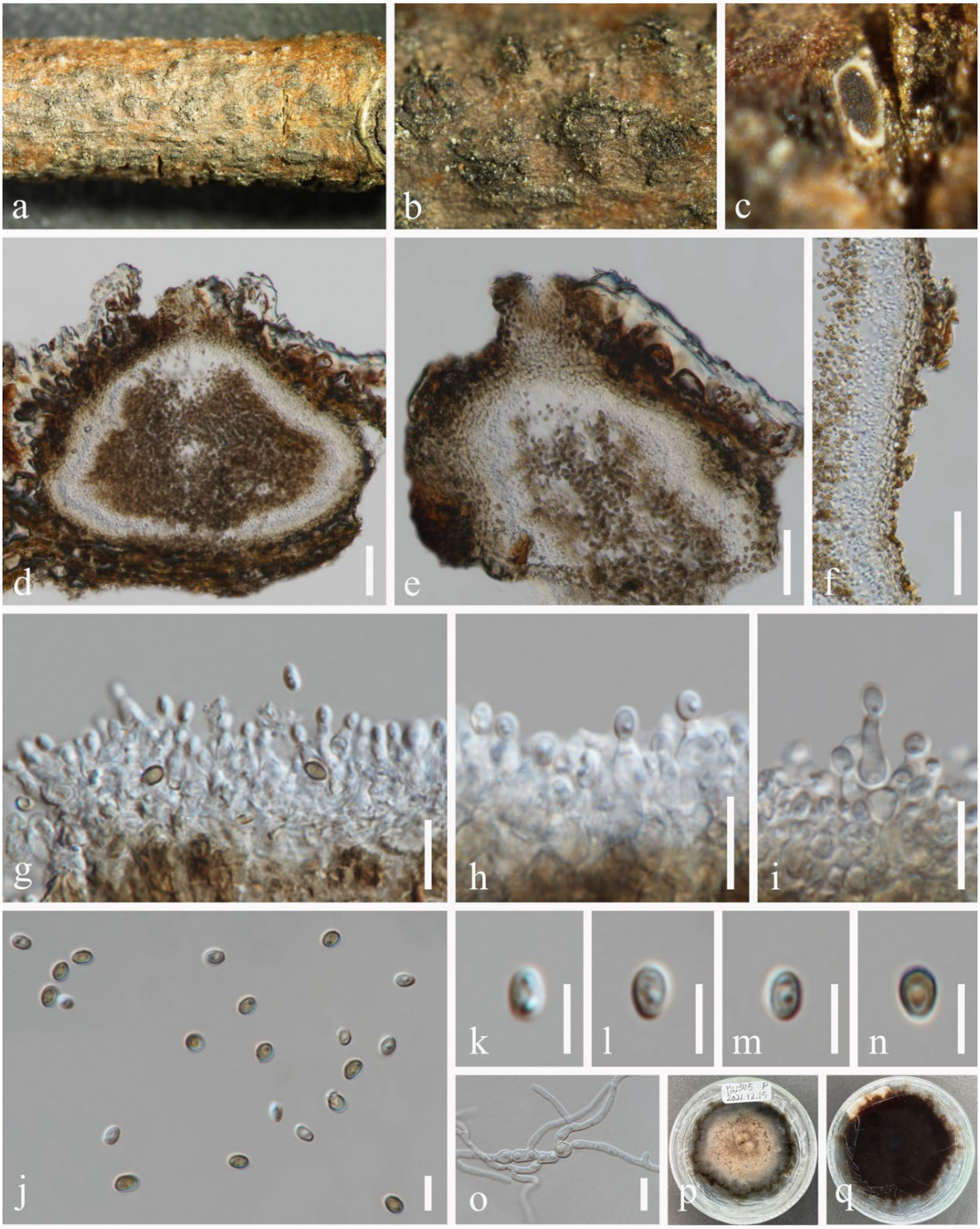

Fig. 28 – *Magnibotryascoma mali* (GZAAS 23-0648, **a new host record**). a, b Conidiomata on host substrate. c–e Vertical section of conidiomata. f Section of peridium. g–i Conidiogenous cells and

developing conidia. j–n Conidia. o Germinating conidium. p, q Colonies after 7 days on PDA (p: upper view, q: bottom view). Scale bars: d, e = 100 µm, f = 20 µm, g–j = 10 µm, k–o = 5 µm.

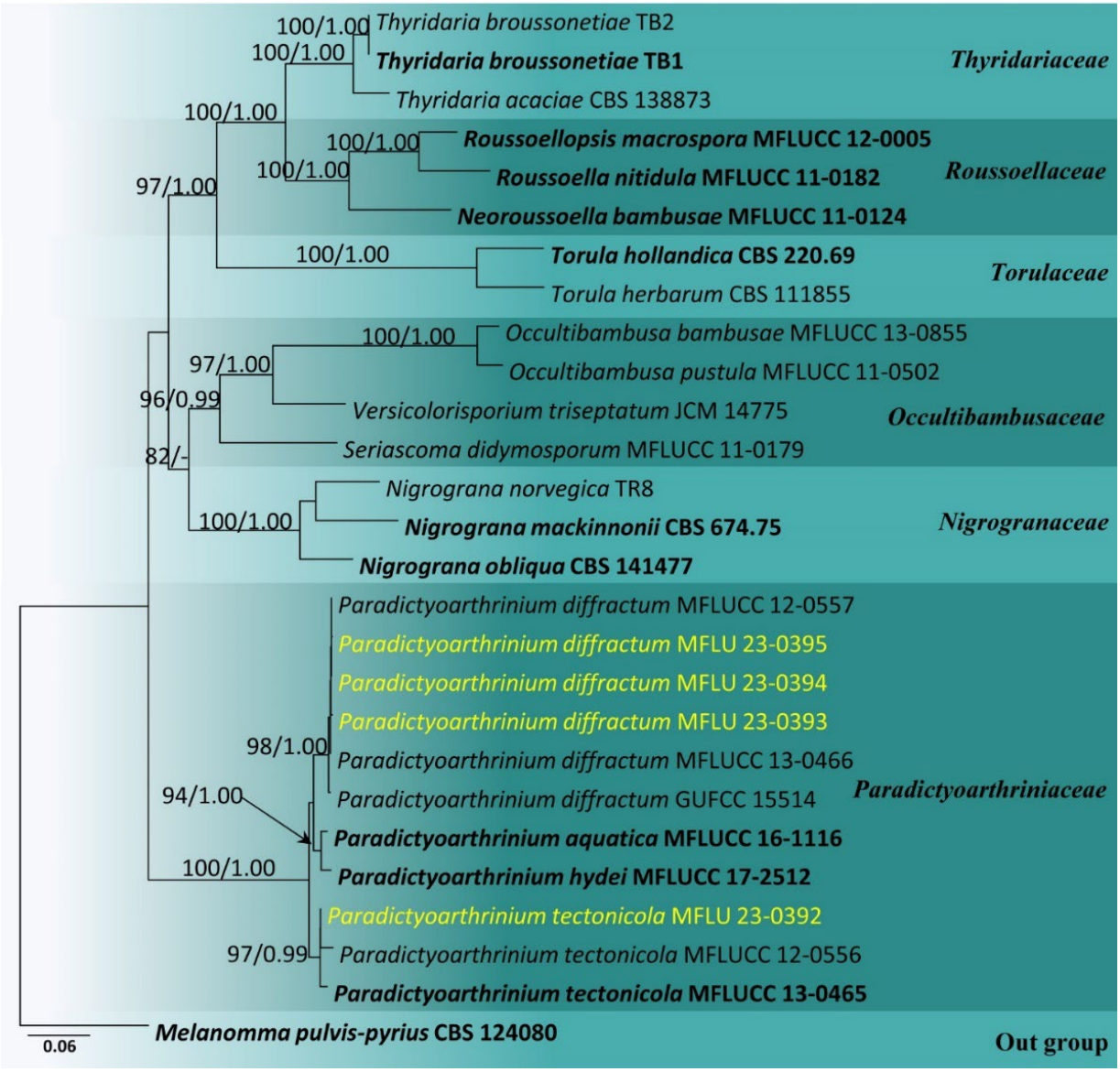

Fig. 29 – Phylogram generated from maximum likelihood analysis is based on combined LSU, ITS, and *rpb2* sequence data. Related sequences of *Paradictyoarthrinium* species were obtained from Liu et al. (2018). *Melanomma pulvis-pyrius* (CBS 124080) is used as the outgroup taxon. Twenty-seven strains were included in the combined gene analyses, comprising 800 characters after alignment (900 characters for LSU, 500 for ITS, and 1,000 for *rpb2*). The best RAxML tree with a final likelihood value of -17377.225426 is presented. The matrix contained 1,271 distinct alignment patterns, with 35.01% of the characters being undetermined or gaps. Estimated base frequencies were as follows: A = 0.253104, C = 0.244057, G = 0.279649, T = 0.223189; substitution rates AC = 1.218587, AG = 3.179551, AT = 1.319328, CG = 0.912251, CT = 7.598733, GT = 1.000000; gamma distribution shape parameter α = 0.867413. ML bootstrap values equal to or greater than 75% and Bayesian posterior probabilities equal to or greater than 0.95 are given above the nodes. Type and ex-type strains are in black bold. New strains are indicated in yellow.

Paradictyoarthrinium diffractum Matsush., Mycological Memoirs 9, 18 (1996)

Index Fungorum number: IF 415849; Facesoffungi number: FoF 01854 Fig. 30

Saprobic on dead stumps and stems of *Cassia* sp. Sexual morph: Undetermined. Asexual morph: *Colonies* on natural substrate, black, powdery, superficial, gregarious, scattered. *Conidiophores* up to 12 µm long, 2–5 µm wide, macronematous, erect to slightly curved, branched to unbranched, constricted at the septa, arising from hyphae. *Conidiogenous cells* blastic, integrated, determinate, and terminal. *Conidia* 9–14 × 6–12 µm ($\overline{x}$ = 12 × 10 µm, n = 30), brown to black, muriform, initially globose to subglobose, becoming ellipsoidal to irregular, solitary or developing in branched chains, with 1– 2 short chains, verrucose, very variable in size and shape; circular to irregular with a protruding basal cell; rounded to truncate at the base.

Culture characters – Colonies on PDA reaching 45 mm diameter after incubating at 25°C for 1 week; colonies from upper view: circular, margin entire, slightly raised, cottony, dense, dark grey; colonies from bottom view: grey.

Material examined – Thailand, Chiang Rai Province, on dead twigs of *Cassia* sp. (*Fabaceae*), 5 February 2022, N. I. de Silva, NID9 (MFLU 23-0393), NID10 (MFLU 23-0394), on dead twigs of *Magnolia* sp. (*Magnoliaceae*), NID 11 (MFLU 23-0394).

GenBank accession numbers – MFLU 23-0393: ITS: PV018455, LSU: PV018451, *rpb2*: PV030957; MFLU 23-0394: ITS: PV018456, LSU: PV018452, *rpb2*: PV030958; MFLU 23-0395: ITS: PV018457, LSU: PV018453, *rpb2*: PV030959.

Known distribution – South Africa (Matsushima 1996), India (Prabhugaonkar & Bhat 2011), and Thailand (Doilom et al. 2017, this study).

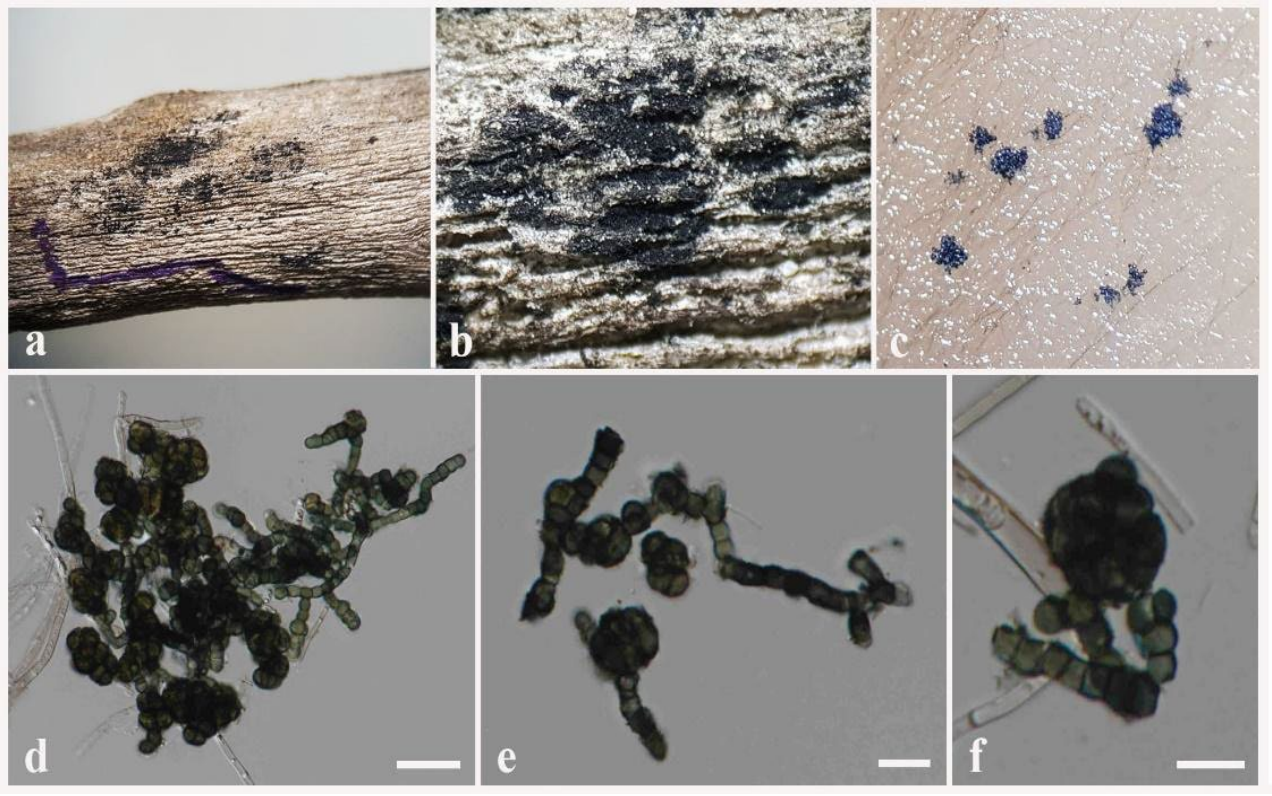

Fig. 30 – *Paradictyoarthrinium diffractum* (MFLU 23-0393, **a new host record**). a The specimen. b Colonies on the host surface. c Colonies on PDA culture plate. d–f Conidia with conidiophores. Scale bars: d = 20 µm, e, f = 10 µm.

Known hosts – On dead twigs in a stream (Matsushima 1996), dead decaying spathe of *Cocos nucifera* (Prabhugaonkar & Bhat 2011), dead stumps and stems of *Tectona grandis* (Doilom et al. 2017), and dead twigs of *Cassia* sp. and *Magnolia* sp. (this study).

Notes –The phylogeny analysis based on combined LSU, ITS, and *rpb2* sequence data indicated that three new strains (MFLU 23-0393, MFLU 23-0394, MFLU 23-0395) clustered with the ex-type strain of *Paradictyoarthrinium diffractum* (GUFCC 15514) and some other strains of *P. diffractum*, with 98% ML, 1.00 BYPP support (Fig. 29). *Paradictyoarthrinium diffractum* was originally described by Matsushima (1996) from a decaying spathe of *Cocos nucifera* collected from a rivulet at Rustenburg, South Africa. This species has since been reported from various host species and geographical locations. Morphologically, the newly obtained strain (MFLU 23-0393) exhibits conidiophores and conidia size ranges that overlap with those of *P. diffractum* (MFLUCC 12–0557) (Doilom et al. 2017). The conidiophores of strain MFLU 23-0393 were up to 12 μm in length and 2–5 μm in width, whereas those of *P. diffractum* (MFLUCC 12–0557) were up to 15 μm long and 3–5.5 μm wide (Doilom et al. 2017). The conidia of both strains were brown to black and muriform, with a new collection (MFLU 23-0393) being 9–14 × 6–12 μm, and *P. diffractum* (MFLUCC 12–0557) (8–)9–11(−14) × (6.5–)8.5–19.5(−13) μm (Doilom et al. 2017). Based on both morphological characteristics and phylogenetic evidence, we report a new host record of *P. diffractum* from dead twigs of *Cassia* species and *Magnolia* sp. in Thailand.

Paradictyoarthrinium tectonicola Doilom & K.D. Hyde, Liu et al., Fungal Diversity 72, 134 (2015)

Index Fungorum number: IF 550900; Facesoffungi number: FoF 00315 Fig. 31

Saprobic on a dead stem of *Ficus septica* (*Moraceae*). Sexual morph: Undetermined. Asexual morph: *Colonie*s on natural substrate, superficial, gregarious, scattered, black, powdery. *Conidiophores* up to 30–35 × 1–3 μm, macronematous, erect to slightly curved, constricted at the septa, arising from hyphae. *Conidiogenous cells* blastic, integrated, terminal, and determinate. *Conidia* 15–25 × 16–20 μm, muriform, subglobose to ellipsoidal, brown to black, verrucose, solitary or developing in branched chains, with 1–3 short chains, very variable in size and shape, circular to irregular with a protruding basal cell, and rounded to truncate at the base.

Culture characters – Colonies on PDA reaching 40 mm diam., after incubation at 25°C for 1 week, colonies from upper view: circular, margin entire, slightly raised, cottony, dense, dark grey, and grey at the bottom view.

Material examined – Thailand, Chiang Mai Province, on a dead stem of *Ficus septica* (*Moraceae*), 15 February 2021, D.S Tennakoon, DC008 (MFLU 23- 0393).

GenBank accession numbers – ITS: PV018458, LSU: PV018454, *rpb2*: PV030960.

Known distribution – Thailand (Liu et al. 2015, this study).

Known hosts – *Tectona grandis* (*Lamiaceae*) (Liu et al. 2015, this study).

Notes – The morphological characteristics of our collection largely overlap with those of *Paradictyoarthrinium tectonicola*. Therefore, we report our collection as a new record of *P. tectonicola* from the dead stem of *Ficus septica* in Thailand. In particular, both isolates share overlapping sizes in their conidiophores (30–35 × 1–3 μm *vs.* 33 × 1.5–3 μm) and conidia sizes (15–25 × 16–20 μm *vs.* 17–21 × 16–19 μm) (Liu et al. 2015). Multi-gene phylogenetic analysis (LSU, ITS, and *rpb2*) further supports this identification, as our collection clusters with *P. tectonicola* isolates (MFLUCC 12-0556 and MFLUCC 13-0465) with 97% ML/ 0.99 BYPP support. *Paradictyoarthrinium tectonicola* was introduced by Liu et al. (2015) from *Tectona grandis* (*Lamiaceae*) in Thailand. Interestingly, while our isolate is also reported from Thailand, it represents a new host record for this species.

Dothideomycetes O.E. Erikss. & Winka

Botryosphaeriales C.L. Schoch, Crous & Shoemaker, Mycologia 98, 1050

Index Fungorum number: IF 501513; Facesoffungi number: FoF 07659

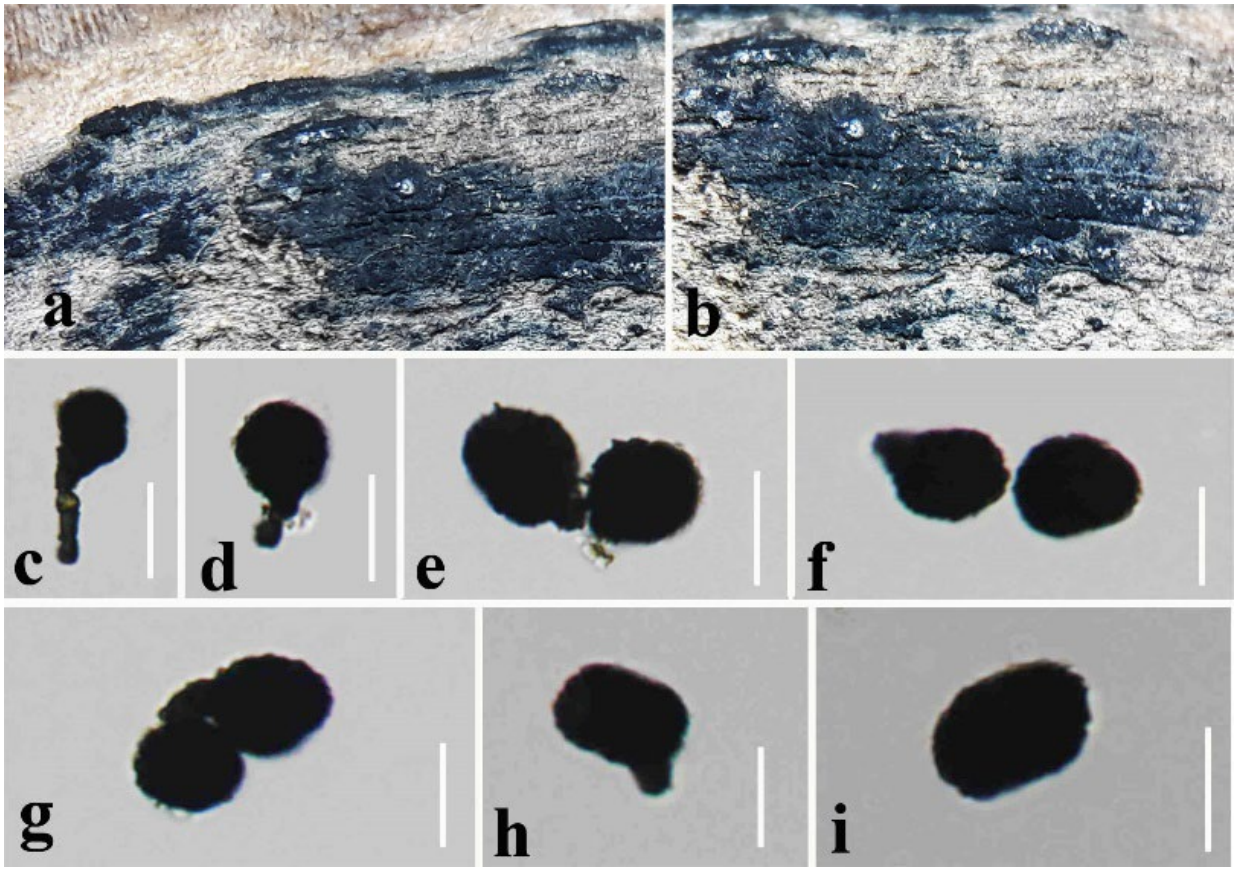

Fig. 31 – ***Paradictyoarthrinium tectonicola*** (MFLU 23- 0393, **a new host record**). a, b Colonies on a host surface. c–i Conidia with conidiophores. Scale bars: c–i = 15 µm.

Botryosphaeriaceae Theiss. & H. Syd, Annales Mycologici 16(1/2), 16 (1918)

Index Fungorum number: IF 80530; Facesoffungi number: FoF 00116

Lasiodiplodia Ellis & Everh., Clendenin, Botanical Gazette 21, 92 (1896)

Index Fungorum number: IF 8708; Facesoffungi number: FoF 00151

Lasiodiplodia was introduced to accommodate *L. tubericola*, which is currently accepted as *L. theobromae* (Liu et al. 2012). Both sexual and asexual morphs have been recorded in *Lasiodiplodia* (Dissanayake et al. 2016). The sexual morph of *Lasiodiplodia* species consists of globose to subglobose ascomata, often with ostioles and uniloculate, and clavate, stipitate asci with hyaline to dark brown, aseptate ascospores (Phillips et al. 2013, 2019). The asexual morph consists of stromatic, immersed or superficial, globose, uni- or multiloculate conidiomata with a central, single, papillate ostiole. *Conidiophores* are usually reduced to conidiogenous cells; if present, they are characterised by hyaline, cylindrical, sometimes septate, and rarely branched conidiophores arising from the inner layer. *Conidiogenous cells* hyaline, cylindrical to conical, holoblastic, and smooth, arising from the inner wall of conidiomata (Phillips et al. 2013). *Conidia* subglobose or oval, smooth, thick-walled, initially hyaline, and become dark brown and striated with maturity (Phillips et al. 2013, 2019). *Pigmented* 1-septate conidia with longitudinal striations and pycnidial paraphyses distinguish *Lasiodiplodia* from other genera in *Botryosphaeriaceae* (Phillips et al. 2013, 2019, Dou et al. 2017). El-Ganainy et al. (2022) accepted 48 species based on morpho-molecular data, and there are 94 *Lasiodiplodia* records available in the Index Fungorum (2025). An updated phylogeny for *Lasiodiplodia* and closely related taxa is shown in Fig. 32.

Lasiodiplodia crassispora T.I. Burgess & P.A. Barber, Mycologia 98(3), 425 (2006)

Index Fungorum number: IF 500235; Facesoffungi number: FoF 06624 Fig. 33

Saprobic on dead grass. Sexual morph: Undetermined. Asexual morph: *Coelomycetes*. *Conidiomata* 70–75 µm × 77–80 µm ($\overline{x}$ = 73 × 78 µm, n = 10), pycnidial, solitary, immersed, becoming erumpent at maturity, formed uniloculate stomata, with globose. *Conidiomata wall* 10–14 µm diam. composed of thin-walled, sub-globose, brown cells of *textura angularis*, inner layer thin, hyaline. *Conidiophores* usually reduced to conidiogenous cells. *Conidiogenous cells* 7–10 µm × 2–4 µm ($\overline{x}$ = 9 × 3 µm, n = 15), lining the pycnidial cavity, holoblastic, hyaline, cylindrical, discrete, determinate, and smooth-walled. *Conidia* 11–14 µm × 6–8µm ($\overline{x}$ = 13 × 7.2 µm, n = 30), oblong to ovoid, straight, rounded at both ends, cylindrical, hyaline, aseptate, with thick walls.

Material examined – Thailand, Chiang Rai Province, Muang, Nang Lae village, on dead grass, 20 May 2021, Achala Rathnayaka, MFLU 23-0262.

GenBank accession numbers – ITS: OR628208, *tef1-α*: OR729891.

Known hosts and distribution – *Adansonia digitata* in Senegal (Cruywagen et al. 2017), *Annona leptopetala*, *A. muricata*, *A. squamosa*, *Mangifera indica* in Brazil (Marques et al. 2013, Machado et al. 2019), *Cinnamomum zeylanicum* in Sri Lanka (Adikaram & Yakandawala 2020), *Corymbia flavescens*, *Corymbia* sp., *Syzygium album* in Australia (Burgess et al. 2019, Sakalidis et al. 2011, Burgss et al. 2006), *Syzygium cordatum* in South Africa (Phillips et al. 2008), *Eucalyptus urophylla* in Uruguay and Venezuela (Burgess et al. 2006, Pérez et al. 2010), *Pterocarpus angolensis* in Africa, Australia and South Africa (Coutinho et al. 2016, Custódio et al. 2018, Mehl et al. 2011), *Sclerocarya birrea* sub sp. *caffra* in South Africa (Mehl et al. 2017), *Vitis vinifera* in Brazil, California, Mexico, South Africa and the United States (Úrbez-Torres et al. 2010, Úrbez-Torres & Gubler 2011, Van Niekerk et al. 2010, et al. 2013, Rangel-Montoya et al. 2021), and *Garcinia subelliptica* in Taiwan region, China (Rathnayaka et al. 2023).

Notes – Morphologically, our collection (MFLU 23-0262) is similar to the holotype of *Lasiodiplodia crassispora* (MURU 407), which was collected from the canker of *Santalum album* in Western Australia (Burgess et al. 2006). The length/ width (L/W) ratio of conidia is similar in both the holotype ($\overline{x}$ = 28.8 × 16, l/w = 1.8) and our collection ($\overline{x}$ = 13 × 7.2 µm, l/w = 1.8) (Burgess et al. 2006). However, the holotype conidia are pigmented before germination, with one septum at maturity and vertical striations, which are not observed in our collection (Burgess et al. 2006). According to multi-gene phylogeny (ITS, *tef1-α*, *tub2*, and *rpb2*), our strain (MFLU 23-0262) clustered with other strains of *L. crassispora* (CBS 118741, CBS 121770, CMW 13488, NCYUCC 19-0391) with 100% ML bootstrap and 1.00 PP support (Fig. 32). Based on morph-molecular analyses, we introduce our collection as a new geographical record of *L. crassispora*.

Neofusicoccum Crous, Slippers & A.J.L. Phillips, Study in Mycology 55, 247 (2006)

Index Fungorum number: IF 500870; Facesoffungi number: FoF 00153

Neofusicoccum was introduced by Crous et al. (2006) with *N. parvum* (Pennycook & Samuels) Crous, Slippers & A.J.L. Phillips as the type species. Some *Neofusicoccum* species are plant pathogens on economically and ecologically important plants, causing diebackand canker. In addition, *Neofusicoccum* has been reported as an endophyte and saprobe on a wide range of hosts (Slippers et al. 2013, Salvatore et al. 2021). The genus contains 71 species epithets in Index Fungorum (2025). An updated phylogeny for *Neofusicoccum* and closely related taxa is shown in Fig. 34.

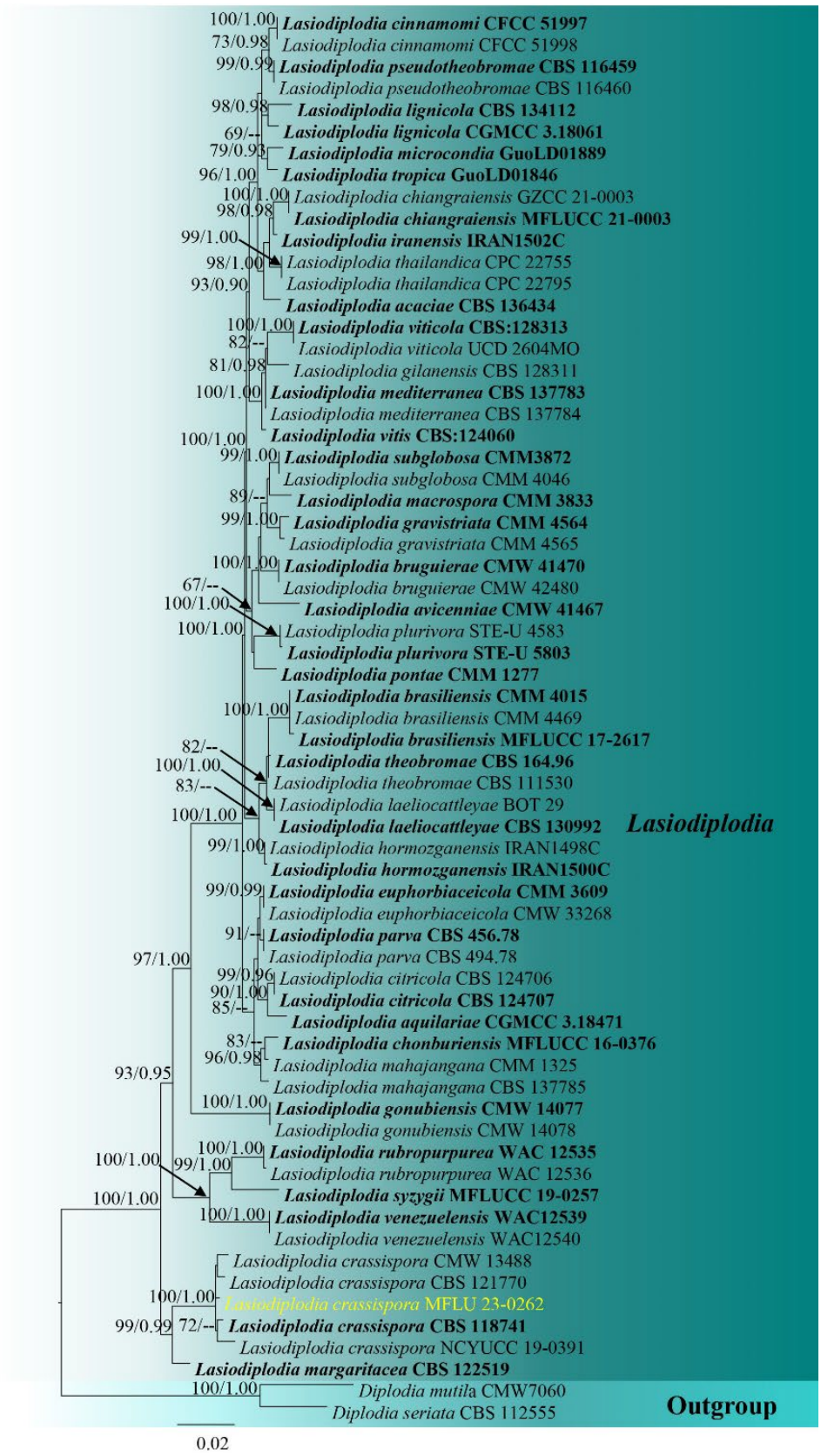

Fig. 32 – Phylogram generated from the maximum likelihood analysis based on the combined ITS, *tef1-α*, *tub2*, and *rpb2* sequence data. Sixty-five strains are included in the combined analyses. The tree

topology of the maximum likelihood analysis is similar to that of the Bayesian analysis. The best RAxML tree with a final likelihood value of -6061.114962 is presented. Evolutionary models applied to all genes are GTR+G. The matrix contained 401 distinct alignment patterns, with 22.27% of the characters being undetermined or gaps. Bootstrap support values for ML greater than 65% and Bayesian posterior probabilities greater than 0.95 are given near nodes, respectively. The tree was rooted with *Diplodia mutila* (CMW7060) and *D. seriata* (CBS 112555). Ex-type strains are in bold. The newly generated sequences are indicated in yellow.

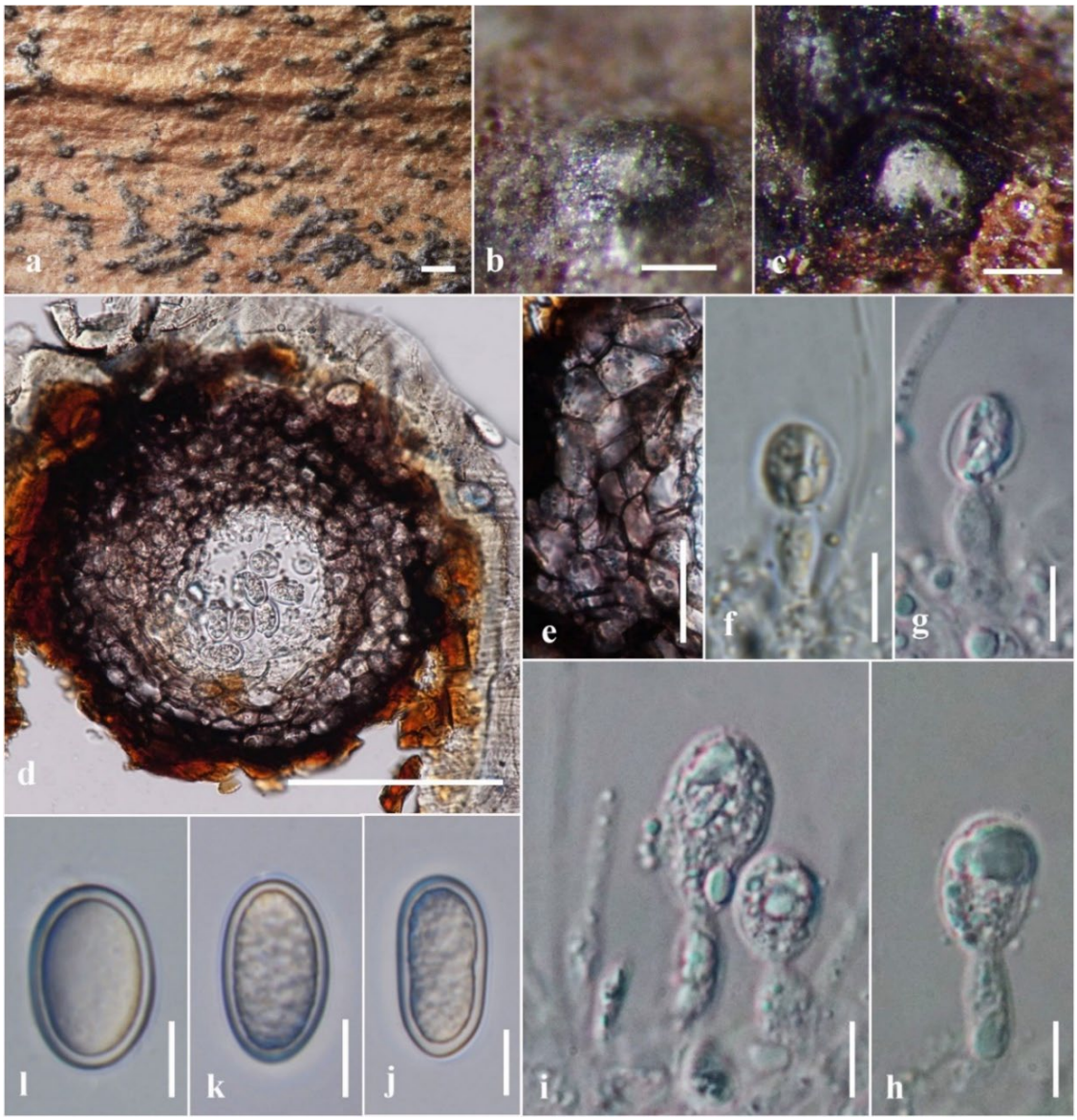

Fig. 33 – *Lasiodiplodia crassispora* (MFLU 23-0262, **a new geographical record**). a Conidiomata on a host substrate. b Close-up of a conidioma erumpent through the host surface. c, d Cross-section of conidioma. e Peridium. f–i Immature conidia attached to conidiogenous cells. j–l Conidia. Scale bars: a = 1 mm, b, c = 100 µm, d = 50 µm, e–l = 5 µm.

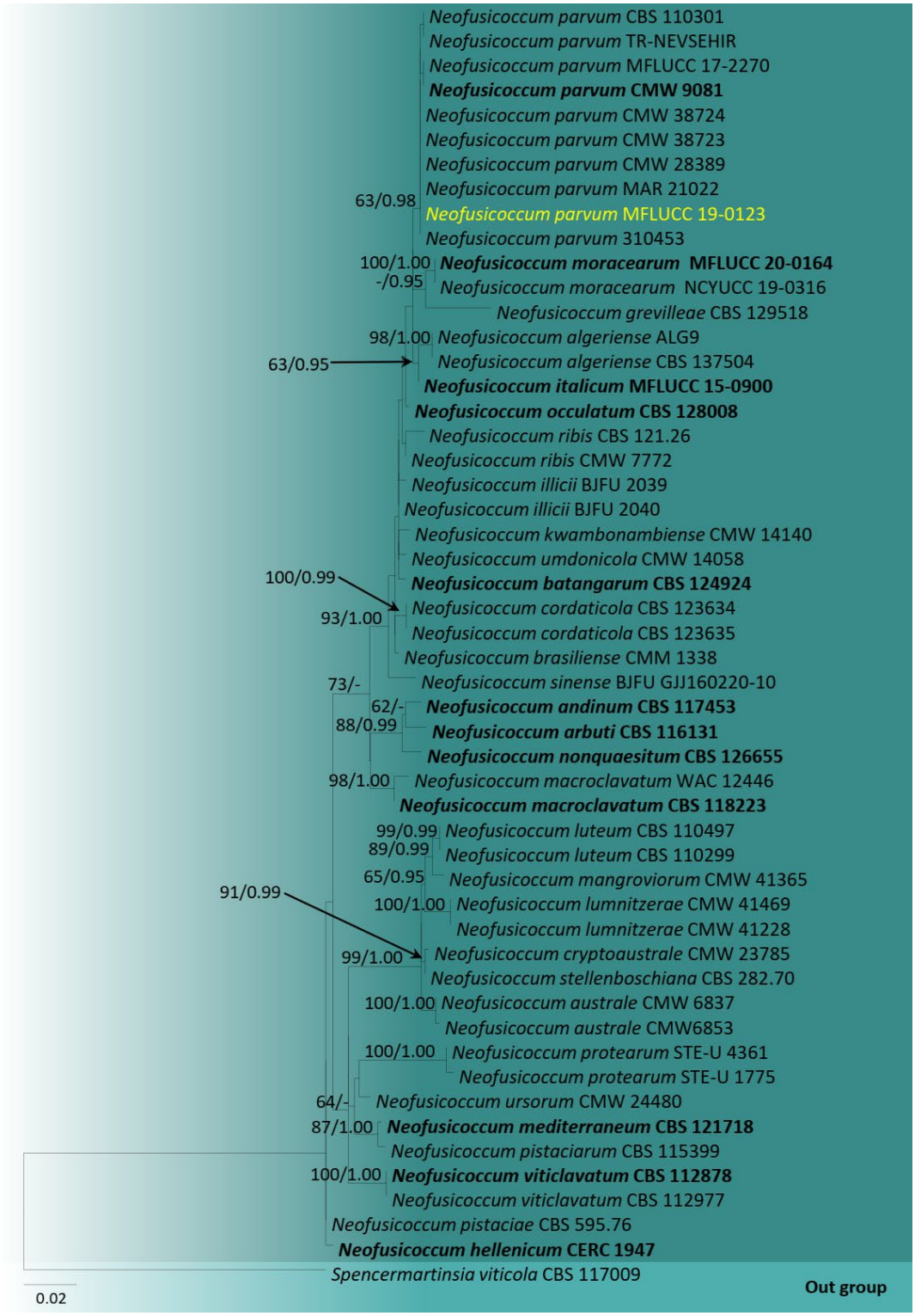

Fig. 34 – Phylogram generated from the maximum likelihood analysis based on combined ITS and *tef1-α* sequence data representing *Neofusicoccum* species. Related sequences are taken from Tennakoon et al. (2021). *Spencermartinsia viticola* (CBS 117009) is used as the outgroup taxon. Fifty-two strains are included in the combined gene analyses, comprising 800 characters after alignment (500 characters for ITS, 300 characters for *tef1-α*). The best RAxML tree with a final likelihood value of -2654.529348 is presented. The matrix contained 249 distinct alignment patterns, with 16.13% of the characters being

undetermined or gaps. Estimated base frequencies were as follows: A = 0.207202, C = 0.291275, G = 0.270358, T = 0.231165; substitution rates AC = 1.124889, AG = 5.902644, AT = 1.169349, CG = 1.132897, CT = 9.453491, GT = 1.000000; gamma distribution shape parameter α = 0.805666. Bootstrap values for maximum likelihood equal to or greater than 60% are given above the nodes. Ex-type strains are in bold. The new strain is indicated in yellow.

Neofusicoccum parvum (Pennycook & Samuels) Crous, Slippers & A.J.L. Phillips, Studies in Mycology 55, 248 (2006)

Index Fungorum number: IF 500879; Facesoffungi number: FoF 02411 Fig. 35

Saprobic on dead twigs of *Magnolia* sp. Sexual morph: *Ascostromata* 100–160 μm high, × 260–330 μm diam ($\overline{x}$ = 135 × 290 μm, n = 10), visible as black dots and on the host tissue, appearing through cracks in bark, solitary or clustered, semi-immersed to erumpent, globose to subglobose. *Peridium* 20–30 μm, comprising two layers, the outer layer composed of dark brown, thick-walled cells of *textura angularis*, and the inner layer composed of light brown to hyaline, thin-walled cells of *textura angularis*. *Hamathecium* comprising 2–3 μm wide, hyaline, hyphae-like, numerous, septate, pseudoparaphyses, slightly constricted at the septa, embedded in a gelatinous matrix. *Asci* 70–110 × 12–20 μm ($\overline{x}$ = 85 × 17 μm, n = 20), 8-spored, bitunicate, fissitunicate, clavate to cylindro-clavate, apically rounded, with ocular chamber, short to long pedicellate. *Ascospores* 13–17 × 5–7 μm ($\overline{x}$ = 15 × 5.5 μm, n = 20), uniseriate at the base, 2–3-seriate at the centre and end, hyaline, ellipsoidal to fusiform, aseptate, wider in the centre, rounded or acute at the ends. Asexual morph: described in Phillips et al. (2013).

Culture characteristics – Colonies on PDA reaching 35 mm diameter after incubation at 25°C for 7 days, colonies from above white, circular, margin entire, raised, dense, fluffy appearance with aerial mycelia; reverse: cream.

Material examined – China, Yunnan Province, Xishuangbanna, on dead twigs of *Magnolia* sp. (*Magnoliaceae*), 27 March 2017, N. I. de Silva, NI176 (MFLU 18-1035), living culture (MFLUCC 19-0123, KUMCC 17-0204).

GenBank accession numbers – ITS: OR742006.

Known distribution – Worldwide distribution, including Australia, Indonesia (Sumatra), Brazil, China (Sichuan), France (Van Niekerk et al. 2004), New Zealand (Alves et al. 2005), Portugal (Phillips et al. 2008), Thailand (Liu et al. 2012, Trakunyingcharoen et al. 2015, Hyde et al. 2020) (this study).

Known hosts – Wide range of host species, including *Actinidia deliciosa*, *A. chinensis*, *Eucalyptus obliqua*, *Populus nigra*, *Prunus cerasoides* (Trakunyingcharoen et al. 2015), *Pinus nigra*, *Vitis vinifera* (Crous et al. 2006, Phillips et al. 2008), *Linum usitatissimum* (Liu et al. 2012), *Vitis vinifera* (Alves et al. 2005), *Mangifera indica* (Mehl et al. 2017, Hyde et al. 2020), and *Magnolia* sp. (this study).

Notes – The phylogenetic analyses of a combined ITS and *tef1-α* sequence dataset indicated that our strain clustered with the ex-type of *Neofusicoccum parvum* (CMW 9081) (Fig. 34). The holotype of *N. parvum* was identified from dead branches of *Populus nigra* in New Zealand (Pennycook & Samuels 1985). Although *N. parvum* has been previously reported on different host species, including *Cinnamomum cassia* (Xu et al. 2022), *Eriobotrya japonica* (Zhai & Zhang 2019), *Eucalyptus* sp. (Chen et al. 2011), *Hevea brasiliensis* (Liu et al. 2017), *Prunus salicina* (Li et al. 2019), and *Vitis* species (Yan et al. 2013) in China, it has not been identified on *Magnolia* species in China. Our collection is the first report of *N. parvum* on *Magnolia* species in China.

Class *Leotiomycetes* O.E. Erikss. & Winka, Myconet 1, 7 (1997)

Subclass *Leotiomycetidae* P.M. Kirk, P. Cannon, Minter & Stalpers (2008)

Marthamycetales P.R. Johnst. & Baral, Johnston et al., IMA Fungus 1(1), 16 (2019)

Index Fungorum number: IF 827852; Facesoffungi number: FoF 19177

Marthamycetaceae Baral, Lantz, Hustad & Minter, Index Fungorum 225, 2 (2015)

Index Fungorum number: IF 551080; Facesoffungi number: FoF 05851

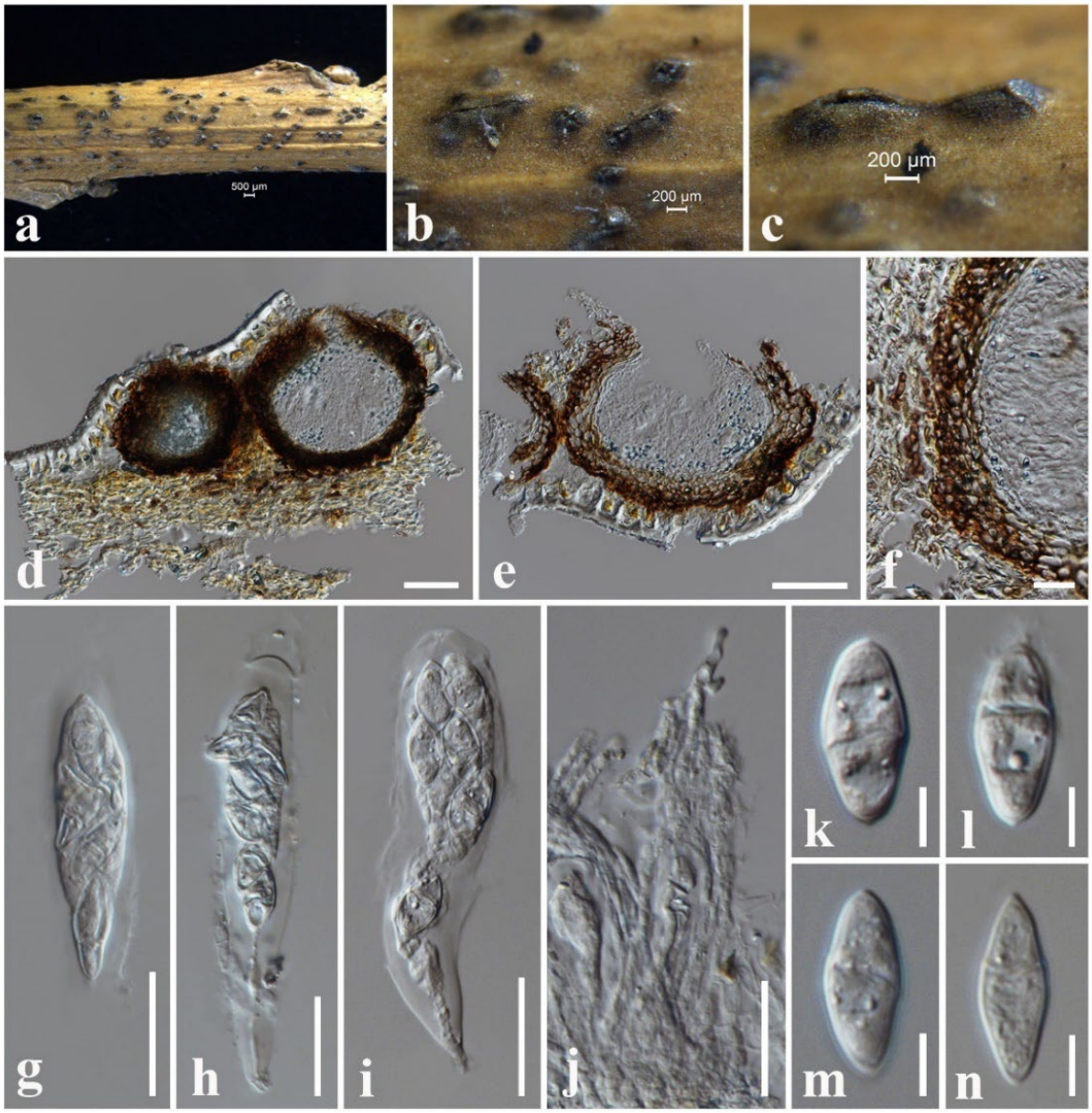

Fig. 35 – ***Neofusicoccum parvum*** (MFLU 18-1035, **a new record**) a, b Appearance of ascomata on substrate, dead branch of *Magnolia* sp. c Close up of ascomata on the host. d, e Vertical sections through ascomata. f Vertical sections showing peridium. g–i Asci. j Pseudoparaphyses. k–n Ascospores. Scale bars: a = 500 µm, b, c = 200 µm, d, e = 50 µm, f = 10 µm, g–j = 20 µm, k–n = 5 µm.

Propolis (Fr.) Corda, Icones fungorum hucusque cognitorum 2, 38 (1838)

Index Fungorum number: IF 4374; Facesoffungi number: FoF 19191

Propolis was described by Fries (1822) as a subgenus of *Stictis*. Later, Corda (1838) elevated *Propolis* to a generic rank and placed it within *Pezizaceae* based on morphological characteristics. Recently, *Propolis* has been associated with *Marthamycetaceae* based on phylogenetic analyses and morphological studies, a classification subsequently accepted by Jaklitsch et al. (2016), Ekanayaka et al. (2019), and Wijayawardene et al. (2018). *Propolis* is recognized as a saprobic genus that includes 26 species (Wijayawardene et al. 2018, Species Fungorum 2025). An updated phylogeny for *Propolis* and closely related taxa is shown in Fig. 36.

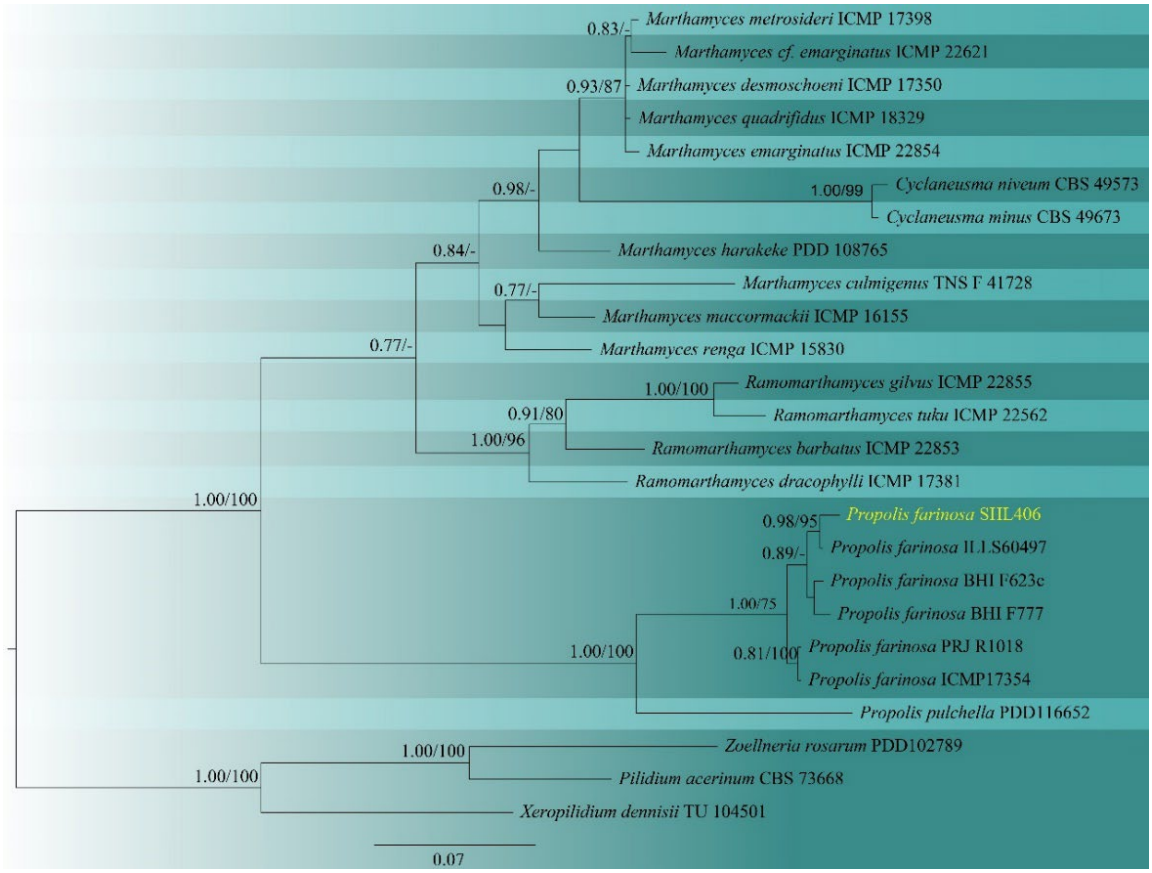

Fig. 36 – Phylogram generated from maximum likelihood analysis based on ITS sequence data. Twenty-five strains were included in the analyses, which comprised 565 characters after alignment. The tree topology of the maximum likelihood analysis is similar to that of the Bayesian analysis. The best RAxML tree with a final likelihood value of -3778.877448 is presented. Estimated base frequencies were as follows: A = 0.235921, C = 0.249680, G = 0.250844, T = 0.263556; substitution rates AC = 1.875712, AG = 2.680128, AT = 1.567019, CG = 0.802624, CT = 4.913941, GT = 1.000000. The evolutionary model SYM+I+G was applied to all the gene regions. Bootstrap support values for ML greater than 75% and Bayesian posterior probabilities greater than 0.75 are given near nodes, respectively. The tree is rooted with *Pilidium acerinum* (PDD 102789), *Xeropilidium dennisii* (TU 104501), and *Zoellneria rosarum* (PDD 102789). The newly generated sequences are indicated in yellow.

Propolis farinosa (Pers.) Fr., Summa vegetabilium Scandinaviae 2, 372 (1849)

Index Fungorum number: IF 433503; Facesoffungi number: FoF 19194 Fig. 37

Saprobic on dead stems. Sexual morph: *Apothecia* 1.5–5 × 1–3 mm ($\overline{x}$ = 3.6 × 2.3 µm, n = 10), scattered to gregarious, immersed or erumpent, circular to angular, or irregular. *Disc* originally developed under host tissue, exposed by tearing or sloughing off the overlying bark, white to slightly grey and pruinose. *Margin* everted, irregular. *Hymenium* 140–170 µm ($\overline{x}$ = 158 µm, n = 10), flat to convex, rough, pruinose, white to slightly brown. *Excipulum* comprises three layers: the outer layer is composed of thick-walled, hyaline *textura prismatica* cells, brown at the middle layer, and the inner layer is composed of *textura angularis* to *textura globulosa*. *Paraphyses* 0.8–1.7 µm ($\overline{x}$ = 1.3 µm, n = 40) wide, longer than asci, filiform, naturally curved, slightly rough, aseptate, hyaline, with apical to irregular narrow branches. *Asci* (110–)115–140(–145) × 11–15 µm ($\overline{x}$ = 134 × 12 µm, n = 47), unitunicate, 8-spored, elongated clavate, straight to slightly curved, uniformly thin-walled, inoperculate, hyaline, with inamyloid and obtuse apex and slightly tapered ends, croziers absent at the base.

Ascospores (80/7/1) 15.3 – 28.3 × 5 – 7 µm ($\bar{x}$ = 20.8 × 5.7 µm, n = 50), partially biseriate, reniform to ellipsoid, with obtuse ends, aseptate, hyaline, thin-walled, slightly rough, with 1–3 large oil guttules, most 2 large oil guttules, and some small oil guttules. Asexual morph: Undetermined.

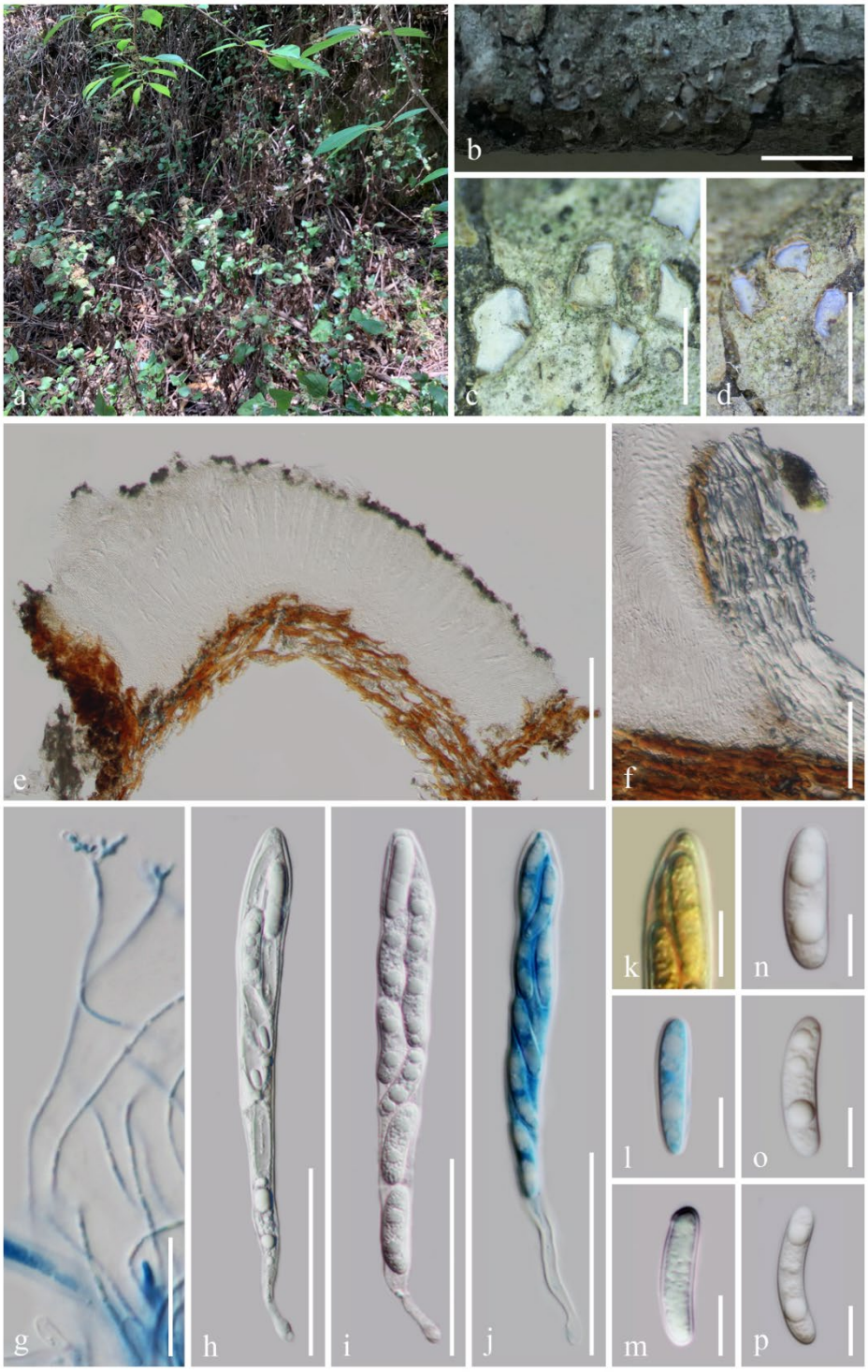

Fig. 37 – *Propolis farinosa* (HKAS 131338, **a new record**). a Habit. b–d Apothecia. e Vertical section of apothecia. f Excipulum. g Paraphyses in cotton blue. h, i Asci. j Asci in cotton blue. k Apex of asci in Melzer's reagent. l Ascospores in cotton blue. m–p Ascospores. Scale bars: b = 0.5 cm, c = 1 mm, d = 2 mm, e = 200 µm, f = 50 µm, g = 20 µm, h–j = 50µm, k–p = 10 µm.

Material examined – China, Yunnan Province, Kunming, Xishan Park, on dead stems, 19 April 2021, Hongli Su, SHL-409 (HKAS 131338).

GenBank accession numbers – ITS: PV455901.

Known distribution – Temperate and boreal forests of North America and Western Europe (Karakehian 2020).

Known hosts – Various dicot and gymnosperm hosts (Karakehian 2020).

Notes – *Propolis farinosa* is characterized by immersed to erumpent apothecia with a white to beige-tinted hymenium, filiform paraphyses with apically branched into irregular, narrower branches, and reniform to ellipsoid ascospores, which are similar to our specimen (HKAS 131338) morphologically (Chlebická 2014). Additionally, phylogenetic analysis indicates that our specimens (HKAS 131338) cluster with *Propolis farinosa* (ILLS60497), with 95% maximum-likelihood bootstrap support and a posterior probability of 0.98. Based on these morphological and phylogenetic similarities, we identified these three collections as *P. farinosa*. *Propolis farinosa* was reported as a common species in temperate and boreal forests of North America and Western Europe (Karakehian 2020). This study presents the first report of *P. farinosa* in China.

Rhytismatales M.E. Barr ex Minter, Hawksworth & Eriksson, Systema Ascomycetum 5(1), 182 (1986)
Rhytismataceae Chevall., Flore Générale des Environs de Paris 1, 439 (1826)

Index Fungorum number: IF 81352; Facesoffungi number: FoF 05946

Tryblidiopsis P. Karst., Bidrag till Kännedom av Finlands Natur och Folk 19, 262 (1871)

Index Fungorum number: IF 5622; Facesoffungi number: FoF 07721

The genus *Tryblidiopsis* comprises four species: *Tryblidiopsis magnesia, T. sichuanensis, T. pinastri,* and *T. sinensis* (Tanney & Seifert 2019). Species within *Tryblidiopsis* are characterized by black apothecia with a covering layer, a covering layer that opens at maturity, filiform hyaline paraphyses, 8-spored asci, and ovoid, ellipsoid, or fusoid ascospores with obvious gelatinous sheaths (Wang et al. 2014, Tanney & Seifert 2019). In this study, we introduce a new species, *T. xizangensis*, from Xizang. An updated phylogeny for *Tryblidiopsis* and closely related taxa is shown in Fig. 38.

Tryblidiopsis xizangensis H.L. Su, K.D. Hyde & Q. Zhao, sp. nov.

Index Fungorum number: IF 903735; Facesoffungi number: FoF 17665 Fig. 39

Etymology – Refers to the type locality, Xizang, in China.

Saprobic on stems. Sexual morph: *Apothecia* 1.5−2 mm in diam ($\overline{x}$ = 1.7 µm, n = 5), 1−2 mm high ($\overline{x}$ = 1.2 µm, n = 5) when dry, scattered to partly gregarious, superficial, erumpent from the bark, cupulate, leathery, and sessile to shortly stipitate. *Disc* a slightly concave surface with a slightly rough, black covering layer (covering stroma) before maturity. *Covering stroma* opened by irregular splits to expose a light brown hymenium. *Margin* involute, slightly rough, black. *Receptacle* cupulate, slightly rough, black. *Stipe* up to 0.8 mm in diam., 0.5−1 mm long when dry, obvious in young ascomata, inconspicuous in mature ascomata. *Covering stroma* 50–70 µm ($\overline{x}$ = 60 µm, n = 10) thick, black, consisting of an outer layer 30–60 µm ($\overline{x}$ = 37 µm, n = 10) thick of carbonaceous, brown, thick-walled cells of *textura angularis*, 5.5–11 × 3.5–6 µm ($\overline{x}$ = 8.3 × 4.8 µm, n = 50) and an inner layer 30–55 µm ($\overline{x}$ = 39 µm, n = 10) thick of hyaline, thin-walled cells of *textura angularis*, 5.5–10 × 3–7.5 µm ($\overline{x}$ = 7.9 × 4.8 µm, n = 50). *Hymenium* 150–185 µm ($\overline{x}$ = 163 µm, n = 10), concave, surface slightly rough, light brown. *Medullary excipulum* 210–310 µm ($\overline{x}$ = 245 µm, n = 10) thick, hyaline, comprised of hyaline branching hyphae of *textura intricata*, filled with gel, 2.6–4.5 µm ($\overline{x}$ = 3.5 µm, n = 70) in diameter. *Ectal excipulum* 30–50 µm ($\overline{x}$ = 41 µm, n = 5) thick, consisting of an outer layer 10–30 µm ($\overline{x}$ = 17 µm, n = 15) thick of carbonaceous, brown, thick-walled cells of *textura angularis*, 6–11.5 × 4.2–8.3 µm ($\overline{x}$ = 7.9 × 6 µm, n = 50) and an inner layer 20–35 µm ($\overline{x}$ = 26 µm, n = 15) thick of hyaline, thin-walled cells of *textura angularis*, 4.6–9.7 × 3.5–6.5 µm ($\overline{x}$ = 7.2 × 4.9 µm, n = 65). *Paraphyses* 1.8–3.1 µm ($\overline{x}$ = 2.4 µm, n = 40) thick, equal to asci, filiform, slightly curved, septate, hyaline, thin-walled, slightly rough,

with swollen, obtuse apical cell and the lower cell in the septum, 3.3–7.4 µm ($\overline{x}$ = 4.8 µm, n = 45) thick. *Asci* 85–120(–135) × 13–21 µm ($\overline{x}$ = 105 × 16 µm, n = 51), clavate, straight to slightly curved, inoperculate, unitunicate, aporhynchous, 8-spored, hyaline, inamyloid, filled with gel and ascospores, with obtuse apexes and slightly tapered bases. *Ascospores* (55/3/2) (17.0–)18.5–27.5(–28.0) × 5.5–8.0(–8.5) µm, ($\overline{x}$ = 22.7 × 6.8 µm, Q =2.0–4.5, Q = 3.4±0.44), partially biseriate, fusiform, one-septate or aseptate, thin-walled, hyaline, rough with some small and/or two large oil guttules, with slightly acute ends, with 1.5–3 µm thick gelatinous sheaths, some septum median with constrictions. Asexual morph**:** undetermined.

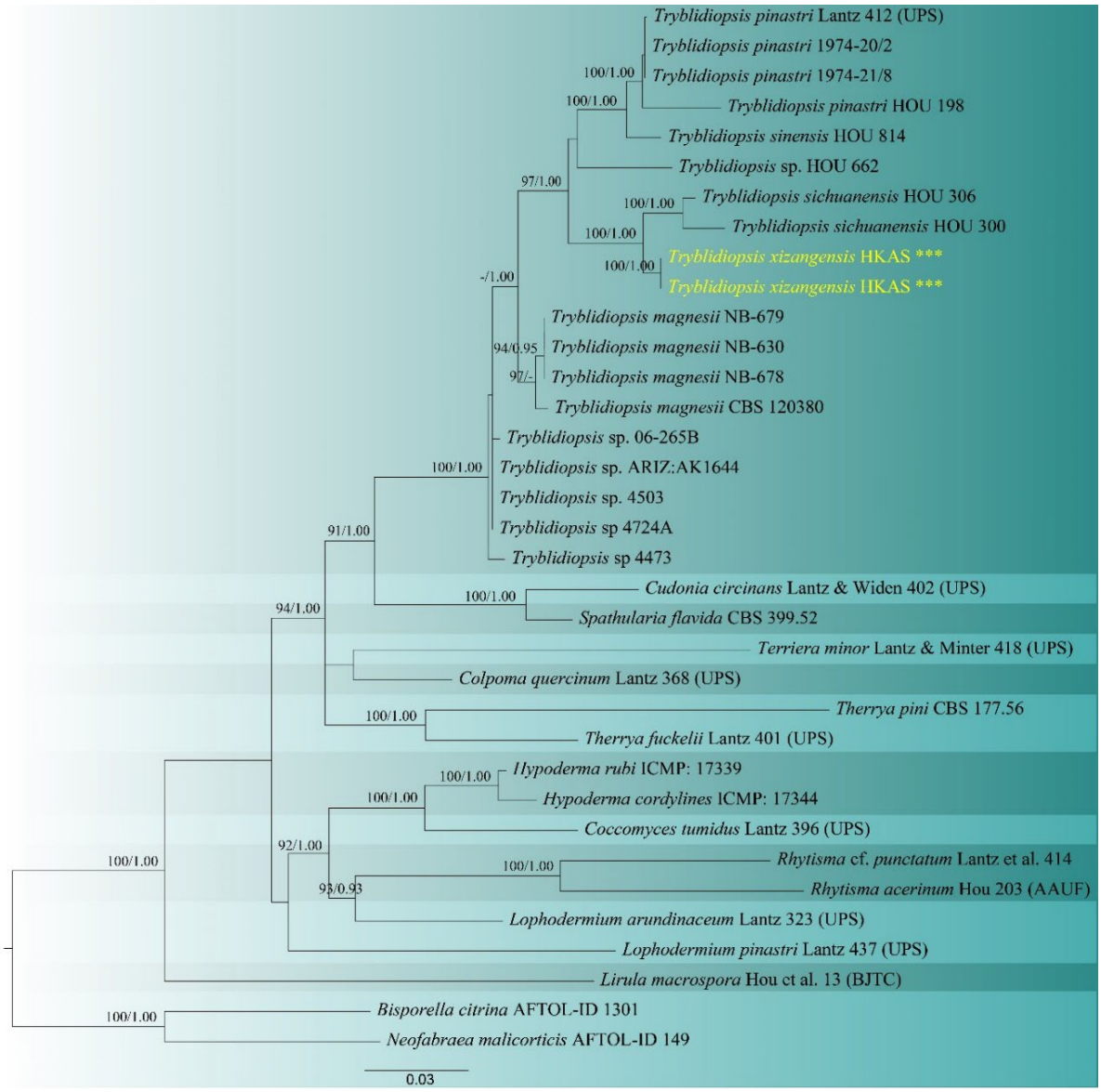

Fig. 38 – Maximum likelihood consensus tree inferred from the combined ITS and LSU sequence alignments. Bootstrap support values for maximum likelihood (ML, first value) of ≥ 90% and Bayesian posterior probabilities of ≥ 0.90 are indicated above the nodes. The tree is rooted to *Bisporella citrina* (AFTOL-ID 1301) and *Neofabraea malicorticis* (AFTOL-ID 149). The newly generated sequences are indicated in red.

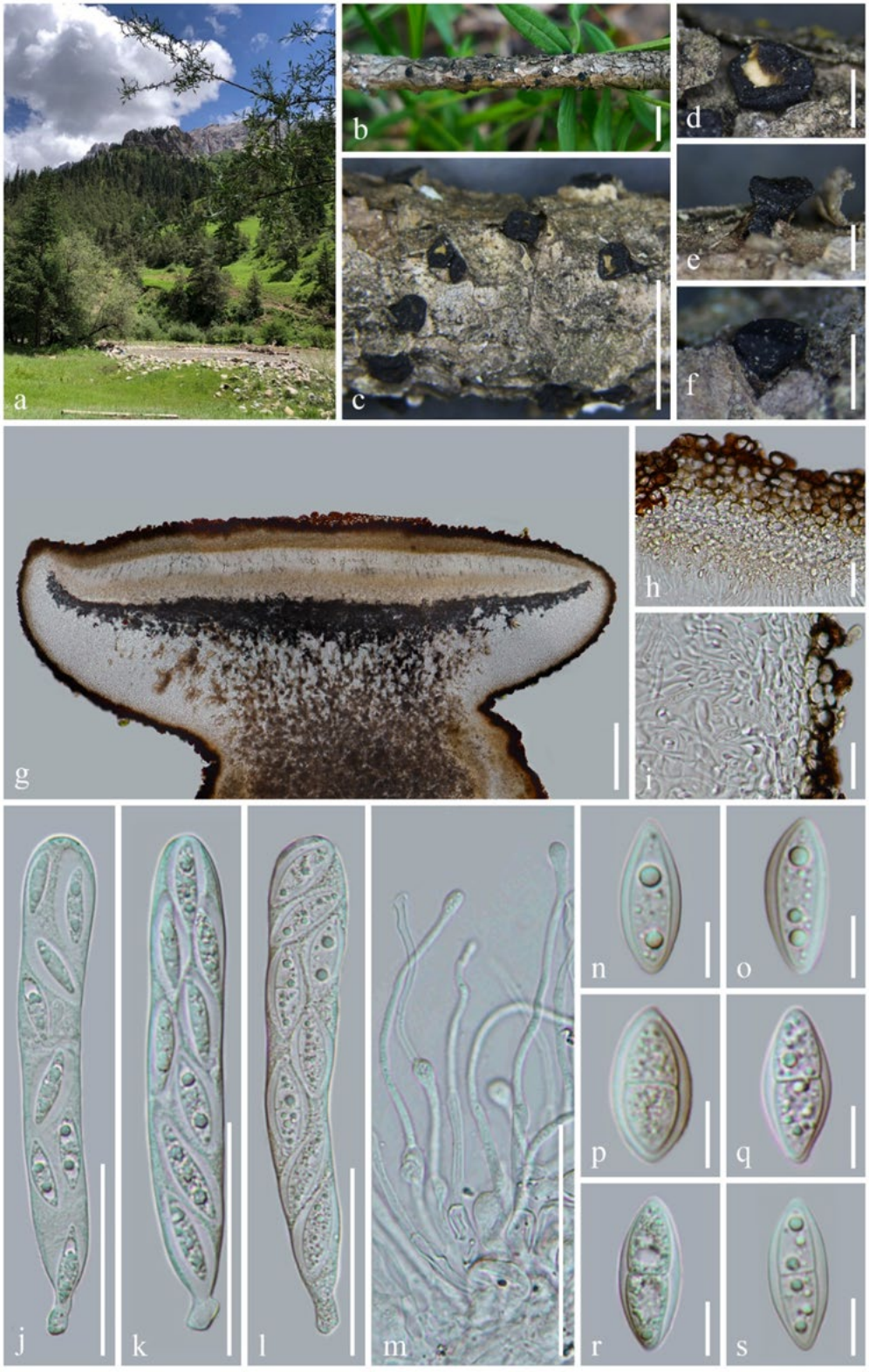

Fig. 39 – ***Tryblidiopsis xizangensis*** (HKAS 46093, **holotype**). a Habitat. b–f Dry and fresh apothecia. g Vertical section of the apothecium. h Covering stroma. i Ectal and medullary excipulum. j–l Asci. m Paraphyses. n–s Ascospores. Scale bars: b = 1 cm, c = 5 mm, d–f = 1 mm, g = 200 µm, h, i = 20 µm, j–m = 50 µm, n–s = 10 µm.

Material examined – China, Xizang, on stems of an unidentified tree, 23 June 2022, Hongli Su SHL 1144 (HKAS 146093, holotype); *ibid*., 21 June 2022, Hongli Su SHL 1085 (HKAS 146094, paratype).

GenBank accession numbers – HKAS 146093: ITS: PV455904, LSU: PV604181; HKAS 146092: ITS: PV455905, LSU: PV604182.

Notes – *Tryblidiopsis xizangensis* is characterized by black apothecia with a black covering layer that opens through irregular splits at maturity, exposing a light brown hymenium when mature, filiform, hyaline paraphyses with a swollen apical cell and the lower cell in the septum, clavate, 8-spored, hyaline asci, fusiform, one-septate or aseptate, hyaline ascospores with some oil guttules and gelatinous sheaths. The species is the only one among the *Tryblidiopsis* species with swollen lower cells in the septum. Additionally, our phylogenetic tree revealed that *T. xizangensis* is a sister to *T. sichuanensis*, with 100% MLBS and 1.00 BPP support. However, they are distinguished by the presence of paraphyses; *T. sichuanensis* lacks paraphyses but has swollen lower cells in the septum.

Class *Sordariomycetes* O.E. Erikss. & Winka, Myconet 1, 10 (1997)

Subclass *Diaporthomycetidae* Senan., Maharachch. & K.D. Hyde, Fungal Diversity 72, 208 (2015)

Index Fungorum number: IF 551051; Facesoffungi number: FoF 00594

Diaporthales Nannf., Nova Acta Regiae Societatis Scientiarum Upsaliensis 8, 53 (1932)

Index Fungorum number: IF 90468; Facesoffungi number: FoF 00593

Diaporthe Nitschke, Pyrenomycetes Germanici 2, 240 (1870)

Index Fungorum number: IF 92244; Facesoffungi number: FoF 00146

Diaporthe (*Diaporthaceae*, *Diaporthales*, *Sordariomycetes*) was established by Fuckel in 1861 and is typified by *Diaporthe alnea* (Wijayawardene et al. 2022b, Index Fungorum, 2025). *Diaporthe* is a genus that comprises important plant pathogens, endophytes, and saprobes and is widely distributed, often associated with economically important plants (Hyde et al. 2014, Norphanphoun et al. 2022). Phylogenetic analyses based on ITS, *cmdA*, *tef1-α*, *β-tubulin*, and *his3* sequence data revealed that *Diaporthe* comprises 13 species complexes and nine singleton species (Norphanphoun et al. 2022). Due to overlapping morphological characters and the cryptic nature of the genus, morphological identification alone is insufficient for precise identification (Norphanphoun et al. 2022, Dissanayake et al. 2024). An updated phylogeny for *Diaporthe* and closely related taxa is shown in Fig. 40.

Diaporthe rosae Samarakoon & K.D. Hyde, Wanasinghe et al., Fungal Diversity 89, 185 (2018)

Index Fungorum number: IF 554072; Facesoffungi number: FoF 03922 Fig. 41

Associated with a leaf spot of *Oroxylum indicum*. Sexual morph: Undetermined. Asexual morph: *Conidiomata* pycnidial, globose to oval, solitary on the host, solitary or aggregated in culture (PDA), semi-immersed, dark brown to black. *Peridium* paraenchymatous, pale brown. *Conidiophores* reduced to conidiogenous cells. *Conidiogenous cells* 7–10 × 2–4 µm ($\overline{x}$ = 8.5 × 2.5 µm, n = 15), cylindrical to ampulliform, tapering towards the apex with periclinal thickening. *Alpha conidia* 5.3–6.7 × 2–3 µm ($\overline{x}$ = 6.2 × 2.5 µm, n = 20), smooth-walled, hyaline, unicellular, and sub-oval to ellipsoidal with bi-guttulate. *Beta conidia* 13–17 × 1–2 µm ($\overline{x}$ = 15 × 1.4 µm, n = 20), hyaline, unicellular, filiform, hook-shaped, with a thicker middle and becoming thinner towards the ends.

Culture characteristics – Colonies on PDA reaching 67–79 mm diam., after incubation at 28°C for 7 days. *Aerial mycelia* fluffy, circular, with entire margins, medium in density, white with emerging dark pigmentation spots, and the production of enormous black stromata on PDA with age, reverse yellow.

Material examined – Thailand, Chiang Rai Province, Phan District, symptomatic on a leaf of *Oroxylum indicum*, 27 September 2021, A. Armand, T38 (MFLU 23-0084), living culture (MFLUCC 23-0056).

GenBank accession number – ITS: OQ919268, *tef1-α*: OQ925954, *β-tubulin*: OQ925955, *CAL:* OQ925953,

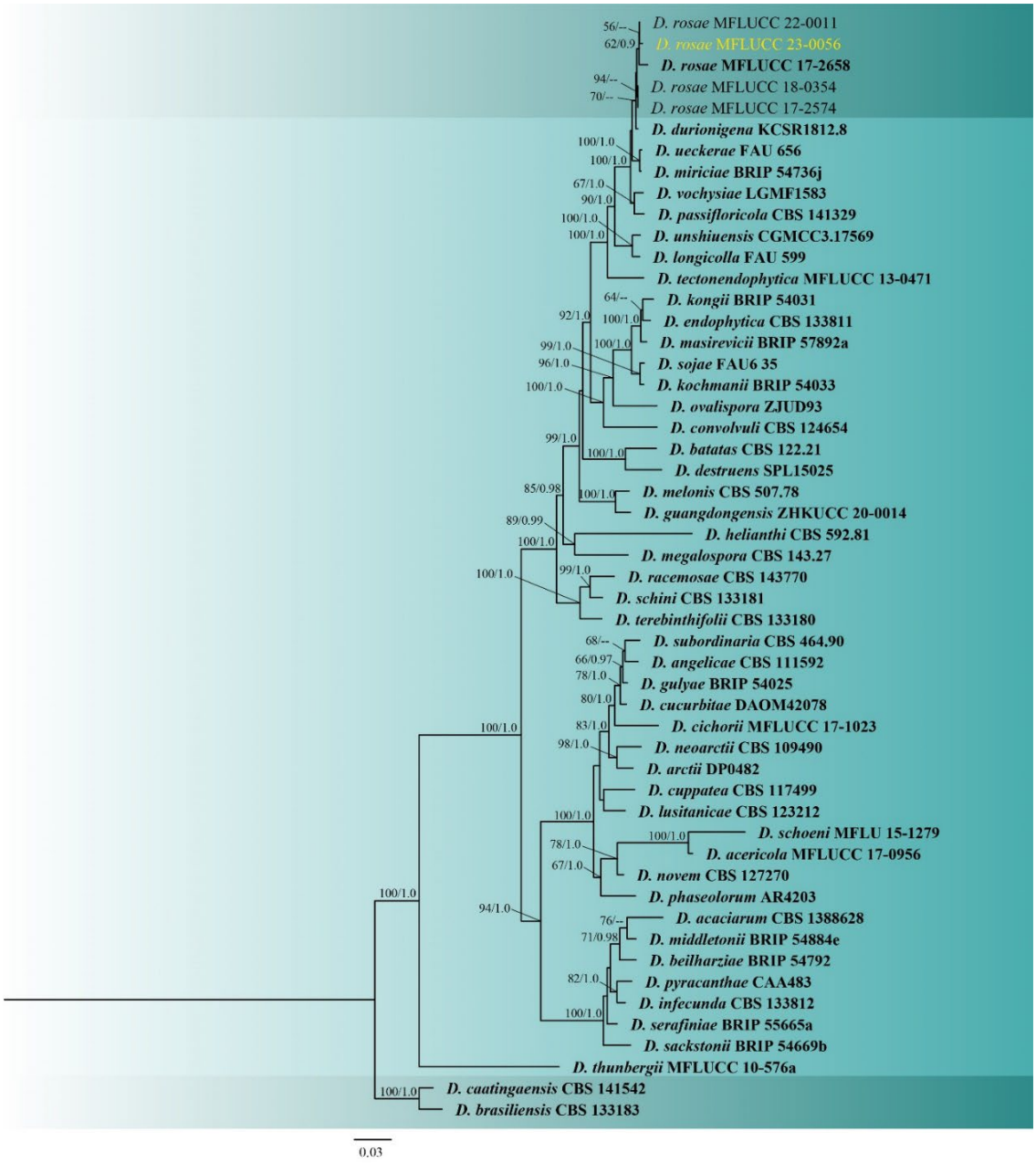

Fig. 40 – Phylogenetic tree generated from maximum likelihood analysis based on a combined ITS, *cmdA*, *tef1-α*, and *β-tubulin* sequence data of *Diaporthe* taxa. Fifty-two strains were included in the combined analyses, which comprised 2,140 characters (575 characters for ITS, 511 characters for *cmdA*, 355 characters for *tef1-α*, and 699 characters for *β-tubulin*) after alignment. The tree topology of the maximum likelihood analysis is similar to that of the Bayesian analysis. The best RAxML tree with a final likelihood value of -15880.006904 is presented. The matrix contained 1,053 distinct alignment patterns, with 22.28% of the characters being undetermined or gaps. The evolutionary models applied to ITS, CAL, *tef*1-α, and β-tubulin genes are TrN+I+G, HKY+G, GTR+I+G, and HKY+G, respectively. Bootstrap support values for ML ≥ 50% (left) and Bayesian posterior probabilities ≥ 0.90 (right) are given near nodes, respectively. The tree is rooted with *Diaporthe caatingaensis* (CBS 141542) and *D. brasiliensis* (CBS 33183). Ex-type strains are in bold. The newly generated sequences are indicated in yellow.

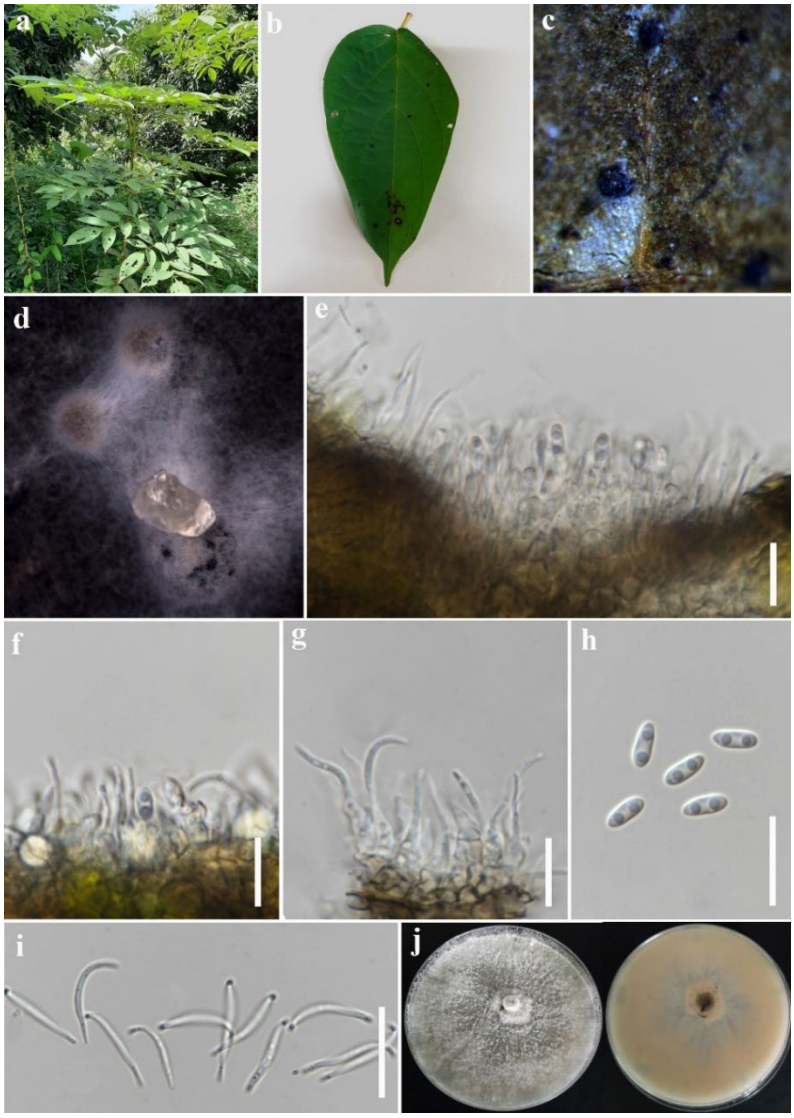

Fig. 41 – *Diaporthe rosae* (MFLU 23-0084, **a new host record**). a Host plant. b Infected leaf. c Fruiting bodies on the host. d Fruiting bodies on the PDA. e–g Conidiogenous cells and conidial attachment. h Alpha conidia. i Beta conidia. j Upper and reverse sides of culture. Scale bars: e–i = 10 µm.

Known distribution (based on molecular data) – Thailand (Perera et al. 2018, Wanasinghe et al. 2018, Huanraluek et al. 2022).

Known hosts (based on molecular data) – *Rosa* sp. (Wanasinghe et al. 2018), *Magnolia champaca* (Perera et al. 2018), *Senna siamea* (Perera et al. 2018), *Nephelium lappaceum* (Huanraluek et al. 2022).

Notes – *Diaporthe rosae* was described on *Rosa* sp. from Thailand (Wanasinghe et al. 2018). The morphological study showed that our strain is similar to *D. rosae* (MFLU 17-1550, holotype). However, our strain (MFLU 23-0084) produced smaller conidiogenous cells (7–10 × 2–4 µm in MFLU 23-0084 *vs.* 7.7–15 × 1.2–2.3 µm in MFLU 17-1550), alpha conidia (5.3–6.7 × 2–3 µm in MFLU 23-0084 *vs.* 5.5–7.5 × 2–3 µm in MFLU 17-1550), and beta conidia (13–17 × 1–2 µm in MFLU 23-0084 *vs.* 12.5–18 × 1–2 µm in MFLU 17-1550) than those of the type strain (Wanasinghe et al. 2018). Combined multi-gene analyses of ITS, *cmdA*, *tef1-α*, and *β-tubulin* revealed that our strain clustered with the ex-type strain of *D. rosae* (MFLUCC 17–2658), exhibiting moderate bootstrap support (62/0.9 ML/PP).

Subclass *Hypocreomycetidae* O.E. Erikss. & Winka, Myconet 1, 6 (1997)

Index Fungorum number: IF 501501; Facesoffungi number: FoF 06512

Fuscosporellales Jing Yang, Bhat & K.D. Hyde, Cryptogamie, Mycologie 37(4): 457 (2016)

Index Fungorum number: IF 552288; Facesoffungi number: FoF 02420

Fuscosporellaceae Jing Yang, Bhat & K.D. Hyde, Cryptogamie, Mycologie 37(4), 457 (2016)

Index Fungorum number: IF 552321; Facesoffungi number: FoF 02421

Mucispora Jing Yang, Bhat & K.D. Hyde, Cryptogamie, Mycologie 37(4), 466 (2016)

Index Fungorum number: IF 552293; Facesoffungi number: FoF 02427

Mucispora was established by Yang et al. (2016) with *Mucispora obscuriseptata* as the type species, based on phylogenetic analyses of three combined loci (LSU, SSU, and *rpb2*). Its asexual morphs are characterized by hairy, dark-coloured colonies. Macronematous and mononematous conidiophores; monoblastic, terminal, and cylindrical conidiogenous cells; and ellipsoidal or obovoid dark brown conidia with septa (Yang et al. 2016, 2017, Wijayawardene et al. 2021, Du et al. 2022). To date, the genus *Mucispora* comprises five species: *M. aquatica*, *M. hydei*, *M. infundibulate*, *M. obscuriseptata*, and *M. phangngaensis*. These species are distributed in southern Thailand and southern China, where they live as saprobes on decaying plant substrates submerged in freshwater (Yang et al. 2016, 2017, Hyde et al. 2020, Wijayawardene et al. 2021, Du et al. 2022). An updated phylogeny for *Mucispora* and closely related taxa is shown in Fig. 42.

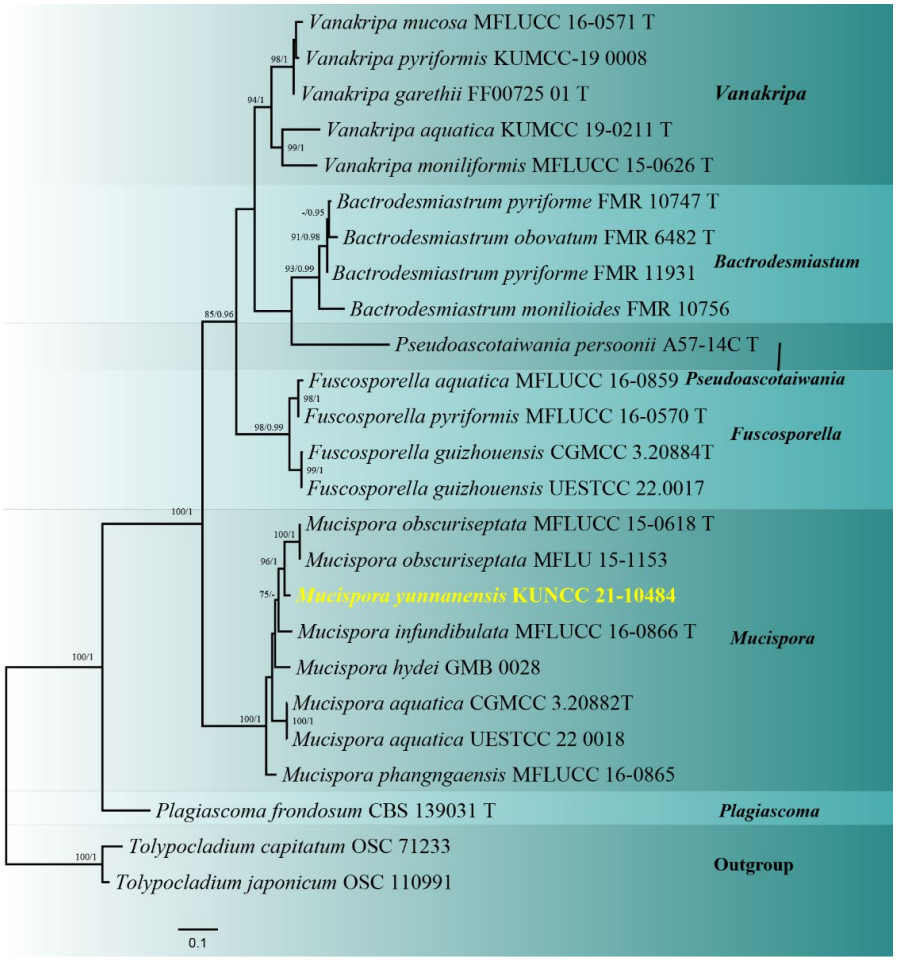

Fig. 42 – Phylogram generated from maximum likelihood analysis based on the combined ITS and LSU sequence data representing the species of *Mucispora* and related taxa. Twenty-six taxa were included in the combined locus alignment that comprised 1,539 characters (LSU: 860, ITS: 679). The best-scoring

RAxML tree with a final likelihood value of -8442.483633 is presented. The matrix contained 708 distinct alignment patterns, with 22.50% of the characters being undetermined or gaps. Estimated base frequencies were as follows: A = 0.218444, C = 0.272182, G = 0.305182, T = 0.204192; substitution rates: AC = 0.853288, AG = 1.693761, AT = 1.290766, CG = 0.450657, CT = 4.396922, GT = 1.0; Bootstrap support values for ML equal to or greater than 75% and BI equal to or greater than 0.95 are given above the nodes. *Tolypocladium capitatum* (OSC 71233) and *T. japonicum* (OSC110991) were used as the outgroup taxa. The newly generated sequence is indicated in yellow bold. The abbreviation T indicates the ex-type strain.

Mucispora yunnanensis R.J. Xu, L. Lei, K.D. Hyde & Q. Zhao, sp. nov.

Index Fungorum number: IF903562; Facesoffungi number: FoF 17300 Fig. 43

Etymology – The epithet "yunnanensis" refers to the type locality, Yunnan Province.

Saprobic on decaying wood in freshwater habitats. Sexual morph: Undetermined. Asexual morph: *Colonies* on natural substrate are effuse, glistening, and black. *Mycelium* partly immersed and partly superficial, consisting of septate, hyaline, and pale brown to brown. *Conidiophores* 70−131 × 5−7 µm ($\overline{x}$ = 96 × 6 µm, n = 15), macronematous, mononematous, solitary, erect, smooth, brown, paler towards the apex, straight or broadly curved, septate, with 2–3 percurrent proliferations. *Conidiogenous cells* 9−13 × 4−7 µm ($\overline{x}$ = 10 × 6 µm, n = 15), monoblastic, integrated, terminal, cylindrical, pale brown to brown, sometimes with successive proliferation. *Conidia* 25−33 × 13−17 µm ($\overline{x}$ = 27 × 15 µm, n = 25), acrogenous, ellipsoidal, obovoid or pyriform, subhyaline when young, rounded at the apex and truncate at the base, smooth, dark brown to black, septate with dark bands, mostly 2-septate and becoming invisible when mature, rarely covered by a hyaline mucilaginous sheath.

Culture characteristics − Conidia germinated on water agar after incubation at room temperature for 24 hours, and germ tubes were produced from basal cells. Colonies growing on PDA reached 8−10 mm in diameter after incubation at 25℃ for 30 days, with light grey to dark grey to brownish grey, dense mycelia on the surface, the centre elevated, and reverse dark grey to brownish grey.

Material examined − China, Yunnan Province, Xishuangbanna, Menghai County, on decaying wood submerged in a freshwater stream, 16 Aug 2021, R.J. Xu, MD-14 (HKAS 131210, holotype); ex-type living culture (KUNCC 21-10484).

GenBank accession numbers – ITS: PV037425, LSU: PV037426.

Notes − *Mucispora yunnanensis* closely resembles *M. aquatica*, *M. infundibulata*, *M. obscuriseptata*, and *M. phangngaensis* in having dark brown to black colonies, macronematous, mononematous, solitary, erect, smooth conidiophores, and ellipsoidal to obovoid conidia with prominent septa when young. However, *M. yunnanensis* can be distinguished from *M. obscuriseptata* by its smaller conidial size (25−33 × 13−17 µm vs. 29−41 × 16−22 µm) (Yang et al. 2016). In addition, a comparison of LSU sequences shows that *M. yunnanensis* (KUNCC 21-10484) differs from *M. obscuriseptata* (MFLUCC 15-0618) by 21/860 bp (2.4%, excluding gap). In comparison, ITS sequences differ by 34/679 bp (5%, excluding gaps) (Jeewon & Hyde 2016). In terms of conidiophore size, *M. yunnanensis* (70−131 × 5−7 µm) has larger conidiophores than *M. infundibulata* (50–65 × 4–6 µm) but smaller than *M. phangngaensis* (170–305 × 5–7 µm) (Yang et al. 2017, Hyde et al. 2020). Furthermore, *M. yunnanensis* is distinguished from *M. aquatica* by the presence of a conidial sheath, which is absent in *M. aquatica* (Du et al. 2022). Phylogenetically, our new taxon, *M. yunnanensis*, forms a well-supported lineage and nests within a clade that includes *M. aquatica*, *M. hydei*, *M. infundibulata*, *M. obscuriseptat*a, and *M. phangngaensis* (Fig. 42).

Glomerellales Chadef. ex Réblová, W. Gams & Seifert, Studies in Mycology 68, 170 (2011)

Index Fungorum number: IF 515429; Facesoffungi number: FoF 09687

Glomerellaceae Locq. ex Seifert & W. Gams, Zhang et al., Mycologia 98(6), 1083 (2007)

Index Fungorum number: IF 504454; Facesoffungi number: FoF 01100

Colletotrichum Corda, Deutschlands Flora in Abbildungen nach der Natur. Dritte Abteilung 3(12), 41 (1831)

Index Fungorum number: IF 7737; Facesoffungi number: FoF 00144

Colletotrichum is a genus within *Glomerellaceae* (Hyde et al. 2020). *Colletotrichum* was introduced by Corda (1831) to accommodate *C. lineola*. Members of this genus are important plant pathogens that cause anthracnose on cosmopolitan hosts worldwide (Cannon et al. 2012, Jayawardena et al. 2020, 2021, Talhinhas & Baroncelli 2021). *Colletotrichum* species are largely asexual, but some have a sexual morph (*Glomerella*) that can be either homothallic or heterothallic (Talhinhas & Baroncelli 2021). These species are characterised by a distinctive hemibiotrophic lifestyle (Jayawardena et al. 2021). There are 344 species and 20 species complexes accepted in *Colletotrichum* (Talhinhas & Baroncelli et al. 2023). An updated phylogeny for *Colletotrichum* and closely related taxa is shown in Fig. 44.

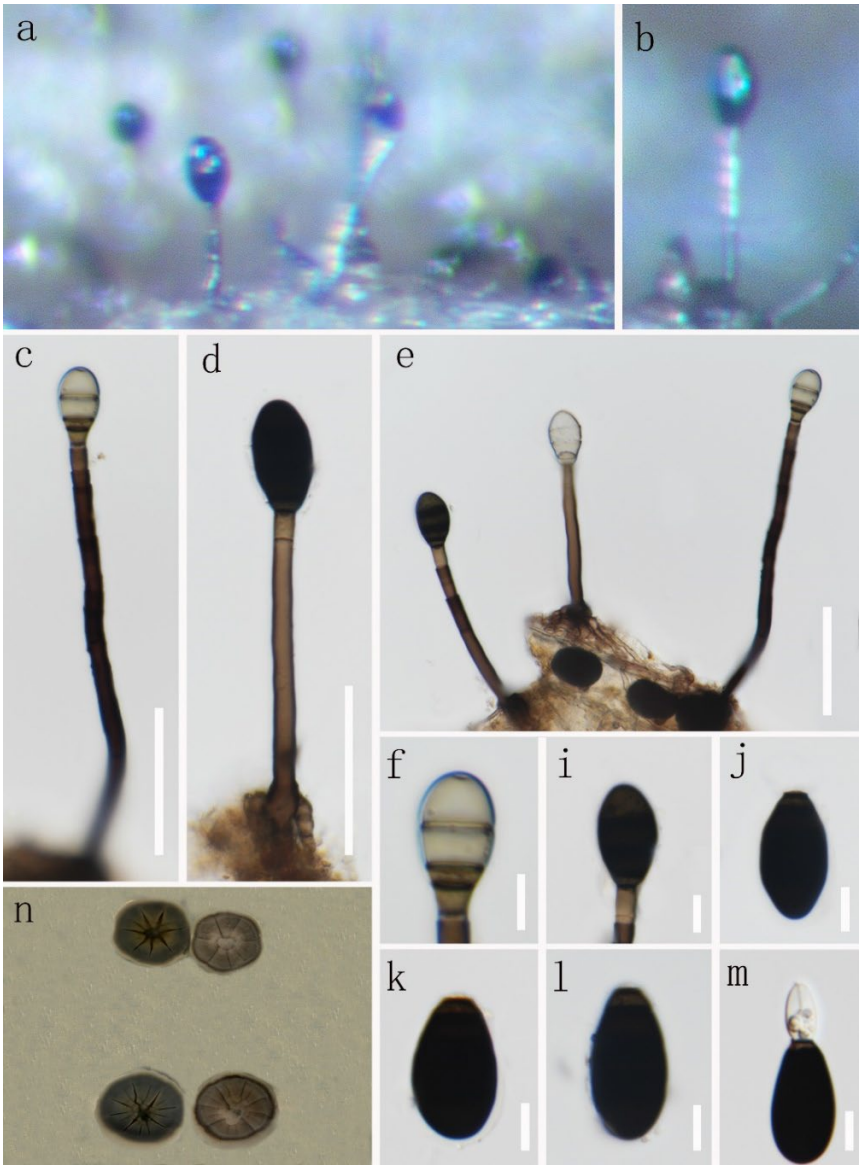

Fig. 43 – *Mucispora yunnanensis* (HKAS 131210, **holotype**). a, b Submerged colonies. c–e Conidiophores, conidiogenous cells with conidia. f–l Conidia. m Germinated conidium. n Colony on PDA. Scale bars: c–e = 50 µm, f–m = 10 µm.

Fig. 44 – Phylogenetic tree obtained from maximum parsimony analysis of a combined ITS, *actin*, *chs-1*, *gapdh*, and *tub2* sequence dataset representing the *Colletotrichum gloeosporioides* species complex.

Ninety-nine strains were included in the combined analyses, which comprised 2,115 characters, of which 1,276 characters were constant, 522 were parsimony-informative, and 317 were parsimony-uninformative. Bootstrap support values for maximum likelihood (ML) and maximum parsimony (MP) ≥ 50% and Bayesian Posterior Probabilities (PP) ≥ 0.90 are indicated at the nodes as ML/MP/PP. The tree is rooted in *C. acidae* (MFLUCC 17-2659) and *C. truncatum* (CBS151.35). The ex-type strains are in bold, and the new isolates of this study are in yellow.

Colletotrichum siamense Prihast., L. Cai & K.D. Hyde, Prihastuti et al., Fungal Diversity 39, 98 (2009)

Index Fungorum number: IF 515410; Facesoffungi number: FoF 03599 Fig. 45

Pathogenic on *Barringtonia asiatica* leaves. Sexual morph: Not observed. Asexual morph: *Conidiomata* pycnidial, solitary, black, sub-globose to globose, semi-submerged, bearing conidial mass. *Conidia* 7.5–18 × 3–4 µm ($\overline{x}$ = 10 ± 1.75 × 3.45 ± 0.45 µm, n = 30), aseptate, hyaline, smooth, uni- to biguttulate, round to cylindrical, apex subrounded to rounded. On PDA: *Conidiophores* rarely observed as hyaline, septate, unbranched, cylindrical to inflated, straight or slightly curved, tapering towards the apex. *Conidiogenous cells* are cylindrical to round, hyaline, smooth, and thin-walled. *Appressoria* pale brown to brown, ovoid, undulate, irregular shape with age, 4.5–8 × 3.5–5 µm ($\overline{x}$ = 6.50 ± 1.15 × 4.10 ± 0.45, n = 10), produced on hyphae and conidia.

Culture Characteristics – Colonies on PDA media, reaching 8.5 cm in diam., when incubated at room temperature (28 ± 2°C) for 7 days, produce white to grey, raised mycelium with an entire (smooth) margin. The reverse is initially white and becomes off-white to yellowish. Aerial mycelium is greyish-white and cottony, with some visible conidial masses.

Material examined – Thailand, Sam Roi Yot District, isolated from symptomatic leaves of *Barringtonia asiatica*, 3 Feb 2023, Herbert Dustin Aumentado, MFLU23-0457, living culture MFLUCC 23-0288.

GenBank accession number – MFLU23-0457: ITS: OR898233, *tub2*: OR900456, *gapdh*: OR900455, *chs-1*: OR900454, *act:* OR900452.

Known distribution – Cosmopolitan (Farr & Rossman 2025, this study).

Hosts – Various hosts (Farr & Rossman 2025), *Barringtonia asiatica* (this study).

Notes – *Colletotrichum siamense* (MFLU23-0457) was isolated directly from a symptomatic leaf of *B. asiatica*. Phylogenetic analysis (Fig. 44) placed *C. siamense* MFLU23-0457 within the *C. siamense* strains with 73/–/0.90 ML, MP, and PP values, respectively. A single-gene comparison of *actin*, *chs-1*, *gapdh*, ITS, and *tub2* between our isolate *C. siamense* (MFLU23-0457) and the type strain *C. siamense* (ICMP18578) revealed minor base pair differences of 9/593 (1.51%), 1/255 (0.39%), 0/298 (0%), 1/277 (0.36%), and 6/402 (1.49%), respectively. Comparison of base pair differences of *actin*, *chs-1*, *gapdh*, ITS, and *tub2* were also done with the type strains of *C. pandanicola*: 3/593 (0.50%), 3/255 (1.17%), 4/298 (1.34%), 1/277 (0.36%), 0/402 (0%) and *C. parvisporum*: 8/593 (1.34%), 1/255 (0.39%), 1/298 (0.35%), 3/277 (1.08%), 2/402 (0.50%) which are synonyms of *C. siamense*. Morphological comparison with the ex-type strain of *C. siamense* showed closely similar conidial dimensions (7.5–18 × 3–4 µm *vs.* 7–18.3 × 3–4.3 µm) and appressoria (4.5–8 × 3.5–5 µm *vs.* 4.7–8.3 × 3.5–5 µm), with no significant differences observed between the ex-type strain and our isolate (MFLUCC 23-0288). Pathogenicity tests confirmed that *C. siamense* (MFLUCC 23-0288) is pathogenic on both wounded and non-wounded *Barringtonia asiatica* leaves, producing brown necrotic lesions. Conidiomata formation was observed starting from seven days post-inoculation. The identical isolate was re-isolated from the infected sites, thus establishing Koch's postulate. No infection was observed in control treatments (Fig. 46). The study presents a new host record and confirms the pathogenicity of *C. siamense* on *Barringtonia asiatica* in Thailand.

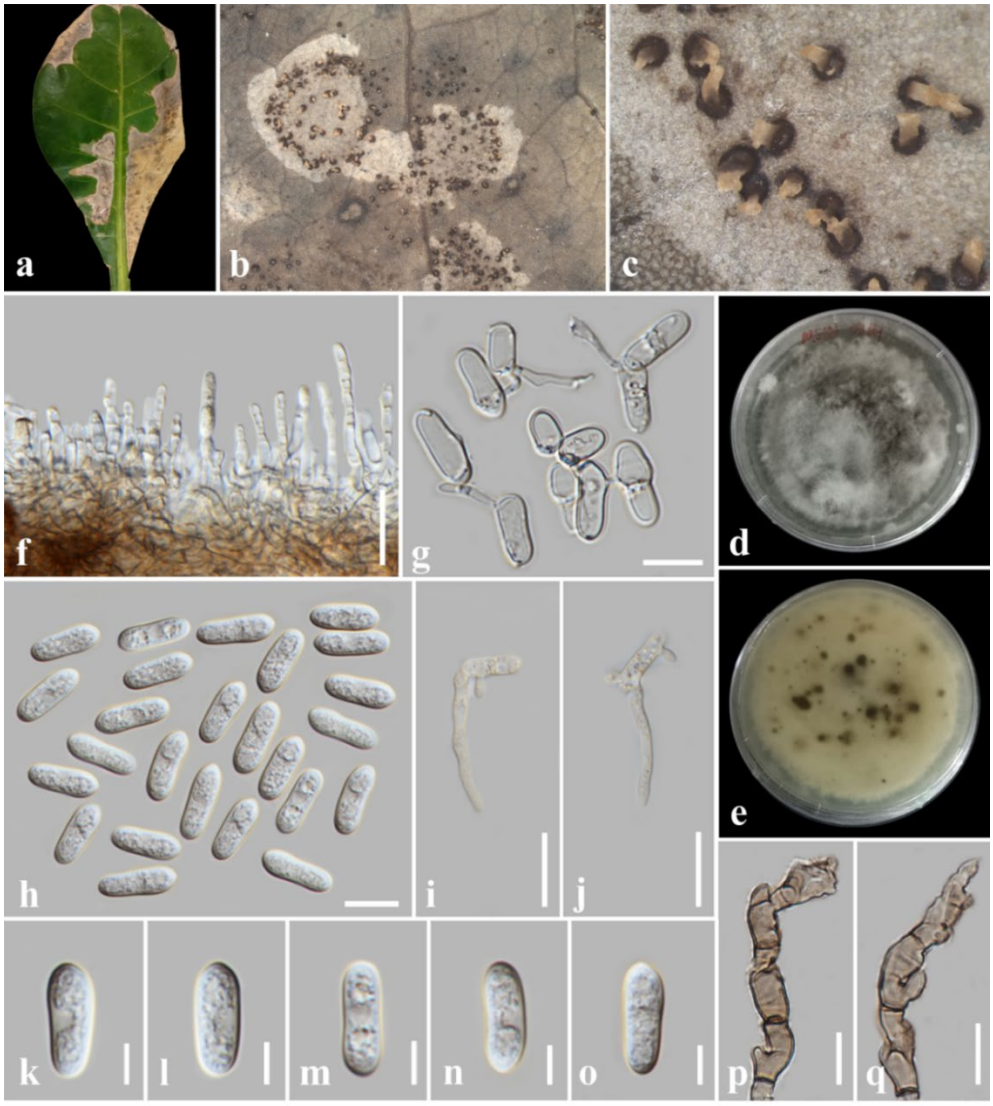

Fig. 45 – *Colletotrichum siamense* (MFLU23-0457, **a new host record**). a Lesions on *Barringtonia asiatica* leaf. b, c Conidiomata oozing orange spore masses on the leaf surface. d, e Colony on PDA at 1-month post-incubation (obverse, reverse). f Conidiophores and conidiogenous cells. g Conidial anastomosis. h, k–o Conidia. i, j Germinating conidia. p, q Appressoria. Scale bars: f = 20 µm, g–j, p–q = 10 µm, k–o = 5 µm.

Colletotrichum subacidae F. Liu, Z.Y. Ma & L. Cai, Liu et al., Studies in Mycology 101, 40 (2022)

Index Fungorum number: IF 841394; Facesoffungi number: FoF 14121 Fig. 47, 48

Associated with the leaf spot of *Bauhinia* species. Sexual morph: Not observed. Asexual morph: *Vegetative hyphae* hyaline, smooth-walled, septate, and branched. *Conidiomata* acervular, dark brown, bearing conidial masses and setae. *Setae* abundant, dark brown, smooth to verruculose, 3–5 septate, 133–170(–180) µm long ($\overline{x}$ = 164 µm, n = 20), cylindrical or serrate base, 4–10 µm diam. ($\overline{x}$ = 7.5 µm, n = 20), acute or subacute at the apex. *Conidiophores* hyaline and densely clustered. *Conidiogenous cells* 15–25 × 2.5–4 µm ($\overline{x}$ = 22 × 3 µm, n = 30), hyaline and cylindrical form. *Conidia* hyaline, smooth-walled, aseptate, curved with parallel walls at the middle part, round and truncate at the base, acute and curved at the apex, guttulate, 20–28 × 2.5–3.8 µm ($\overline{x}$ = 23.5 × 3 µm, n = 30).

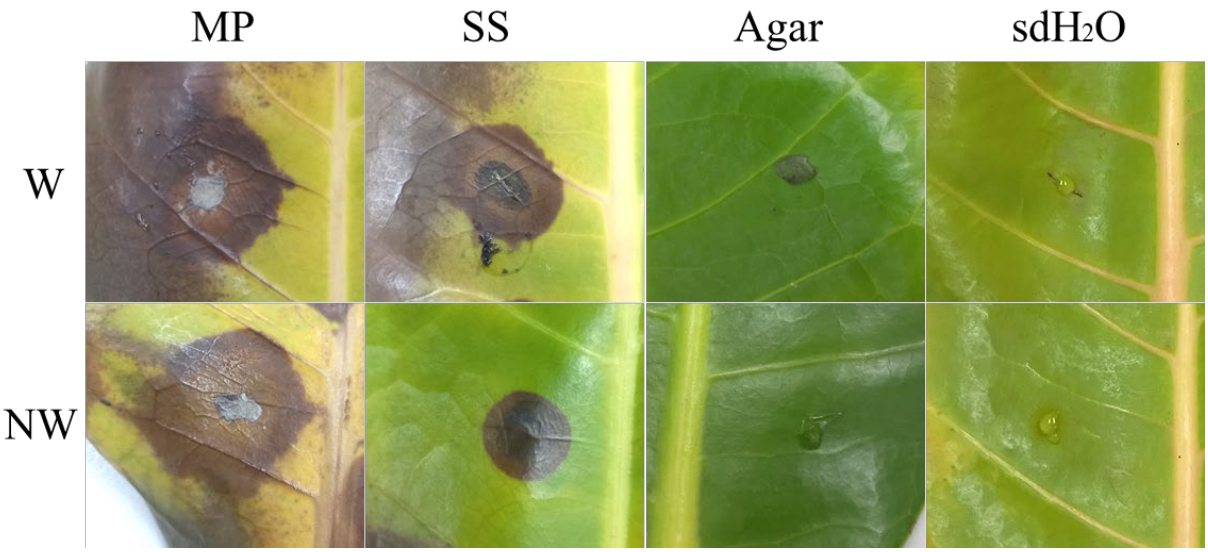

Fig. 46 – Pathogenicity testing on *Barringtonia asiatica* leaves. Symptoms at 14 days post-inoculation. Pathogen inoculations using a mycelial plug (MP) and a spore suspension (SS). W: Wounded, NW: Non-wounded. Control inoculations were done using blank agar and sterile distilled water (sdH_2O).

Culture characteristics – Colonies on PDA reaching 50–57 mm diam. After 7 days of incubation at 28°C, the aerial mycelia are velvety, circular, undulated at the margins, medium-dense, white, and becoming smoke grey with age; the reverse is the same colour. Appressoria formed in slide culture, 4–10 (−12) × 3–5 µm ($\overline{x}$ = 8.5×3.8 µm, n = 20), formed on mycelia and conidia, brown, mostly round or oval (produced by conidia), seldom slightly oblong (produced by mycelia), variable in size, appressoria complex formation present.

Material examined – Thailand, Chiang Rai Province, Muang Chiang Rai District, Tha Sud, a symptomatic leaf of Bauhinia sp., 29 December 2021, A. Armand, C32-2 (MFLU 23-0069), living culture (MFLUCC 23-0045).

GenBank accession numbers – ITS: OQ368730, *TUB2*: OQ470730, *gapdh*: OQ383226, *chs-1*: OQ383225, *actin*: OQ383224.

Known distribution (based on molecular data) – China (Liu et al. 2022).

Known hosts (based on molecular data) – *Tetrastigma obovatum*, *Asparagus officinalis*, *Hosta* sp., *Ailanthus altissima* (Liu et al. 2022).

Notes – *Colletotrichum subacidae* clusters phylogenetically with other strains of this species (Fig. 47), although it exhibits significant interspecies variation. The most phylogenetically similar species, *C. acidae*, shares low sequence similarity with *C. subacidae* at *act* (96.8%), *chs-1* (98%), *gapdh* (92.6%), and *tub2* (98%). Comparisons between the newly isolated strain (MFLUCC 23-0045) and the type strain of *C. subacidae* (LC13857) revealed sequence similarities of 98.2% for *act*, 98.6% for *chs-1*, 97.8% for *gapdh*, and 99% for *tub2*. Morphologically, *C. subacidae* (LC13857) differs from *C. acidae* in the shape and size of appressoria (oblong to subcylindrical, 8–25 × 5–8 µm *vs.* round, oval, or irregular, 11–23 × 9–18 µm), size of conidiogenous cells (9–20 × 2–4.5 µm *vs.*1–2 × 2–3.5 µm), and conidial shape of *C. acidae* conidia are more strongly curved than those of *C. subacidae* (Samarakoon et al. 2018). *Colletotrichum subacidae* (MFLUCC 23-0045) was identical to the type strain, with minor differences in the size of setae and conidia. Based on morphological comparison and phylogenetic analysis, the strain was identified as *C. subacidae*.

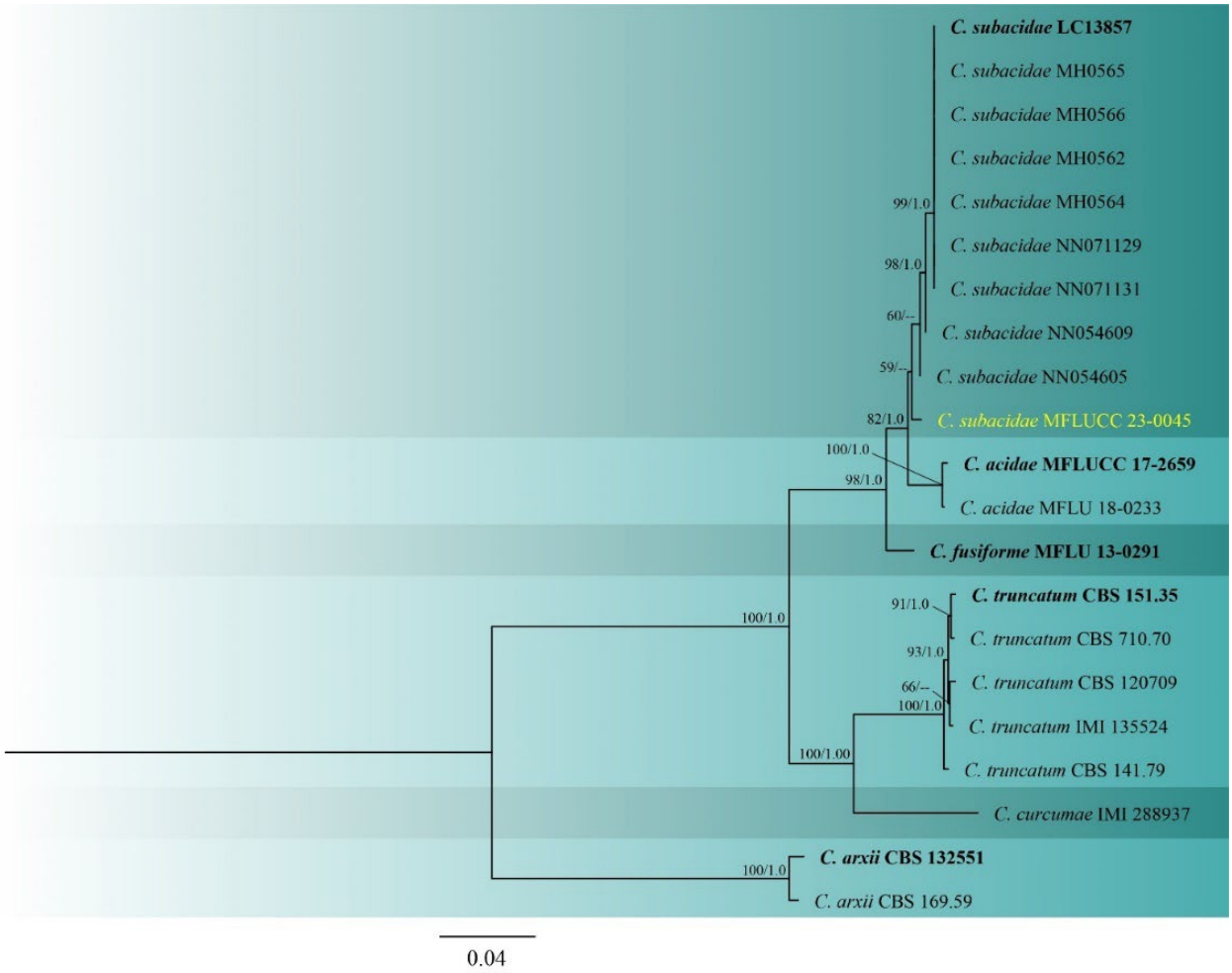

Fig. 47 – Phylogenetic tree of the *Colletotrichum truncatum* species complex based on maximum parsimony, generated by a combined ITS, *actin, chs-1, gapdh*, and *tub2* sequence data. The tree was rooted with *Colletotrichum arxii* (CBS 132511) and *C. arxii* (CBS 169.59). Maximum-likelihood bootstrap values ≥ 50% and Bayesian posterior probabilities ≥ 0.90 are shown near the nodes. Type strains are in bold, and the newly generated isolate is in yellow.

Pleurotheciales Réblová & Seifert, Réblová, Seifert, Fournier & Štěpánek, Persoonia 37, 63 (2015)
Index Fungorum number: IF 813228; Facesoffungi number: FoF 06531

Pleurotheciaceae Réblová & Seifert, Réblová, Seifert, Fournier & Štěpánek, Persoonia 37, 63 (2015)
Index Fungorum number: IF813229; Facesoffungi number: FoF 05316

Phaeoisaria Höhn., Mathematisch-naturwissenschaftliche Klasse, Abteilung 118, 330 (1909)
Index Fungorum number: IF 9305; Facesoffungi number: FoF 05521

Phaeoisaria was established by Höhnel (1909) and typified by *P. bambusae* Höhn. The genus comprises 30 species that produce indeterminate synnemata with septate or aseptate, obovoidal, ellipsoidal, fusiform-cylindrical, or falcate conidia formed on a sympodially developing rachis. Members of *Phaeoisaria* are saprobic, commonly found on decaying wood, plant debris, or soil sediments (Sutton 1973, Deighton 1974, Castañeda et al. 2002, Seifert et al. 2011, Mel'nik 2012, Cheng et al. 2014, Crous et al. 2015, Liu et al. 2015, Réblová et al. 2016). The phylogenetic tree generated in this study is shown in Fig. 49.

Fig. 48 – *Colletotrichum subacidae* (MFLU 23-0069, **a new host record**). a, b. Infected leaves. c Fruiting body on the host. d Setae formed on the host leaf. e Setae formed on PDA. f Conidiogenous cells and conidial attachment. g, h. Conidia. i Appressoria. j Upper and reverse sides of culture. Scale bars: d–f = 50 µm, g = 20 µm, h, i = 10 µm.

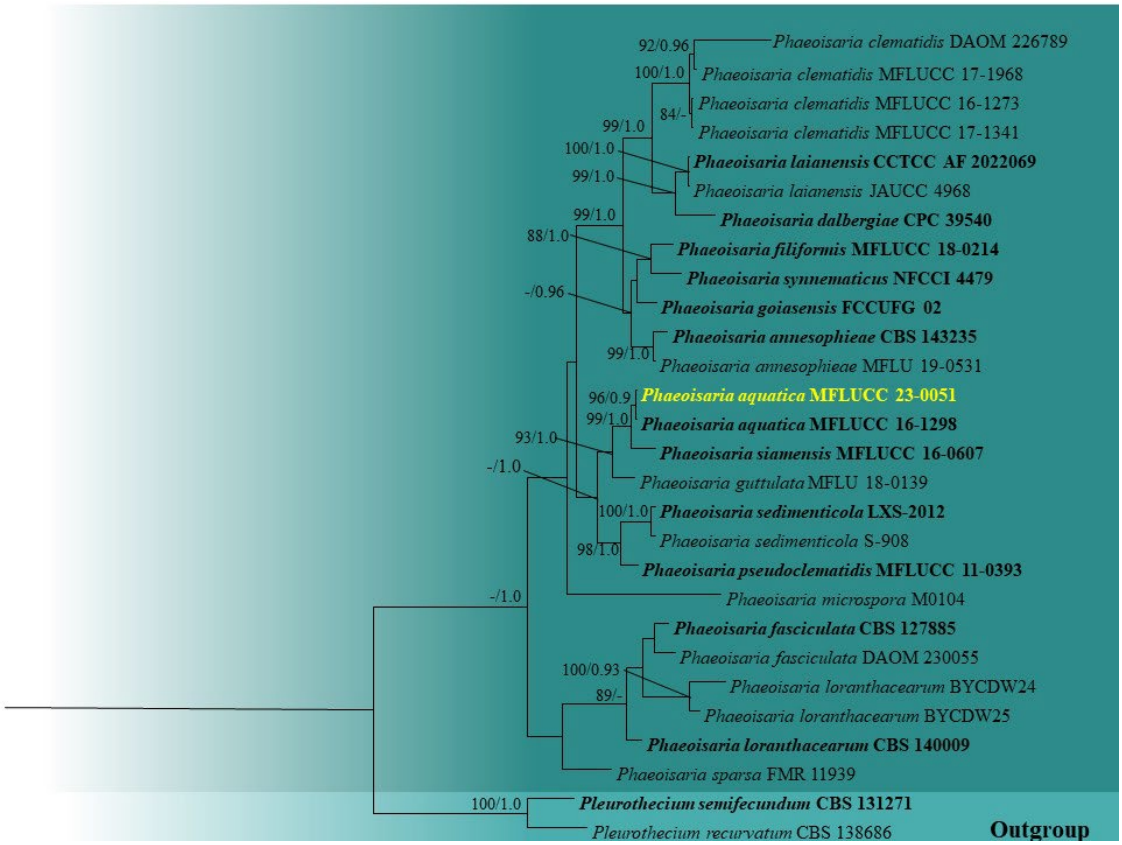

Fig. 49 – Phylogenetic tree generated from Bayesian analysis based on combined ITS, LSU, *rpb2*, and SSU sequence data. Twenty-seven strains were included in the combined analyses, which included 4,010 characters (ITS = 535, LSU = 787, *rpb2* = 1,031, and SSU = 1,657) after alignment. The topology of the Bayesian analysis is similar to that of the maximum likelihood analysis. The best RAxML tree with a final likelihood value of -10922.470271 is presented. Estimated base frequencies were as follows: A = 0.229958, C = 0.262428, G = 0.293712, T = 0.213902; substitution rates AC = 1.554430, AG = 2.491612, AT = 1.326313, CG = 1.765727, CT = 6.981695, GT = 1.000000; gamma distribution shape parameter α = 0.420469. The evolutionary model TIM2ef+G, GTR+I+G, GTR+G, and TrN were applied to ITS, LSU, *rpb2*, and SSU sequence data. Bootstrap support values for ML ≥ 75% and Bayesian posterior probabilities ≥ 0.90 are indicated near nodes. The tree is rooted with *Pleurothecium recurvatum* (CBS 138686) and *P. semifecundum* (CBS 131271). Ex-type strains are in bold. The newly generated sequence is indicated in yellow.

Phaeoisaria aquatica Z.L. Luo, X.J. Su & K.D. Hyde, Luo et al., Mycological Progress 17(5), 514 (2018)

Index Fungorum number: IF 821837; Facesoffungi number: FoF 03411 Fig. 50

Saprobic on *Nyariophyton zizyphifolium* woody litter. Sexual morph: Undetermined. Asexual morph: Hyphomycetous. *Conidiomata* synnematal, *Synnemata* 305–716 × 13–24 µm ($\bar{x}$ = 495 × 17.6 µm, n = 10), scattered, erect to flexuous, velvety, dark brown to black, formed of parallel and compressed conidiophores, broad at the base and apical fertile area. *Conidiophores* macronematous, synnematous, dark brown to brown, smooth, branched, septate, with flared conidiogenous cells in the upper half. *Conidiogenous cells* 10.5–22 × 2.8–4.5 µm ($\bar{x}$ = 16 × 3.4 µm, n = 10), polyblastic, integrated, terminal, and intercalary, sympodial, frequently discrete, smooth, hyaline to pale brown, attenuated into a tip, denticulate, with one to multiple denticulate conidiogenous loci. *Conidia* 4.8–7.7 × 1.8–3.7 µm ($\bar{x}$ = 6 × 2.6 µm, n = 30), ellipsoidal to obovoidal, hyaline, straight, aseptate, smooth-walled.

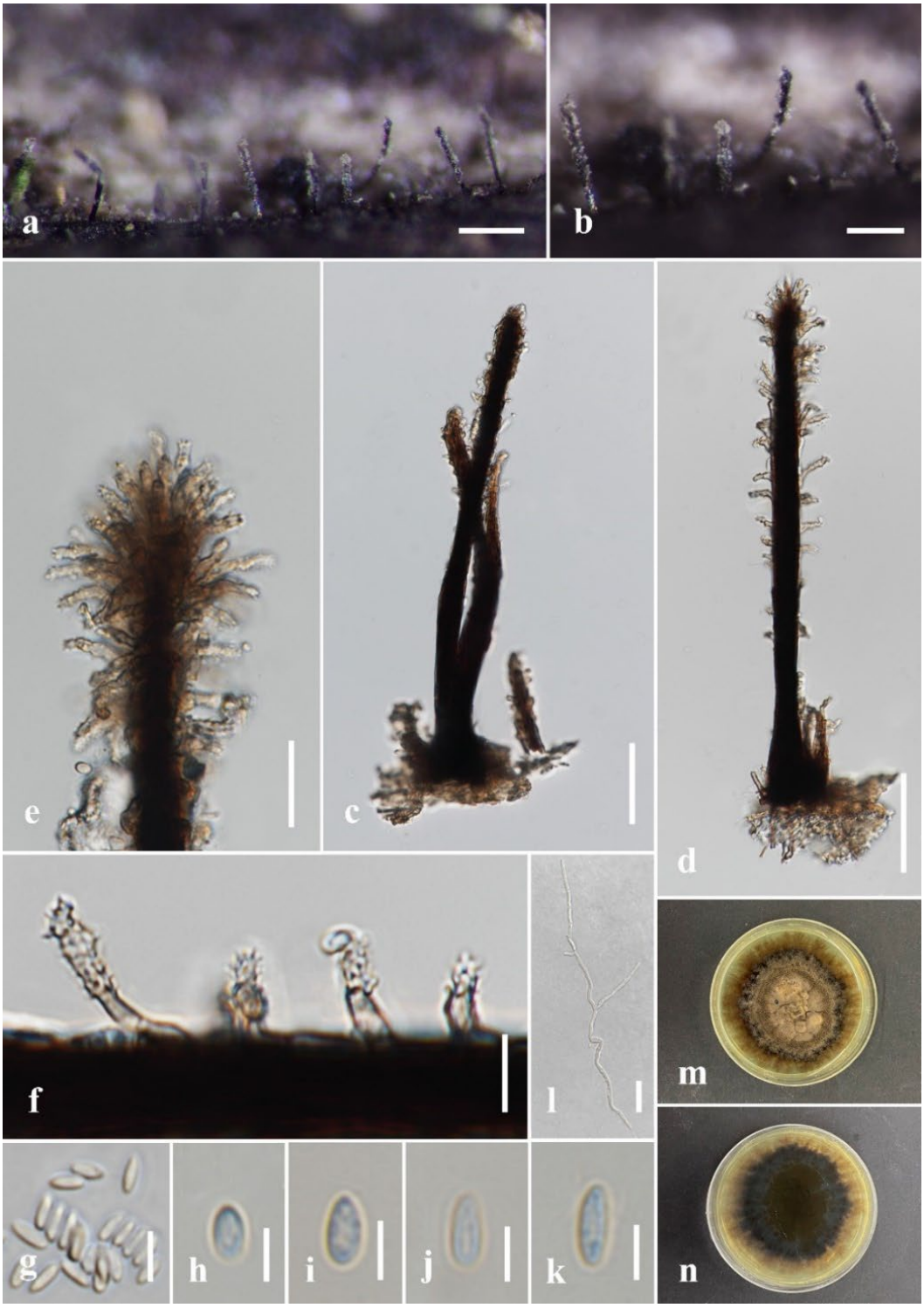

Fig. 50 – ***Phaeoisaria aquatica*** (MFLUCC 23–0051, **a new record**) a, b Colonies on wood. c d Conidiophores. e, f Conidiogenous cells with conidia. g–k Conidia. l Germinated conidium. m, n Colony on PDA from above and reverse. Scale bars: a = 200 µm, b = 100 µm, c, d = 50 µm, e, l = 20 µm, f, g = 10 µm, h–k = 5 µm.

Culture characteristics – Conidia germinating on PDA after 24 hrs., Germ tubes growing from both sides. *Colonies* on potato dextrose agar (PDA), reaching 2 cm diam. After incubating at 28°C for 14

days, solitary, flat or effuse, circular, slightly rough at the surface with fimbriate margin, cream at the center, greenish-brown towards the periphery, olive green at the edge, on the reverse olivaceous dark green to dark brown, surrounded by olive green to brown at the margin. Mycelium is semi-immersed in the substrate.

Material examined – Thailand, Chiang Rai Province, on decaying wood of *Nayariophyton zizyphifolium* (*Malvaceae*), 26 March 2022, N. Afshari 1C1T2R1b (MFLU 23-0075), living culture MFLUCC 23-0051.

GenBank accession numbers – ITS: OQ913674, LSU: OQ913689, SSU: OQ913710, *rpb2*: OQ984995.

Known distribution (based on molecular data) – Yunnan, China (Luo et al. 2018), Thailand (Boonmee et al. 2021)

Known hosts (based on molecular data) – Submerged decaying wood (Luo et al. 2018, Boonmee et al. 2021).

Notes – A BLASTn search of ITS sequences revealed that our strain shares 100% similarity with *P. aquatica*. Phylogenetic analysis further demonstrated that *P. aquatica* (MFLUCC 23-0051) clusters with the type strain *P. aquatica* (MFLUCC 16–1298) with 96% ML and 0.9 BPP statistical support (Fig. 49). Luo et al. (2018) introduced *P. aquatica* (MFLUCC 16–1298) as a novel species collected from the Jinsh River in China. Subsequently, Boonmee et al. (2021) reported *P. aquatica* (MFLU 21-0071) from Thailand, isolated from submerged decaying wood. In contrast, MFLUCC 23-0051, described in this study, was collected from dead wood of *Nayariophyton zizyphifolium*. Our strain shares key morphological characteristics, including the dimensions and shape of conidia, conidiophores, and conidiogenous cells, as well as dark brown synnemata. All morphological data, coupled with the phylogenetic results, provided robust evidence to assign our collection as a new host record.

Hypocreales Lindau, Die Natürlichen Pflanzenfamilien nebst ihren Gattungen und wichtigeren Arten 1(1), 343 (1897)

Index Fungorum number: IF 90477; Facesoffungi number: FoF 02091

Bionectriaceae Samuels & Rossman, Study in Mycology 42, 15 (1999)

Index Fungorum number: IF 82088; Facesoffungi number: FoF 01367

Gliomastix Guéguen, Bulletin de la Société Mycologique de France 21, 240 (1905)

Index Fungorum number: IF 8345; Facesoffungi number: FoF 12997

Gliomastix was introduced by Guéguen (1905) and was initially typified by *Gliomastix chartarum* (= *Torula chartarum* Corda). However, Hughes (1958) re-examined the type material and, based on priority, synonymized *G. chartarum* and *G. convoluta* (Harz) E.W. Mason as *G. murorum* (Corda) S. Hughes var. *murorum*. As a result, *G. murorum* is considered the type species in many accepted references (Barron 1968, Dickinson 1968, Arx 1970, Ellis 1971, Kendrick & Carmichael 1973). Initially classified as a section within *Acremonium*, the phylogenetic study by Summerbell et al. (2011) demonstrated that *Gliomastix* is a distinct genus in the family *Bionectriaceae*. The members of *Gliomastix* are mostly saprobes on decomposing organic residue and soil-inhabiting (Song et al. 2008). The species are characterized by phialides borne on short conidiophores, which are smooth or granularly coated. *Conidia* produced by the phialides as chains or slimy masses (Dickinson 1968, Ellis 1971). There are 47 epithets in Index Fungorum (2025); however, only seven species have DNA sequence data (Vu et al. 2019). An updated phylogeny for *Gliomastix* and closely related taxa is shown in Fig. 51.

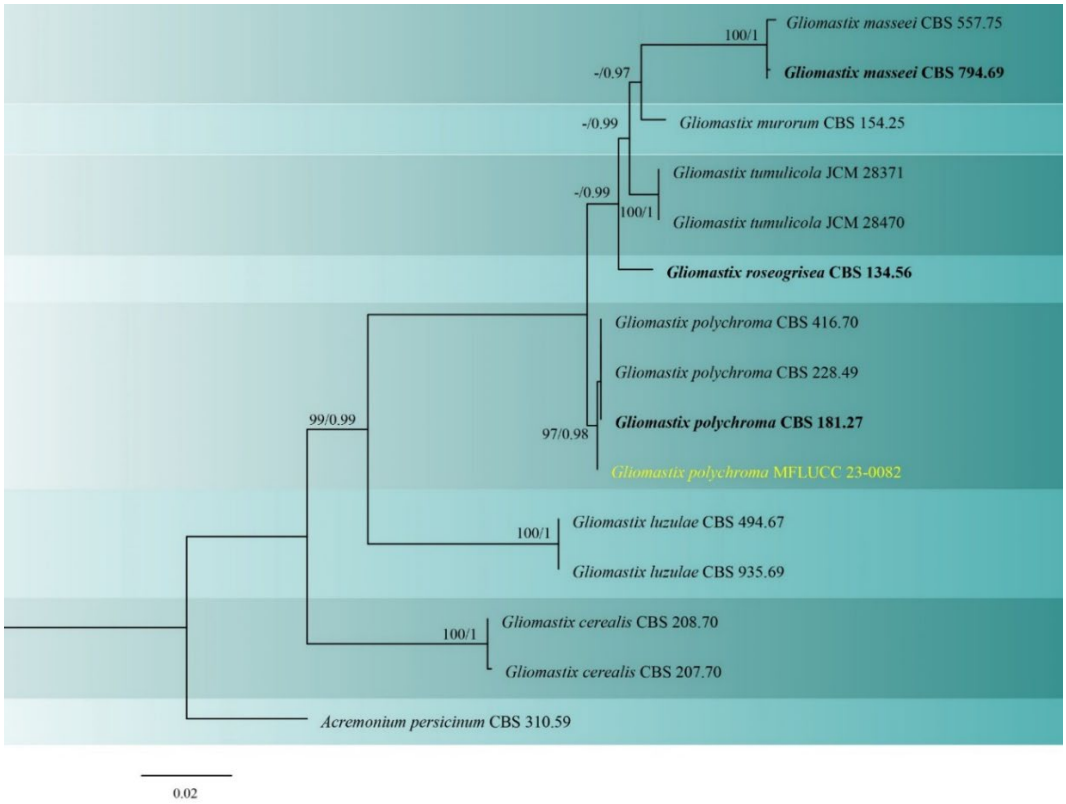

Fig. 51 – RAxML tree of *Gliomastix* based on concatenated ITS–LSU sequence data. Fifteen strains were included in the combined analyses, which comprised 1314 characters after alignment. The tree topology of the maximum likelihood analysis is similar to that of the Bayesian analysis. The best-scoring RAxML tree, with a value of -2627.619840, is presented as a final ML optimization likelihood. The matrix contained 158 distinct alignment patterns, with 4.20% of the characters being undetermined or gaps. Estimated base frequencies were as follows: A = 0.236264, C = 0.254063, G = 0.290887, T = 0.218787; substitution rates AC = 1.517394, AG = 0.968386, AT = 1.111626, CG = 0.322930, CT = 4.181166, GT = 1.000000. The evolutionary model GTRGAMMA was applied to all the gene regions. Bootstrap support values for ML ≥ 80% and BYPP ≥ 0.9 are shown as ML/BYPP near the nodes. The isolate used in the present study is shown in red. Type strains are indicated in black bold. The tree is rooted with *Acremonium persicinum* (CBS 310.59). The scale bar represents the expected number of nucleotide substitutions per site.

Gliomastix polychroma (J.F.H. Beyma) Matsushima, Icones Microfungorum a Matsushima Lectorum (Kobe), 77 (1975)

Index Fungorum number: IF 314513; Facesoffungi number: FoF 14328 Fig. 52

Endophytic on *Oryza sativa.* Sexual morph: Undetermined. Asexual morph: Hyphomycetous. *Hyphae* 1–2.4 µm in width, hyaline, septate. *Conidiophores* 11–27 × 1.5–2 µm ($\overline{x}$ = 16 × 2 µm, n = 10), hyaline, smooth, mononematous, cylindrical, gradually decreasing in width towards the tip. *Conidiogenous cells* 2–8 × 1–2 µm ($\overline{x}$ = 3.5 × 1.2 µm, n = 10), hyaline, smooth, mostly encompassing a single phialide, sometimes on a small extended cell. *Conidia* observed in both aggregated slimy masses and long dry chains, 2.5–5 × 2–3 µm ($\overline{x}$ = 3.8 × 2.5 µm, n = 30), hyaline to pale brown, aseptate, smooth, ellipsoidal or broadly round with a truncate base.

Culture characteristics – Colonies on PDA reaching 40–46 mm diameter in 7 days at 27 °C, initially greyish white with a grey circle in the centre, undulated edges in the margin, floccose, after six weeks turning to dull dark green, mostly around the margin; reverse yellowish-white colour with a dark grey spot at the centre.

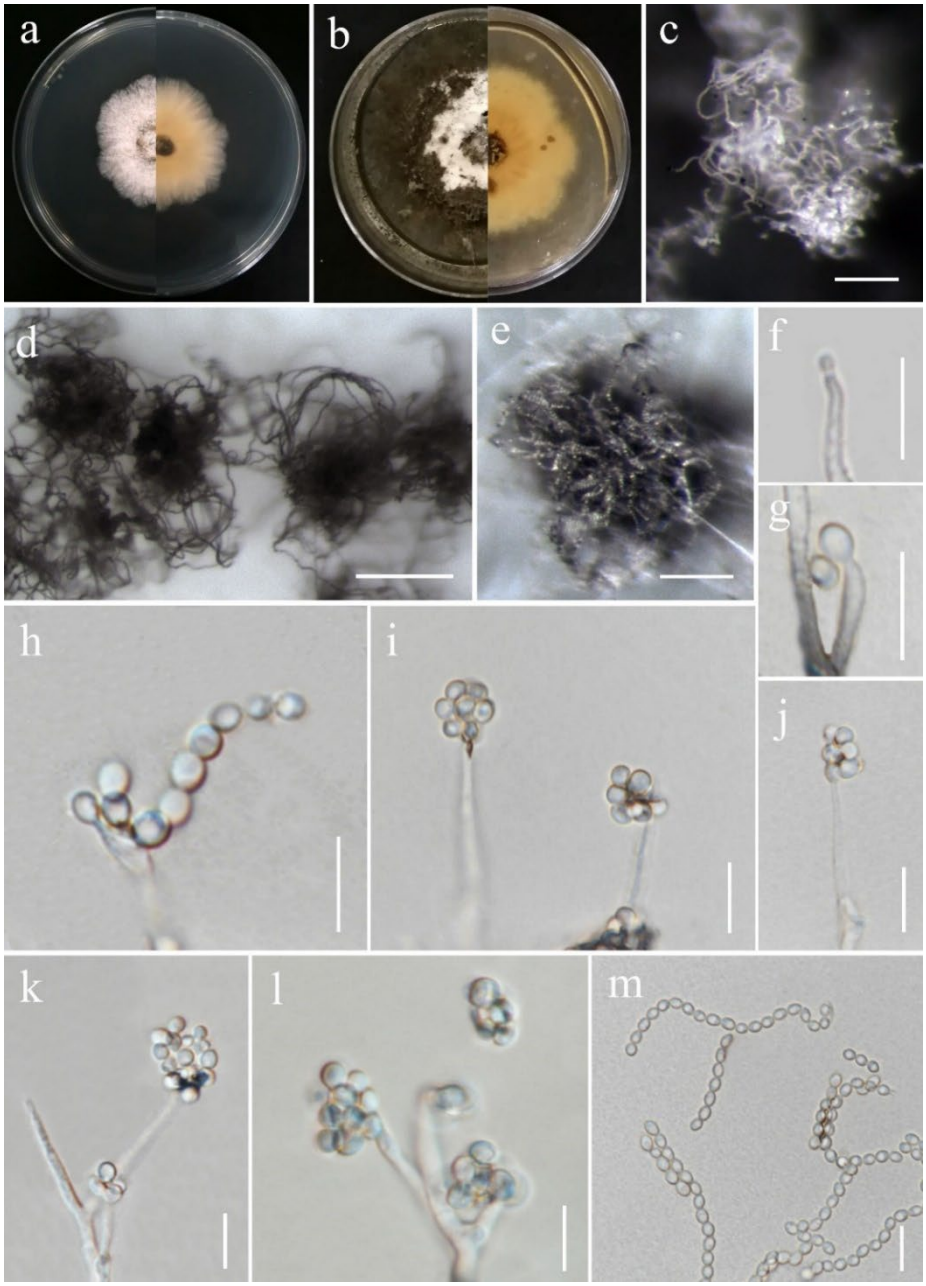

Fig. 52 – *Gliomastix polychroma* (MFLU 23-0268, **a new host record**). a Above and reverse of the colony on PDA after a week. b Above and reverse of a colony on PDA after six weeks. c–e Close-up structures of conidiophores and conidia on culture. f, g Conidiophores and conidial attachment on conidiogenous cells. h Conidiophores and conidiogenous cells bear conidia in a chain. i–l Conidiophores and conidiogenous cells bearing conidia with various shapes in slimy heads. m Conidia in a chain. Scale bars: c–e = 200 µm, f–m = 10 µm.

Material examined – Thailand, Chiang Rai Province, Muang Chiang Rai District, Mae Yao Subdistrict, on the stem of *Oryza sativa* (*Poaceae*), 17 December 2021, Sahar Absalan, MS92b (MFLUCC 23-0082).

GenBank accession numbers – ITS: OR077587, LSU: OR077588.

Notes – Summerbell et al. (2011) provide a phylogenetic tree based on LSU to clarify the position of *Acremonium* and related genera within the *Hypocreales*. They included the ex-type isolate of *Oospora*

polychroma J.F.H. Beyma, the basionym of *G. polychroma*, which is considered a type strain (CBS 181.27). The phylogenetic tree (Fig. 51) showed that our strain clustered with other strains in a clade of *G. polychroma* with 97% ML/0.98 PP. However, the conidia exhibit two distinct shapes: chains and mucoid masses, which have not been reported in previous studies for this species. However, they were observed in *G. mororum* (Dickinson 1968, Hammill 1981, Kiyuna et al. 2011).

Ophiocordycipitaceae G.H. Sung, J.M. Sung, Hywel-Jones & Spatafora, Sung et al., Studies in Mycology 57, 35 (2007)

Index Fungorum number: IF 504190; Facesoffungi number: FoF 01315

Hirsutella Pat., Revue Mycologique. (Toulouse) 14(54), 67 (1892)

Index Fungorum number: IF 8538; Facesoffungi number: FoF 19187

Hirsutella, initially introduced with a single entomopathogenic species, has evolved into a diverse group comprising over 70 species, encompassing various forms of pathogens affecting insects, mites, nematodes, and soil habitats (Doassans & Patouillard 1892, Chen et al. 2000, Ciancio et al. 2013, Simmons et al. 2015, Qu et al. 2021). The genus is characterized by swollen or inflated phialides with tapering necks and mucilaginous packets containing one or several conidia (Doassans & Patouillard 1892, Qu et al. 2021). Despite well-discussed morphological analyses, the lack of molecular data poses a challenge to species identification, as only a quarter of *Hirsutella* species have molecular data available (Xiao et al. 2019, Qu et al. 2021). *Hirsutella* species have been reported across numerous countries and continents, predominantly in tropical and subtropical regions (Doassans & Patouillard 1892, Chen et al. 2000, Kurihara et al. 2009, Ciancio et al. 2013, Yuan et al. 2020, Qu et al. 2021). An updated phylogeny for *Hirsutella* and closely related taxa is shown in Fig. 53.

Hirsutella minnesotensis Sen Y. Chen, Xing Z. Liu & F.J. Chen, Chen et al., Mycologia 92(5), 820 (2000)

Index Fungorum number: IF 467590; Facesoffungi number: FoF 17778 Fig. 54

Parasitic on termites (*Termitidae*, *Macrotermitinae*), with a dark brown host covered with white hyphae and forming light brown to purple stromata. Sexual morph: *Stromata* 8–12 cm long, 1–3 mm wide, branched or unbranched, stipitate, arising from the head of the host. *Stipe* 5 cm long, 1.5 mm wide, fibrous, cylindrical, light grey to purple in color. *Fertile head* 2–5 cm long, 2–3 mm diam., light grey to pale brownish. *Perithecia* 240–330 × 125–210 µm ($\overline{x}$ = 285 × 168 µm, n = 30), vertically immersed in the axis within the fertile head, brown to dark brown, oval-shaped, thick-walled. *Peridium* 25–40 µm ($\overline{x}$ = 32 µm, n = 60) wide, comprises three layers: textura globulosa outer layer, textura angularis to textura prismatica inner layer. *Asci* 120–185 × 6–9 µm ($\overline{x}$ = 152 × 7.5 µm, n = 60), 8-spored, cylindrical to clavate, hyaline, possessing a prominent thickened apex. *Apical cap* 5–8 × 4–6 µm ($\overline{x}$ = 6.5 × 5 µm, n = 60) diam., thick, hemispherical, hyaline. *Ascospores* 90–130 × 2–3.5 µm ($\overline{x}$ = 110 × 2.8 µm, n = 60), filiform, smooth-walled, hyaline, multiseptate, and do not break into secondary spores. Asexual morph: *Hyphomycetes*. *Synnemata* 1.8–2.5 cm long, 0.3–1 mm wide, single, light grey to purple, produced at the terminal part of the stroma, cylindrical, tapering upwards. *Conidiophore* 25–40 µm wide ($\overline{x}$ = 32 µm, n = 40), branched or unbranched, septate, hyaline. *Phialide* 9–18 × 3–5 µm ($\overline{x}$ = 13.5 × 4 µm, n = 40), monophialidic or occasionally polyphialidic, hyaline, cylindrical to clavate. *Conidia* 4–7.5 × 2–3.5 µm ($\overline{x}$ = 5.7 × 2.8 µm, n = 60), 1-celled, broadly ellipsoidal to subglobos or fusiform, hyaline, developing along the tip of the phialide.

Material examined – China, Anhui Province, Huangshan City, She County, at 165 m, 29.879 N'' 118.608 E, parasitic on termite (*Termitidae*, *Macrotermitinae*), on soil, 1 July 2023, Jianwei Liu, SX23139 (HKAS 132215); SX23139J (GZCC 24-0173).

GenBank accession numbers – HKAS 132215: ITS: PQ469944, LSU: PQ469941, SSU: PQ472487, *tef-1α*: PQ569881, *rpb1*: PQ569895: GZCC 24-0173: ITS: PQ469945, LSU: PQ469942, SSU: PQ472488, *tef-1α*: PQ569882, *rpb1*: PQ569896.

Known distribution (based on molecular data) – USA, China (Chen et al. 2000, Shu et al. 2015).

Known hosts (based on molecular data) – second-stage juvenile of *Heterodera glycines* (Chen et al. 2000, Shu et al. 2015).

Notes – *Hirsutella minnesotensis* was introduced by Chen et al. (2000) and originally isolated from a second-stage juvenile of *Heterodera glycines* in Minnesota, USA. Our phylogenetic analysis revealed that the new isolate (HKAS 132215) clusters closely with *H. minnesotensis* (CBS115627) (Fig. 53). Morphologically, our isolate is almost identical to *H. minnesotensis,* except for its small conidia. Since *H. minnesotensis* is characterized only by ITS gene sequences, the ITS region of our isolate (HKAS 132215) showed no significant differences from *H. minnesotensis* (CBS115627) (Chen et al. 2000). Based on these findings, we identified our new isolate as *H. minnesotensis*. This represents the first report of *H. minnesotensis* parasitizing termites (*Termitidae*, *Macrotermitinae*), expanding its known host range. Additionally, this study provides the first description of the sexual morphology of *H. minnesotensis* from China. *Tolypocladium inflatum* (OSC 71235) and *T. ophioglossoides* (NBRC 106332).

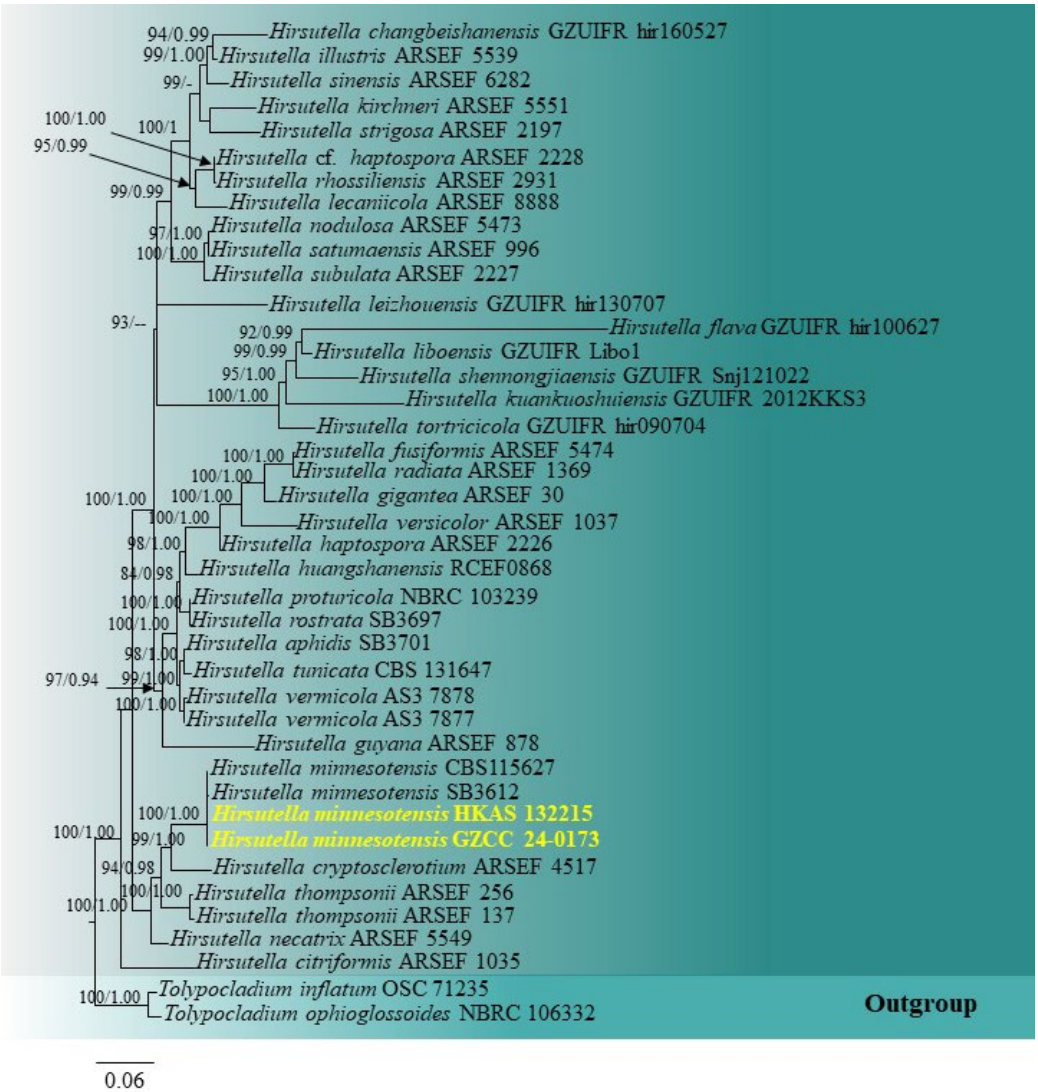

Fig. 53 – Phylogram generated from maximum likelihood analysis based on combined ITS, LSU, SSU, *tef1-α,* and *rpb1* sequence data. Forty-one strains were included in the combined analyses, which comprised 4,272 characters (551 characters for ITS, 814 characters for LSU, 1,358 characters for SSU,

878 characters for *tef1-α*, and 671 characters for *rpb1*) after alignment. The tree topology of the maximum likelihood analysis is similar to that of the Bayesian analysis. The best RAxML tree with a final likelihood value of -31688.504873 is presented. Estimated base frequencies were as follows: A = 0.233021, C = 0.281623, G = 0.282944, T = 0.202412; substitution rates AC = 1.540111, AG = 3.052859, AT = 1.003088, CG = 1.604297, CT = 5.374687, GT = 1.000000; gamma distribution shape parameter α = 0.506634. The evolutionary model GTR+I+G was applied to all the gene regions. Bootstrap support values for ML ≥ 75% and Bayesian posterior probabilities ≥ 0.90 are given near nodes, respectively. The tree is rooted with *Tolypocladium inflatum* (OSC 71235) and *T. ophioglossoides* (NBRC 106332). The newly generated sequences are indicated in yellow.

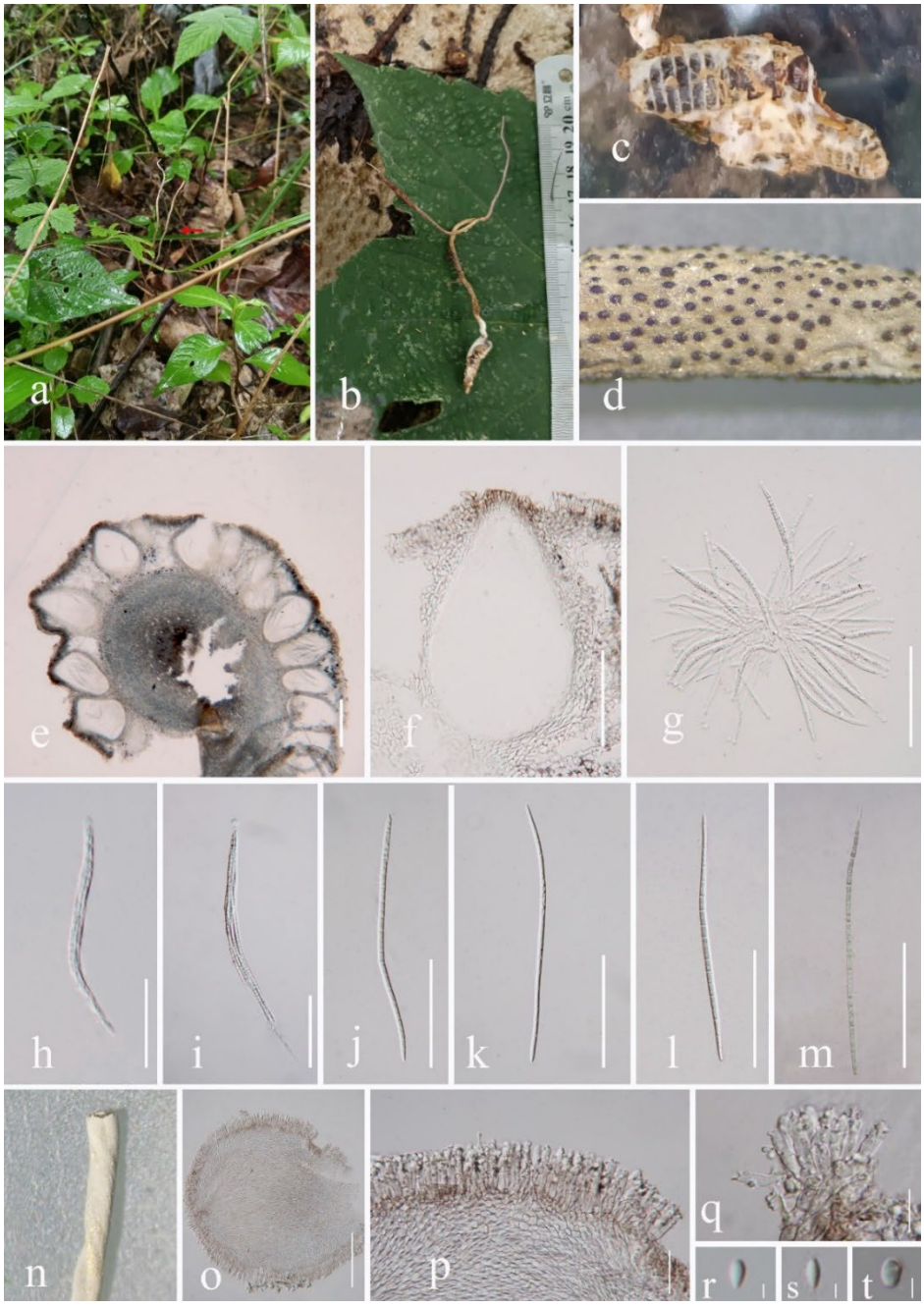

Fig. 54 – *Hirsutella minnesotensis* (HKAS 132215, **a new host record**) a Habitat. b Overview of the host and stromata. c Host. d Vertical sections showing the perithecia. e, f Perithecia. g–i Asci.

j–m Ascospores. n Synnemata. o–q Conidiophores. r–t Conidia. Scale bars: e = 200 μm, f, g, o =100 μm, h–m = 50 μm, p = 20 μm, q = 10 μm, r–t = 3 μm.

Polycephalomycetaceae Y.P. Xiao, Y.B. Wang, T.C. Wen, H. Yu & K.D. Hyde, Xiao et al., Fungal Diversity 120, 23 (2023)

Index Fungorum number: IF 559469; Facesoffungi number: FoF 10730

Pleurocordyceps Y.J. Yao, Y.H. Wang, S. Ban, W.J. Wang, Yi Li, Ke Wang & P.M. Kirk, Wang et al., Journal of Systematics and Evolution 59(5), 1074 (2021)

Index Fungorum number: IF 570683; Facesoffungi number: FoF 10737

Wang et al. (2021) introduced the new generic name *Pleurocordyceps* and proposed relevant new combinations based on its distinct characteristics. The genus is defined by lateral, fertile, pulvinate stromata near the tip in the sexual morph and the presence of the two types of conidia in Petri dish culture in the asexual morph. Additionally, Wang et al. (2021) provided a key to the 11 accepted *Pleurocordyceps* species. *Pleurocordyceps* is distinguished from closely related genera by its lateral, fertile, pulvinate stromata near the tip in the sexual morph and by the presence of two types of phialides and conidia in the asexual morph (Wang et al. 2021, Xiao et al. 2023). In addition to parasitizing insects, the majority of species in this genus are fungal parasites (Wang et al. 2015, Xiao et al. 2023). An updated phylogeny for *Pleurocordyceps* and closely related taxa is shown in Fig. 55.

Pleurocordyceps yunnanensis (Hong Yu bis, Y.B. Wang & Y.D. Dai) Y.H. Wang, S. Ban, W.J. Wang, Yi Li, Ke Wang, P.M. Kirk & Y.J. Yao, Wang et al., Journal of Systematics and Evolution 59(5), 1076 (2021)

Index Fungorum number: IF 570681; Facesoffungi number: FoF 17063 Fig. 56

Parasitic on *Ophiocordyceps* species. Sexual morph: Synnemata arising from the stromata and stipe of *Ophiocordyceps* sp. or the total wasp's corpses, unbranched, solitary or alternating on the stalk of *Ophiocordyceps* sp.; without synnemata on the fertile part of *Ophiocordyceps* sp., clavate or spatulate, unbranched, straight, 0.5–1.5 mm ($\overline{x}$ = 1 mm, n = 20) long, 100–500 μm ($\overline{x}$ = 300 μm, n = 20) wide. *Terminal* portion of a synnema covered by a viscous mass, clavate, subulate, or capitate; white, cream-coloured. *Phialides* of two types: α-phialides arising from the conidial mass of the synnema; β-phialides developing from the stipe. α-phialides 8.5–18.5 × 0.7–1.8 μm ($\overline{x}$ = 13.5 × 1.3 μm, n = 50), β-phialides 5.5–11.5 × 1.2–2.5 μm ($\overline{x}$ = 8.5 × 1.8 μm, n = 40), smooth, hyaline, solitary. α-conidia 1.5–2.1 μm ($\overline{x}$ = 1.8 μm, n = 50) diam., globose, one-celled, smooth-walled; β-conidia 2.6–3.8 × 1.3–2.2 μm ($\overline{x}$ = 3.2 × 1.7 μm, n = 50) fusiform or droplet-shaped, one-celled, smooth-walled, hyaline. Asexual morph: Undetermined.

Culture characteristics – Colonies on PDA 2–3 cm in diameter after 15 days at 25 °C, white to cream-coloured, with red pigment production. Synnemata emerging after 20 d, solitary, clavate, 1.2–2.5 mm long, with an enlarged globose fertile head on the top, white at first, cream-coloured with age. α-phialides 6.5–17.5 × 0.8–1.6 μm ($\overline{x}$ = 12 × 1.2 μm, n = 50), arising on the conidial mass of the synnema, smooth, hyaline. β-phialides 9–21 × 0.8–2.1 μm ($\overline{x}$ = 15 × 1.5 μm, n = 50), arising on the stipe, smooth, hyaline, solitary. α-conidia 1.8–2.6 μm ($\overline{x}$ = 2.2 μm, n = 50) diam, globose, one-celled, smooth-walled; β-conidia 2.2–3.5 × 1.2–1.9 μm ($\overline{x}$ = 2.9 × 1.5 μm, n = 50) fusiform, one-celled, smooth-walled, hyaline.

Material examined – China, Liaoning Province, Tieling City, on *Ophiocordyceps* sp., 10 August 2022, YuYang TL25 (GZAAS 22-2051), living culture (GZCC 22-2051).

GenBank accession numbers – GZAAS 22-2051: ITS: OR762894, LSU: OR762898, SSU: OR762896, *rpb1*: OR765991, *rpb2*: OR765993, *tef1-α*: OR765996; GZCC 22-2051: ITS: OR762895, LSU: OR762899, SSU: OR762897, *tef1-α*: OR765995, *rpb1*: OR765992, *rpb2*: OR765994.

Known distribution (based on molecular data) – China (Wang et al. 2015).

Known hosts (based on molecular data) – *Ophiocordyceps nutans (Ophiocordycipitaceae)* and stink bugs (Wang et al. 2015).

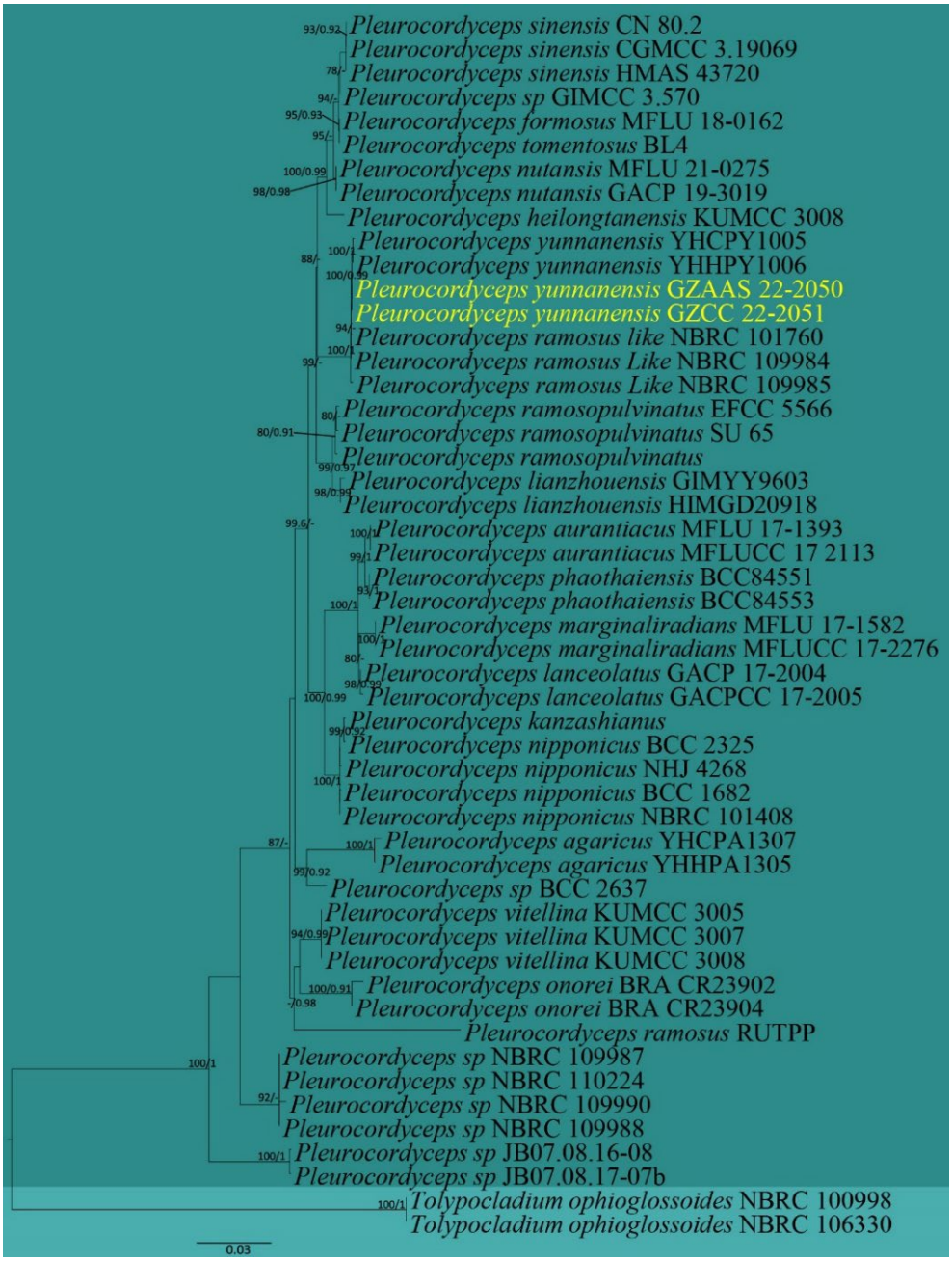

Fig. 55 – Phylogram generated from maximum likelihood analysis based on combined ITS, LSU, SSU, *tef1-α*, *rpb1*, and *rpb2* sequence data. Fifty-one strains were included in the combined analyses, which comprised 4,784 characters (538 for ITS, 843 for ITS, 945 for SSU, 833 for *tef1-α*, 662 for *rpb1*, and 963 for *rpb2*) after alignment. The tree topology of the maximum likelihood analysis is similar to that of the Bayesian analysis. The best RAxML tree with a final likelihood value of -14581.867251 is presented. Estimated base frequencies were as follows: A = 0.240791, C = 0.267040, G = 0.276332, T = 0.215838; substitution rates AC = 1.256723, AG = 3.210482, AT = 1.161173, CG = 1.131251, CT = 6.632724, GT = 1.000000; gamma distribution shape parameter α = 0.828459. The evolutionary model GTR+I+G was applied to all the gene regions. Bootstrap support values for ML greater than 75% and Bayesian posterior probabilities greater than 0.90 are given near nodes, respectively. The tree is rooted with *Tolypocladium ophioglossoides* (NBRC 100998; NBRC 106330). Type strains are in bold. The newly generated sequences are indicated in yellow.

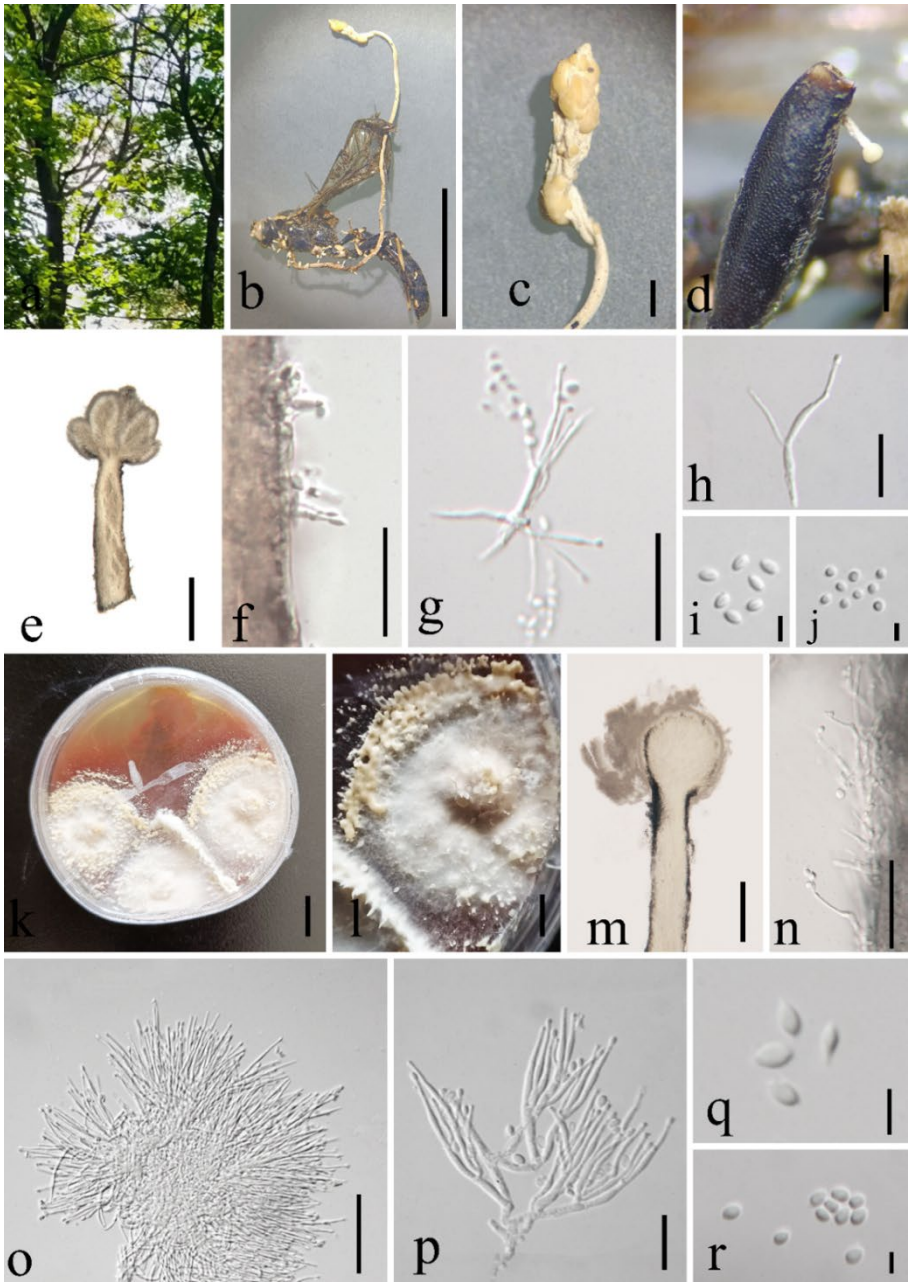

Fig. 56 – *Pleurocordyceps yunnanensis* (GZAAS 22-2051, **a new host record**) a Habitat. b Overview of host. c Colony on the surface of stromata. d, e Synnemata. f β-phialides. g, h α-phialides. i β-conidia. j α-conidia. k, l Culture from above. m Synnemata. n β-phialides. o, p α-phialides q β-conidia. r α-conidia. Scale bars: b, k =1 cm, c, d, l = 0.1 cm, e, m = 300 μm, f, g, n, o = 20 μm, h, p = 10 μm, i, j, q, r = 3 μm.

Notes – The new collections clustered with *Pleurocordyceps yunnanensis* (Fig. 55). *Pleurocordyceps yunnanensis* was previously reported as a parasite on *Ophiocordyceps* species and wasps (*Hymenoptera*) obtained from forest litter in Liaoning Province, China. The holotype was described as parasitizing *Ophiocordyceps nutans* (*Ophiocordycipitaceae*) and stink bugs. In this study, *Ophiocordyceps* species and wasp corpses were identified as hosts of *P. Yunnanensis* (Wang et al. 2015). The morphology of the new collections is closely similar to *P. Yunnanensis*, confirming that *Ophiocordyceps* species and wasps serve as new hosts for this fungus.

Stachybotryaceae L. Lombard & Crous, Crous et al., Persoonia 32, 283 (2014)

Index Fungorum number: IF 90922; Facesoffungi number: FoF 05320

Grandibotrys L. Lombard & Crous, Lombard et al., Persoonia 36, 189 (2016)

Index Fungorum number: IF 815992; Facesoffungi number: FoF 05548

Grandibotrys was introduced by Lombard et al. (2016) for stachybotrys-like fungi, with *G. pseudotheobromae* L. Lombard & Crous. as a type species, along with *G. xylophila* L. Lombard & Crous. Later, *Grandibotrys hyalinus* N.G. Liu, Hongsanan & K.D. was introduced (Hyde et al. 2017). Members of *Grandibotrys* have been collected from decaying dead wood in Nepal and Thailand (Lombard et al. 2016, Hyde et al. 2017). An updated phylogeny for *Grandibotrys* and closely related taxa is shown in Fig. 57. Based on phylogeny and morphological analysis, this study reports a new host and geographic record for *G. pseudotheobromae*.

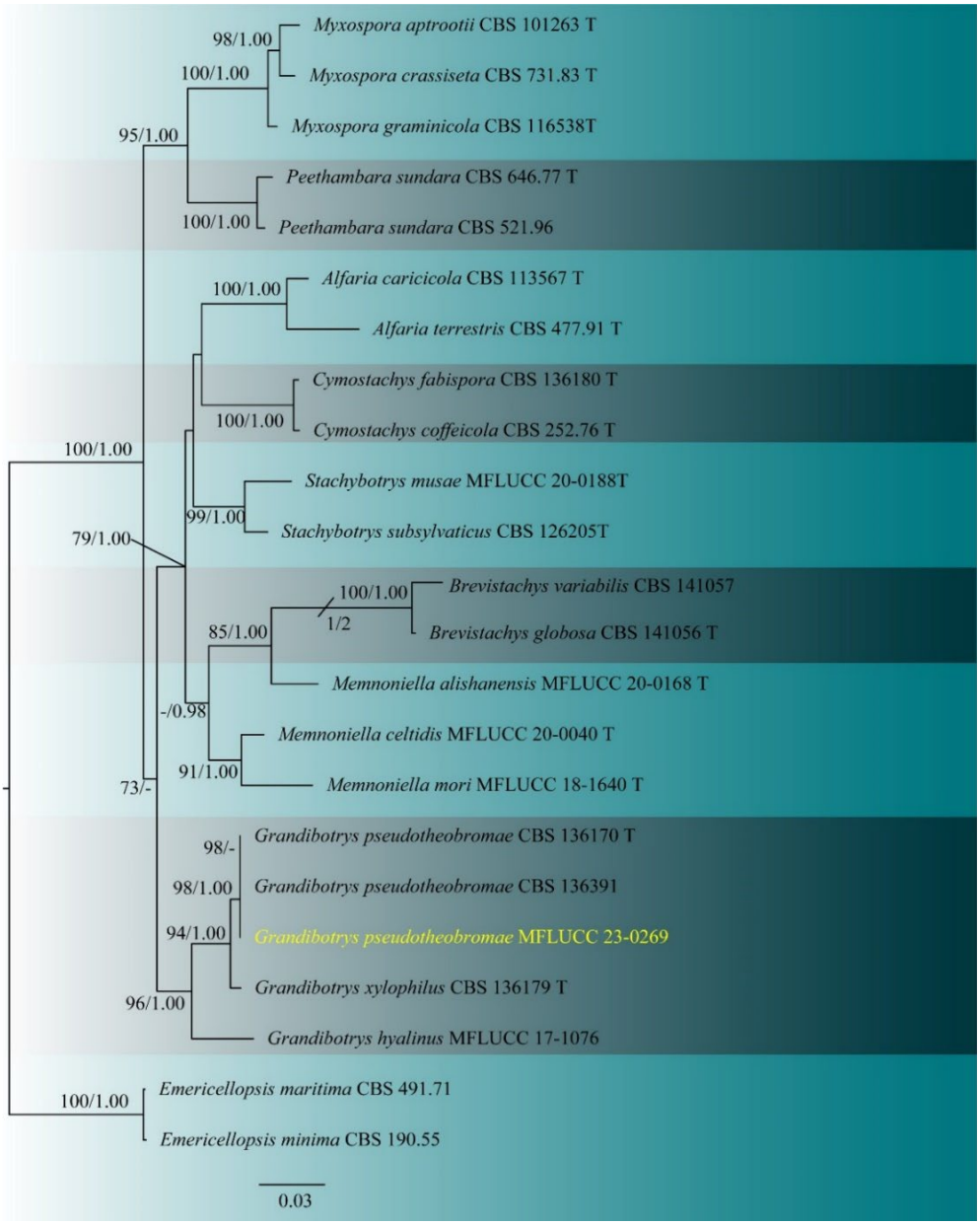

Fig. 57 – Phylogram generated from maximum likelihood analysis based on combined LSU and ITS sequence data. Twenty-three strains were included in the combined analyses, which comprised 1,317

characters (801 characters for LSU, 516 characters for ITS) after alignment. The tree topology of the maximum likelihood analysis is similar to that of the Bayesian analysis. The best RAxML tree with a final likelihood value of -5389.861631 is presented. Estimated base frequencies were as follows: A = 0.240272, C = 0.262543, G = 0.287058, T = 0.210127; substitution rates AC = 2.395561, AG = 2.395561, AT = 2.002558, CG = 1.167244, CT = 6.830089, GT = 1.000000; gamma distribution shape parameter α = 0.167831. The evolutionary model GTR+I+G was applied to all the gene regions. Bootstrap support values for ML greater than 75% and Bayesian posterior probabilities greater than 0.90 are given near nodes, respectively. The tree is rooted with *Emericellopsis maritima* (CBS 491.71 and CBS 190.55). Ex-type strains are designated by the addition of 'T' after the strain number. The newly generated sequences are indicated in yellow.

Grandibotrys pseudotheobromae L. Lombard & Crous, Lombard et al., Persoonia 36, 189 (2016)

Index Fungorum number: IF 815993; Facesoffungi number: FoF 15064 Fig. 58

Saprobic on a dead stem of *Euphorbia tirucallis*. Sexual morph: Undetermined. Asexual morph: hyphomycetous. *Colonies* on natural substrate effuse with velvety. Mycelium immersed, composed of smooth, septate hyphae. *Conidiophores* 200–300 × 4–5.5 μm length ($\overline{x}$ = 240–4.8 μm, n = 10), macronematous, mononematous, erect, solitary or in groups, bearing at their apex a whorl of 2–4 conidiogenous cells, unbranched to branched, thin-walled, smooth, septate, hyaline. *Conidiogenous cells* 24–25.5 × 4.5–5.5 μm ($\overline{x}$ = 24.5–5 μm, n = 10), monophialidic, terminal, integrated, determinate, clavate to subcylindrical to fusiform, with a mammiform apex and rounded base, hyaline. *Conidia* 21–25 × 13–15 μm ($\overline{x}$ = 23.5–14.5 μm, n = 10) acrogenous, aseptate, limoniform, guttulate, olivaceous green to dark brown.

Culture characteristics – Conidia germinated on water agar within 15 hours, and the hyaline germ tubes were produced from both sides. Colonies on PDA reached around 5 cm diam. after incubation for 30 days, forming white, outwardly radiating colonies.

Material examined – Thailand, Chiang Rai Province, Mae Fah Luang University, on a dead stem of *Euphorbia tirucallis* (*Euphorbiaceae*), 28 February 2021, J.Y. Zhang, Y41-1 (MFLU 23-0465), living culture, MFLUCC 23-0269.

GenBank accession numbers – ITS: OR742097, *tef1-α*: OR791262, *β-tubulin*: OR791263.

Known distribution (based on molecular data) – Nepal (Lombard et al. 2016).

Known hosts (based on molecular data) – Decaying wood (Lombard et al. 2016).

Notes – Lombard et al. (2016) introduced *Grandibotrys pseudotheobromae*, originally isolated from decaying wood in Nepal. Our new collection aligns well with the description of *G. pseudotheobromae*, exhibiting mononematous, hyaline conidiophores that bear a whorl of 2–4 conidiogenous cells at the apex, monophialidic conidiogenous cells with a mammiform apex, and limoniform, olivaceous conidia. Phylogenetic analysis confirmed that our new isolate clustered with *G. pseudotheobromae* (CBS 136391 and CBS 136170) with 94% ML/1.00 PP support (Fig. 57). Based on both phylogenetic and morphological evidence, we identified our isolate as *G. pseudotheobromae*, representing a new report from Thailand and *Euphorbia tirucalli* (*Euphorbiaceae*).

Pleurotheciales Réblová & Seifert, Réblová et al., Persoonia 37, 63 (2015)

Index Fungorum number: IF 813228; Facesoffungi number: FoF 06531

Pleurotheciaceae Réblová & Seifert, Réblová et al., Persoonia 37, 63 (2015)

Index Fungorum number: IF 813229; Facesoffungi number: FoF 05316

Pleurothecium Höhn., Berichte der Deutschen, Botanischen Gesellschaft 37, 154 (1919)

Index Fungorum number: IF 9475; Facesoffungi number: FoF 05317

Pleurothecium was introduced by Höhnel (1919) with *Pleurothecium recurvatum* (≡ *Acrothecium recurvatum*) as the type species. Currently, *Pleurothecium* has 21 epithets (Index Fungorum 2025), of which only two species, *P. recurvatum* and *P. semifecundum*, are known by their

sexual morphs (Réblová et al. 2012). Most species of *Pleurothecium* have been reported as saprobes from freshwater habitats (Réblová et al. 2016, Hyde et al. 2023). An updated phylogenetic tree of *Pleurothecium* species is provided in Fig. 59.

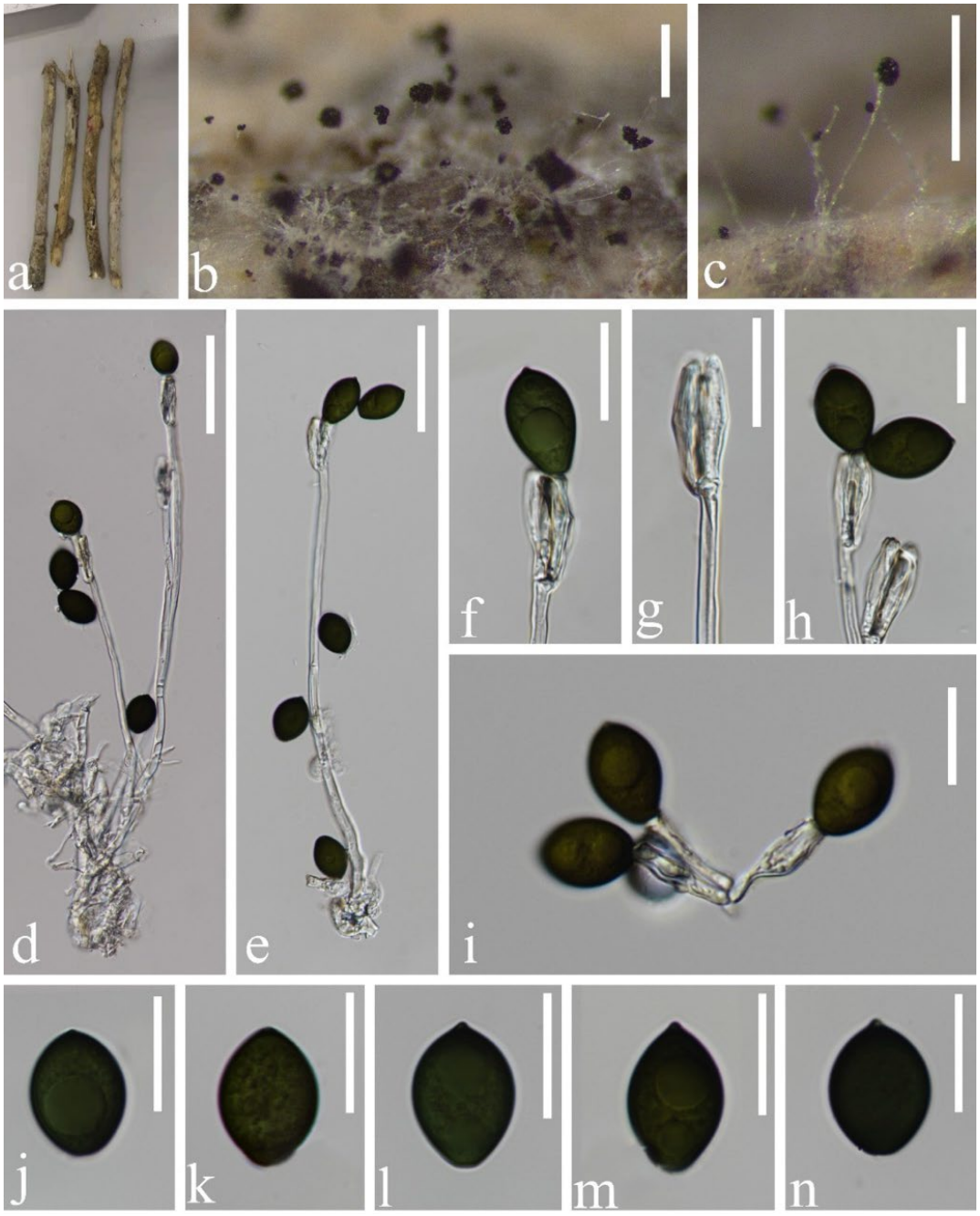

Fig. 58 – *Grandibotrys pseudotheobromae* (MFLU 23-0465, **a new host record**). a Host. b, c Conidiophores on the host surface. d, e Conidiophores. f–i Conidiogenous cells attached to conidia. j–n Conidia. Scale bars: b, c = 200 µm, d, e = 50 µm, f–n = 20 µm.

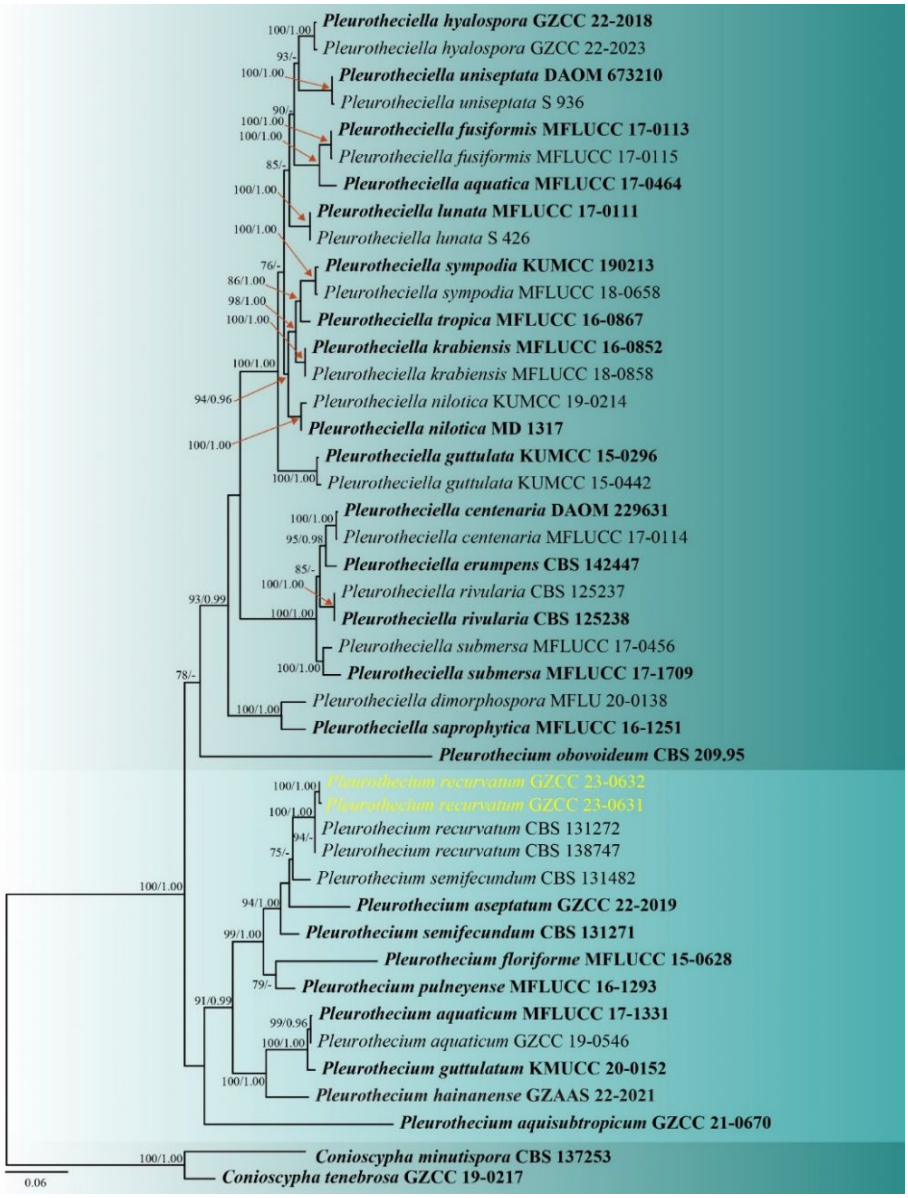

Fig. 59 – Phylogram generated from maximum likelihood analysis based on combined ITS, LSU, SSU, and *rpb2* sequence data representing the species of *Pleurotheciaceae*. Forty-four taxa were included in the combined analyses, which comprised 3,490 characters (656 characters for ITS, 865 for LSU, 957 for SSU, and 1,012 for *rpb2*). The tree topology of the maximum likelihood analysis is similar to that of the Bayesian analysis. Bootstrap support values for ML ≥ 75% and Bayesian posterior probabilities ≥ 0.95 are given near nodes, respectively. *Conioscypha minutispora* (CBS 137253) and *C. tenebrosa* (GZCC 19-0217) were used as the outgroup taxa. Ex-type strains are in bold. The newly generated sequences are indicated in yellow.

Pleurothecium recurvatum (Morgan) Höhn., Centralblatt für Bakteriologie, Parasitenkunde und Infektionskrankheiten, Abteilung 2(60), 26 (1923)

Index Fungorum number: IF 276190; Facesoffungi number: FoF 05453 Fig. 60

Saprobic on decaying wood. Asexual morph: *Colonies* on the substratum superficial, effuse, and white. *Mycelium* composed of partly immersed, partly superficial, hyaline, septate, branched hyphae with small, glistening conidia. *Conidiophores* macronematous, mononematous, subcylindrical, straight,

unbranched, 244–391 µm long ($\bar{x}$ = 329 µm, n = 15), 4–6.5 µm wide ($\bar{x}$ = 5 µm, n = 15), smooth, septate, brown, paler towards the apex. *Conidiogenous cells* polyblastic, integrated, terminal, sympodial, denticles, subcylindrical, 35–50 µm long ($\bar{x}$ = 39 µm, n = 15) and 4–4.5 µm wide ($\bar{x}$ = 4.3 µm, n = 15), subhyaline to pale brown. *Conidia* solitary, acrogenous, fusiform or clavate, straight or slightly flexuous, 20–23 µm × 6–7.5 µm ($\bar{x}$ = 21 × 7 µm, n = 20), rounded at the apex, tapering towards the base, aseptate, often with 4 guttules in each cell, hyaline, smooth-walled.

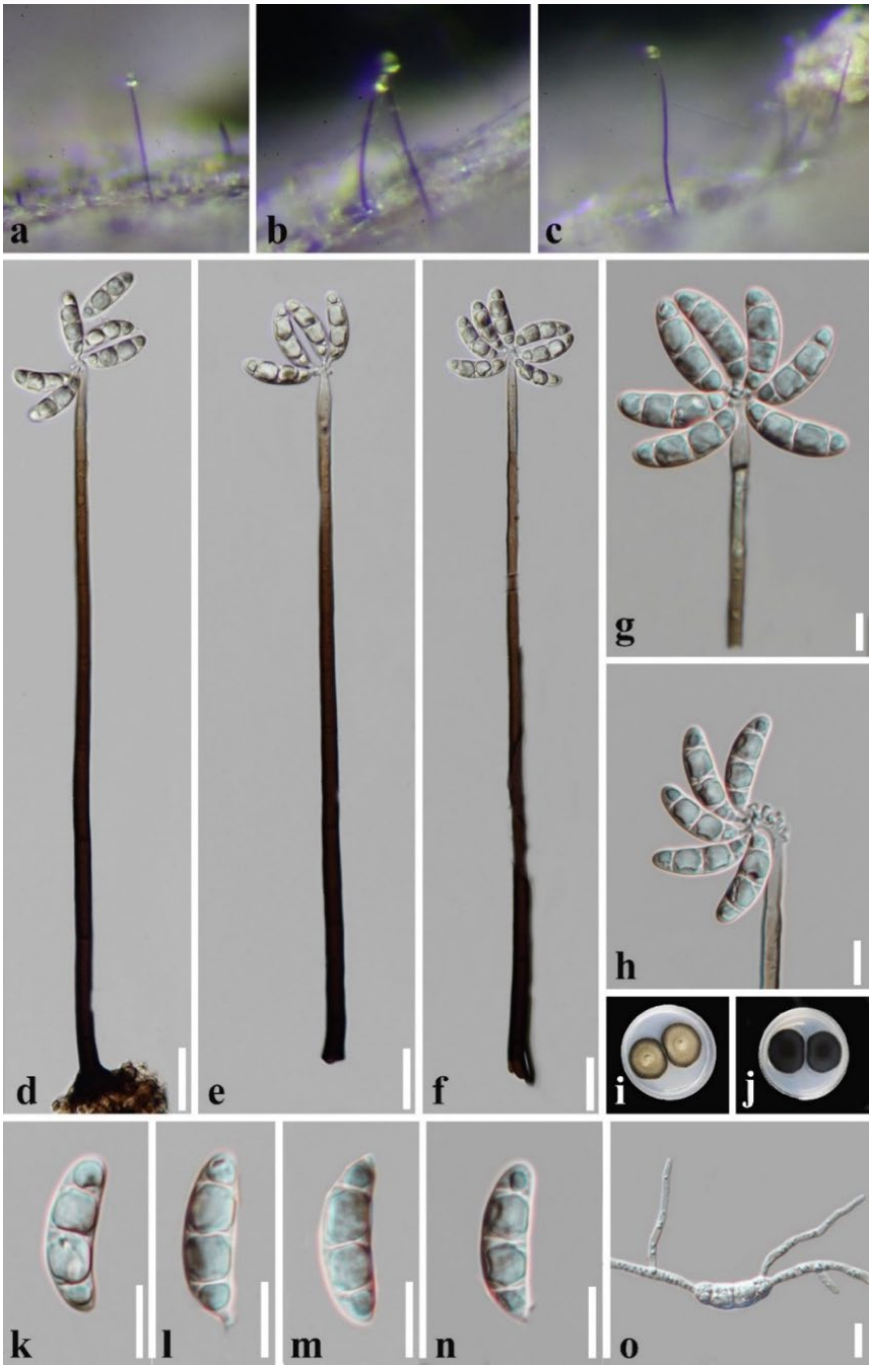

Fig. 60 – *Pleurothecium recurvatum* (GZAAS 23-0618, **a new record**). a–c Colonies on dead wood. d–f Conidiophores, conidiogenous cells, and conidia. g, h Conidiogenous cells bearing conidia. i, j Colony on PDA from above and below. k–n Conidia. o Germinating conidium. Scale bars: d–f, k–n = 20 µm. g, h, o = 10 µm.

Culture characteristics – Conidia germinate on water agar, producing germ tubes from conidia within 12 hours. Colonies growing on PDA, circular, with a flat surface, entire edge, reaching 32 mm in 30 days at 25°C, and brown to dark brown.

Material examined – China, Guizhou Province, Longli County, on decaying wood in a terrestrial habitat, 3 December 2020, Jian Ma, LLSB7 (GZAAS 23-0618), living culture, GZCC 23-0632. *Ibid*., LLSB5 (GZAAS 23-0617), living culture (GZCC 23-0631).

GenBank accession numbers – GZCC 23-0632: ITS: OR999429, LSU: OR999431; GZCC 23-0631: ITS: OR999430, LSU: OR999432.

Known distribution (based on molecular data) – Canada, the Czech Republic, and Sweden (Réblová et al. 2012).

Known hosts (based on molecular data) – *Carpinus betulus*, *Quercus* sp., and *Salix fragilis*, (Réblová et al. 2012).

Notes – *Pleurothecium recurvatum* was introduced by Höhnel (1919) based on morphological characteristics. In the phylogenetic analyses, our strain clusters with *P. recurvatum,* with 100 ML/1.00 PP support (Fig. 59). Morphologically, our isolate exhibits characteristics consistent with the asexual morph of *P. recurvatum* (Réblová et al. 2012). Therefore, we identified it as *P. recurvatum*. This study documents the discovery of this species in a terrestrial habitat in China.

Subclass *Xylariomycetidae* O.E. Erikss & Winka, Myconet 1, 12 (1997)

Index Fungorum number: IF 501509; Facesoffungi number: FoF 06514

Amphisphaeriales D. Hawksw. & O.E. Erikss., Systema Ascomycetum 5(1), 177 (1986)

Index Fungorum number: IF 00672; Facesoffungi number: FoF 90458

Apiosporaceae K.D. Hyde, J. Fröhl., Joanne E. Taylor & M.E. Barr, Sydowia 50 (1), 23 (1998)

Index Fungorum number: IF 81935; Facesoffungi number: FoF 00629

Neoarthrinium Ning Jiang, Jiang, Voglmayr, Ma, Xue, Piao & Li, MycoKeys 92, 36 (2022)

Index Fungorum number: IF 843845; Facesoffungi number: FoF 19190

Neoarthrinium was introduced by Jiang et al. (2022), with *Neoarthrinium lithocarpicola* as the type species. The species of this genus are characterized by cylindrical, septate, verrucose, and flexuous conidiophores, occasionally reduced to conidiogenous cells. *Conidiogenous* cells are erect, blastic, and clustered along hyphae, hyaline to pale brown, smooth, doliiform, subglobose to lageniform, and sometimes branched. *Conidia* are brown to dark brown, smooth to finely roughened, subglobose, ellipsoid to lenticular, with a longitudinal germ slit, and occasionally elongated to ellipsoidal (Jiang et al. 2022). An updated phylogeny for *Neoarthrinium* and closely related taxa is shown in Fig. 61.

Neoarthrinium bambusae J.W. Liu, Senan & K.D. Hyde, sp. nov.

Index Fungorum number: IF 903854; Facesoffungi number: FoF 14213 Fig. 62

Etymology – refers to the host genus *Bambusa*.

Saprobic on a dead sheath of *Bambusa dolichoclada. Hyphae* hyaline, branched, septate. Sexual morph: Undetermined. Asexual morph: *Hyphae* 2–3.5 µm diam., hyaline, branched, septate. *Conidiophores* basauxic, mononematous, straight, narrow, cylindrical, verrucose, and hyaline, with thick, transverse septa that appear as stripes. *Conidiogenous cells* 7–15 × 2–3 µm ($\overline{x}$ = 12 × 2.5 µm, n = 20), erect, blastic, aggregated in clusters on hyphae, integrated and terminal, hyaline to olivaceous, smooth, cylindrical, aseptate, branched. *Conidia* 6–10 × 4–6 µm ($\overline{x}$ = 7 × 4.5 µm, n = 25), subglobose, pyriform to lenticular, pale brown becoming brown, smooth, with a longitudinal germ slit.

Culture characteristics – Colonies grew on PDA at 20 °C in the dark, attaining a diameter of 3 cm within 7 days; fluffy, flat, spreading, with sparse aerial mycelium, a circular margin, a white surface, and a reverse that was white to off-white. Sporulation occurs after 30 days at 20 °C.

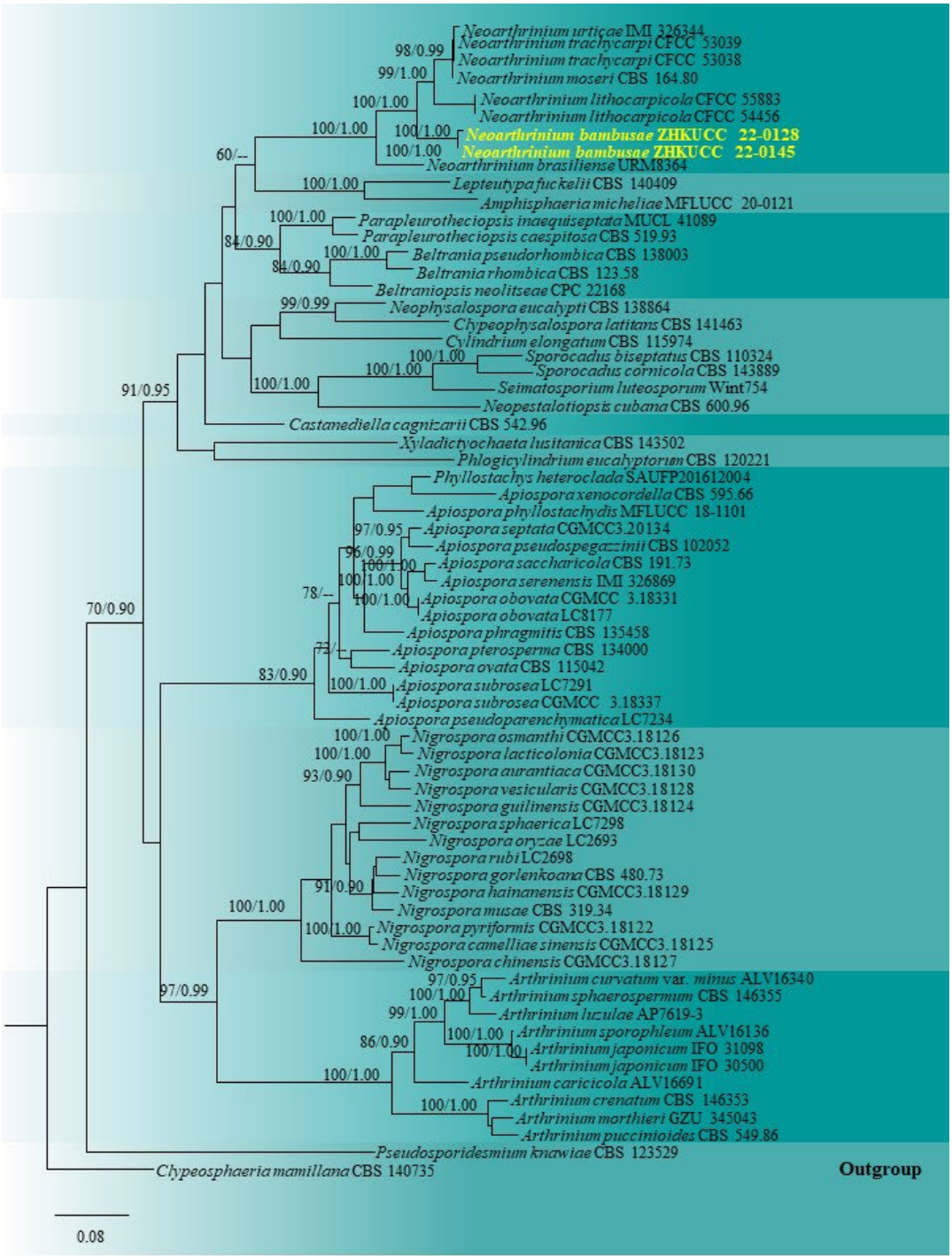

Fig. 61 – Phylogram generated from maximum likelihood analysis based on combined ITS, LSU, *β-tubulin,* and *tef1-α* sequence data of 67 taxa, which comprised 2,540 characters (ITS = 588, LSU = 881, *β-tubulin* = 549, *tef1-α* = 522). The best-scoring RAxML with a final likelihood value of -29576.288449 is presented. The matrix contained 1,393 distinct alignment patterns, with 24.65% of the characters being undetermined or gaps. Estimated base frequencies were as follows: A = 0.236635, C = 0.288169, G = 0.226537, T = 0.248659; substitution rates: AC = 0.984449, AG = 3.233412, AT = 1.483517, CG = 0.954343, CT = 4.314399, GT = 1.0; gamma distribution shape parameter α = 0.232351. Maximum likelihood bootstrap values ≥ 50% and Bayesian posterior probabilities ≥ 0.90 (MLBS/BYPP) are

labelled at each node. The tree is rooted with *Clypeosphaeria mamillana* (CBS 140735). The new isolate is indicated in yellow.

Material examined – China, Guangdong Province, Guangzhou City, Haizhu District, (23°06'28.4"N 113°16'51.6 "E), on dead sheath of *Bambusa dolichoclada* Hayata (*Poaceae*), 15 June 2020, I.C. Senanayake, 84-1 (ZHKU 22-0071, holotype), ex-type cultures ZHKUCC 22-0128, ZHKUCC 22-0145.

GenBank accession numbers – ZHKUCC 22-0128: ITS: PV647994, LSU: PV647999, *tef1-α*: PV665644; *β-tubulin*: PV665646; ZHKUCC 22-0145: ITS: PV647995, LSU: PV648000, *tef1-α*: PV665645; *β-tubulin*: PV665647.

Notes – The sequence data of ITS, LSU, *tef1-α*, and *β-tubulin* for our isolates (ZHKUCC 22-0128, ZHKUCC 22-0145) indicate that *Neoarthrinium* is the closest match in NCBI blast. The combined gene analysis of ITS, LSU, *tef1-α*, and *β-tubulin* revealed that our isolates were genetically close to *Neoarthrinium trachycarpum* and *N. urticae*, but genetically distinct from them, forming a clade with MP/BI values of 100/1.00 bootstrap support. Our collection differs morphologically from *N. trachycarpum* by its broad hyphae, large, cylindrical conidiogenous cells, and olivaceous to pale brown, subglobose, pyriform to lenticular conidia. *Neoarthrinium trachycarpum* is an endophyte on diseased branches of *Trachycarpus fortunei* (Yan et al. 2019).

Furthermore, our collection is morphologically distinct from *N. urticae* by its narrow hyphae, conidiophores with hyaline septa, large, cylindrical conidiogenous cells, and olivaceous to pale brown, subglobose, pyriform, or lenticular conidia. *Neoarthrinium urticae* was collected from *Urtica dioica* L. (Ellis 1965, Jiang et al. 2022). *Neoarthrinium brasiliense* has been collected from the leaves of *Lafoensia pacari* as an endophyte from Brazil. This species differs from our collection in its ampulliform, or doliiform, conidiogenous cells and acroperogenous conidia, which form singly or in chains to form clusters of varied shapes with a longitudinal germ slit (dos Santos 2024). *Neoarthrinium moseri* has blastic, hyaline, smooth, lageniform conidiogenous cells aggregated in clusters and subglobose to ellipsoid dark brown conidia with a longitudinal germ slit (Gams 1995, Jiang et al. 2022). This species was isolated from the petioles of *Mauritia minor* Burret in Colombia. *Neoarthrinium lithocarpicola* was collected from *Lithocarpus glaber* (Thunb.) Nakai from China. This species differs from our collection in having globose to subglobose, hyaline to pale brown conidiogenous cells, measuring 5.5–8 × 2.5–3.5 μm, brown to dark brown, smooth to finely roughened, subglobose to lenticular, and occasionally occurring in elongated to ellipsoidal forms. Therefore, based on morphological and molecular evidence, we establish our collection (ZHKU 22-0071) as a new species, *Neoarthrinium bambusae*.

Pestalotiopsidaceae Maharachch. & K.D. Hyde, Senanayake et al., Fungal Diversity 73, 106 (2015)

Index Fungorum number: IF 551178; Facesoffungi number: FoF 0666

Pestalotiopsis Steyaert, Bulletin du Jardin botanique de l'État à Bruxelles 19, 300 (1949)

Index Fungorum number: IF 9272; Facesoffungi number: FoF 00154

Pestalotiopsis was separated from *Pestalotia* by Steyaert (1949). Species of *Pestalotiopsis* are widely distributed and occur in various habitats worldwide, including soil, plant debris, and living plant tissues (Maharachchikumbura et al. 2014, Liu et al. 2017, Ariyawansa & Hyde 2018, Sun et al. 2023). These fungi are known to cause diseases in a wide range of plants, including trees, shrubs, and crops (Song et al. 2014, Moslemi & Taylor 2015, Hlaiem et al. 2018). Additionally, some *Pestalotiopsis* species produce beneficial metabolites and have potential applications in bioremediation and the degradation of plastic waste (Russell et al. 2011, Xu et al. 2014, 2016). An updated phylogeny for *Pestalotiopsis* and closely related taxa is shown in Fig. 63.

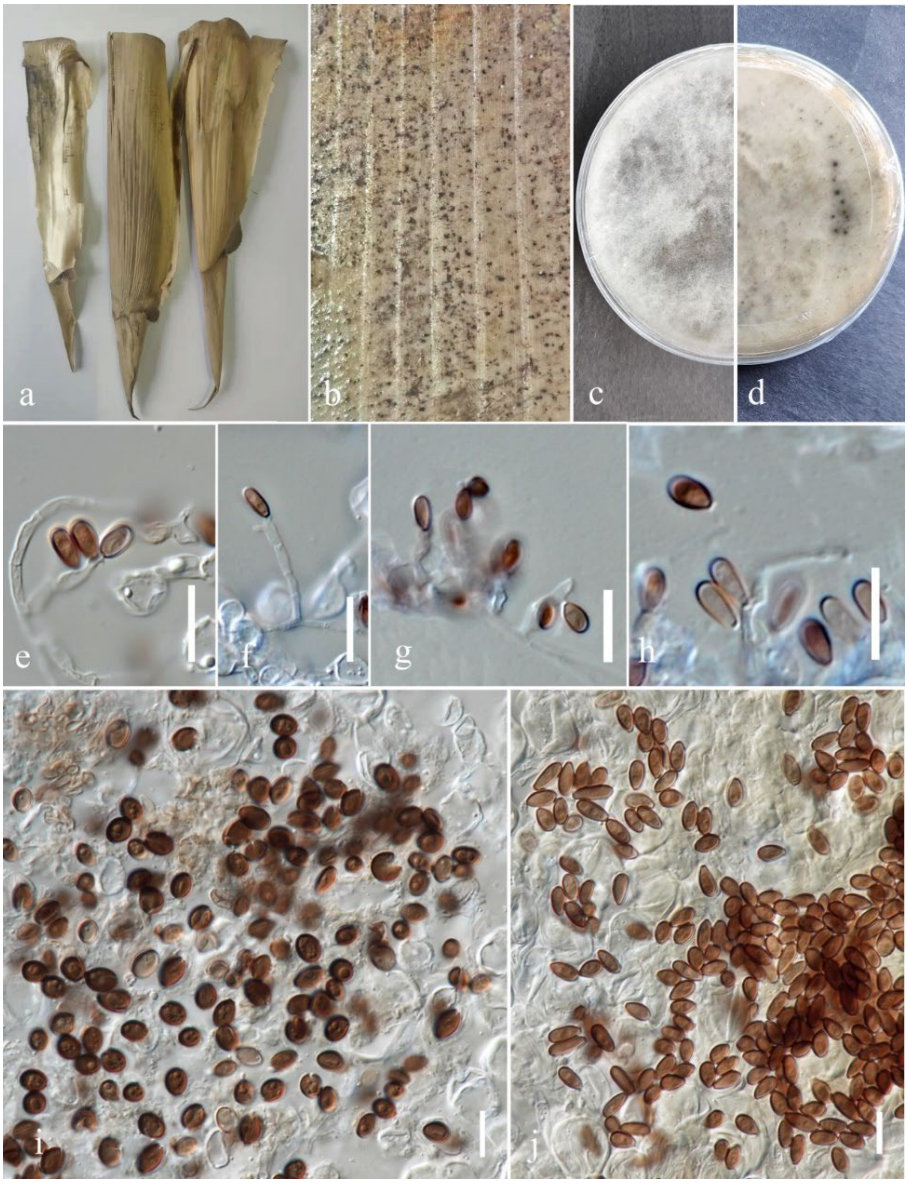

Fig. 62 – ***Neoarthrinium bambusae*** (ZHKU 22-0071, **holotype**) a Specimen examined. b Conidial clusters on the substrate. c Upper view of culture on PDA. d Reverse view of culture on PDA. e–h Conidiogenous cells attached to the conidia. i, j Conidia. Scale bars: e–j = 15 µm.

Pestalotiopsis chamaeropis Maharachch., K.D. Hyde & Crous, Maharachchikumbura et al., Studies in Mycology (2014)

Index Fungorum number: IF 809735; Facesoffungi number: FoF 11691 Fig. 64

Associated with leaf spots of *Spineless yucca*. Sexual morph: Undetermined. Asexual morph: *Conidiomata* solitary or aggregated, subglobose to globose, dark, semi-immersed or erumpent, exuding black conidial masses. *Conidiophores* hyaline, smooth, simple, and reduced to conidiogenous cells. *Conidiogenous cells* 2–3 µm wide, cylindrical to subcylindrical, hyaline, smooth. *Conidia* 15–23 × 4–7 µm ($\overline{x}$ = 19 × 6 µm, n = 40), brown, fusiform, straight to slightly curved, 4-septate, basal cell obconic with a truncate base, hyaline to pale brown, smooth-walled, 2–5 µm long; three median cells 10–14 µm long, brown, septa darker than the rest of the cell, somewhat constricted at the septa; second cell from base brown, 3–5 µm long; third cell brown, 3–5 µm long; fourth cell brown, 3–55 µm long; apical cell 2–5 µm long, hyaline, conic to acute; with 2–3 tubular appendages on apical cell, inserted at different

loci in a crest at the apex of the apical cell, unbranched, 7–15 µm long; single basal appendage, unbranched, tubular, centric, 3–7 µm long.

Material examined – China, Yunnan Province, Kunming City, Yiliang District, Yangzonghai Garden, on leaves of *Spineless yucca*, 20 February 2023, H.W. Shen, 2347 (HGUP 23-0006), living culture GUCC 23-0020.

GenBank accession numbers – ITS: OR731395, *tef1-α*: OR735526, *β-tubulin*: OR735527.

Known distribution (based on molecular data) – Australia (Moslemi & Taylor 2015), China (Liu et al. 2017, Zheng et al. 2023), Italy (Maharachchikumbura et al. 2014), Japan (Nozawa et al. 2019), Portugal (Santos et al. 2022), South Korea (Park et al. 2017), and Tunisia (Hlaiem et al. 2018).

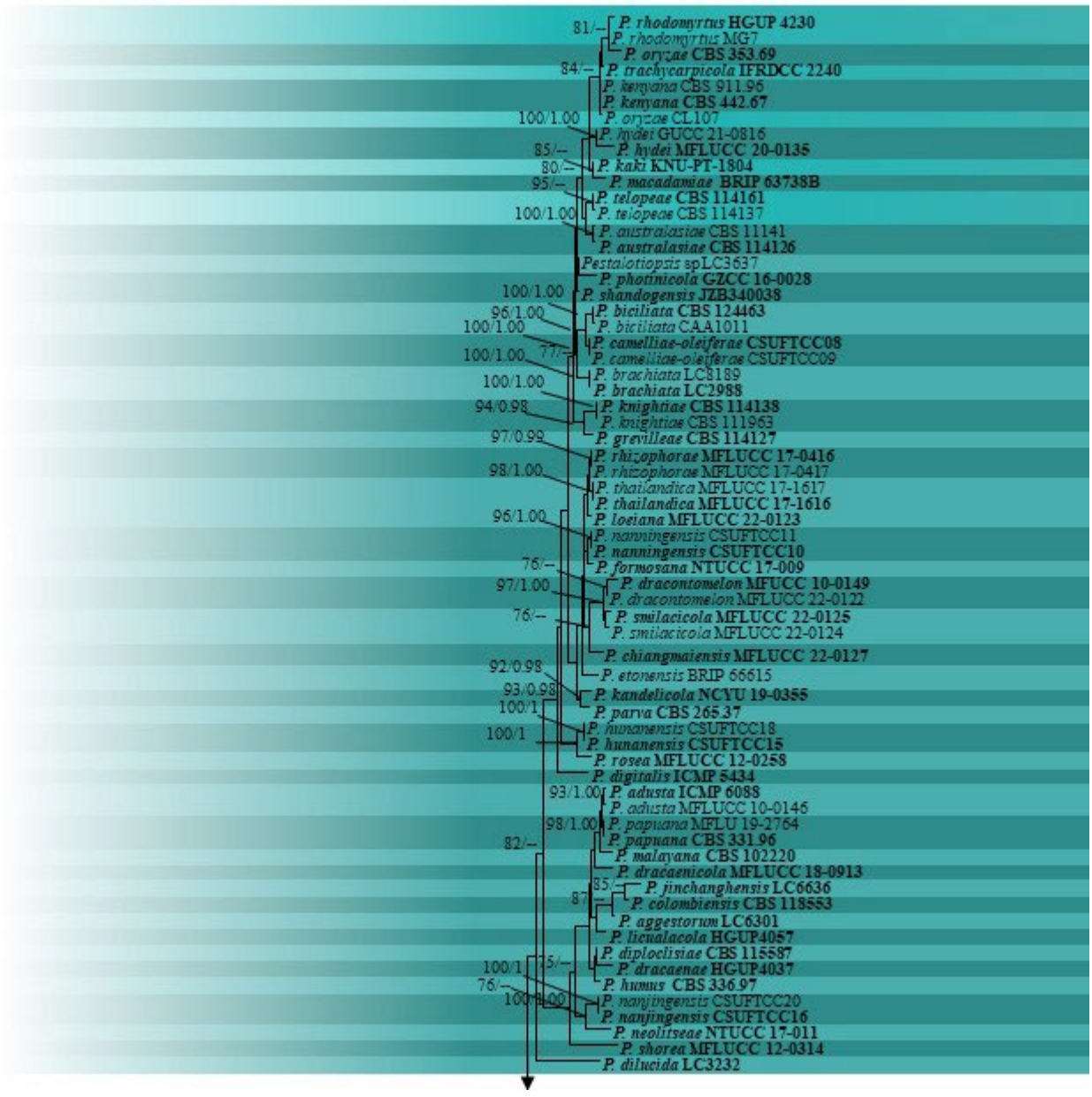

Fig. 63 – Phylogram generated from maximum likelihood analysis based on combined ITS, *tef1-α*, and *β-tubulin* sequence data. One hundred thirteen strains were included in the combined analyses, which comprised 1,518 characters (541 for ITS, 548 for *tef1-α*, and 429 for *β-tubulin*) after alignment. The tree topology of the maximum likelihood analysis is similar to that of the Bayesian analysis. The best

RAxML tree with a final likelihood value of -11962.607820 is presented. Estimated base frequencies were as follows: A = 0.235641, C = 0.293366, G = 0.210231, T = 0.260762; substitution rates AC = 1.144961, AG = 3.584236, AT = 1.214569, CG = 1.011543, CT = 4.559912, GT = 1.000000. The evolutionary model GTR+I+G was applied to all the gene regions. Bootstrap support values for ML ≥ 75% and Bayesian posterior probabilities ≥ 0.95 are given near nodes, respectively. The tree is rooted with *Neopestalotiopsis protearum* (CBS 114178) and *N. cubana* (CBS 600.96). Ex-type strains are in bold. The newly generated sequences are indicated in yellow.

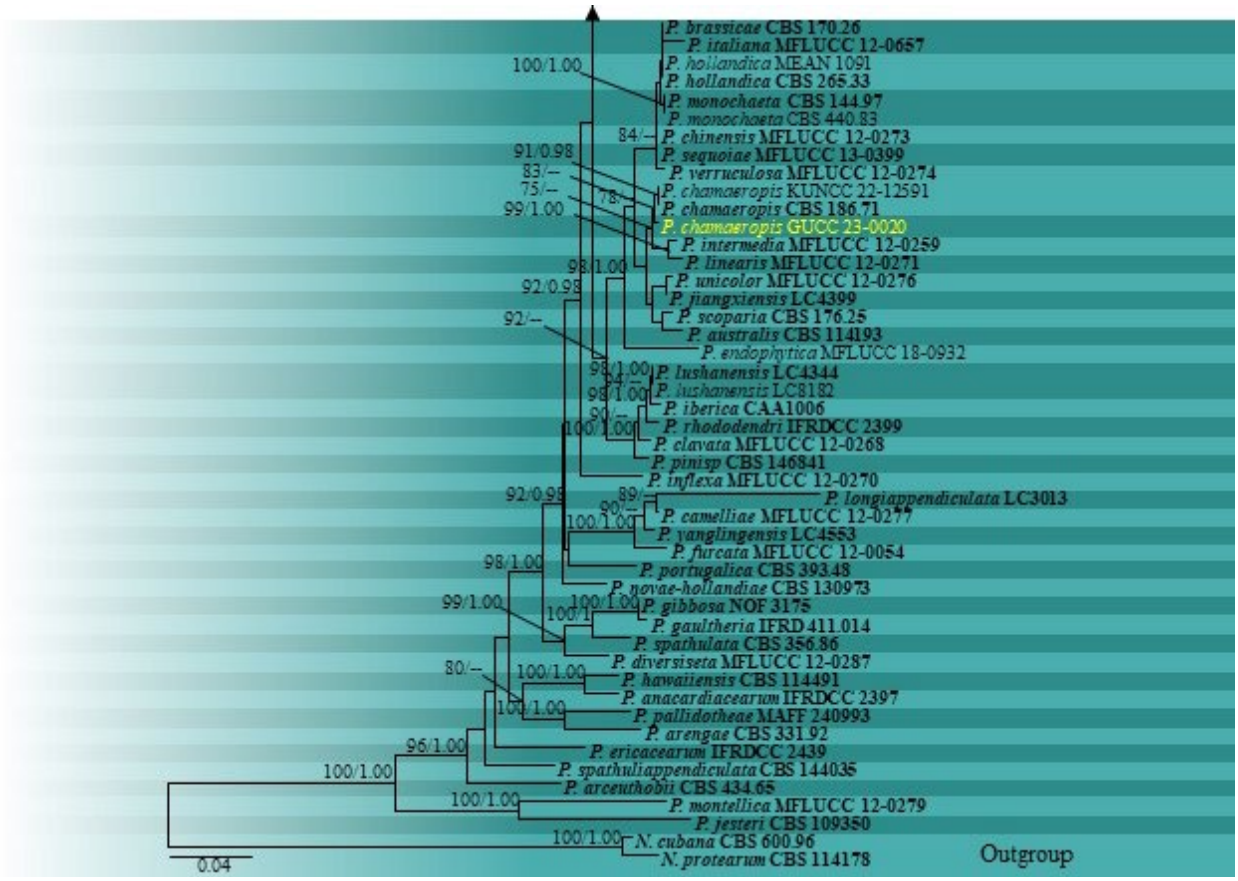

Fig. 63 – Continued.

Known hosts (based on molecular data) – *Aronia melanocarpa* (Park et al. 2017), Blueberry (Zheng et al. 2023), *Camellia* sp. (Jiang et al. 2017, Liu et al. 2017, Chen et al. 2021), *Castanopsis fissa* (Jiang et al. 2022), *Chamaerops humilis* (Maharachchikumbura et al. 2014), *Cunninghamia lanceolata* (Jiang et al. 2022), *Cyclobalanopsis* sp. (Jiang et al. 2022), *Erica arborea* (Hlaiem et al. 2018), *Eurya nitida* (Qiu et al. 2022), *Phyllostachys heteroclada* (Jiang et al. 2022), *Pieris japonica* (Nozawa et al. 2019), *Prostanthera rotundifolia* (Moslemi & Taylor 2015), *Quercus* sp. (Jiang et al. 2022), *Rosa* sp. (Peng et al. 2022), and *Vaccinium corymbosum* (Santos et al. 2022).

Notes – The collection was obtained from dead leaves of *Spineless yucca* in Yunnan Province, China, and identified as *Pestalotiopsis chamaeropis*, supported by both morphological and phylogenetic analyses. Our isolate clustered with the reference strain of *P. chamaeropis* (CBS 186.71) in the combined ITS, *tef1-α*, and *β-tubulin* sequence data phylogeny (Fig. 63). A comparison of ITS, *tef1-α*, and *β-tubulin* sequences with these two strains reveals 0, 3, and 1 base pair difference. Therefore, we introduced our collection as a new host record of *Pestalotiopsis chamaeropis*.

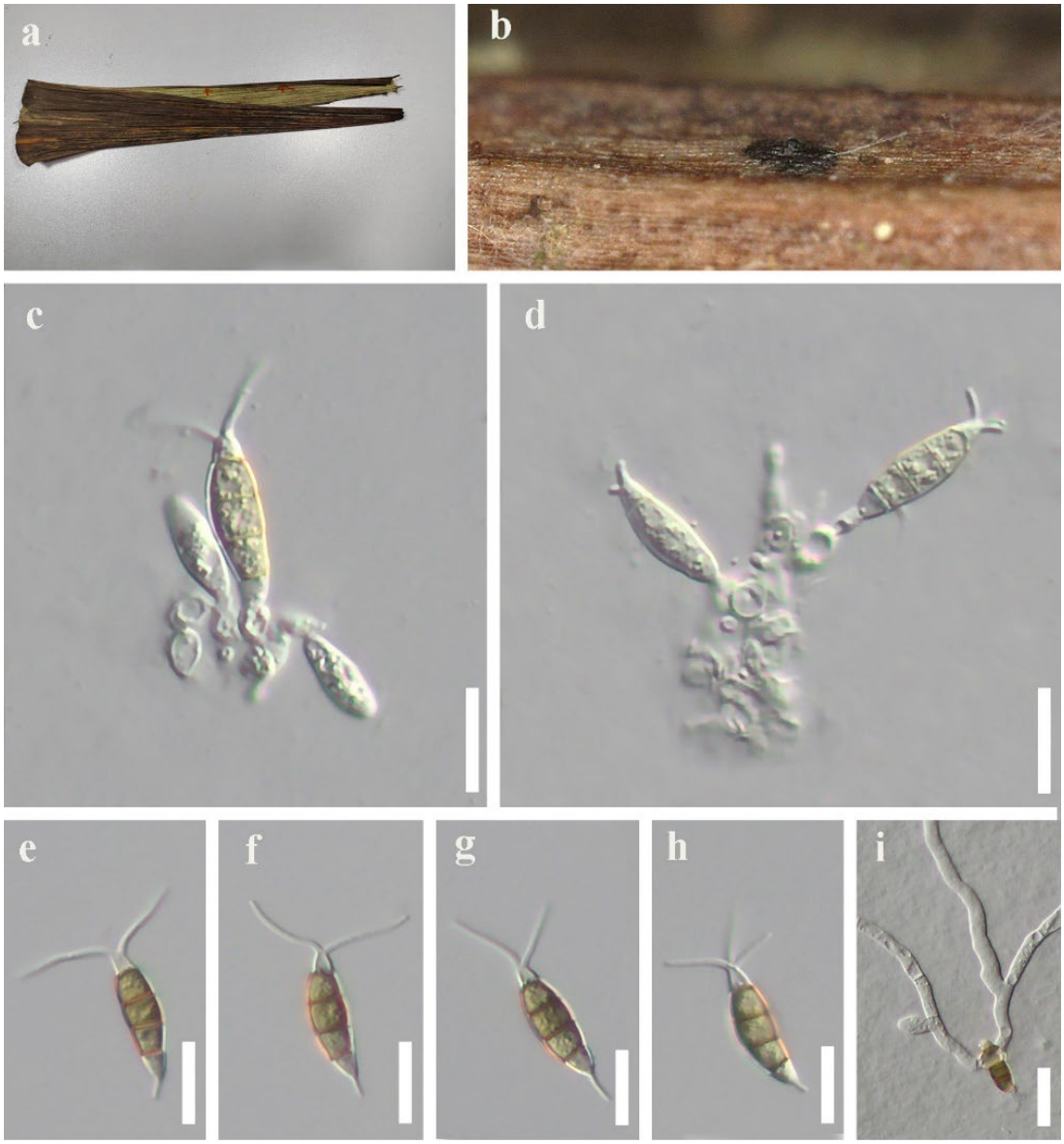

Fig. 64 – *Pestalotiopsis chamaeropis* (GUCC 23-0020, **a new host record**). a Host. b Conidiomata on the host surface. c, d Immature conidia attached to conidiogenous cells. e–h Conidia. i Germinated conidium. Scale bars: c–i = 10 µm.

Sporocadaceae Corda, Icones fungorum hucusque cognitorum 5, 34 (1842)

Index Fungorum number: IF 81408; Facesoffungi number: FoF 06111

Immersidiscosia Kaz. Tanaka, Okane & Hosoya, Persoonia 26, 94 (2011)

Index Fungorum number: IF 519746; Facesoffungi number: FoF 13575

Immersidiscosia was introduced by Tanaka et al. (2011) to accommodate *I. eucalypti* as the type species. This genus is characterized by deeply immersed, pycnidioid conidiomata that originate intra- or subepidermally, with a conidiomatal beak bearing periphyses. To date, only the type species are available in this genus; thus, additional specimen collections are needed to expand this genus. An updated phylogeny for *Immersidiscosia* and closely related taxa is shown in Fig. 65.

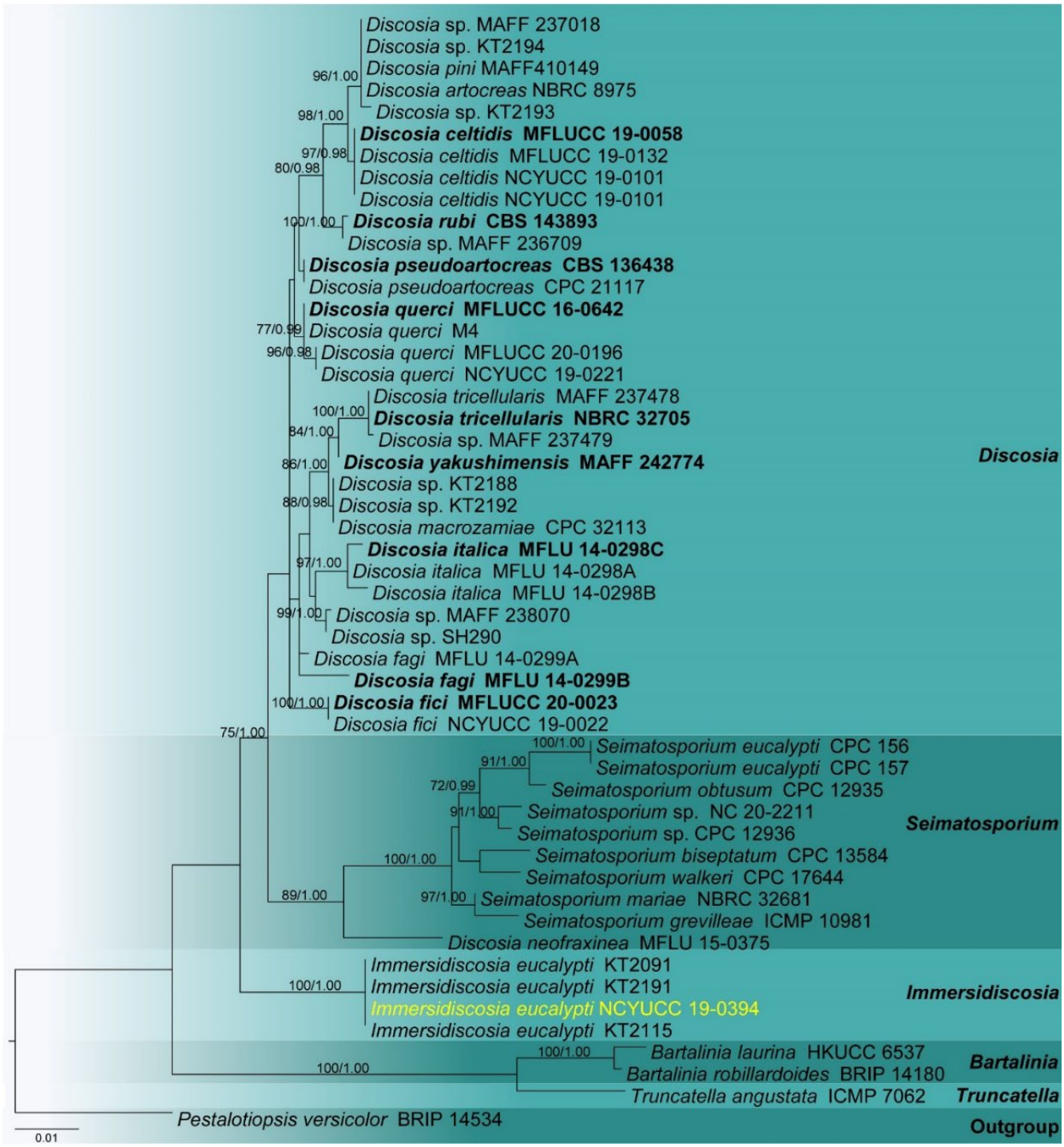

Fig. 65 – Phylogram generated from maximum likelihood analysis based on combined LSU and ITS sequence data. Fifty-one strains were included in the combined analyses, which comprised 1,447 characters (879 characters for LSU, 568 characters for ITS) after alignment. The tree topology of the maximum likelihood analysis is similar to that of the Bayesian analysis. The best RAxML tree, with a final likelihood value of -4353.814129, is presented. Estimated base frequencies were as follows: A = 0.257848, C = 0.211048, G = 0.257848, T = 0.273256; substitution rates AC = 1.335193, AG = 3.602899, AT = 1.168130, CG = 1.026300, CT = 5.892783, GT = 1.000000; gamma distribution shape parameter α = 0.691033. The evolutionary model GTR+I+G was applied to all the gene regions. Bootstrap support values for ML ≥ 75% and Bayesian posterior probabilities ≥ 0.90 are given near nodes,

respectively. The tree is rooted with *Pestalotiopsis versicolor* (BRIP 14534). Ex-type strains are in bold. The newly generated sequences are indicated in yellow.

Immersidiscosia eucalypti (Pat.) Kaz. Tanaka, Okane & Hosoya, Tanaka et al., 26, 94 (2011)

Index Fungorum number: IF 519747; Facesoffungi number: FoF 03385 Fig. 66

Saprobic on dead leaves of *Celtis formosana* L. (*Cannabaceae*). Sexual morph: Undetermined. Asexual morph: Coelomycetous. *Conidiomata* 100–150 × 250–300 µm, conspicuous, pycnidial, stromatic, amphigenous, scattered or aggregated, immersed, flattened or concave at the centre with a convex margin and a relatively thin stromatic base, rounded, black, glabrous, epidermal, unilocular or multilocular. *Conidiomata wall* 10–15 µm wide, thin-walled, composed of several layers of small, flattened, brown to dark brown pseudoparenchymatous cells, cells towards the inside light brown, arranged in a *textura angularis*, fusing and indistinguishable from the host tissues. *Conidiophores* reduced to conidiogenous cells, arising from the upper cells of the basal stroma. *Conidiogenous cells* 8–10 × 1–3 µm ($\overline{x}$ = 9.2 × 2 µm, n = 20), subcylindrical, developing directly on the innermost layer of the conidiomata wall, phialidic, each producing a single conidium, integrated, hyaline, smooth-walled. *Conidia* 15–22 × 2–4 µm ($\overline{x}$ = 18 × 3.3 µm, n = 40), hyaline, fusiform to cylindrical, thin-walled, smooth, straight or slightly curved, 3-septate, slightly constricted at septa, with cells of unequal width, basal cell obconic, with a truncate base, apical cell subconical with a rounded apex, apical and basal cells with an unbranched, filiform, flexuous or straight appendage; apical and basal appendages 10–12 µm ($\overline{x}$ = 11.2 µm, n = 20).

Culture characteristics – *Colonies* on PDA, 10–20 mm in diameter after 2 weeks, medium dense, raised, with a smooth surface and an entire edge, fluffy to velvety with smooth aspects, colony from upper view, white to cream; from bottom view, yellowish-white with white to cream mycelium.

Material examined – China, Taiwan Province, Fanlu Township area, dead leaves of *Celtis formosana*, 16 August 2017, Danushka Tennakoon, TC12 (NCYU19-0406), living culture, NCYUCC 19-0394.

GenBank accession numbers – ITS: OR759965, LSU: OR759976.

Known distribution (based on molecular data) – China, France, Italy, and Japan (Tanaka et al. 2011, Hyde et al. 2017, this study).

Known hosts (based on molecular data) – *Ardisia japonica*, *Celtis formosana*, *Eucalyptus* spp., *Laurus nobilis*, *Quercus myrsinifolia*, *Q. pubescens* (Tanaka et al. 2011, Hyde et al. 2017, this study).

Notes – Our collection (NCYUCC 19-0394) resembles *Immersidiscosia eucalypti* in having immersed, scattered or aggregated, pycnidial conidiomata, subcylindrical, phialidic conidiogenous cells and hyaline, fusiform to cylindrical, 3-septate conidia with apical and basal appendages (Tanaka et al. 2011). In particular, conidiogenous cells (8–10 × 1–3 *vs.* 5–20 × 1.5–2 µm) and conidia (15–22 × 2–4 *vs.* 15–19.5 × 2.5–3 µm) dimensions overlap, confirming that our strain is *I. eucalypti* (Tanaka et al. 2011). However, our collection shows slightly different conidiomata dimensions (100–150 × 250–300 *vs.* 200–370 × 320–480 µm). Phylogeny also indicates that our collection (NCYUCC 19-0394) clusters with other *I. eucalypti* strains (KT2091, KT2191, and KT2115) in a 100% ML, 1.00 BYPP-supported clade (Fig. 65). *Immersidiscosia eucalypti* has been reported from various host species, and this is the first record from *Celtis formosana*.

Neopestalotiopsis Maharachch., K.D. Hyde & Crous, Studies in Mycology 79, 135 (2014)

Index Fungorum number: IF 809759; Facesoffungi number: FoF 01545

Neopestalotiopsis belongs to the pestalotioid group, which also includes *Pestalotiopsis* and *Pseudopestalotiopsis* (Maharachchikumbura et al. 2014). The genus comprises pestalotiopsis-like taxa, characterized by versicolorous median cells and indistinct conidiophores (Maharachchikumbura et al.

2014). Species of *Neopestalotiopsis* are widely distributed in tropical and temperate regions, where they exhibit pathogenic, endophytic, and saprobic lifestyles (Maharachchikumbura et al. 2014, Bezerra et al. 2018, Freitas et al. 2019). Following previous studies by Konta et al. (2023) and Sun et al. (2023), and based on the Index Fungorum database (Index Fungorum 2025), we include 88 *Neopestalotiopsis* species in this study. An updated phylogeny for *Neopestalotiopsis* and closely related taxa is shown in Fig. 67.

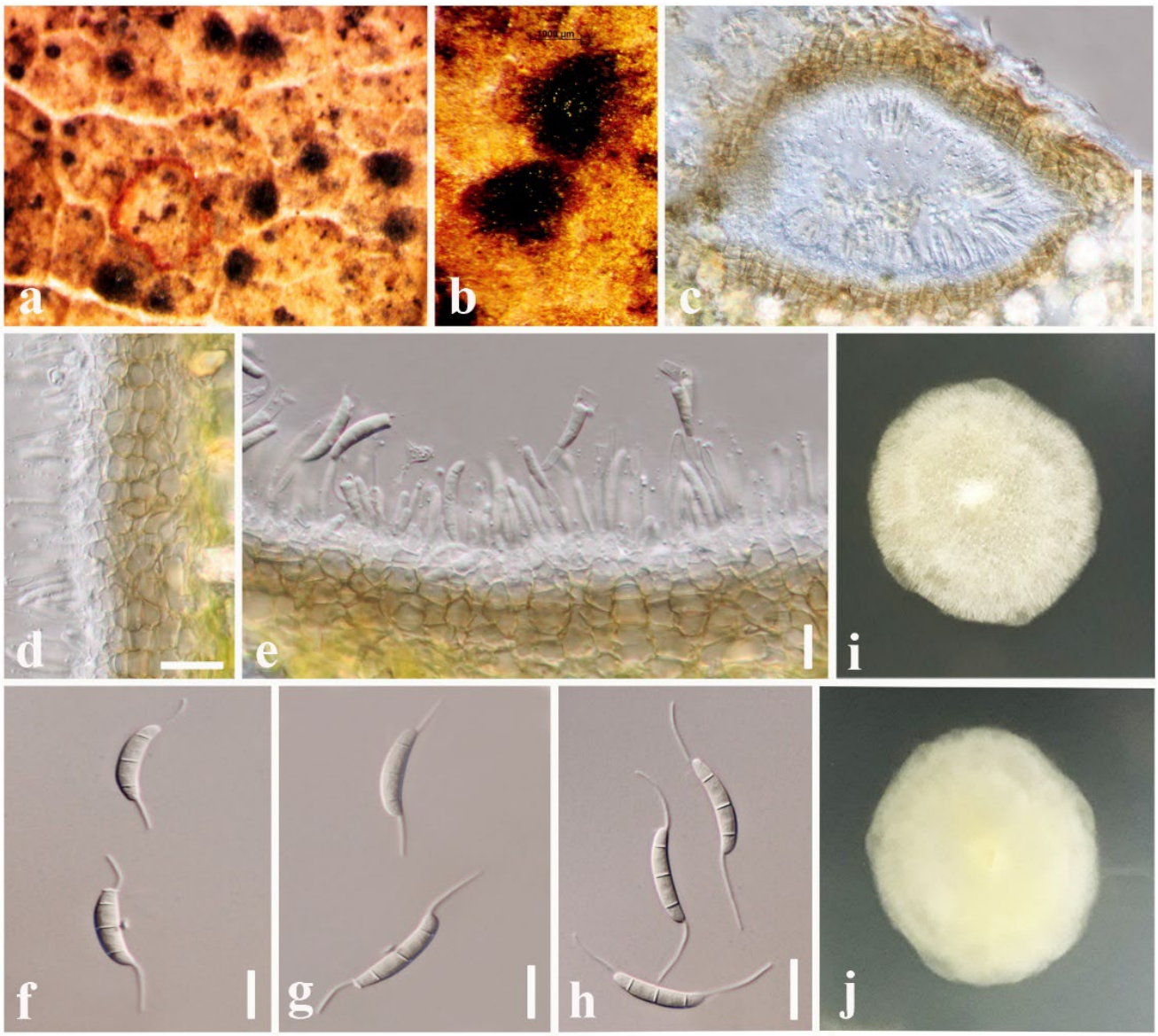

Fig. 66 – ***Immersidiscosia eucalypti*** (NCYU19-0406, **new host and geographical records**). a Appearance of conidiomata on the host. b Close-up of conidiomata. c Section of conidioma. d Conidioma wall. e Conidiogenous cells with developing conidia. f–h Conidia. i Colony from above (on PDA). j Colony from below (on PDA). Scale bars: c = 60 µm, d = 15 µm, e–h = 10 µm.

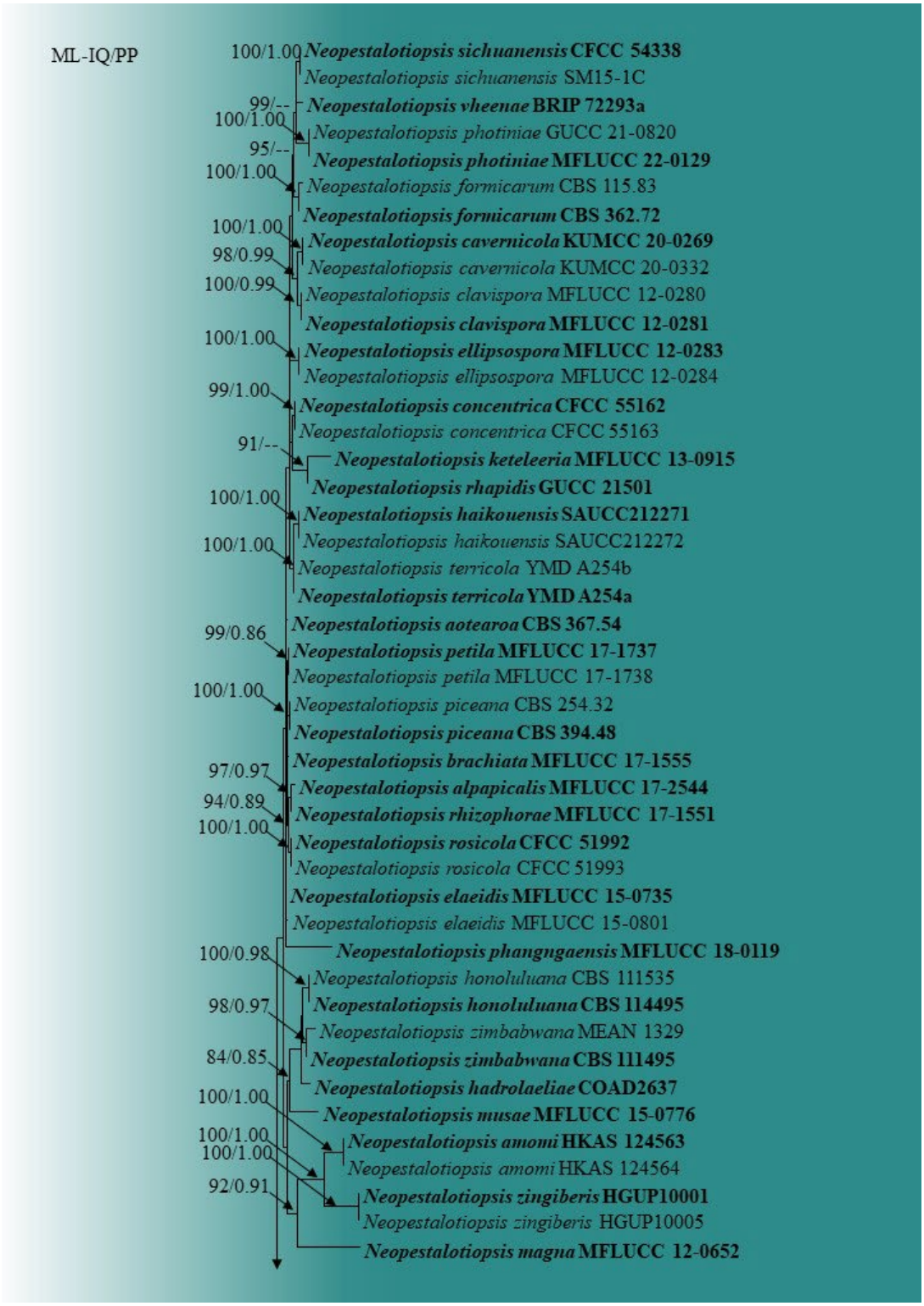

Fig. 67 – Phylogram generated from maximum likelihood analysis (IQ) based on the combined ITS, *β-tub,* and *tef-1α* sequence data of *Neopestalotiopsis*. One hundred and forty strains of *Neopestalotiopsis* were included in the combined analysis, which comprised 1681 characters (511 characters for ITS, 768 characters for *β-tubulin*, 402 characters for *tef-1α*). The tree topology of the maximum likelihood analysis is similar to that of the Bayesian analysis. The best RAxML tree with a final likelihood value of -9498.452 is presented. Maximum likelihood bootstrap values ≥ 80% and Bayesian posterior

probabilities ≥ 0.8 (MLBS/BYPP) are given at the nodes. The tree is rooted with *Pestalotiopsis knightiae* (CBS 114138 and CBS 111963) and *P. diploclisia* (CBS 115585 and CBS 115587). Ex-type strains are in bold, and the taxon described in this study is in yellow.

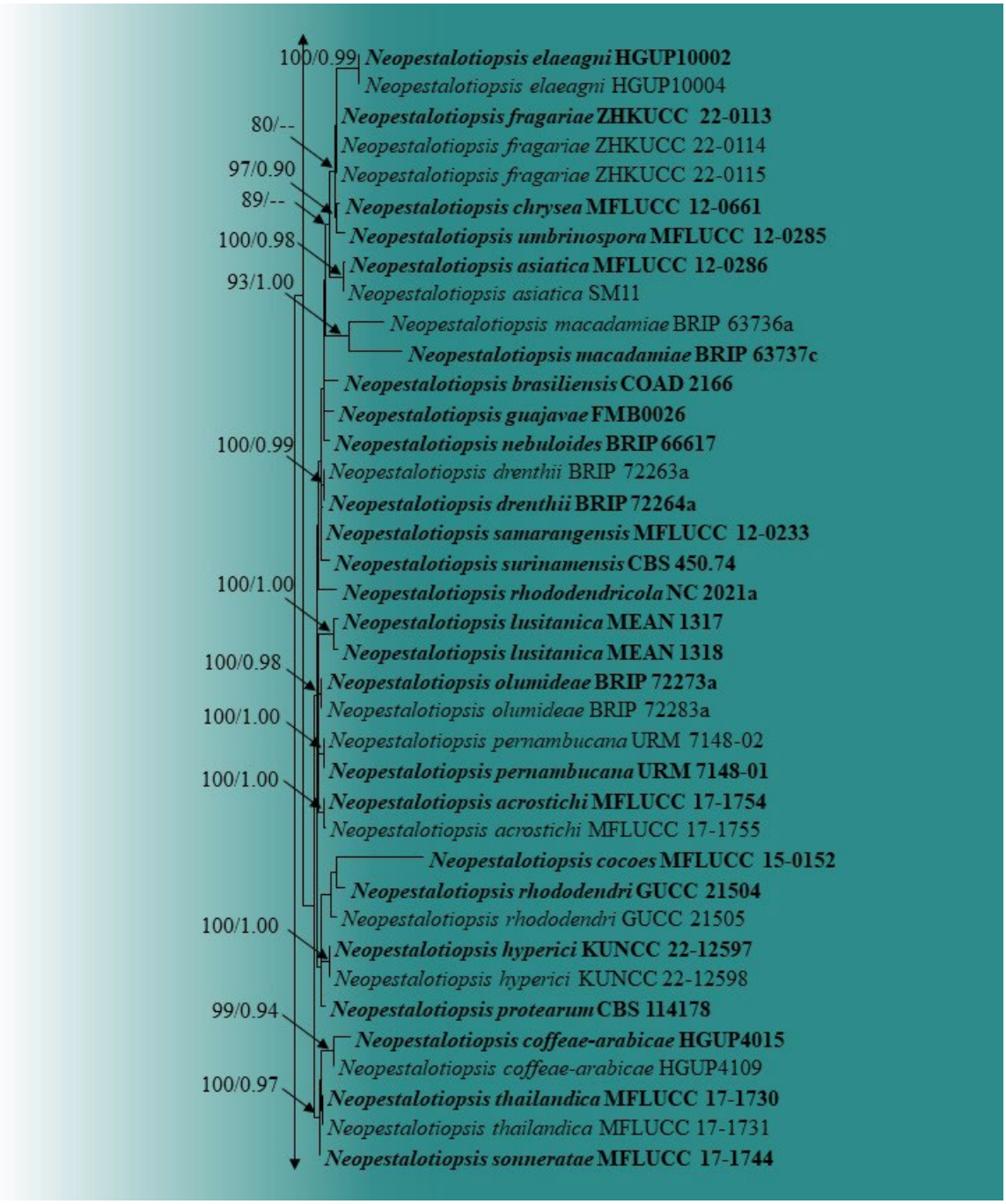

Fig. 67 – Continued.

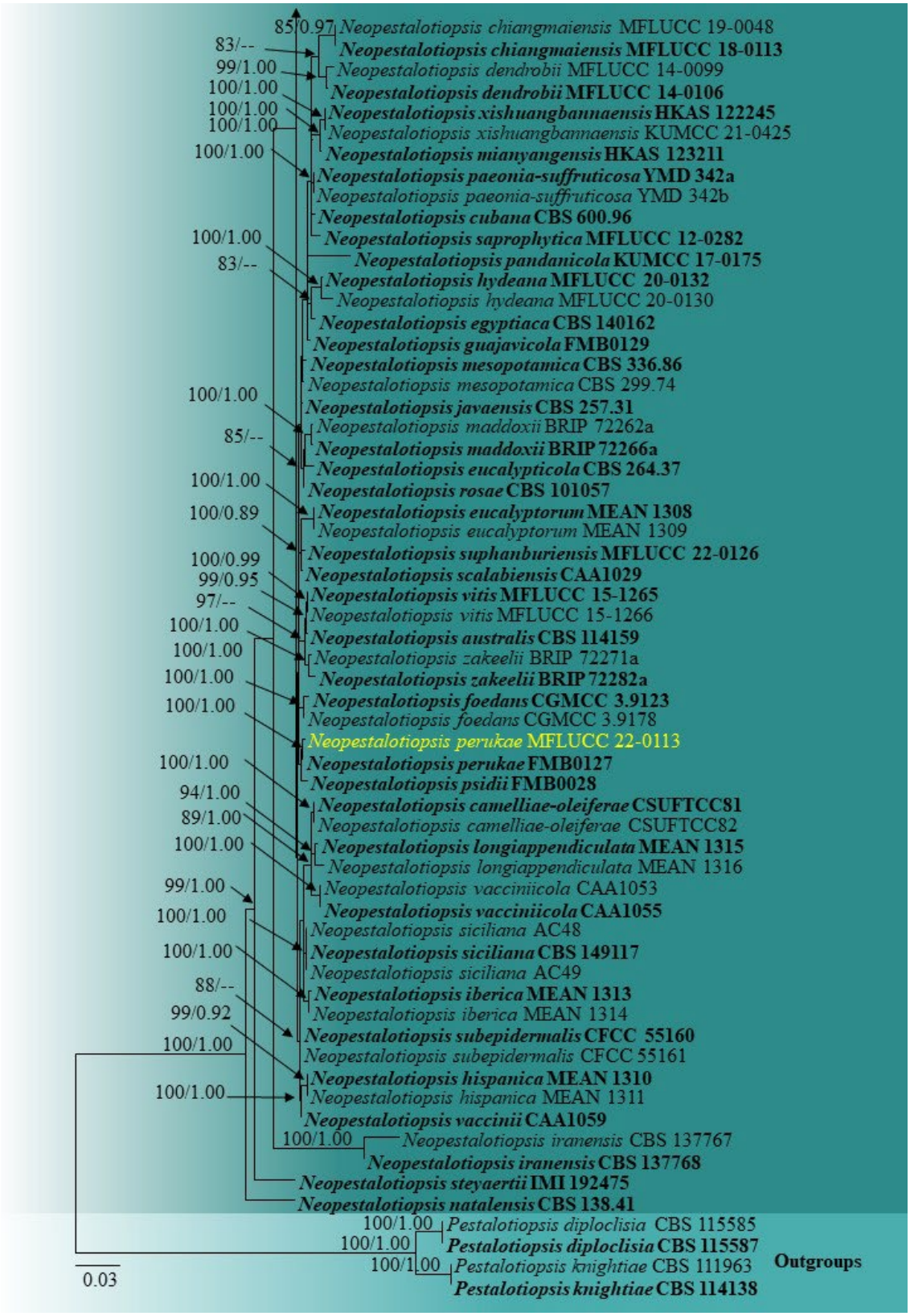

Fig. 67 – Continued.

Neopestalotiopsis perukae I.U. Haq, S. Ijaz & N.A. Khan, Pakistan Journal of Agricultural Science 58, 1306 (2021)

Index Fungorum number: IF 840637; Facesoffungi number: FoF 15048 Fig. 68

Associated with leaf spots of *Antidesma* sp. *Leaf spots* circular, pale brown. Sexual morph: Undetermined. Asexual morph: *Pycnidia* 500–1000 µm diam ($\overline{x}$ = 722 µm, n = 5), semi-immersed or partly erumpent on MEA, globose to sub-globose, brown to black, releasing a black, slimy, globose, glistening mass of conidia. *Conidiophores* ampulliform to cylindrical, mostly reduced to conidiogenous cells. *Conidiogenous cells* holoblastic, discrete or integrated, filiform to cylindrical, hyaline, smooth-walled, slightly widened at the base, and truncated at the apex. *Conidia* 19–25 × 5–8 µm ($\overline{x}$ = 22.7 × 6.4 µm, n = 40), fusiform to ellipsoidal to obovoid, straight to slightly curved, 4-septate, constricted somewhat at septa; basal cell 2–5 µm long ($\overline{x}$ = 3.8 µm, n = 30), obconic with truncate base, rugose and thin-walled; three median cells, subcylindrical to doliiform, versicolourous, pale to dark brown, septa darker than the rest of the cells; second cell from base 3–6 µm long ($\overline{x}$ = 4.4 µm, n = 30); third median cell 2.5–5 µm long ($\overline{x}$ = 4 µm, n = 30); fourth cell 3–6 µm long ($\overline{x}$ = 3.9 µm, n = 30); apical cell 2.5–5 µm long ($\overline{x}$ = 3.6 µm, n = 30), conic, subcylindrical, hyaline, thin- and smooth-walled, with 1–4 tubular apical appendages (mostly 3) arising from the apical crest, flexuous, unbranched, 8–26 µm long ($\overline{x}$ = 20 µm, n = 20), basal appendage 2.5–7 µm long ($\overline{x}$ = 4.5 µm, n = 20), single, tubular, unbranched, centric.

Culture characteristics – Colonies on MEA reaching approximately 70 mm in diameter, after 7 days of incubation at 25 °C, forming dense mycelia and round colonies with entire margins; colonies appear white on both the upper and lower surfaces and produce black pycnidia.

Material examined – Thailand, Chiang Mai Province, Doi Lo District, on *Antidesma* sp., 15 October 2019, D. Gomdola, DG310 (MFLU 22-0173), living culture MFLUCC 22-0113.

GenBank accession numbers– ITS: OP681140, *tef-1α*: OQ850147, *β-tubulin*: OQ850149.

Known distributions – Pakistan (Ul Haq et al. 2021) and Thailand (this study).

Known hosts – *Antidesma* sp. (*Phyllanthaceae*) (this study), *Psidium guajava* (*Myrtaceae*) (Ul Haq et al. 2021).

Notes – Based on the multigene phylogenetic analyses of the concatenated ITS, *β-tub*, and *tef-1α* matrices of *Neopestalotiopsis*, our isolate (MFLUCC 22-0113) clustered with the ex-type strain of *Neopestalotiopsis perukae* (FMB0127) with 100% ML and 1.00 PP support (Fig. 67). Excluding gaps, a pairwise nucleotide comparison between MFLUCC 22-0113 and *N. perukae* (FMB0127) revealed no difference in *β-tub* (681 bp). However, a 0.4% and 0.5% difference was observed in the ITS and *tef-1α* regions, respectively. Furthermore, conidial features match the species concept of the pestalotioid group, specifically those of *Neopestalotiopsis* (Maharachchikumbura et al. 2012, 2014). Our isolate shares a morphology similar to that of *N. perukae* (FMB0127), characterized by fusiform to ellipsoidal, 4-septate conidia with three versicolored median cells (Ul Haq et al. 2021). Conidia of MFLUCC 22-0113 are 19–25 µm long and 5–8 µm wide, while those of *N. perukae* are 18.3–21.1 µm long and 5.6–7.2 µm wide (Ul Haq et al. 2021). Based on morphology and multigene phylogenetic analyses, we establish MFLUCC 22-0113 as a new host and geographical record, isolated for the first time from leaf spots of *Antidesma* sp. in northern Thailand.

Xylariales Nannf., Nova Acta Regiae Societatis Scientiarum Upsaliensis Ser 48(2), 66 (1932)

Index Fungorum number: IF 90505; Facesoffungi number: FoF 12988

Melanographium Sacc., Annales Mycologici 11(6), 557 (1913)

Index Fungorum number: IF 8891; Facesoffungi number: FoF 13787

Saccardo (1913) established the genus *Melanographium* with *M. spleniosporum* as the type species. This genus currently comprises 15 species; however, sequence data are available for only two, with the majority of species classified based on morphological observations (Hyde et al. 2020, Boonmee et al. 2021). Due to the limited molecular data, the taxonomic placement of the remains is uncertain. Wijayawardene et al. (2018) later classified *Melanographium* as a genus incertae sedis within

Sordariomycetes. The genus is characterized by its superficial, effuse colonies, unbranched, straight to flexuous, brown conidiophores, polyblastic conidiogenous cells with sympodial proliferation, and holoblastic, reniform, aseptate, and solitary conidia (Ellis 1963, 1971). An updated phylogeny for *Melanographium* and closely related taxa is shown in Fig. 69.

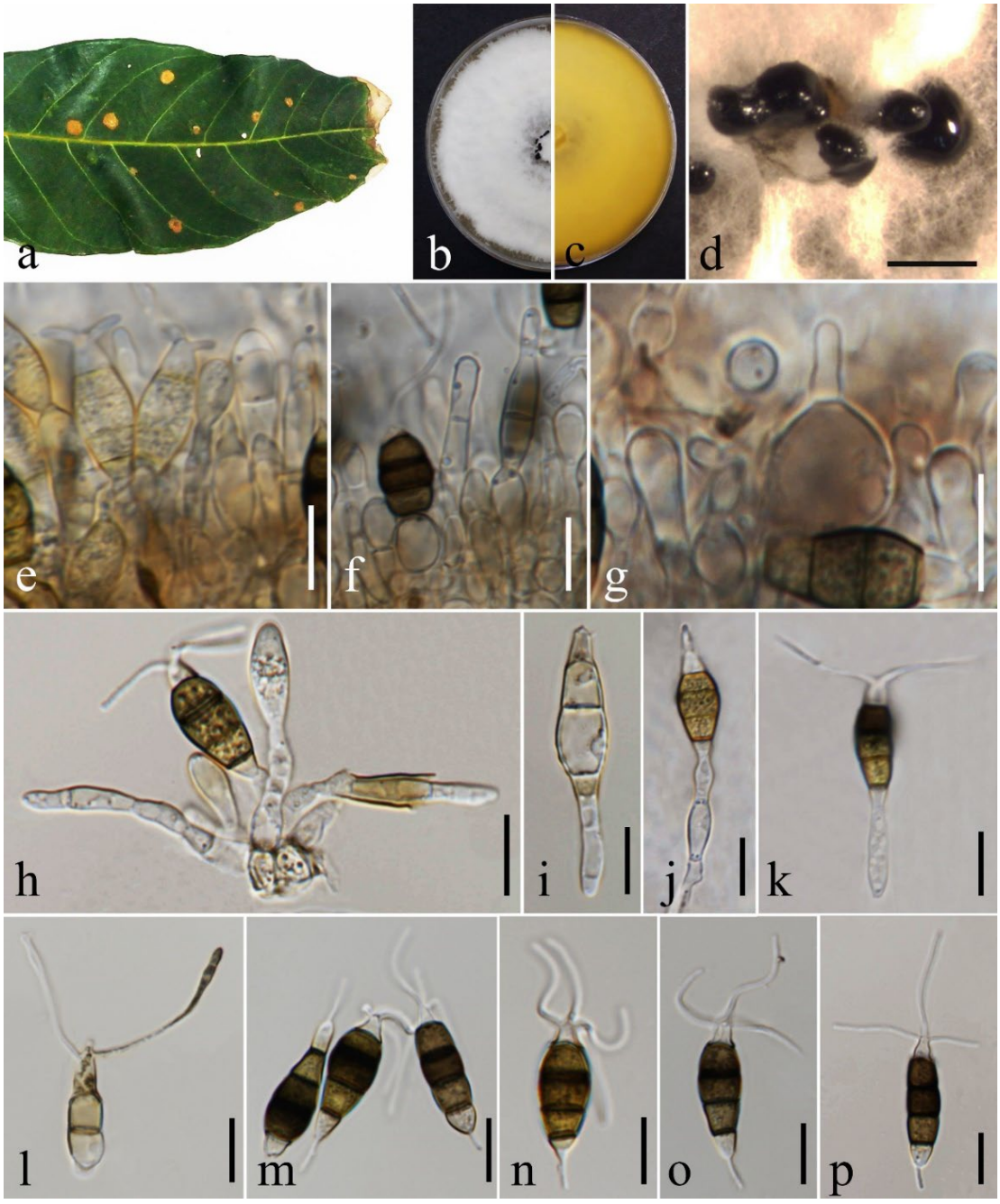

Fig. 68 – *Neopestalotiopsis perukae* (MFLUCC 22-0113, **a new host and geographical record**). a Specimen. b, c Upper view (left) and bottom view (right) of colony on MEA. d Pycnidia on MEA. e–g Conidiogenesis. h–k Attachment of conidia. l Immature conidium with appendages.m–p Conidia bearing apical and basal appendages. Scale bars: d = 1000 μm, e–p = 10 μm.

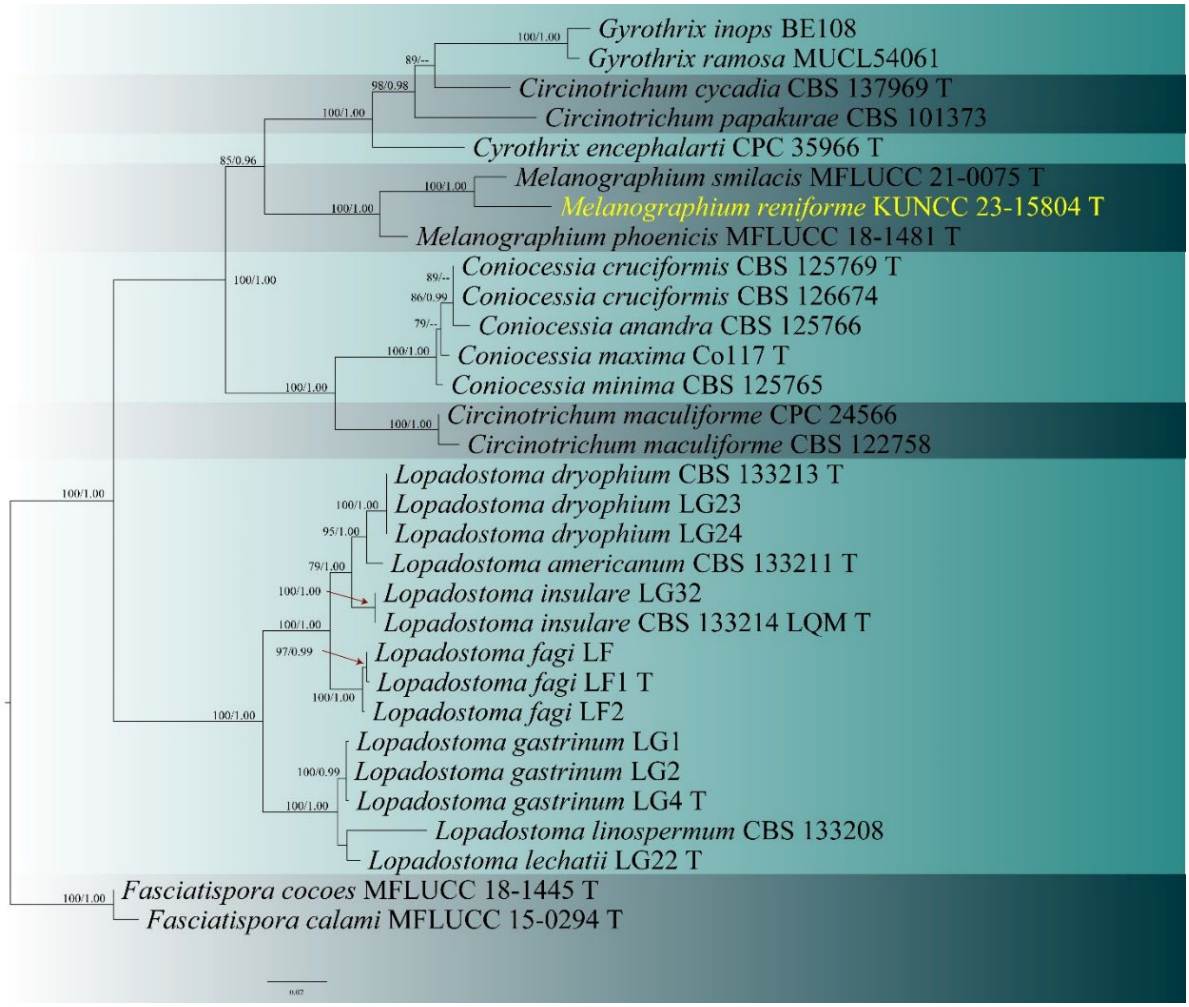

Fig. 69 – Maximum likelihood phylogenetic tree based on a combined LSU and ITS sequence data of Melanographium taxa and related genera. Thirty-one strains were included in the combined analyses, which comprised 1,500 characters (ITS: 1–600bp; LSU: 601–1,500bp) after alignment. *Fasciatispora cocoes* (MFLUCC 18-1445) and *Fasciatispora calami* (MFLUCC 15-0294) were used as outgroup taxa. The tree topology of the maximum likelihood analysis is similar to that of the Bayesian analysis. The best RAxML tree with a final likelihood value of -6424.598674 is presented. Estimated base frequencies were as follows: A = 0.261794, C = 0.217459, G = 0.275262, T = 0.245485; substitution rates AC = 1.181909, AG = 2.387082, AT = 1.803172, CG = 0.947131, CT = 5.381398, GT = 1.000000; gamma distribution shape parameter α = 0.551593. The evolutionary model GTR+I+G is applied to all the genes. Bootstrap support values for ML greater than 75% and Bayesian posterior probabilities greater than 0.90 are given near nodes, respectively. The newly generated sequences are indicated in yellow.

Melanographium reniforme Y. Y. Yang, Gomes de Farias & K. D. Hyde, sp. nov.

Index Fungorum number: IF 903449; Facesofungi number: FoF 15183 Fig. 70

Etymology – The species epithet "*reniforme*" refers to the fungus having reniform ascospores.

Saprobic on the dead stem of an unidentified plant. Sexual morph: Not observed. Asexual morph: *Colonies* on the substratum are superficial, tufted, dark brown to black, effuse, and hairy. *Mycelium* mostly immersed, composed of pale brown hyphae, branched, and septate. *Conidiophores* 435–617 µm long ($\bar{x}$ = 533 µm, n = 10), 3.9–4.5 µm wide ($\bar{x}$ = 4.2 µm, n = 10), macronematous, erect, loose fascicles, straight or slightly flexuous, unbranched, smooth, multi-septate, brown to pale brown towards the apex,

dark brown below, subcylindrical, thick-walled. *Conidiogenous cells* mono- to polytretic, integrated, terminal, subcylindrical, subhyaline to pale brown, sympodial, cicatrized, and have pale scars. *Conidia* 14–24 µm long ($\overline{x}$ =18 µm, n=30), 8–12 µm wide ($\overline{x}$ =10 µm, n = 30), holoblastic, acropleurogenous, solitary, reniform or obovoid, pale brown when immature, become brown to dark brown when mature, smooth-walled, aseptate, guttulate when immature. *Conidial secession* schizolytic.

Culture characteristics – culture was established from a germinating conidium. The colony slowly grew on PDA medium, reaching 4.5 cm in diameter after 18 days at room temperature (20–22℃), with white, round, velvety, dense mycelia that radiated outward, and a reverse side that was yellowish.

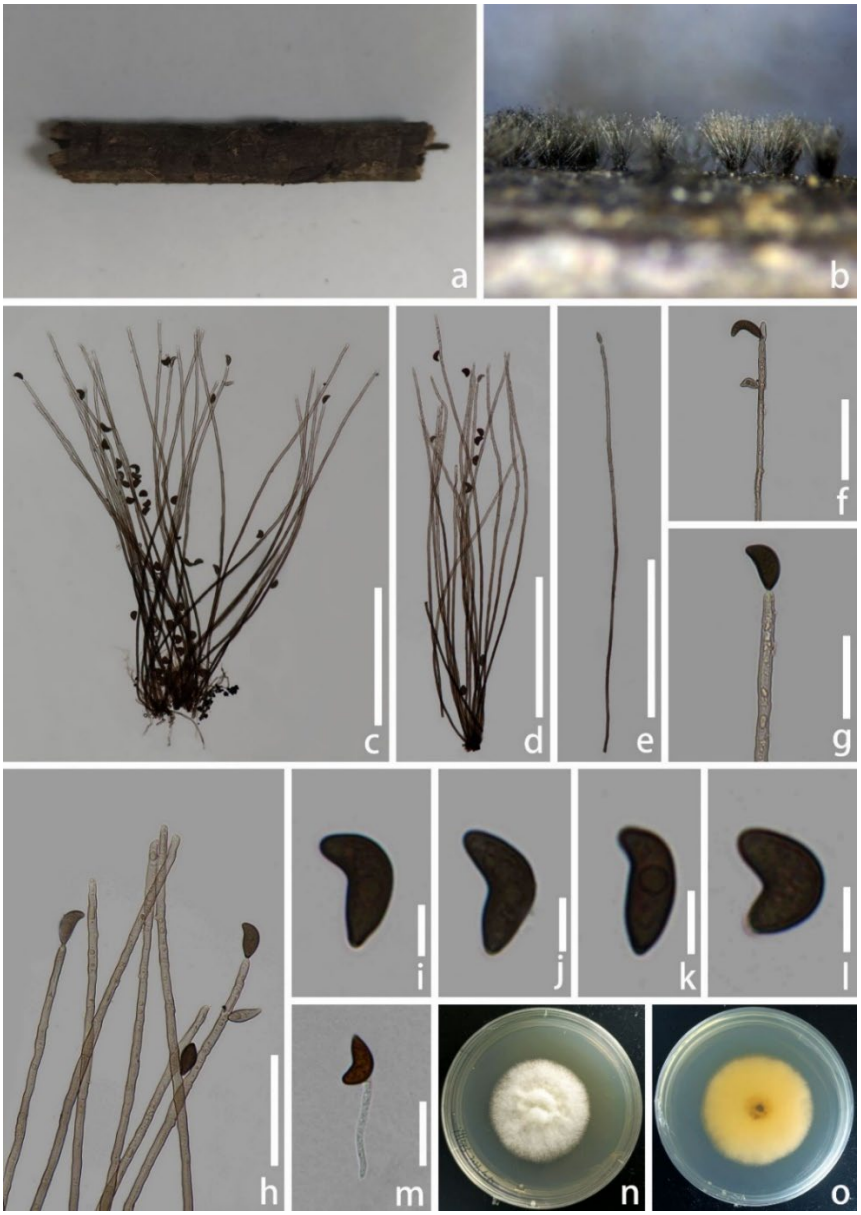

Fig. 70 – *Melanographium reniforme* (HAKS 131232, **holotype**). a Natural substrate. b Appearance of colonies on natural substrate. c, d fascicled conidiophores. e Conidiophores with conidiogenous cells and conidia. f–h Apex of conidiophores with developing conidia. i–l conidia. m Germinated conidium. n, o Culture on PDA from the surface and reverse. Scale bars: c–e = 200 µm, f, h = 50 µm, g, m = 25 µm, i–l = 10 µm.

Material examined – China, Yunnan Province, Jinghong City, Banna Wild Elephants Valley, on a dead stem of an unidentified plant, 9 September 2022, Yanyan Yang, YYY343 (HKAS 131232, holotype), living culture KUNCC 23-15804.

GenBank accession numbers – ITS: OR813920, LSU: OR813921.

Notes – *Melanographium reniforme* was found on dead wood in China. Phylogenetic analyses placed the new strain in a sister clade to *Melanographium smilacis* (MFLU 21-0075) with 100% ML and 1.00 BYPP support. *Melanographium smilacis* was first introduced to the genus *Melanographium* by Boonmee et al. (2021). The sequence comparisons revealed 29 bp (6%) differences in a 482 bp fragment of ITS between *M. reniforme* and *M. smilacis* (MFLU 21-0075). Morphologically, *M. reniforme* and *M. smilacis* exhibit effused and tufted colonies, characterized by brown conidiophores, reniform or obovoid, and brown conidia. However, *M. smilacis* differs from *M. reniforme* in having flexuous conidiophores that are geniculate near the apex (270–561 × 2–7 μm). Therefore, we introduce our isolate (HKAS 131232) as a new species of *Melanographium* based on phylogenetic analysis and morphological comparison.

Xylariaceae Tul. & C. Tul. Selecta Fungorum Carpologia, Tomus Secundus. Xylariei - Valsei - Sphaeriei 2, 3 (1863)

Index Fungorum number: IF 81528; Facesoffungi number: FoF 00070

Xylaria Hill ex Schrank, Baiersche Flora 1, 200 (1789)

Index Fungorum number: IF5832; Facesoffungi number: FoF 000696

Xylaria is the largest genus of *Xylariaceae*, with *X. hypoxylon* as the type species (Peršoh et al. 2009, Wijayawardene et al. 2022b). Species of *Xylaria* are primarily recognized for their distinctive morphological features, including large stromata, cylindrical asci with an elongated stipe, and dark ellipsoidal ascospores in both sexual and geniculosporium-like asexual forms (Ju & Rogers 1996, Stadler et al. 2013). Most *Xylaria* species function as saprobes, thriving on damp, decomposing dicotyledonous wood; however, some are also found on monocotyledons, fruits, seeds, and fallen leaves (Hsieh et al. 2010, Ju & Hsieh 2023), while others are endophytes (Ma et al. 2022). An updated phylogeny for *Xylaria* and closely related taxa is shown in Fig. 71.

Xylaria grammica (Mont.) Mont., Nova acta Regiae Societatis Scientiarum Upsaliensis 3, 1(1), 128 (1851)

Index Fungorum number: IF 195134; Facesoffungi number: FoF 14125 Fig. 72

Sprobes on *Quercus* sp. Sexual morph: *Stromata* cylindrical, fusiform to cylindrical, clavate, solitary, unbranched, rarely branched near the base, with the apex obtusely rounded or tapering to a sterile point, on a long, well-defined, slender, smooth, and black stipe. Arising from a somewhat discoid base, 4–8 cm in height and 0.7–1.5 cm in diameter. *Exterior* dull brown, with longitudinal cracks, exposing the underlying dark area, and cream-coloured remaining areas appear as vertical stripes, with the crust very minutely granulated in parallel. Interior white to yellowish-brown, becoming hollow and loosening, with an irregular rhombus texture. *Perithecia* immersed, subglobose, 0.4–1.2 mm in diameter. *Ostiole* punctiform, situated in the dark stripes. *Asci* cylindrical, 8-spored, 72–160 (109) μm long, the spore-bearing parts 62–81 × 4–5 μm ($\overline{x}$ = 71 × 4.5 μm, n = 30), with apical apparatus bluing in Melzer's reagent, tubular with a slightly flared apex, 2–3.4 × 1.5–2.4 μm ($\overline{x}$ = 2.7 × 1.9 μm, n = 30). *Ascospores* 7−19 × 4−9 μm ($\overline{x}$ = 14 × 6.5 μm, n = 30), uniseriate, ellipsoid, with an olive to brown smooth wall, straight, and with 1−2-guttulate. Asexual morph: Not observed.

Known hosts – *Ardisia nervosa* (*Myrsinaceae*) (Okane et al. 2012), *Dendrobium aphyllum*, *D. nobile*, *D. chrysanthum*, *D. chrysotoxum*, *D. crystallinum*, and *D. fimbriatum* (Chen et al. 2013), *Licuala spinosa* (*Arecaceae*), *Polyalthia simiarum* (*Annonaceae*), *Polyalthia simiarum* (*Annonaceae*) (Okane et al. 2012), *Protium heptaphyllum* (Fierro-Cruz et al. 2017), *Salacia chinensis* (*Celastraceae*), and *Saprosma longifolium* (*Rubiaceae*) (Okane et al. 2012),

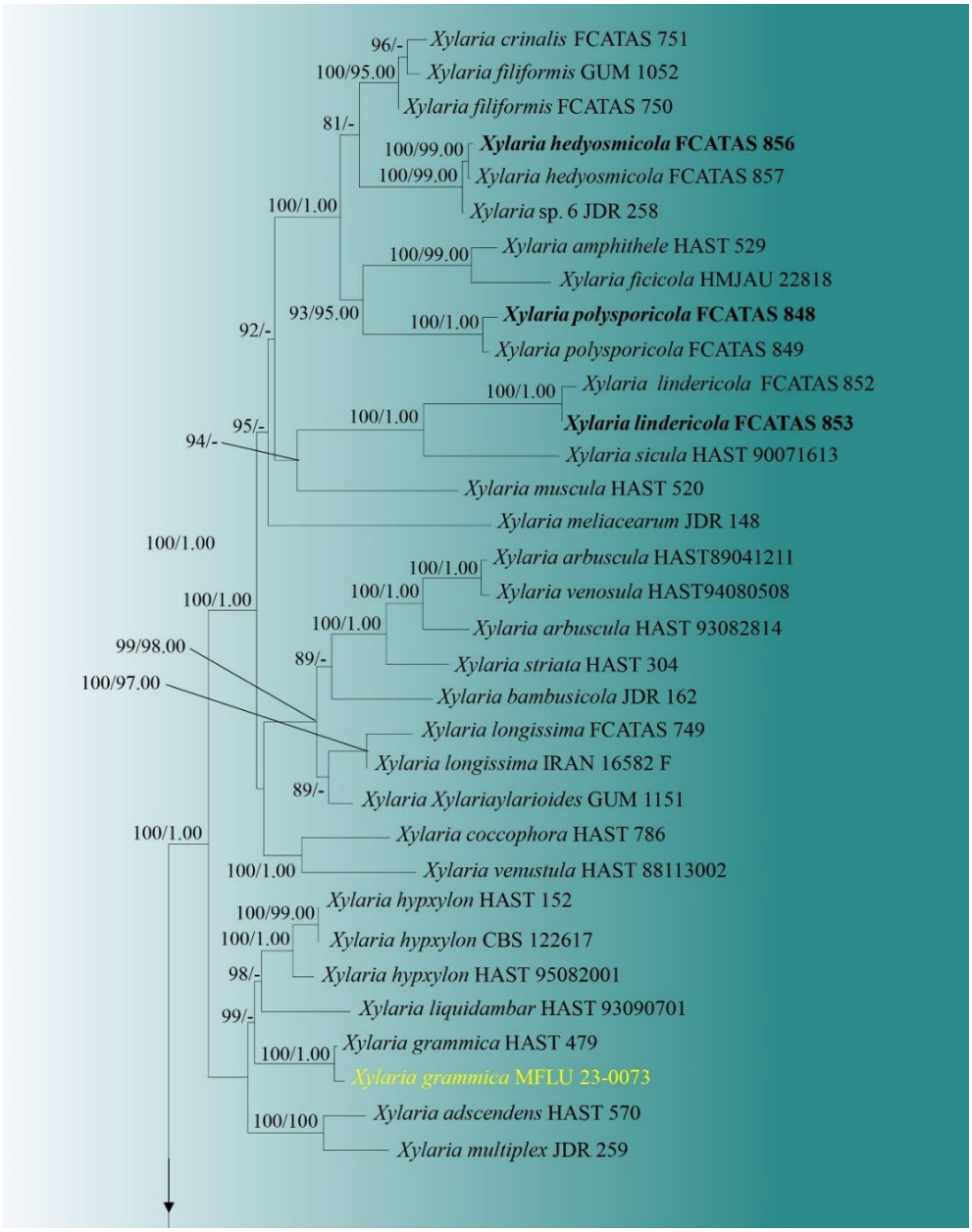

Fig. 71 – Phylogram generated from maximum likelihood analysis based on combined ITS, *rpb2*, and *β-tubulin* sequence data of the *Xylariaceae*. Maximum-likelihood bootstrap support values greater than or equal to 60% and Bayesian posterior probabilities greater than or equal to 0.95 are shown near the nodes, respectively. The tree was rooted with *Hypoxylon trugodes* (MUCL 54794), *Hypoxylon ticinense* (CBS 115271), and *Daldinia loculatoides* (CBS 113279). Seventy-four strains were included in the combined analyses, which comprised 3,348 characters (584 characters for ITS, 1,190 characters for *rpb2*, and 1,572 characters for *β-tubulin*). The tree topology of the maximum likelihood analysis is similar to that of the Bayesian analysis. The best RAxML tree with a final likelihood value of -86198.836 is presented. Estimated base frequencies were as follows: A = 0.239, C = 0.278, G = 0.238, T = 0.245, substitution rates AC = 1.15531, AG = 4.89267, AT = 1.15531, CG = 1.00000, CT = 7.03206, GT = 1.00000; gamma distribution shape parameter α = 0.802. All the type specimens are in bold. The newly generated sequences are indicated in yellow.

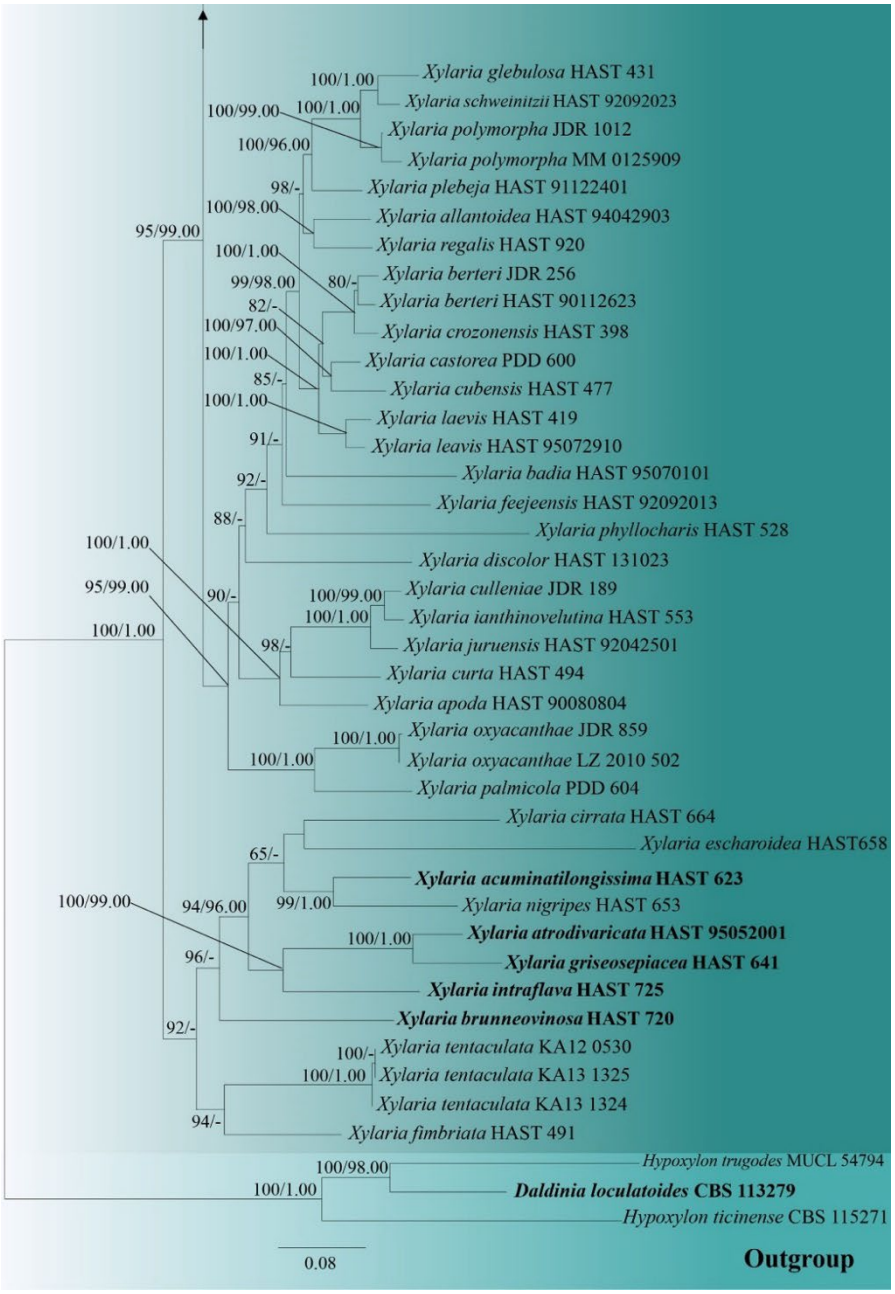

Fig. 71 – Continued.

Material examined – Thailand, Chiang Mai Province, Chomthong District, on *Quercus kingiana* (*Fagaceae*), 18 October 2021, MC Samarakoon, DI015 (MFLU23-0073, a new host record).

GenBank accession numbers – ITS: OQ652943, *rpb2*: OQ674150, *β-tubulin*: OQ674151.

Known distribution – Brazil (da Silva Cruz & Cortez 2015), China (Chen et al. 2013), Colombia (Fierro-Cruz et al. 2017), India (Kshirsagar et al. 2009), Malaysia (Lee et al. 2002), Taiwan (Hashemi et al. 2015), Thailand (Whalley et al. 2015, Becker et al. 2020, Ma et al. 2022, this study).

Notes – Our collection morphologically resembles *X. grammica* in its cracking of the stromatic crust and the presence of rows of ostioles within the cracks. Our phylogenetic analysis based on combined ITS, *rpb2*, and *tub2* data revealed that our strain clusters with *X. grammica* (HAST 479), with 100% maximum-likelihood support and a Bayesian posterior probability of 1.00. We report our isolate (MFLU 23-0073) as a new host record from *Quercus kingiana* in Thailand.

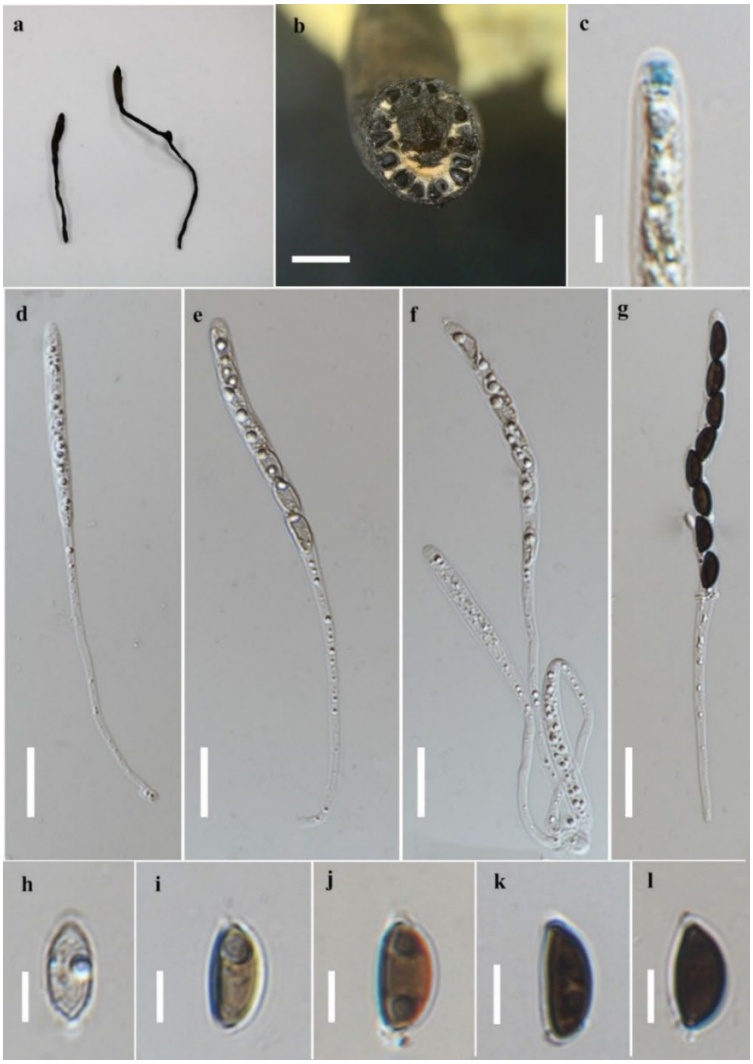

Fig. 72 – ***Xylaria grammica*** (MFLU23-0073, **a new host record**): a Stromata habit. b Section of ascoma. c Apical ring. d–g Asci. h–l Ascospores. Scale bars: b = 1 mm, c = 5 µm, d–g = 20 µm, h–l= 5 µm.

Phylum ***Basidiomycota*** R.T. Moore, Botanica Marina 23(6), 371 (1980)
Subphylum ***Agaricomycotina*** Doweld, Prosyllabus Tracheophytorum. Tentamen Systematis Plantarum Vascularium (Tracheophyta) (Moscow) (2001)
Class ***Agaricomycetes*** Doweld, Tentamen Systematis Plantarum Vascularium (Tracheophyta) (Moscow) (2001)
Agaricales Underw., Moulds, mildews and mushrooms. A guide to the systematic study of the Fungi and Mycetozoa and their literature (New York) 97 (1899)

Index Fungorum number: IF 90508; Facesoffungi number: FoF 14342

Agaricaceae Chevall., Flore Générale des Environs de Paris 1, 121 (1826)

Index Fungorum number: IF 80434; Facesoffungi number: FoF 14343

Coniolepiota Vellinga, Vellinga, Sysouphanthong & Hyde, Mycologia 103(3), 502 (2011)

Index Fungorum number: IF 518493; Facesoffungi number: FoF 19185

Coniolepiota is a monotypic genus consisting of a single species, *C. spongodes* (Berk. & Broome) Vellinga (Vellinga et al. 2011). The type species is characterized by medium- to large-sized white basidiomata completely covered with lilac to purple-grey, powdery velar warts. It possesses small hyaline ellipsoid to oblong basidiospores, four-spored basidia, the presence of cheilocystidia, the absence

of pleurocystidia and clamp connection, as well as a powdery pileus covering composed of irregularly shaped hyphae. An updated phylogeny for *Coniolepiota spongodes* and closely related taxa is shown in Fig. 73.

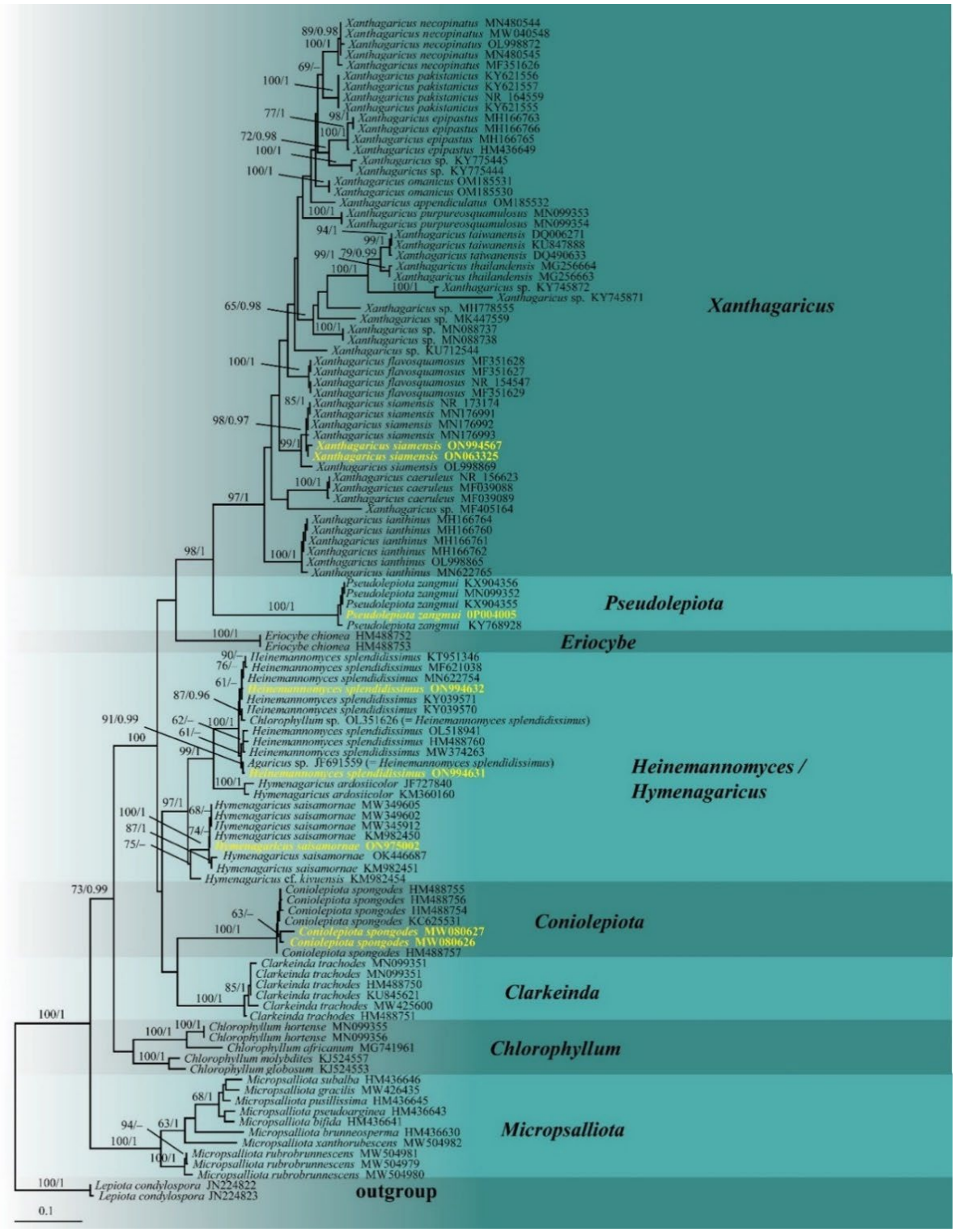

Fig. 73 – Phylogram generated from maximum likelihood analysis of *Agaricaceae* based on ITS sequence data. Totally, 112 sequences are included in the analyses, comprising 723 characters after

alignment. The best RAxML tree with a final likelihood value of -9301.954593 is presented. The matrix contained 487 distinct alignment patterns, with 10.56% of the characters being undetermined or gaps. Estimated base frequencies were as follows: A = 0.228398, C = 0.223926, G = 238676, T = 0.309000; substitution rates AC = 1.229884, AG = 3.697926, AT = 1.260755, CG = 0.709063, CT = 4.037652, GT = 1.000000; gamma distribution shape parameter α = 0.379081. Bootstrap values (ML/BI) are given above the branches. Bootstrap values for maximum likelihood ≥ 60 and Bayesian posterior probabilities ≥ 0.95 are placed above the branches. *Lepiota condylospora* (JN224822, JN224822) is used as the outgroup taxon. The newly generated strains are in yellow.

Coniolepiota spongodes (Berk. & Broome) Vellinga, Vellinga et al., Mycologia 103(3), 502 (2011)

Index Fungorum number: IF 518494; Facesoffungi number: FoF 19195 Figs. 74, 75

Pileus 35–70 mm diam., firstly hemispherical, expanding to convex, applanate to plano-concave when mature, with straight margin; when young, completely covered with a thick layer of powdery velar warts, greyish magenta (14 E4-8), fallen or thinner layer when mature, with white background; marginal zone powdery or with appendiculate remnants, concolorous with those on center. *Lamellae* free, white to yellowish white (4A2) when mature, broadly ventricose, crowded, with 3 lamellulae, with an eroded edge. *Stipe* 65–90 × 6–10 mm, cylindrical, slightly wider at the base; from the annular zone downward, the base is covered with crowded concolorous powder as on the pileus, absent at the apex zone, with a white background. *Annulus* with an annular zone or remnants, as on the pileus margin. *Context* white in pileus; white, hollow in stipe. *Smell and taste* were not tested. *Spore* print white.

Fig. 74 – Fresh basidiomata of *Coniolepiota spongodes* in situ (a new record). a, b Strain HNL503450. c, d Strain HNL503122.

Basidiospores [50, 2, 2] l × w = 4.5–6.5 × 2.4–3.8 µm, avl × avw = 5.2 × 3.1 µm, Q = 1.43–2.03, avQ = 1.70; in side view ellipsoid to oblong, with rounded apex, oblong in frontal view, hyaline, slightly thick-walled, dextrinoid. *Basidia* 15–19 × 5–10 µm, short clavate, hyaline, slightly thick-walled, 4-spored. *Cheilocystidia* 15–22 × 5–10 µm, clavate to broadly clavate, hyaline, thick-walled. *Pleurocystidia* absent. *Pileus* covering covered with various shapes of hyphae, cylindrical, irregular, branched, t-shaped, 3–12 µm wide, cylindrical elements 18–55 µm long. *Stipe* covering is similar to the pileus covering. *Clamp connections* absent.

Habitat and distribution – solitary, saprotrophic, on soil, found in Oudomxay and Xiangkhouang Provinces of North Laos.

Material examined – Laos, Oudomxay Province, Xay District, 25 July 2014, P. Sysouphanthong, PS2014-1451 (HNL503122); Xiangkhouang Province, Phonsavan District, 22 May 2016, P. Sysouphanthong, PS2016-5 (HNL503450).

GenBank accession numbers – HNL503122: ITS: MW080626; HNL503450: ITS: MW080627.

Notes – Vellinga et al. (2011) reported that *Coniolepiota spongodes* are distributed in Malaysia, Singapore, Sri Lanka, and Thailand. Furthermore, Hosen et al. (2013) reported the species from Bangladesh and China. This study reports the species from Laos based on morphology (Figs. 74–75) and molecular evidence (Fig. 73).

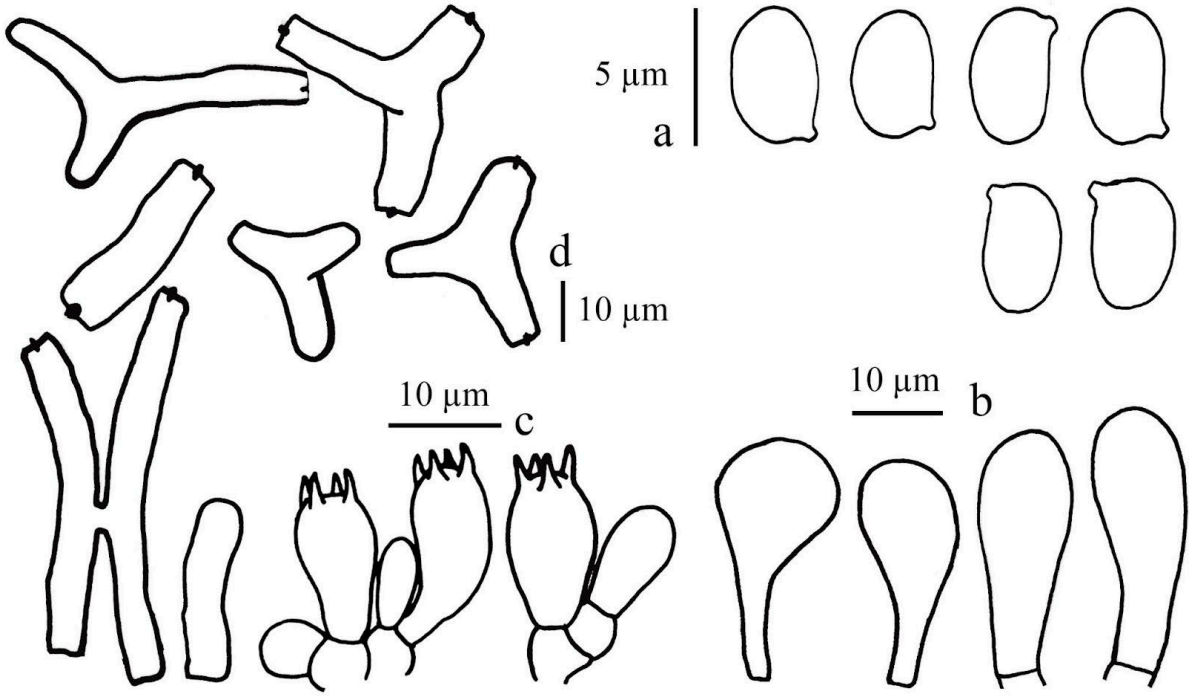

Fig. 75 – Microcharacters of *Coniolepiota spongodes* (HNL503450). a Basidiospores. b Cheilocystidia. c Basidia. d Elements on the pileus covering.

Heinemannomyces Watling, Belgian Journal of Botany 131(2), 133 (1999)

Index Fungorum number: IF 27918; Facesoffungi number: FoF 19176

Heinemannomyces is a monotypic genus belonging to *Agaricaceae*, and *H. splendidissima* is the type species (Watling 1998). The species is characterised by woolly-floccose or woolly arachnoid velar remnants on the pileus and stipe with chestnut brown to greyish red, dark blue to bluish grey lamellae, pale yellow and ellipsoidal ovoid basidiospores, presence of cheilocystidia, absence of pleurocystidia and clamp connections (Watling 1998, Hosen et al. 2018). An updated phylogeny for *Heinemannomyces* and closely related taxa is shown in Fig. 73.

Hymenagaricus Heinem., Bulletin du Jardin Botanique National de Belgique 51(3/4), 465 (1981)

Index Fungorum number: IF 17814; Facesoffungi number: FoF 19188

Hymenagaricus (*Agaricaceae* Chevall.) comprises 20 accepted species, with *H. hymenopileus* (Heinem.) Heinem. as the type species (He et al. 2019, Kalichman et al. 2020). *Hymenagaricus* is characterized by small to medium-sized basidiomata, covered squamules on the pileus with epithelial to hymeniform cells, yellow to pale brown basidiospores, the presence of cheilocystidia, and the absence of pleurocystidia and clamp connections (Heinemann & Little Flower 1984, Little Flower et al. 1997, Kumla et al. 2021, 2023, Hussain et al. 2024). An updated phylogeny for *Hymenagaricus* and closely related taxa is shown in Fig. 73.

Hymenagaricus saisamornae J. Kumla & N. Suwannarach, Kumla et al., Chiang Mai Journal of Science 48(3) (2021)

Index Fungorum number: IF 838223; Facesoffungi number: FoF 19198 Figs. 76, 77

Pileus 12–35 mm diam., firstly conical to hemispherical, expanding to campanulate or convex, applanate when mature, with straight incurved margin; when young with glabrous at the center, brown (7E5-8) to reddish brown (8E5-8), with concolorous minute scattered squamules towards the margin, soon broken around the center and form a glabrous patch at the center, with concolorous squamules around the patch, with concolorous minute scattered squamules towards the margin, with a white background when young and becoming pinkish to pale red (9A2-3) when mature; marginal zone with minute concolorous squamules and white appendiculate remnants. *Lamellae* free, white when young, reddish grey to dull red (9B2-3) when mature, broadly ventricose, crowded, with 4 lamellulae, with an eroded edge. *Stipe* 25–70 × 5–8 mm, cylindrical, from annulus downward base covered with concolorous minute squamules as on the pileus, fragile or absent when mature, smooth at apex zone, background white and turning dull red to greyish red (9C3-4) when touched. *Annulus membranous* white, with concolorous minute squamules as on the pileus margin. *Context* white in pileus; white, hollow in the stipe, turning dull red to greyish red (9C3-4). *Smell and taste* not tested. *Spore print* dark brown.

Basidiospores [25,1,1] l × w = 5.3–6.8 × 4–4.8 µm, avl × avw = 5.73 × 4.30 µm, Q = 1.22–1.50, avQ = 1.33; in side view ellipsoid ovoid, with rounded apex, brown, slightly thick-walled, dextrinoid. *Basidia* 18–25 × 6–10 µm, clavate, hyaline, slightly thick-walled, 4-spored. *Cheilocystidia* 15–35 × 7–15 µm, clavate to broadly clavate, hyaline, thick-walled. *Pleurocystidia* absent. *Pileus* covering trichoderm composed of erect cylindrical hyphae and elements, element cells 20–60 × 5–12 µm. *Stipe* covering is similar to the pileus covering. *Clamp connections* absent.

Fig. 76 – *Hymenagaricus saisamornae* *in situ* **(**HNL503426, **a new record).**

Habitat and distribution – grow in clusters as saprotrophic, on soil, found in Vientiane, central North Laos.

Material examined – Laos, Vientiane Capital, Xaythany District, Houayyang Preserve Forest, 17 Nov. 2015, P. Sysouphanthong, PS199 (HNL503426).

GenBank accession numbers – HNL503426: ITS: ON975002.

Note – *Hymenagaricus saisamornae* was originally described from Thailand (Kumla et al. 2021). A specimen from Laos is morphologically identical to the type specimens from Thailand, with the only noticeable difference being the larger size of the basidiomata in the Lao specimens. However, all other characters are similar (Figs. 76–77). The phylogenetic analysis revealed that the two Lao specimens are identical to the sequences in GenBank (Fig. 73).

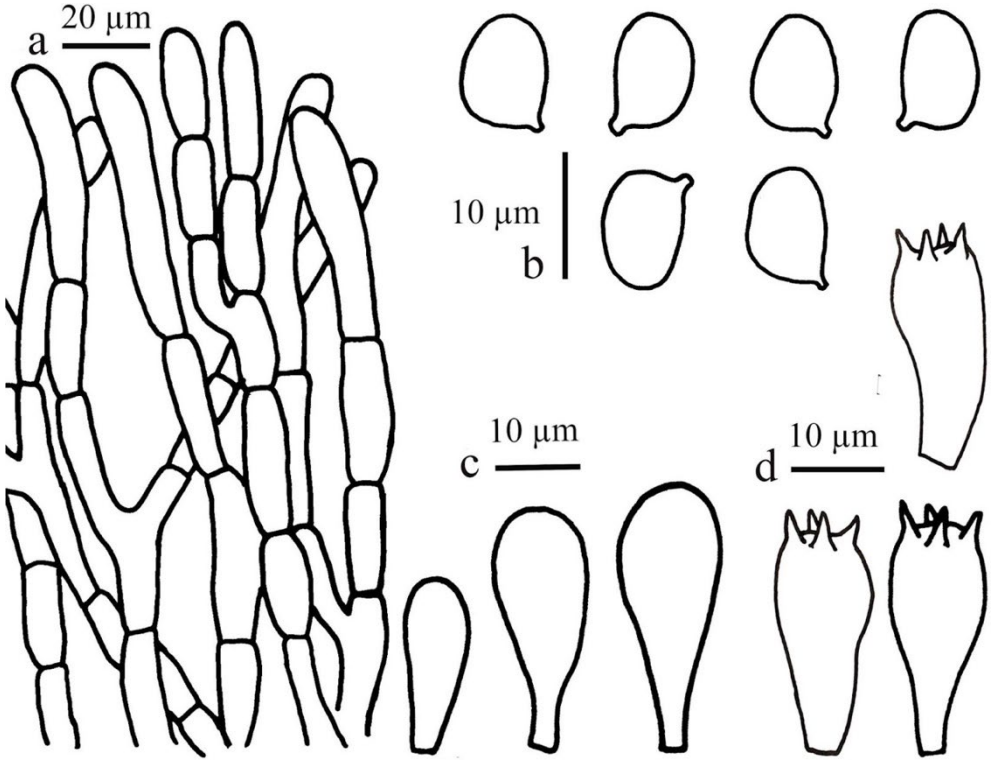

Fig. 77 – Microcharacteristics of *Hymenagaricus saisamornae* (HNL503426). a Basidiospores. b Basidium. c Cheilocystidia. d Pileus covering.

Leucocoprinus Pat., Journal of Botany 2, 16 (1888)

Index Fungorum number: IF 17956; Facesoffungi number: FoF 19189

Leucocoprinus Pat. (1888), a member of the *Agaricaceae* (Kalichman et al. 2020), is characterized by white, dextrinoid, and metachromatic basidiospores, as well as the absence of clamp connections (Vellinga 2001a). *Leucocoprinus* is distinguished from the closely related genus *Leucoagaricus* primarily by its more robust and persistent basidiomata, a typically non-striate cap, and the lack of a germ pore or hyaline cover on its basidiospores (Singer 1986). *Leucocoprinus* comprises over 80 recognized species, with the majority distributed in tropical climates (Vellinga 2001a, Kibby 2019). A well-known representative is *L. birnbaumii*, a yellow species often found growing in plant pots and greenhouses worldwide (Kibby 2019). The type species of *Leucocoprinus* is *L. cepistipes* (Sowerby) Pat. A stable taxonomic framework for this clade encompassing both *Leucoagaricus* and *Leucocoprinus* is crucial for accurately classifying the cultivated fungi of attine ants (Chapela et al. 1994). *Leucocoprinus* represents the oldest available genus-level name for the combined clade. Molecular data confirmed that

Leucoagaricus and *Leucocoprinus* are monophyletic (Liang et al. 2010, Vellinga et al. 2011, Ge et al. 2015, Hussain et al. 2018, Asif et al. 2024). Further subdivision of the clade into more than two taxa is not feasible due to significant overlap in characteristics among the subgroups, which would likely obscure rather than clarify our understanding of their evolutionary relationships (Vellinga et al. 2015). Building upon phylogenetic analyses, Redhead (2023) proposed a taxonomic revision involving the transfer of the type species of *Leucoagaricus*, *La. rubrotinctus*, along with several other species within the *Leucoagaricus* section and those exhibiting a reddening reaction upon injury, into the genus *Leucocoprinus* (Redhead 2023). An updated phylogeny for *Leucocoprinus* and closely related taxa is shown in Fig. 78.

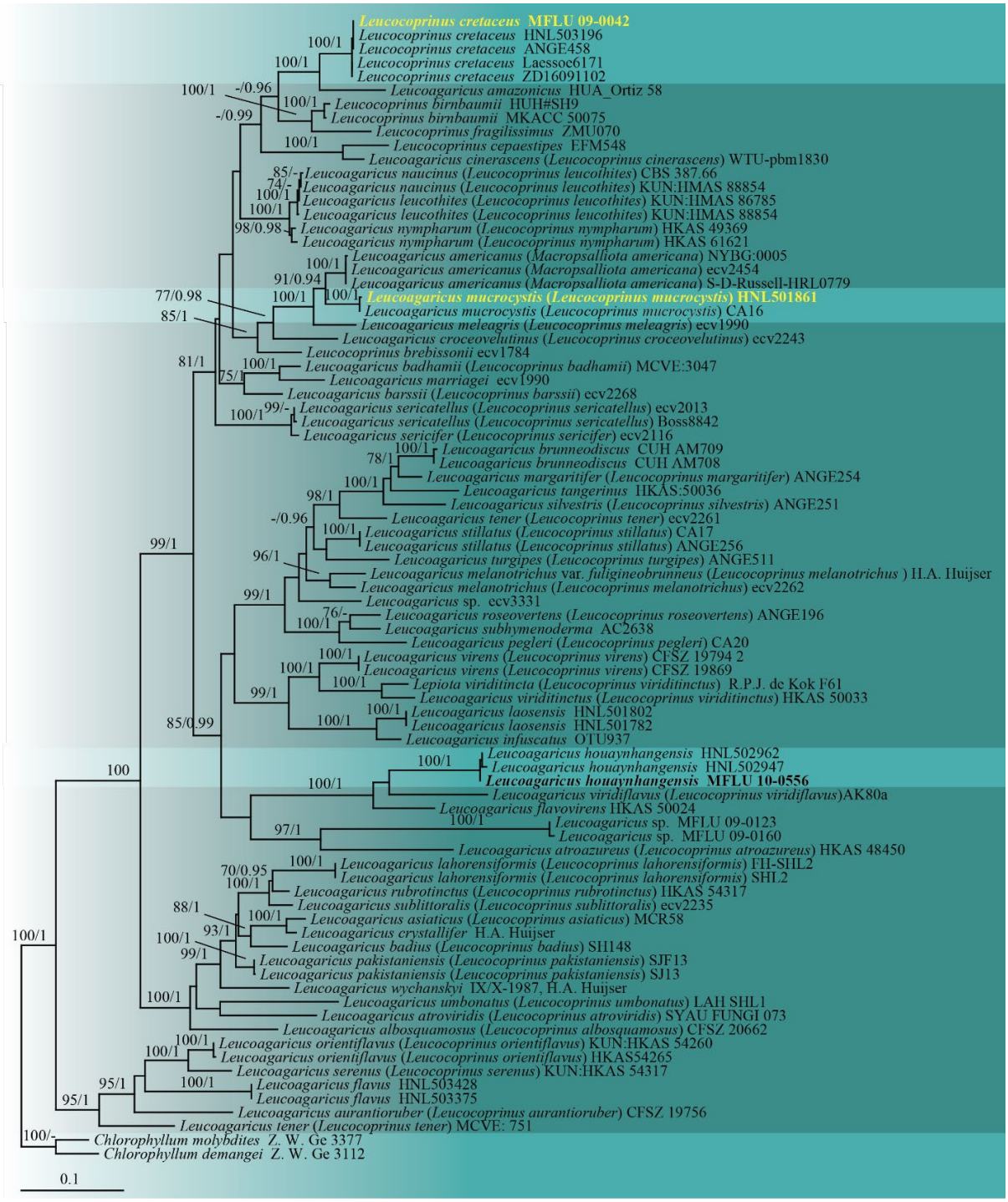

Fig. 78 – Phylogram generated from the maximum likelihood analysis of *Leucoagaricus* based on the combined ITS and LSU sequences. Bootstrap values for maximum likelihood equal to or greater than ≥ 60 and Bayesian posterior probabilities ≥ 0.95 are placed above the branches. *Chlorophyllum demangei* (Pat.) Z.W. Ge & Zhu L. Yang and *Chl. Molybdites* (G. Mey.) Massee was used as the outgroup taxa. A total of 83 sequences were included in the analyses, comprising 1,657 characters after alignment (774 characters for ITS and 883 characters for LSU). The best RAxML tree with a final likelihood value of -19825.972161 is presented. The matrix contained 869 distinct alignment patterns, with 33.01% of the characters being undetermined or gaps. Estimated base frequencies were as follows: A = 0.257226, C = 0.186854, G = 0.256734, T = 0.299186; substitution rates AC = 1.404754, AG = 3.110980, AT = 1.553207, CG = 0.680137, CT = 5.124544, GT = 1.000000; gamma distribution shape parameter α = 0.271750.

Leucocoprinus cretaceus (Bull.) Locq., Bulletin Mensuel de la Société Linnéenne de Lyon 14, 93 (1945)

Index Fungorum number: IF 287726; Facesoffungi number: FoF 3137 Fig. 79, 80

Pileus 20–80 mm diam., when young subglobose, to oblong, expanding to paraboloid or campanulate, then umbonate to concave when fully mature, with a straight margin and becoming reflexed with age; with white squamules on a white fibrillose background. *Margin* with white granular squamules, with white remnants in the mature stage. *Lamellae* free, broadly ventricose, 4–8 mm wide, crowded, white, with 5 lamellulae series, with a white eroded edge. *Stipe* 55–110 × 5–14 mm, wider at the base and tapering to the apex, covered with white squamules, on a white background, turned pale red to pastel red (8A3-4) when touched. *Annulus* cuff-like, white, attached at the upper part of the stipe, often fragile when mature. *Context* in pileus white, up to 5 mm wide; in stipe, white, turned pale red to pastel red as on the pileus surface, hollow. *Smell* soft. *Taste* not tested. *Spore print* white.

Basidiospores [50, 1, 1] 7.5–11.5 × 5–7.5 µm, avl × avw= 8.63 × 6.12 µm, Q = 1.23–1.53, Qav = 1.41, in side-view broadly ellipsoidal to ellipsoid amygdaliform, with a germ pore, in frontal view ellipsoid, hyaline, thick-walled, dextrinoid. *Basidia* 15–20 × 8–15 µm (av. = 17.5 × 11.5 µm, n = 50), lavate, hyaline, thin-walled, 4-spored. *Pleurocystidia* absent. *Cheilocystidia* 25–65 × 5–15 µm (av. = 45 × 10 µm, n = 50), fusiform, clavate to narrowly clavate with or without a short appendage at apex, branched, hyaline, thin-walled. *Pileus* covering a trichoderm made up of cylindrical to oblong hyphae, terminal elements cylindrical, utriform, clavate with or without a short appendage at apex 55–110 × 5–12 µm, slightly thick-walled, hyaline. *Stipe* covering is the same as the pileus covering. *Clamp connections* absent.

Material examined – Thailand, Chiang Mai Province, Mae Taeng District, Pha Deng Village, 10 July 2007, P. Sysouphanthong (MFLU 09-0042).

GenBank accession numbers – ITS: MZ605938.

Habitat and distribution – Solitary to a cluster, saprotrophic, on the soil or compost of leaf litter. The species was found in northern Thailand.

Notes – *Leucocoprinus cretaceus* is easily recognised in the field, having white basidiomata, a long stipe, and white squamules on the pileus and stipe. Morphologically, the basidiospores are broadly ellipsoidal to ellipsoid amygdaliform with a germ pore. The cheilocystidia are fusiform to clavate, with or without a short appendage at the apex, and the pileus and stipe covering are trichodermal. *Leucocoprinus cretaceus* is found in both tropical and temperate regions (Vellinga 2001a, Birkebak 2010). The broad distribution of the species was discussed by Niveiro et al. (2013). Several species of *Leucocoprinus* have been recorded in Thailand, including *Leucocoprinus birnbaumii*, *L. brebissonii*, *L. breviramus*, *L. cepaestipes*, *L. fragilissimus*, and *L. otsuensis* (Chandrasrikul et al. 2011). Additionally, *L. cretaceus* has been collected and sequenced from Thailand. However, these collections have not been described in terms of their morphological characteristics or published.

Fig. 79 – *Leucocoprinus cretaceous* in situ (MFLU 09-0042, **a new record)**.

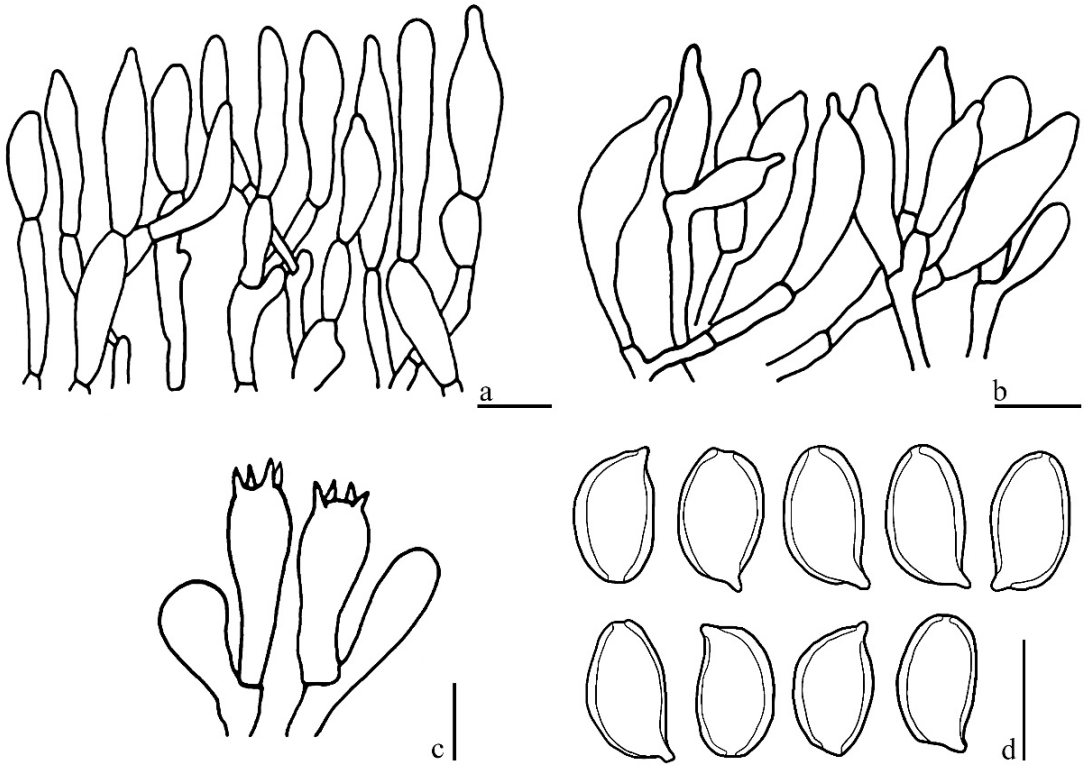

Fig. 80 – Microcharacteristics of *Leucocoprinus cretaceous* (MFLU 09-0042, **a new record**). a Pileus covering. b Cheilocystidia. c Basidia. d Basidiospores. Scale bars: a–b = 20 μm, c–d = 10 μm.

Leucocoprinus mucrocystis (Pegler) M. Asif, Saba & Vellinga, Asif, Saba & Raz, Mycologia 116(4), 615 (2024)

Index Fungorum number: IF 901241; Facesoffungi number: FoF 19196 Fig. 81–82

Pileus 20–45 mm, obtusely conical to parabolic or campanulate, expending convex to subumbonate or umbonate, slightly applanate when fully mature, with straight margin; when young glabrous, reddish brown to dark brown (8E6-8, 8F6-8), with concolorous squamose umbo, with finely squamose to squamose around umbo towards the margin, light brown to brown (7D6-8, 7E6-8) on a white background, turned brownish orange to light brown or brown (6C6-8, 7D6-8) when touched or cut; marginal zone with concolorous finely squamose to squamose, with or without remnants in the mature stage. *Lamellae* 4–7 mm wide, free, broadly ventricose, white, turned brownish orange to light brown or brown (6C6-8, 7D6-8) when touched, crowded, more than 5 lamellulae layers, with concolorous serulate to eroded edge. *Stipe* 35–80 × 5–10 mm, cylindrical or slightly wider downward base, white to orange white or pale orange (6A2-3), turned brownish orange to light brown or brown (6C6-8, 7D6-8) when touched or cut, covered with finely squamose to squamose from annulus zone downward base, light brown to brown (7D6-8, 7E6-8). Annulus attached at the upper side of the stipe, membranous, white on the upper side, with light brown to brown (7D6-8, 7E6-8) and squamose at the underside. *Context* up to 6 mm wide, with white stipe, hollow; both pileus and stipe contexts turned brownish orange to light brown or brown (6C6-8, 7D6-8) when touched. *Odor* slightly strong. *Taste* not tested. *Spore print* white.

Fig. 81 – *Leucoagaricus mucrocystis* *in situ* (HNL501861, **a new record**).

Basidiospores [50, 2, 2] 7–8.3 × 4–4.8 µm, avl × avw = 7.60 × 4.3 µm, Q =1.62–1.82, Qav = 1.74, inside-view oblong ovoid to oblong-amygdaliform with rounded or slightly acute apex, in frontal view ellipsoid to oblong, hyaline, slightly thick-walled, without a germ pore, dextrinoid, congophilous,

metachromatic. *Basidia* 20–26 × 8–10 µm (av. = 22.7 × 9.1 µm, n = 50), lavate, hyaline, slightly thick-walled, 4-spored. *Pleurocystidia* absent. *Cheilocystidia* 10–50 × 4–10 µm (av. = 28.2 × 6.5 µm, n = 50), abundant, composed of chains of various elements, clavate, oblong, cylindrical, rarely fusiform, forked or with outgrowths, multiseptated, often branched, hyaline, slightly thick-walled. *Pileus* covering a trichoderm made up of erect, oblong to cylindrical, multiseptated, branched, terminal elements 20–80 × 4–8 µm, pale yellow to pale brown parental and intracellular pigments. *Stipe* 3–4 septate, 20–50 × 4–8 µm, covering a trichoderm comprised of erect cylindrical elements, hyaline to pale brown parental and intracellular pigments. *Clamp connections* absent.

Material examined – Laos, Vientiane, Xaythany District, Houay Yang Preserves Forest, 25 June 2014, Phongeun Sysouphanthong, HNL501861.

GenBank accession numbers – ITS: OP102589.

Habitat and distribution – Solitary or in a small cluster with few basidiomata, found in mixed deciduous forest with the domination of *Castanopsis* spp.

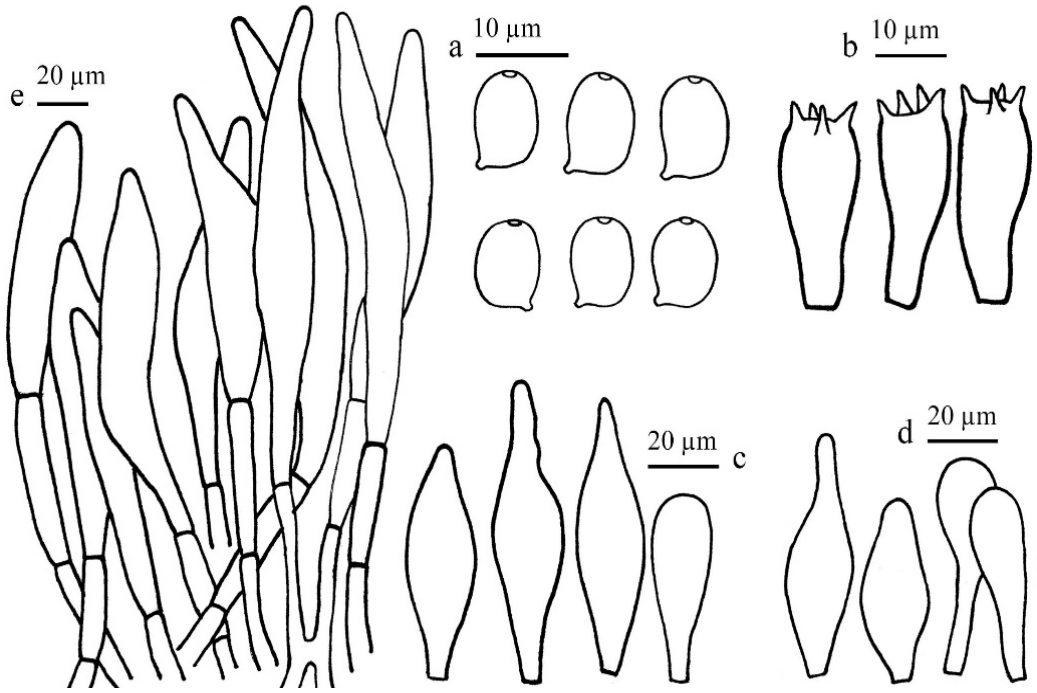

Fig. 82 – Microcharacteristics of *Leucoagaricus mucrocystis in situ* (HNL501861, **a new record**). a Basidiospores. b Basidia. c–d Cheilocystidia. e Pileus covering.

Lepiota (Pers.) Gray, Natural Arrangement of British plants 1, 601 (1821)

Index Fungorum number: IF 17938; Facesoffungi number: FoF 14344

Lepiota belongs to the family *Agaricaceae*. This genus comprises 450 species, divided into six sections based on their morphological characteristics and distribution in tropical and temperate zones (Dennis 1952, Vellinga 2001a, He et al. 2019). Molecular studies illustrated that the species and sections are not monophyletic (Vellinga 2003, Liang et al. 2018, Hou & Ge 2020, Hyde et al. 2020). An updated phylogeny for *Lepiota* and closely related taxa is shown in Fig. 83.

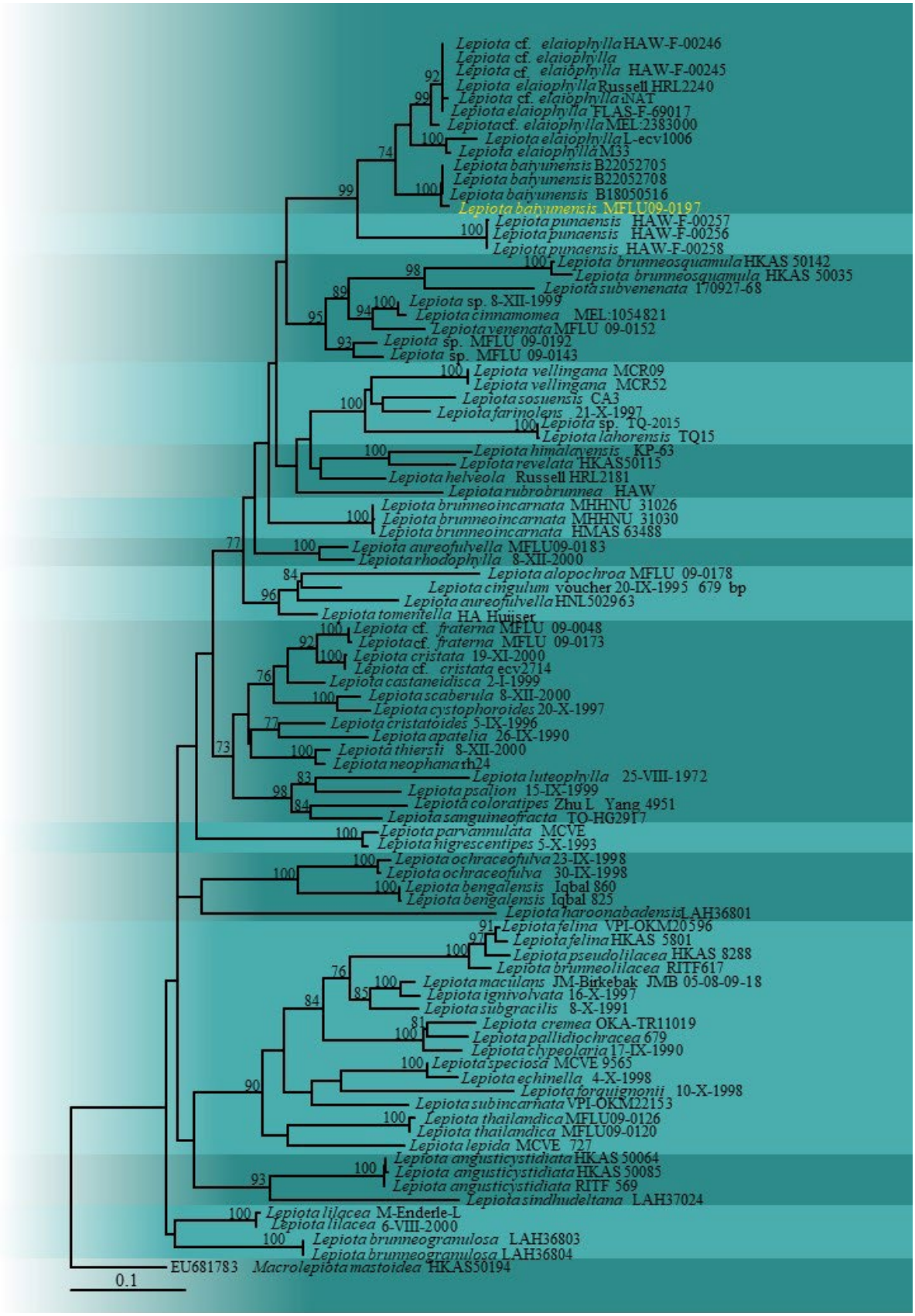

Fig. 83 – Maximum likelihood tree based on ITS sequences, showing the phylogenetic position of *Lepiota baiyunensis*, rooted with *Macrolepiota mastoidea*, ML ≥ 70 are displayed around nodes. The

final matrix contained 304 distinct alignment patterns, and the likelihood of the best-scoring ML tree was -5168.453068. The final matrix contained 304 distinct alignment patterns, and the likelihood of the best-scoring ML tree was -5168.453068; tree-length = 19.347074. Estimated base frequencies were as follows; A = 0.224326, C = 0.229448, G = 0.242828, T = 0.303398; substitution rates AC = 2.581696, rate AG = 10.304919, rate AT = 4.108383, rate CG = 0.765329, rate CT = 11.113504, rate GT = 1.000000; gamma distribution shape parameter α = 0.310488. The newly generated strains are in yellow.

Lepiota baiyunensis Y.S. Liang & L.H. Qiu, Liang et al., Phytotaxa 606(1), 8 (2023)

Index Fungorum number: IF 848014; Facesoffungi number: FoF 19197 Fig. 84–85

Pileus 12 mm, umbonate, with wide umbo, margin inflexed; covered by brown (6E4-6) squamules at umbo, turned dark brown when dried, with brown (6E4-6) fine squamules or squamulose fibrillose towards the margin, on greyish-yellow (4B4, 3B4-5) fibrillose background; in margin zone with distant squamules, sulcate. *Lamellae* free, greyish-yellow (2B4, 3B4-5), ventricose, 3.8–4 mm wide, with an eroded edge, slightly crowded. *Stipe* 24 × 1.3–2 mm, cylindrical or tapering to apex; covered with white to pale yellow (3A3) fibrillose, surface brown (6E4-6), with finely brown (6E4-6) squamules at base zone on pale yellow fibrillose. *Context* yellowish-white (1A2) in pileus, 2 mm wide at the umbo of the pileus; in stipe hollow, concolorous with the surface. *Taste and smell* were not tested. *Spore print* white.

Basidiospores [25,1,1] 6–8 (9) × 3.8–5 µm, 7.12 × 4.07 µm, on average, Q = 1.5–2, avQ = 1.75, inside view oblong ovoid, amygdaliform, with rounded apex, with or without suprahilar depression, in frontal view oblong ovoid, hyaline, slightly thick-walled, congophilous, dextrinoid, cyanophilous, not metachromatic. *Basidia* 22–25 × 7–8 µm, clavate, hyaline, with hyaline drops or mucilaginous inside, 4-spored. *Lamella* edge sterile. *Cheilocystidia* 16–23 × 8–11 µm, mostly clavate, with or without long pedicellate, hyaline, with pale yellow mucilaginous content, branched, and slightly thick-walled. *Pleurocystidia* absent. *Pileus* covering a trichoderm made up of narrowly clavate to cylindrical, pheropeduncate elements, 32–187 × 10-15 µm, slightly thick-walled, parietal and intracellular pigment, clavate, with white to pale brown hyphae under the elements layer, 3–8.75 µm wide. *Stipe* covering of squamules, trichoderm, the same as those in the pileus covering. *Clamp connections* present in all tissues.

Material examined – Thailand, Chiang Rai Province, Muang Chiang Rai District, Mae Fah Luang University, 11 July 2009, P. Sysouphanthong, MFU090197.

GenBank accession numbers – ITS: PV017891.

Habitat and distribution – Gracious or dispersed across soil enriched with decomposing leaves from a monsoon evergreen forest in China (Liang et al. 2023), Thailand (this study).

Notes – Phylogenetically, *Lepiota baiyunensis* was closely related *to L.* cf. *elalophylla*, *L. elalophylla*, and *L. punaensis*, which were easily distinguished from this species (Liang et al. 2023). The features that distinguish *Lepiota* cf. *elalophylla* are as follows: a dull yellow background; appressed scales that split into small scales as the pileus expands; brown or reddish-brown context following cutting; equal stipe; larger spores (7–7.2 × 3.7–3.8) and basidia (23.1–28.7 × 7.2–8.8 µm) (Stallman 2019). According to Wartchow et al. (2008) and Ferreira & Cortez (2012), *L. elalophylla* is identified by its cream background covered in yellowish brown squamules, lemon yellow lamellae, a slimmer stipe with brown squamules, and relatively larger spores (5.4–7 × 2.5–4.3 µm) and basidia (15.1–22.5 × 5.7–7.6 µm). *Lepiota punaensis* is distinguished by its off-white to white lamellae, warm brown fibrils that break into tiny scales, and off-white backdrop (Stallman et al. 2020). Currently, only a single report of *L. baiyunensis* has been found in China (Liang et al. 2023). Phylogenetic analyses (Fig. 87) revealed that *L. baiyunensis* (MFU-90197) belongs to the same clade as other reported strains and represents the first report from Thailand.

Fig. 84 – *Lepiota baiyunensis* *in situ* (MFU090197, **a new record**).

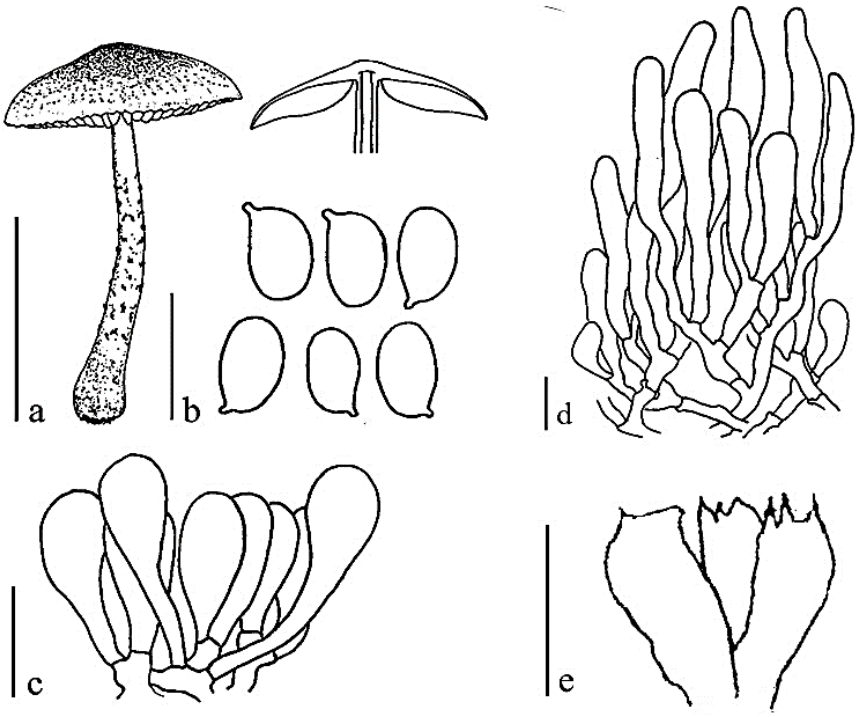

Fig. 85 – *Lepiota baiyunensis*. a Basidiocarp and section. b Basidiospores. c Cheilocystidia. d Pileus covering. e. Basidia. Scale bars: a = 10 mm, b–d =10 µm, e = 20 µm.

Pseudolepiota Z.W. Ge, Ge & Yang, Phytotaxa 312(2), 252 (2017)

Index Fungorum number: IF 820481; Facesoffungi number: FoF 19192

Pseudolepiota is a monotypic genus, consisting of a single species, *Ps. zangmui* Z.W. Ge. This species is recognized by small to medium-sized basidiomata, which are white to orange white and covered with violet-brown to ruby squamules, broadly ellipsoid to ellipsoid-ovoid white basidiospores, presence of cheilocystia, absence of pleurocystidia and clamp connections, and a hymenodermal pileus covering (Ge & Yang 2017, Sysouphanthong et al. 2021). An updated phylogeny for *Pseudolepiota* and closely related taxa is shown in Fig. 73.

Pseudolepiota zangmui Z.W. Ge., Ge & Yang, Phytotaxa 312, 252 (2017)

Index Fungorum number: IF 820482; Facesoffungi number: FoF 07068 Figs. 86–87

Pileus up to 35 mm, at first campanulate, expanding to slightly convex, covered with violet-brown (10F7-8), darker at the center, rough and with concolorous crowded squamules around the center, towards the margin, on a white background. *Lamellae* up to 4 mm wide, slightly crowded, 4–5 lamellulae series, and an eroded edge, free, initial white, and greyish-orange (5B3) when mature. *Stipe* 20–30 × 3–6 mm, cylindrical, slightly wider at the base, covered with white to yellowish-white fibrillose. *Annulus* unclear, with white fibrillose. *Context* white in the pileus, white in the stipe, turning reddish when touched, hollow. *Spore print* whitish. *Taste and smell* not tested.

Basidiospores [25,1,1] 4.5–5.5 × 3.2–4.5 µm, avl × avw = 5.04 × 3.80 µm, Q = 1.28–1.48, avQ = 1.35, broadly ellipsoid to ellipsoid-ovoid, hyaline, slightly, without a germ pore. *Basidia* 13–18 ×4.5–5.3 µm, clavate, 4-spored, rarely 2-spored. *Cheilocystidia* 13–27 × 8–15 µm, short clavate to broadly clavate, rarely utriform and narrowly utriform, hyaline. *Pleurocystidia* absent. *Pileus* covering hymenoderm composed of 3–5 layers of elements, oblong to cylindrical, element cells 15–25 × 4–12 µm, slightly thick-walled, with smooth pale-yellow pigments in upper layers, with encrusted walls in lower layers. *Clamp connections* absent.

Habitat and distribution – in small groups with few basidiomata, saprotrophic and terrestrial in deciduous forests dominated by *Castanopsis* spp.

Material examined – Laos, Oudomxay Province, Xay District, Houay Houm Village, 25 June 2014, Ph. Sysouphanthong, P2014-204 (HNL501875).

GenBank accession numbers – HNL501875: ITS: OP004005.

Notes – Ge & Yang (2017) described *Pseudolepiota zangmui* from tropical southwest China, and later, Sysouphanthong et al. (2021) reported the species from north Thailand. This study presents a new record of the species from Laos. *Pseudolepiota* is a monotypic genus, and while it shares morphological similarities with *Xanthagaricus*, molecular analyses have since distinguished it from *Xanthagaricus* (Ge & Yang 2017, Sysouphanthong et al. 2021).

Fig. 86 – *Pseudolepiota zangmui* in situ (HNL503426, **a new record**).

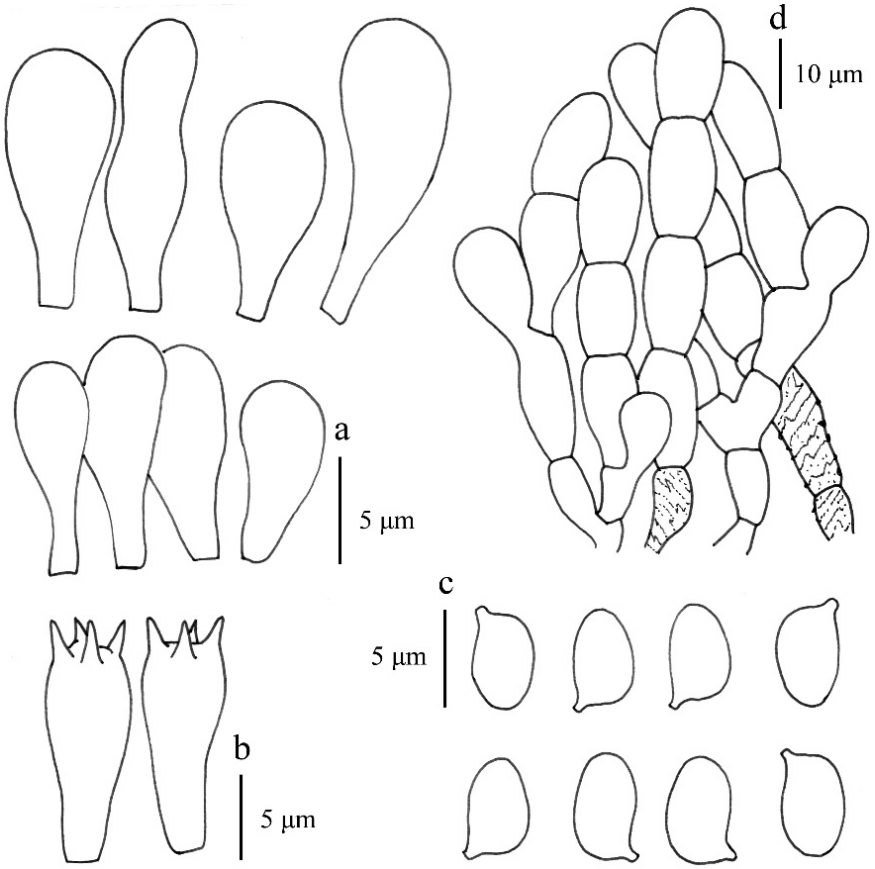

Fig. 87 – Microcharacteristics of *Pseudolepiota zangmui* (HNL503426, **a new record**). a Basidiospores. b Basidia. c Cheilocystidia. d Pileus covering.

Xanthagaricus (Heinem.) Little Flower, Hosag. & T.K. Abraham, New Botanist 24, 93 (1997)

Index Fungorum number: IF 28406; Facesoffungi number: FoF 06314

Xanthagaricus is a saprotrophic genus known for its small-sized basidiomata (Little Flower et al. 1997, Vellinga et al. 2011, Hosen et al. 2018). This genus is characterized by small to medium-sized basidiomata with a squamulose pileus cell. It features yellow to yellowish-brown basidiospores, the presence of cheilocystidia, and the absence of both pleurocystidia and clamp connections (Heinemann & Little Flower 1984, Little Flower et al. 1997, Hussain et al. 2018, Sysouphanthong et al. 2021). An updated phylogeny for *Xanthagaricus* and closely related taxa is shown in Fig. 73.

Xanthagaricus siamensis Yuan S. Liu & S. Lumyong, Phytotaxa 437(1), 17 (2020)

Index Fungorum number: IF 556936; Facesoffungi number: FoF 06314 Figs. 88, 89

Pileus 15–65 mm diam., initially campanulate to parabolic, expanding to umbonate to plano-convex with a straight to slightly incurved margin. It is completely covered with brown (7E6-8) fibrillose squamules when young, which soon open with concolorous towards the margin on white to greyish-violet (19C3-4) when mature, with white to light brown (7D4-5) appendicular remnants. *Lamellae* 4–5 lamellulae series, free, white (4A1) when young, becoming pinkish (11A2) to dull green (25D3-4), greenish-grey to dull green (25E2-3) when mature. *Stipe* 40–80 × 3–8 mm, cylindrical, covered with white light brown (7D4-5) fibrillose, clouded at the annular zone. Context white and thin in the pileus, white and hollow in the stipe. *Taste and smell* not tested.

Basidiospores [50,2,2] 4.2–5.8 × 2.5–3.3 µm, avl × avw = 5.04 × 2.90 µm, Q = 1.50–2.15, avQ = 1.7, ellipsoid to oblong ovoid, smooth, pale yellow to light brown, without a germ pore. *Basidia* 12–17×

5–8 µm, clavate, hyaline, 4-spored. *Pleurocystidia* absent. *Cheilocystidia* are abundant, 10–25 × 6–12 µm, varying in shape from narrow clavate to broadly clavate, rarely utriform, and often branched, hyaline, thin-walled. *Pileus* covering a cutis composed of light, cylindrical hyphae and elements, elements 30–65 × 3–8 µm, with light brown intracellular pigments. *Stipitipellis* is a cutis composed of cylindrical hyphae and elements, 3.5–8.5 µm wide. *Clamp connections* absent.

Material examined – Laos, Oudomxay Province, Xay District, Houay Houm Village, 6 September 2014, Ph. Sysouphanthong, PS2014-1015 (HNL502686); Vientiane, Xaythany District, Houayyang Preserve Forest, 10 October 2015, Ph. Sysouphanthong, PS111 (HNL503338).

GenBank accession numbers – HNL503338: ITS: ON063325; HNL502686: ITS: ON994567.

Habitat and distribution – grow in saprotrophic groups on the soil in a forest dominated by *Castanopsis* spp.

Notes – *Xanthagaricus siamensis* was introduced from northern Thailand (Liu et al. 2020). Laos specimens are identical to the type specimens by morphology, but Lao specimens have larger basidiomata, basidiospores, and longer elements of pileus covering (Figs. 88–89). Moreover, the molecular analysis of ITS sequence data also confirmed identification (Fig. 73).

Fig. 88– *Xanthagaricus siamensis* *in situ*. (HNL502686, **a new record**).

Polyporaceae Fr. ex Corda, Icones Fungorum 3, 49 (1839)

Index Fungorum number: IF 81203; Facesoffungi number: FoF 19178

Ganoderma P. Karst., Revue mycologique Toulouse 3(9), 17 (1881)

Index Fungorum number: IF 17639; Facesoffungi number: FoF 06334

Ganoderma was established by Karsten (1881) with *Polyporus lucidus* (Curtis) Fr. (= *Ganoderma lucidum* (Curtis) P. Karst.) as the type species (Moncalvo & Ryvarden 1997). The genus has a worldwide distribution but is predominantly found in tropical and temperate regions, including Africa, the Americas, Europe, and Asia, especially in the Greater Mekong Subregion (GMS) (Luangharn et al. 2021). *Ganoderma* is pathogenic, inflicting various diseases on plants (Dai et al. 2007). Some are medicinal mushrooms that are ecologically and economically important (Luangharn et al. 2020). *Ganoderma* is characterized by laccate and laccate basidiocarps and double-walled basidiospores. An update on morphology and molecular data for this genus was reported (Luangharn 2019a, 2029b, 2021, He et al. 2022, Sun et al. 2022). An updated phylogenetic tree of *Ganoderma* species is provided in Fig. 90.

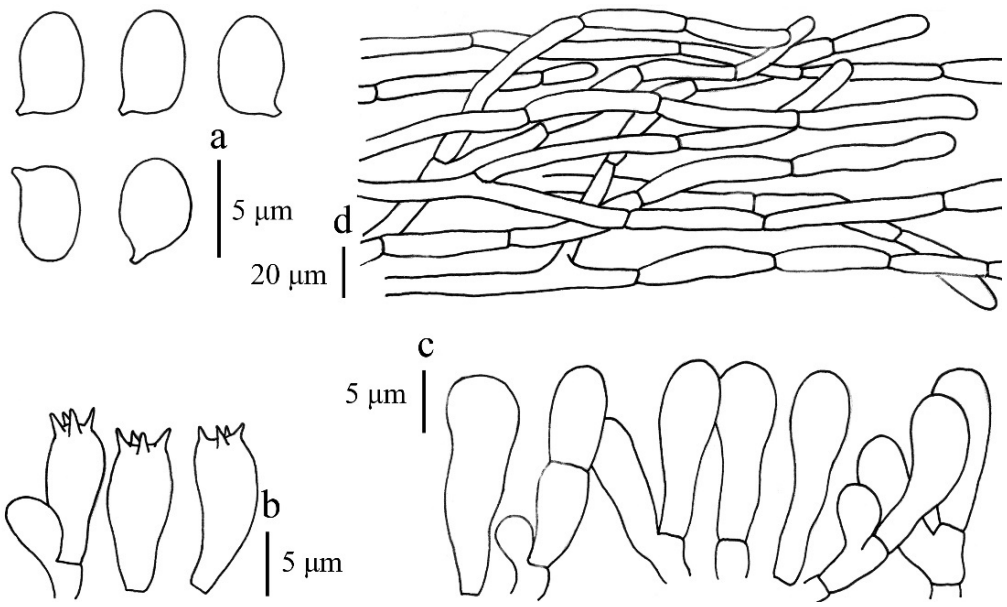

Fig. 89 – Microcharacteristics of *Xanthagaricus siamensis* (HNL503426, **a new record**). a Basidiospores. b Basidia. c Cheilocystidia. d Pileus covering.

Ganoderma alpinum B.K. Cui, J.H. Xing & Y.F. Sun, Studies in Mycology 101, 332 (2022)

Index Fungorum number: IF 839671; Facesoffungi number: FoF 17744 Fig. 91

Basidiomata annual to perennial, subdimidiate, perennial, sessile, woody, and hard when dry. *Pileus* up to 28 cm in length, 16 cm in width, and 1.5–3 cm thick, sub-flabellate to flabelliform, applanate, ungulate, sessile or short stipitate, with a distinctly contracted base. *Pileus surface* dull, glabrous, with concentric furrows and radial wrinkles. *Pileus color* distinct concentric zones with light brown to brown at the center, slightly pale orange and pale brown when extended to the margin at old age on the upper surface, separated by a layer of context. *Margin* up to 2–3 cm thick, thinner and lighter than the base, soft, round, subacute to obtuse, entire, slightly wavy, cracked when dry, with pale yellow to grayish brown, thick toward the margin and downward toward the poreless marginal part of the hymenophore. *Pore surface* white to cream when fresh, clay buff to dark brown when dry, and immediately discolored when bruised. *Pores* circular, 5–6 per mm, dissepiments slightly thick, and entire. *Tube layers* up to 2 cm long, yellowish to brownish, with non-stratified. *Context* up to 2.5 cm thick, mostly cinnamon brown to dark brown, homogeneous of cuticle cells, with black melanoid lines, usually separated layers of context tissue at base, and hard corky and fibrous context.

Hyphal system trimitic; generative hyphae with clamp connections; all hyphae IKI –, CB +; tissues darkening in KOH. *Generative hyphae in context* 0.8–3.2 μm ($\overline{x}$ = 2.4, *n* = 30) in diam., in context colourless, abundant thin-walled, composed of narrow and sparingly branched; skeletal hyphae 2.3–6.7 μm ($\overline{x}$ = 4.8, n = 30) diam., pale yellowish brown, thick-walled with a wide to narrow lumen or sub-solid, arboriform and flexuous; binding hyphae in context colourless, thick-walled, branched and flexuous, up to 2.5 μm diam. *Generative hyphae in tubes* 2–4 μm diam., thin-walled with colourless; skeletal hyphae 3–5.5 μm diam., pale brown, thick-walled with a wide to narrow lumen or sub-solid, with arboriform and flexuous; binding hyphae in tubes up to 2 μm diam., thick-walled with colourless, some branched and flexuous. *Pileipellis* 20–30 × 5–8 μm, composed of clamped generative hyphae, thick-walled, apical cells clavate, slightly inflated and flexuous, yellowish brown, and forming a regular palisade. *Basidiospores* broadly ellipsoid to ovoid, truncated, yellowish brown, IKI –, CB +, double-walled with distinctly thick walls, exospore wall smooth, endospore wall with dense spinules, (5.8–)6.1–7.2(–7.8) × (3.6–)4.2– 5.2(–5.6) μm, L = 6.38 μm, W = 4.71 μm, Q = 1.39–1.44 (n = 60/2) with the

turgid vesicular appendix excluded); (7.2–)7.5–8.9(–9.2) × (3.9–)4.2–5.1(–5.8) µm, L = 7.95 µm, W = 4.73 µm, Q = 1.69–1.72 (n = 60/2, with the turgid vesicular appendix included). *Basidia* 20–30 × 11–16 µm, barrel-shaped, thin-walled, colourless. *Basidioles* 10–18 × 5–11 µm, clavate, thin-walled, colourless. *Cystidia* and *cystidioles* absent.

Material examined – Thailand, Chiang Rai Province, Muang District, Mae Fah Luang University, 20°0′52″N, 99°52′27″E, alt., 392 m, 11 November 2023, T. Luangharn, LT 2023-083, MFLU 25-0191.

GenBank numbers – ITS: PV616857.

Known distribution – Known only from southwestern China and Thailand (this study).

Host and habitat – Solitary on the decayed stump of an unidentified tree species.

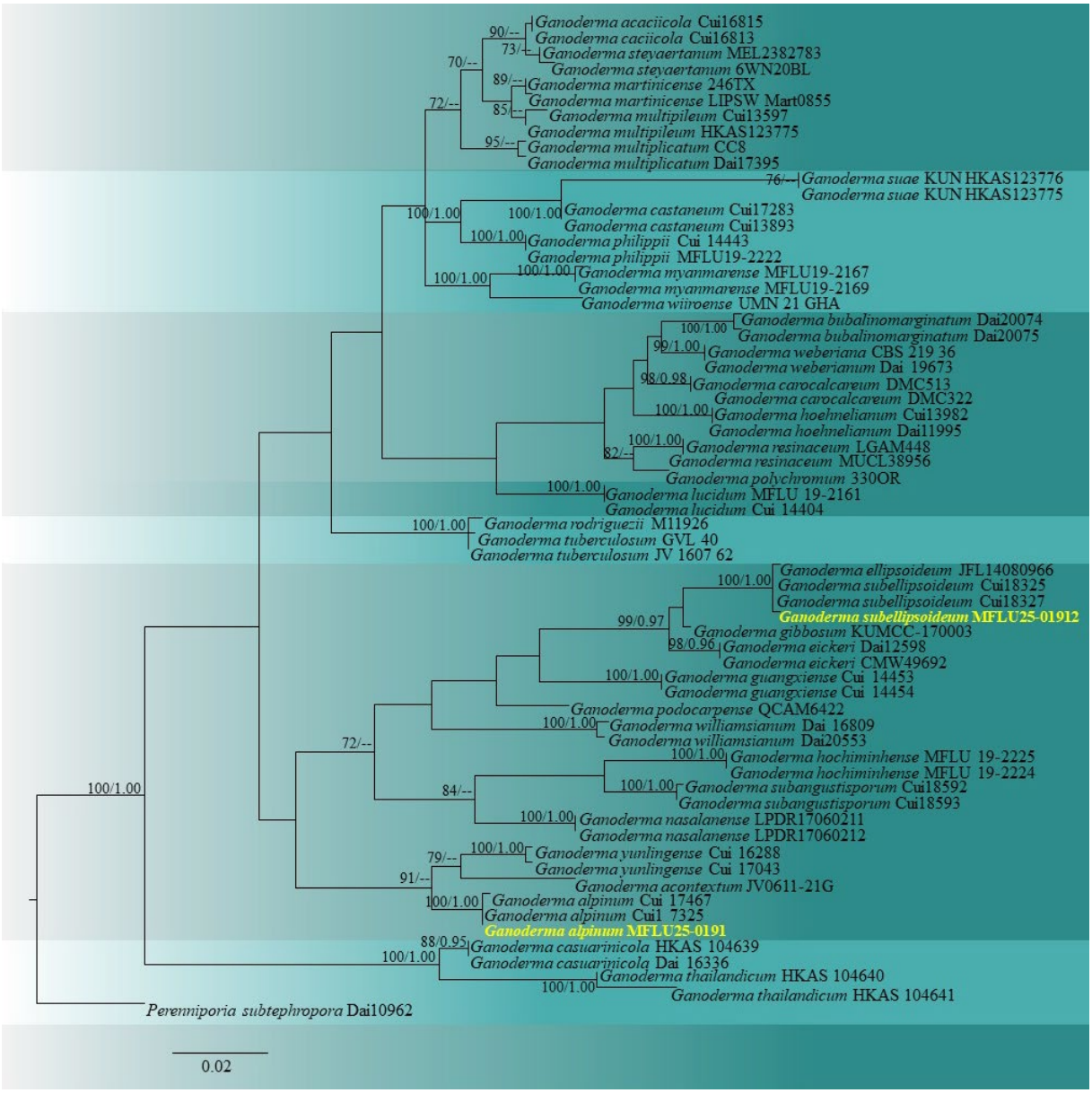

Fig. 90 – Phylogram generated from the maximum likelihood (ML) analysis based on the ITS and LSU sequences for *Ganoderma* species. The tree is rooted with *Perenniporia subtephropora* (Dai10962). The ML bootstrap supports (≥ 70%), and BI posterior probabilities (≥ 0.95) are denoted near the respective nodes. The taxa originating from this study are shown in black bold. Sixty-five strains are included in the combined analyses, which comprise 1,949 characters (614 for ITS, 1,335 for LSU) after alignment,

of which 1,630 characters were constant, 273 characters were variable and parsimony-informative, and 46 characters were parsimony-uninformative. The tree topology obtained from the maximum likelihood analysis is congruent with that from the Bayesian analysis. The proportion of invariable sites was 0.375. Estimated base frequencies were A = 0.263, C = 0.196, G = 0.267, T = 0.274; substitution rates AC = 0.88182, AG = 3.77630, AT = 1.77105, CG = 0.6352, CT = 5.77334, GT = 1.000000; and the gamma distribution shape parameter α = 0.698. The best RAxML tree with a final likelihood value of -6168.328927 is presented. Estimated base frequencies were as follows: A = 0.242107, C = 0.242209, G = 0.274991, T = 0.240693; substitution rates AC = 1.704526, AG = 3.853574, AT = 1.285674, CG = 1.184574, CT = 9.89482, GT = 1.000000; gamma distribution shape parameter α = 0.189089.

Fig. 91 – *Ganoderma alpinum* (MFLU25-0191, **a new record**). a–c Mature basidiomes on host, d Pure culture on PDA incubated for 2 weeks, e Pore characteristics, f, g, k Hyphae of context in KOH, h–j Basidiospores. Scale bars: a, b = 2 cm, d = 3 cm, d = 1 cm, e = 500 µm, f, g, k = 10 µm, h–j = 5 µm.

Ganoderma subellipsoideum B.K. Cui, J.H. Xing & Y.F. Sun, Studies in Mycology 101, 348 (2022)

Index Fungorum number: IF 839681; Facesoffungi number: FoF 17745 Fig. 92

Basidiomata annual, sessile (without stipe), perennial, subdimidiate, lateral stipe, woody, hard. *Pileus* up to 18 cm in length, 6–13 cm in width, and 10.8–3 cm thick, solitary, sub-circular to flabelliform, applanate. *Pileal surface* dull when dried, glabrous, with dense concentric furrows. *Pileus color* dark yellowish brown to near black when fresh, becoming yellowish brown or greyish brown when dried. *Margin* actively growing, up to 0.8–2.5 cm thick, and the obtuse is entire, thinner, and lighter than the base. *Pore surface* white when fresh, turning darker when bruised, cream to buff when dry. *Pores*

circular, 6–8 per mm; dissepiments moderately thick and entire. *Tube layers* up to 6–9 mm long, dark brown, stratified by a layer of context. *Context* up to 1.2 cm thick, cinnamon brown, homogeneous, with black melanoid lines, hard corky when dried.

Hyphal system trimitic; generative hyphae with clamp connections; all hyphae IKI –, CB +; tissues darkening in KOH. *Generative hyphae in context* 2–4 µm diam, colourless, thin-walled; skeletal hyphae in context 2–5 µm diam, pale brown, thick-walled with a wide to narrow lumen or sub-solid, arboriform and flexuous; binding hyphae in context up to 1.5 µm diam, colourless, thick-walled, branched and flexuous. *Generative hyphae in tubes* 2–3 µm diam, colourless, thin-walled; skeletal hyphae in tubes 2–4 µm diam, yellowish brown, thick-walled with a wide to narrow lumen or sub-solid, arboriform and flexuous; binding hyphae in tubes up to 1 µm diam, colourless, thick-walled, branched and flexuous. *Pileipellis* composed of clamped generative hyphae, 30–40 × 3–5 µm, thick-walled, apical cells clavate, flexuous, pale yellowish brown, forming a regular palisade. *Basidiospores* 6–6.9(–7) × 4–5.3(–5.5) µm, L = 6.46 µm, W = 4.62 µm, Q = 1.36–1.44 (n = 60/2, with the turgid vesicular appendix excluded); (8–)8.2–9.6(–10) × (4–)4.2–5.2(–6) µm, L = 8.89 µm, W = 4.69 µm, Q = 1.89–1.9 (n = 60/2), with the turgid vesicular appendix included), ellipsoid, truncated, yellowish brown, IKI –, CB +, double-walled with moderately thick walls, exospore wall smooth, endospore wall with dense spinules. *Basidia* 12–17 × 9–11 µm, barrel-shaped, thin-walled, colourless. *Basidioles* 11–15 × 6–10 µm, broadly clavate, thin-walled, colourless. *Cystidia* and *cystidioles* absent.

Fig. 92 – *Ganoderma subellipsoideum* (MFLU 25-0192, **new host and geographical records**). a–c Mature basidiomes on loving host, d Pure culture on PDA incubated for 10 days, e Pore

characteristics, f Hyphae of thama, g–i Hyphae of context in KOH, j–k Basidiospores. Scale bars: b, c = 2 cm, e = 500 µm, f, i = 20 µm, g, h = 15, j–k = 10 µm.

Material examined – Thailand, Chiang Rai Province, Muang District, Mae Fah Luang University, 20°0′52″N, 99°52′27″E, alt. 392 m, 11 November 2023, T. Luangharn, LT 2023-099, MFLU 25-0192.

GenBank accession numbers – ITS: PV616858, LSU: PV616861.

Known distribution – Known only from southwestern China and Thailand (this study).

Host and habitat – Solitary on the living tree of *Callistemon viminalis*.

Strophariaceae Singer & A.H. Sm., Mycologia 38(5), 503(1946)

Index Fungorum number: IF 81444; Facesoffungi number: FoF 19183

Agrocybe Fayod, Annales des Sciences Naturelles, Botanique 9, 358 (1889)

Index Fungorum number: IF 17034; Facesoffungi number: FoF 19184 Fig. 93

Agrocybe was introduced by Fayod (1889) with *Agrocybe praecox* as the type species. *Agrocybe* consists of agaricoid fungi producing small to medium-sized stipitate basidiomata with attached lamellae. These fungi have a dull brown spore print, a hymeniform pileipellis, and a broad germ pore, characterized by saprobic growth in grasslands, soil, litter, and dead wood. *Agrocybe* was traditionally classified in *Bolbitiaceae*; molecular phylogenetic analyses have suggested that it is a polyphyletic genus belonging to the *Strophariaceae* (Matheny et al. 2006, Tóth et al. 2013, Malysheva et al. 2019). He et al. (2019) documented 100 species, and Li et al. (2023) introduced a new commercially cultivated species, *Agrocybe striatipes*.

Agrocybe retigera (Speg.) Singer, Lilloa 22, 493 (1951)

Index Fungorum number: IF 292342; Facesoffungi number: FoF 17283 Fig. 94

Pileus convex or campanulate at first, becoming plano-convex with a broad central bump; whitish yellow (2A2); 1.3–2.9 cm in diameter; hygrophanous in humid conditions, wrinkled in dry conditions, with some or entirely rough-reticulated; bald. *Margin* entire, thin, not striate. *Lamellae* yellowish white (1A2) when young, becoming greyish brown (5D3) to brown (5E5) eventually, with the same colour on the edge, ventricose, even, 1 tier. *Stipe* white (1A1) to yellowish white (1A2), bald, equal above and swollen at base, hollow, 26–83 × 2–6 mm, lacking a partial veil, basal mycelium white. *Context* white (1A1). *Spore print* brown (9F3). *Odour* pleasant.

Basidiospores 8.7–14.2 × 6.4–10.7 µm, Q = 1.3–1.8, Q_m = 1.54, ellipsoid to oblong, smooth, with a double wall, greyish yellow (3B6), apically truncate with a 1 µm germ pore. *Basidia* 17.9–25.6 × 8.7–11.4 µm, clavate, hyaline, thin-walled, 4-spored. *Pleurocystidia* 22.6–55.4 × 10.9–25.6 µm, utriform to pyriform, thin-walled, with some having a broadly rounded apex. *Cheilocystidia* and *Caulocystidia* not observed. *Hymenophoral trama* irregular. *Pileipellis* irregular epithelium and thin *Stipitipellis* euhymeniderm. *Clamp connections* present in all tissues.

Material examined – Thailand, Chiang Rai Province, Muang Chiang Rai District, Huai Sak Subdistrict, 19°47’N, 99°54’E, alt. 400 m, solitary or gregarious on the open lawn, 4 June 2020, Yuwei Hu, HYW24 (MFLU 24-0042).

GenBank accession numbers – MFLU 24-0042: ITS: PP930816, LSU: PP930820.

Known distribution – America (Li et al. 2023), Argentina (Singer 1950), Brazil (Cortez & da Silveira 2005), China (Liu et al. 2021), India (Watling & Abraham 1986), Thailand (this study).

Notes – *Agrocybe retigera* is a tropical and subtropical species found in America and Asia, characterized by its lacunose-rugose pileus surface (either on the entire pileus or near the margin), large basidiospores, and hymenophoral cystidia that are vesiculose with a broadly rounded apex (Spegazzini 1922, Singer 1950, Niveiro et al. 2020). In this study, the pileus surface is somewhere or entirely rough-reticulated, with basidiospores 8.7–14.2 × 6.4–10.7 µm. *Pleurocystidia* are utriform to pyriform, consistent with the diagnostic features of *A. retigera*. *Cheilocystidia and Caulocystidia* were not

observed, likely because the specimens examined were young. Phylogenetic analysis showed that our collection (MFLU 24-0042) clustered with another *A. retigera* (JAUCC 2154), with 100% MPBS and 1.00 BYPP bootstrap support (Fig. 93). This study provides a new geographic record for *A. retigera* from an open lawn in Thailand.

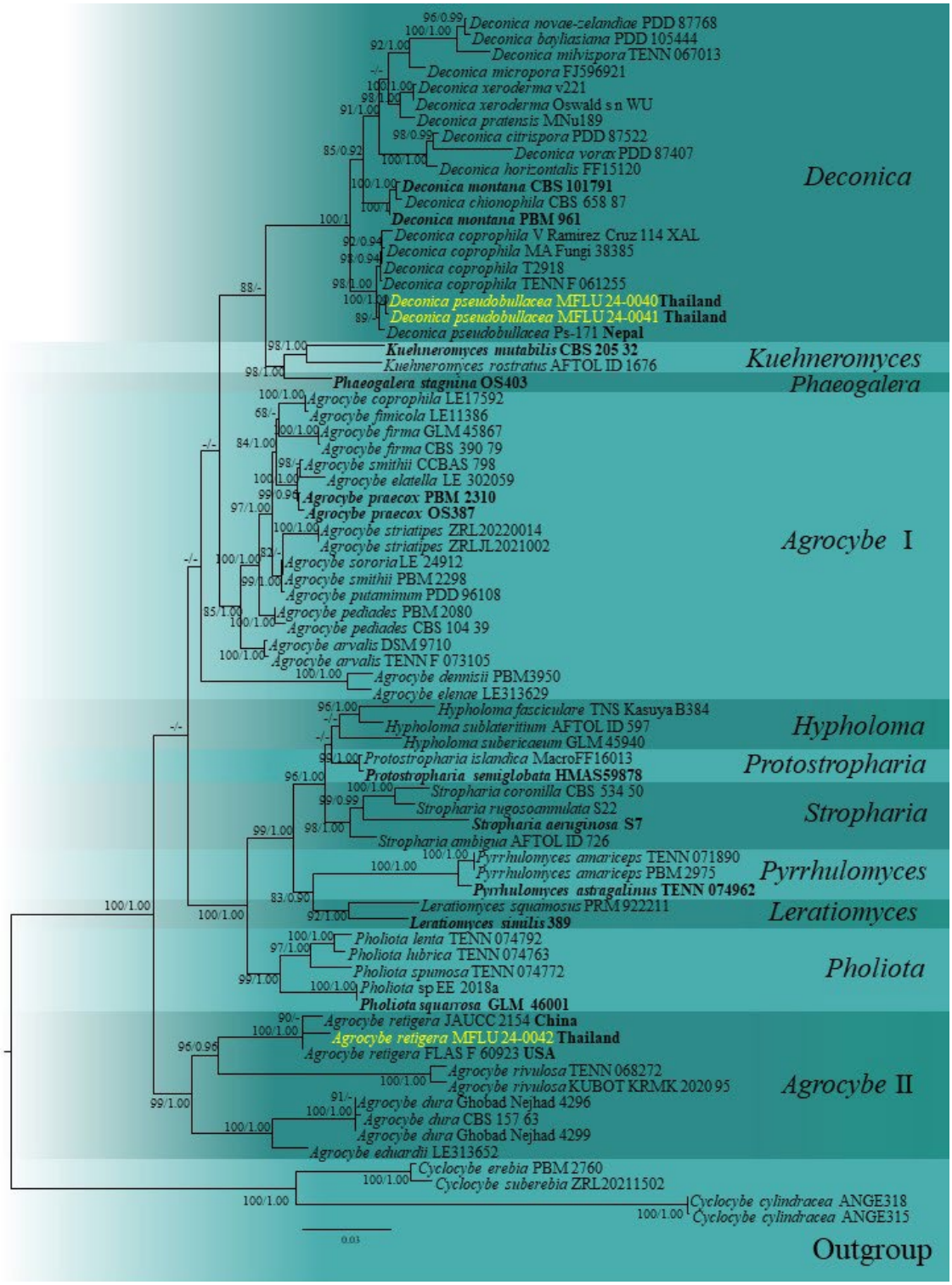

Fig. 93 – Phylogram generated from the maximum likelihood analyses based on the combined ITS and LSU sequence data of the genus *Agrocybe* and *Deconica*. Seventy-four strains are included in the

combined analyses. The Bayesian analysis is similar to maximum likelihood analysis. The best RAxML tree with a final likelihood value of -12895.288 is presented. The evolutionary model TVM+F+R3 and TN+F+R3 are applied separately to the ITS and LSU genes. The matrix contained 763 distinct alignment patterns, with 22.37% of the characters being undetermined or gaps. Bootstrap support values for ML ≥ 60% and Bayesian posterior probabilities ≥ 0.90 are given near nodes, respectively. The tree was rooted with *Cyclocybe erebia* (PBM 2760), *Cyclocybe suberebia* (ZRL20211502), and *C. cylindracea* (ANGE 318 and ANGE315). Ex-type strains are in bold. The newly generated sequences are indicated in yellow.

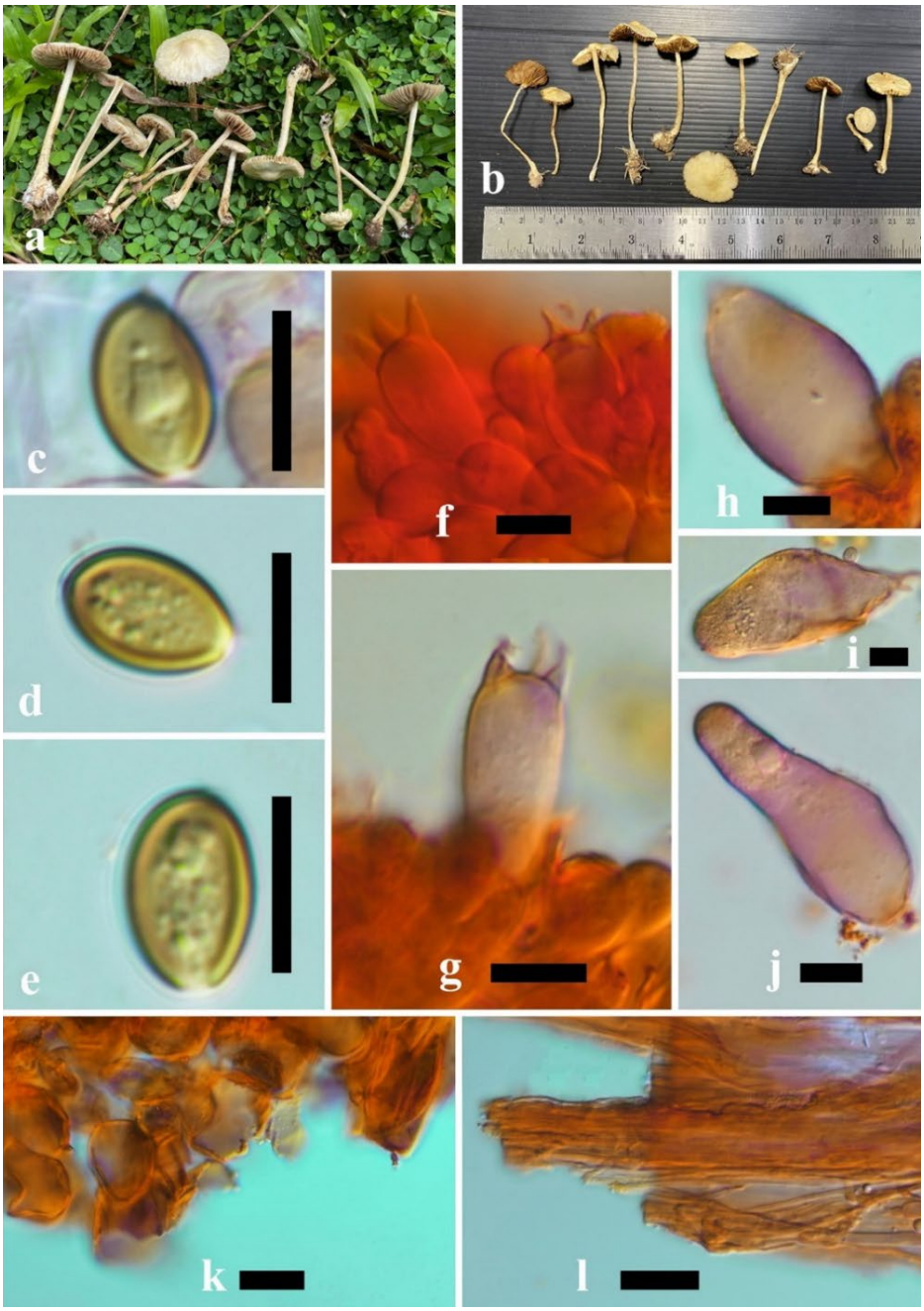

Fig. 94 – *Agrocybe retigera* (MFLU 24-0042, **a new record**). a, b Basidiomata in the field. c–e Basidiospores. f, g Basidia. h–j Pleurocystidia. k Pileipellis. l Stipitipellis. Scale bars: c–j = 10 µm, k–l = 20 µm.

Deconica (W.G. Sm.) P. Karst., Bidrag till kännedom av Finlands natur och folk 32, 26 (1879)

Index Fungorum number: IF 17469; Facesoffungi number: FoF 19186

Deconica was introduced by Smith (1870) as a subgenus of *Agaricus* L., and Karst (1879) proposed elevating it to the generic level. *Deconica* basidiomata occur on plant debris, grasses, mosses, rotten wood, trunks, and dung; they have mycenoid, collybioid, crepidotoid, or omphaloid basidiomata; conical, convex, or hemispherical, dry or viscid pileus with or without an umbo; adnate to broadly adnate, brown to purple-brown lamellae; and a slender stipe when present (Noordeloos 2011). He et al. (2019) recorded 44 *Deconica* species, and Ramírez-Cruz et al. (2020) described two new species of *Deconica*.

Deconica pseudobullacea (Petch) Ram. Cruz & Guzmán, Ramírez et al., Sydowia 64(2), 218 (2012)

Index Fungorum number: IF 800726; Facesoffungi number: FoF 17284 Fig. 95

Pileus 0.2–0.3 cm in diameter, 0.1–0.2 cm in height, hemispherical to convex, non-umbonate, greyish brown (6D3) in the middle, light brown (6D5) towards the margin, surface smooth, bald, translucent-striate margin. *Lamellae* subdecurrent, regular, even, light brown (5D5), 1 tier, *Stipe* 9.5–13.4 × 0.4–0.5 mm, central, cylindrical, slightly swollen towards the apex and base, smooth to fibrillose with numerous scales, fibrous, hollow, basal mycelial pad present, a fibrillose partial veil present, falling towards the base with age. *Context* fine, and thin, and colour does not change with exposure to the air. *Odor* not distinct. *Spore print* purplish brown (11F6).

Basidiospores 9–13.3 × 6–8.3 µm, Q = 1.3–2, Q_m = 1.62, with a hexagonal shape in the upper view and ellipsoid in the side view, greyish yellow (2C4) to olive (3E5), with a relatively thick wall, apically truncate with a 1 µm germ pore. *Basidia* 14.9–27.3 × 8.2–11.8 µm, clavate to cylindrical, hyaline, 4-spored. *Pleurocystidia* 24.4–40.6 × 8.4–12 µm, narrowly utriform to fusiform, hyaline, thin-walled. *Cheilocystidia* 13.2–24.6 × 5.6–8.8 µm, fusiform to cylindrical, hyaline, thin-walled. *Caulocystidia* not observed. *Hymenophoral trama* is irregular. *Pileipellis* an intricate trichoderm. *Stipitipellis* is an irregular hymeniderm. *Clamp connections* present in all tissues.

Material examined – Thailand, Mukdahan Province, Dong Luang District, Phang Daeng Subdistrict, 16°47"N, 104°26"E, alt. 180 m, solitary or gregarious on the cow manure, 19 August 2020, Song-Ming Tang, 2020081909 (MFLU 24-0040), Allen G. T. Niego AG20053 (MFLU 24-0041).

Known distribution – Nepal (Ramírez-Cruz et al. 2020), Thailand (this study).

GenBank accession numbers – MFLU 24-0040: ITS: PP930817, LSU: PP930821; MFLU 24-0041: ITS: PP930818, LSU: PP930822.

Notes – *Deconica pseudobullacea* is a tropical and subtropical species found in Asia, characterized by coprophilous, small basidiomata, relatively long stipes with a fibrillose partial veil, and hexagonal basidiospores. This finding was previously recorded by Ramírez-Cruz et al. (2012) and Ramírez-Cruz et al. (2020). *Deconica pseudobullacea* is morphologically similar to *D. coprophila*, while *D. pseudobullacea* has relatively small basidiomata and a longer stipe. Based on the phylogenetic analyses, our collections (MFLU 24-0040, and MFLU 24-0041) clustered with another *D. pseudobullacea* (Ps-171) with 89% MPBS bootstrap support (Fig. 93). This study provides a new geographical record for *D. pseudobullacea*, which is reported from cow dung in Thailand.

Polyporales Gäum., Vergleichende Morphologie der Pilze 503 (1926)

Index Fungorum number: IF90565; Facesoffungi number: FoF 16751

Steccherinaceae Parmasto, Conspectus Systematis Corticiacearum 169 (1968)

Index Fungorum number: IF81420; Facesoffungi number: FoF 15448

Trullella Zmitr., Folia Cryptogamica Petropolitana (Sankt-Peterburg) 6, 104 (2018)

Index Fungorum number: IF827466; Facesoffungi number: FoF 16752

Trullella was established with *T. dentipora* (Ryvarden & Iturr.) Zmitr., as the type species (Miettinen & Ryvarden 2016). Species of *Trullella* are characterized by a combination of pileate or laterally stipitate basidiomata, typically featuring a light brownish, smooth upper surface with coloured

zones (Miettinen & Ryvarden 2016). They possess a dimitic hyphal system characterized by clamped cyanophilous generative hyphae and cylindrical, thin-walled, smooth basidiospores. Recently, Index Fungorum (2025) listed eight species worldwide. An updated phylogeny is shown in Fig. 96.

Fig. 95 – *Deconica pseudobullacea* (MFLU 24-0040, MFLU 24-0041, **a new record**). a, b Basidiomata in the field (MFLU 24-0040). c Basidiomata in field (MFLU 24-0041). d, e Basidiomata of *Deconica coprophila* in the field (HKAS 131327). f, g Basidiospores. h, i Basidia. j Pleurocystidia. k Cheilocystidia. l Pileipellis. m Stipitipellis. Scale bars: f–k = 10 µm, l–m = 20 µm.

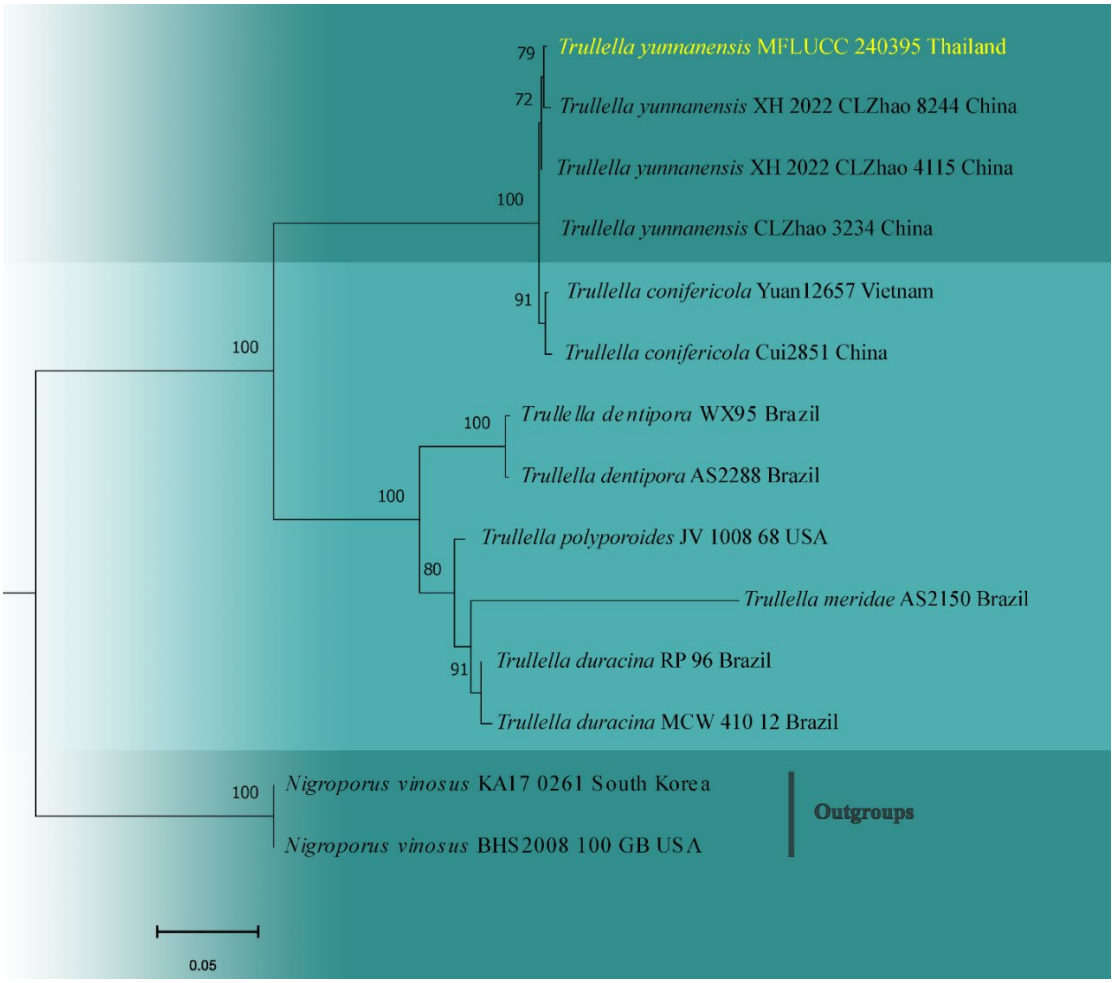

Fig. 96 – Phylogenetic tree (RAxML) obtained from the DNA sequence data of the ITS dataset. Phylogenetic analyses were inferred from ITS sequences comprising 14 taxa, including 12 *Trullella* species and two outgroup species of *Nigroporus vinosus* (BHS2008) and *N. vinosus* (KA170261). The final dataset comprised 647 total characters, including gaps after alignment. Our specimen grouped with the strains of *T. yunnanensis* and forms a sister clade with *T. conifericola*. Bootstrap values (BS) from maximum likelihood (ML) greater than 70% are indicated above the nodes. The tree is rooted with *Nigroporus vinosus* (BHS2008) and *Nigroporus vinosus* (KA170261). Newly recorded species from Thailand are indicated in yellow.

Trullella yunnanensis C.L. Zhao, He, Dong & Zhao, Kew Bull 78(1), 216 (2023)

Index Fungorum number: IF 843170; Facesoffungi number: FoF 16637 Figs. 97, 98

Basidiomata annual, solitary, laterally stipitate. *Pileus* 1.5−6 cm wide, up to 1 mm thick, reniform to semi-circular, applanate, smooth, zonate, and radially striate, cream to yellowish when young, light brown upon maturity on the upper surface. *Margin* entire, acute. *Pores* 7−8 per mm, small and round, dissepiments thin and entire, white to cream when young, light brown upon maturity. *Stipe* up to 4 cm long, up to 6 mm in diameter, with a cylindrical shape. *Corky* up to 0.2 mm thick, creamy, and leathery in dried condition. *Tubes* up to 0.3 mm long, concolorous with the hymenium surface, with corky.

Basidiospores (3.4–)3.7–5.6(– 5.7) × 1.6–2.4 µm, L = 4.9 µm, W = 2 µm, Q = 2.15–2.33, Q_m = 2.42 (n = 30), cylindrical and curved, thin-walled, smooth, colourless. *Basidia*. 7−12 × 5−7.5 µm, clavate to barrel-shaped, with four sterigmata clamped at base. *Basidioles* dominant, pear-shaped, and slightly smaller than basidia. *Cystidia and cystidioles* absent. *Hyphal structure* dimitic hyphal system and

clamped generative hyphae, all tissues unchanged in KOH. *Context* 3−5 µm in diam., generative hyphae dominant, colourless, thin-walled, and branched; skeletal hyphae 4−5.5 µm in diam., colourless, thick-walled, and unbranched. *Tubes*: hyphal pegs common 25−40 × 15−30 µm. *Culture characteristics* non-fluffy with greyish white. *Odour and taste* undetermined.

Material examined – Thailand, Chiang Rai Province, Mae Fah Luang District, 20 October 2023, S. Khyaju, MFLU24-0322.

GenBank accession numbers – ITS: PQ452693.

Habitat – on a decaying log, mixed coniferous forests.

Known distribution – China (Cao et al. 2021, He et al. 2023), Thailand (this study).

Notes – The newly recorded species, *Trullella yunnanensis*, is described based on morphological characteristics and phylogenetic analyses of the ITS sequence. In the present study, our strain is nested within the *T. yunnanensis* clade and forms a sister clade with *T. conifericola*. However, *T. yunnanensis* has 7−8 pores per mm, whereas *T. conifericola* has 10–12 pores per mm. This study supports the prediction by He et al. (2023) that *T. yunnanensis* could be found in East Asia. Furthermore, additional investigations may lead to the discovery of new taxa and the accumulation of further records in this region.

Fig. 97 – *Trullella yunnanensis* (MFLU 24-0322, **a new record**). a–c Basidiomata. d Pore surface. Scale bars: a, b = 2 cm, d = 1 mm.

Russulales Kreisel ex P.M. Kirk, P.F. Cannon & J.C. David, Ainsworth & Bisby's Dictionary of the fungi 9, 11 (2001)

Index Fungorum number: IF 90569; Facesoffungi number: FoF 19181

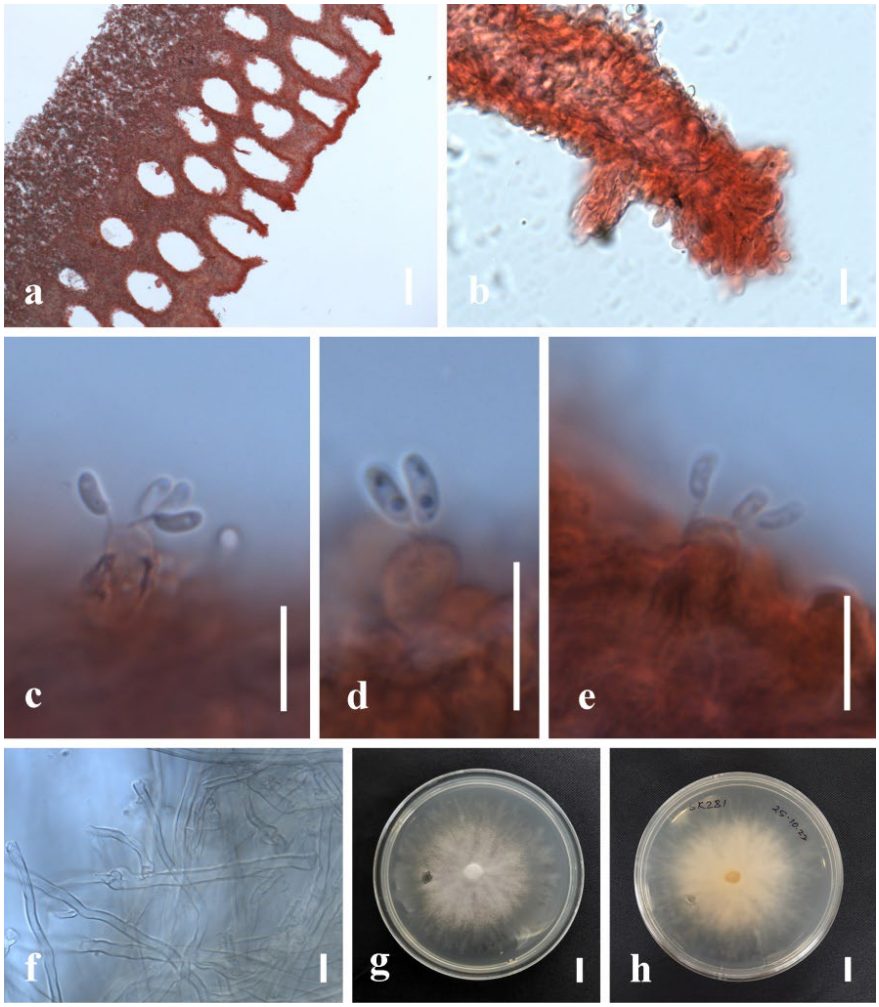

Fig. 98 – *Trullella yunnanensis* (MFLU 24-0322, **a new record**). a Section of the hymenium and hyphal pegs. b A hyphal peg in the wall of the hymenium pore. c–e Basidia and basidiospores. f Hyphae from context. g Culture in PDA (upper view). h Culture in PDA (bottom view). Scale bars: a = 100 µm, b–f = 10 µm, g, h = 1 cm.

Russulaceae Lotsy, Truffe 2, 708 (1907)

Index Fungorum number: IF 81358; Facesoffungi number: FoF 19180

Lactarius Pers. Tentamen dispositionis methodicae Fungorum 63 (1797)

Index Fungorum number: IF17895; Facesoffungi number: FoF 02521

Lactarius has been recognized under different names since the 17th Century, with one of the earliest significant contributions being made by the German mycologist Christiaan Hendrik Persoon, who used the name *Lactaria* and published seven species (Persoon 1797). The genus is characterized by the exudation of latex and the amyloid ornamentation of its basidiospores. To date, approximately 450 species have been recorded, with the majority of studies focusing on taxa from Europe and North America (Wijayawardene et al. 2022b). Members of *Lactarius* are defined by their agaricoid, brittle basidiomata lacking both a volva and an annulus, typically featuring a centrally positioned stipe. The basidiospores display amyloid ornamentation with various types of arrangements of ridges and warts, and sometimes winged, lamellar trama composed of lactifers, sphaerocytes, and connecting hyphae; hymenial and dermatocystidia are thin-walled with various types of apices and contents. *Pilear and Stipe trama* is composed of nests of sphaerocytes, and clamp connections are absent (Heilman-Clausen et al.

1998). *Lactarius* is usually ectomycorrhizal and is one of the most encountered mushrooms in subalpine to temperate forests. At present, the genus is classified into three subgenera: *L.* subg. *Lactarius* (Fr. ex J. Kickx f.) Kauffman, *L.* subg. *Russularia* (Fr.) Kauffman, and *L.* subg. *Plinthogalus* (Berk.) & A.H. Sm. (Buyck et al. 2010). An updated phylogeny for *Lactarius* and closely related taxa is shown in Fig. 99.

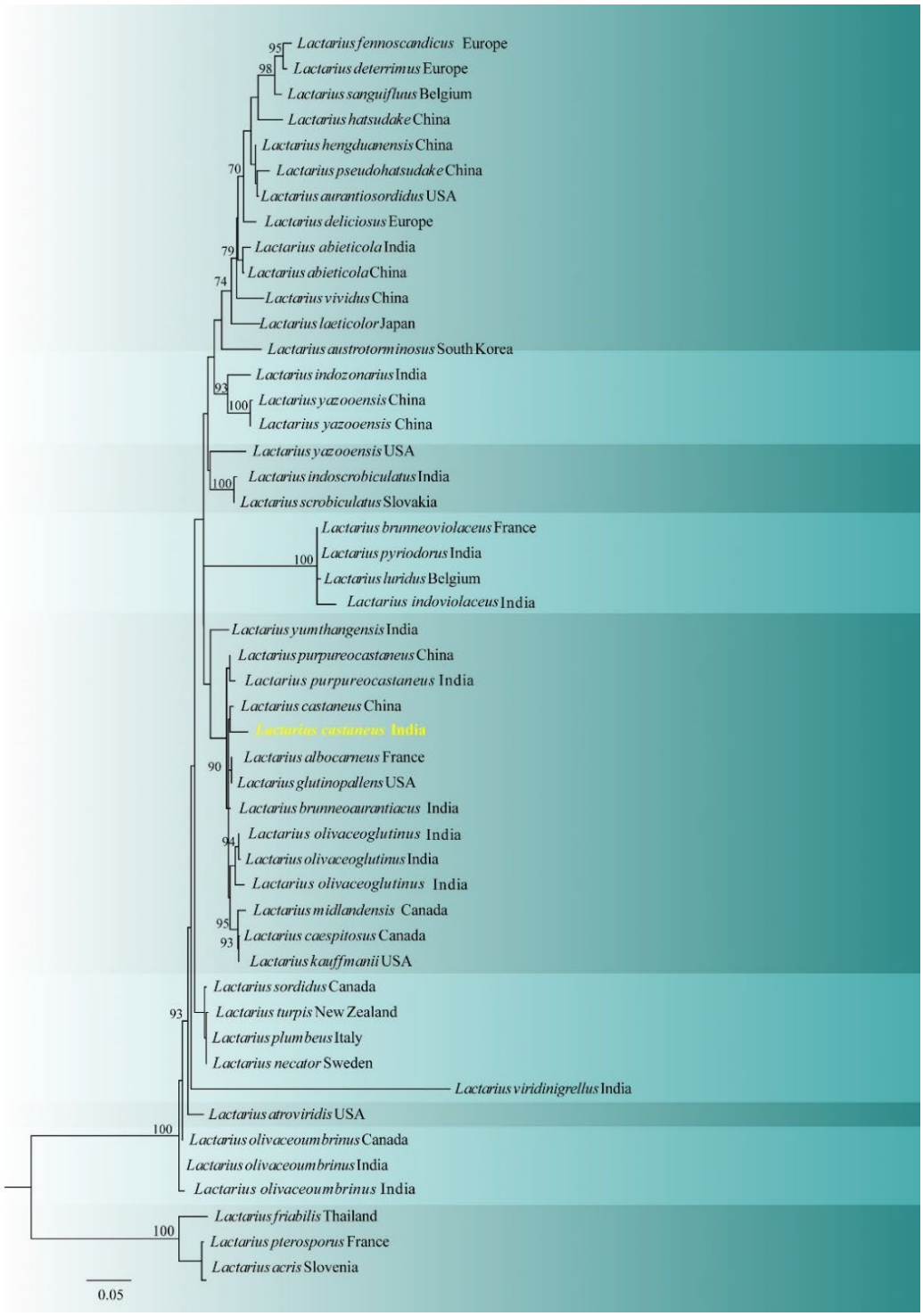

Fig. 99 – A maximum likelihood (ML) phylogram inferred from raxmlGUI 2.0 based on nrITS sequence data. The sequences derived from the Indian specimens of *Lactarius castaneus* are shown in red and

bold. Bootstrap support values (≥ 70%) obtained from the ML analysis are shown above or below the branches at nodes.

Lactarius castaneus W.F. Chiu, Lloydia 8(1), 34 (1945)

Index Fungorum number: IF 287456; Facesoffungi number: FoF 19199 Figs. 100, 101

Pileus 40–55 mm in diam., hemispheric to applanate; surface heavily glutinous, smooth, undulated. *Pileus surface* light brown to yellowish brown (5–6D5), not peeling easily; brittle in consistency; margin decurved, regular to slightly wavy, entire. *Lamellae* adnate, subdistant (10 L+l/cm at pilear margin), sometimes forked near the juncture of the stipe; lamellulae in 5–6 series; orange white (5A2) turning to light orange to greyish orange (5A–B4) on bruising; edge entire. *Stipe* 15–35 × 5–1 mm, central, clavate to subclavate, smooth, pale orange to light orange (5A3–4) to brownish orange (5C4) in maturity with yellowish-white granular spots. *Context* thick at the pileus, hollow in the stipe, light orange to greyish orange (5A–B4), no change with 3% KOH and $FeSO_4$, it immediately becomes brownish yellow with guaiac. *Latex* scarce, white, turning exposed lamellae light orange (5A4) after a few seconds, slightly acrid. *Taste* very acrid. *Odor* mild and earthy.

Basidiospores 7.2–8.9–9.7 × 6.2–7.3–8.1 µm, (n = 30, Q = 1.02–1.21–1.36), usually globose to ellipsoid; ornamentation amyloid; up to 0.9 µm high, composed of high ridges mostly aligned in a zebroid pattern but never forming a complete reticulum, ridges appear as bands surrounding the basidiospores; suprahilar spot inamyloid. *Basidia* 38–82 × 8–10.5 µm, clavate to subclavate, 4-spored; sterigmata 5–7 × 0.8–1 µm. *Pleuromacrocystidia* moderate, 71–115 × 9.5–13 µm, emergent up to 51 µm, subcylindric with rounded apices, originating from the subhymenium region; content fibrous, granular. *Pleuropseudocystidia* 2–4 µm wide, mostly non-emergent, cylindrical to rarely tortuous at apex. *Lamellae edge* fertile with basidia, basidioles, and cystidia. *Cheilomacrocystidia* 32–75 × 8.6–12 µm, emergent up to 35.7 µm, subcylindric with rounded apices; content fibrous and granular. *Subhymenium* up to 15 µm thick, pseudoparenchymatous. *Lamellar trama* composed of lactifers, sphaerocytes, and connecting hyphae. *Pileipellis* up to 148 µm thick, ixotrichoderm, composed of erect, branched, multiseptated hyphae (16–60 × 1–3 µm), sometimes with lactifers under a layer of gluten. *Stipitipellis* up to 69 µm thick, ixotrichoderm, composed of erect, multiseptated hyphae (18–45 × 1.5–3 µm) under a layer of gluten.

Habitat and distribution – Growing in solitary on soil in association with *Abies* in sub-alpine forests of the Tawang District of Arunachal Pradesh.

Material examined – India, Arunachal Pradesh, Pankang Teng Tso (PTSO) Lake, Tawang District, 27°37.512"N, 91°51.574"E, 3703 m a.s.l., 22 July 2021, *I. Bera*, IB 21-013 (CAL 1888).

GenBank accession numbers – ITS: OP806907.

Notes – The slimy, azonate pileus, unchanging latex, zebroid ornamented basidiospores, and well-defined ixotrichoderm pileipellis undoubtedly place *Lactarius castaneus* within *Lactarius* sect. *Glutinosi*, subsect. *Pallidini* Bon (Heilmann-Clausen et al. 1998). Morphologically, *L. castaneus* is distinctive by its medium-sized, light brown to yellow-brown pileus with an undulated surface, pileus covered by a thick layer of gluten; stout, clavate to subclavate pale orange stipe; subdistant lamellae that bruise greyish orange on bruising; acrid-tasting latex; large, zebroid ornamented basidiospores, and an ixotrichoderm type of pileipellis make *L. castaneus* unique in the field. The original description by W.F. Chiu could not be located; therefore, the morphological observations were compared with those documented in China by Wang (2007). In addition, the current specimen closely aligns with Wang (2007), which, although minor differences were noted, such as more crowded lamellae, a thicker gluten layer on the pileipellis (200–300 µm), and slightly larger basidiospores (8)8.5–10.5(–11) × (6.5–)7–8.5(–9.5) µm. Based on nrITS phylogenetic analysis (Fig. 99), the studied specimen clusters with Chinese *L. castaneus* (MF508962) in a distinct clade, thereby confirming its identity.

The notably glutinous pileus of *L. castaneus* is similar to that of the Japanese species *L. glutininitens* Har. Takah, which also features a smooth, glabrous, azonate, and strongly glutinous

pileus, consistent with an ixotrichoderm pileipellis (Takahashi 2001). However, *L. glutininitens* differs in having a pale greyish brown to pale greyish pileus, larger basidiospores (8.5–11 × 7–8.5 µm), shorter cystidia (pleuro: 35–90 × 7–10 µm; cheilo: 22–30 × 5–7.5 µm) with acute to mucronate apices, and a cutis-type of stipitipellis lacking a gluten layer. To date, they differentiate *L. glutininitens* from the described species (Takahashi 2001). Evidence of *L. castaneus* has not been documented from India to date, and thus the studied specimen represents a new record for the Indian mycoflora.

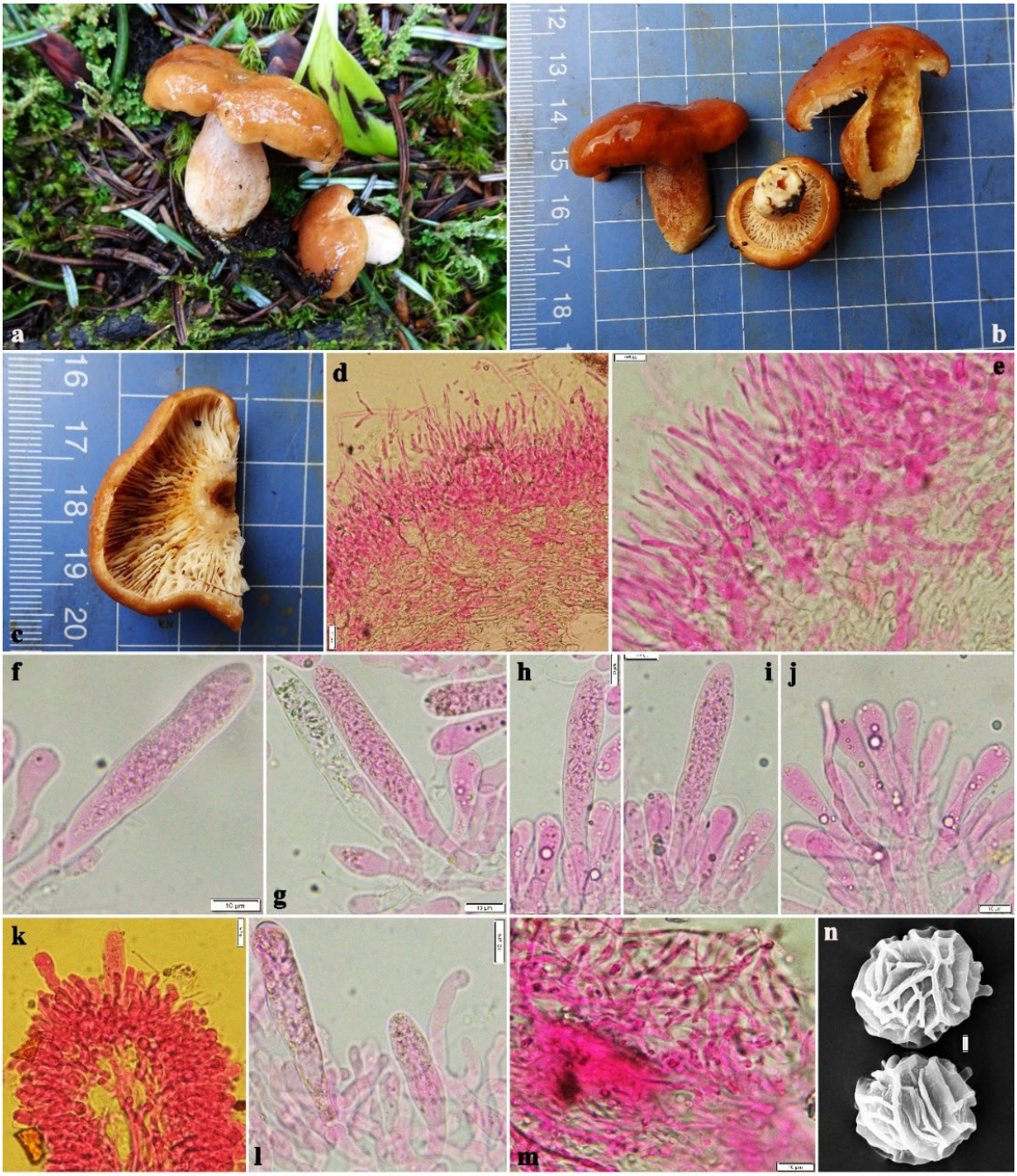

Fig. 100 – *Lactarius castaneus* (CAL 1888, **a new record**). a, b Fresh basidiomata in the field and at base camp. c Latex turning cut lamellae orange. d, e Transverse section through pileipellis. f–i Pleuromacrocystidia. j Pleuropseudocystidia. k, l Cheilomacrocystidia. m Transverse section through stipitipellis. n Basidiospore. Scale bars: d = 20 µm, e–m = 10 µm, n = 1 µm

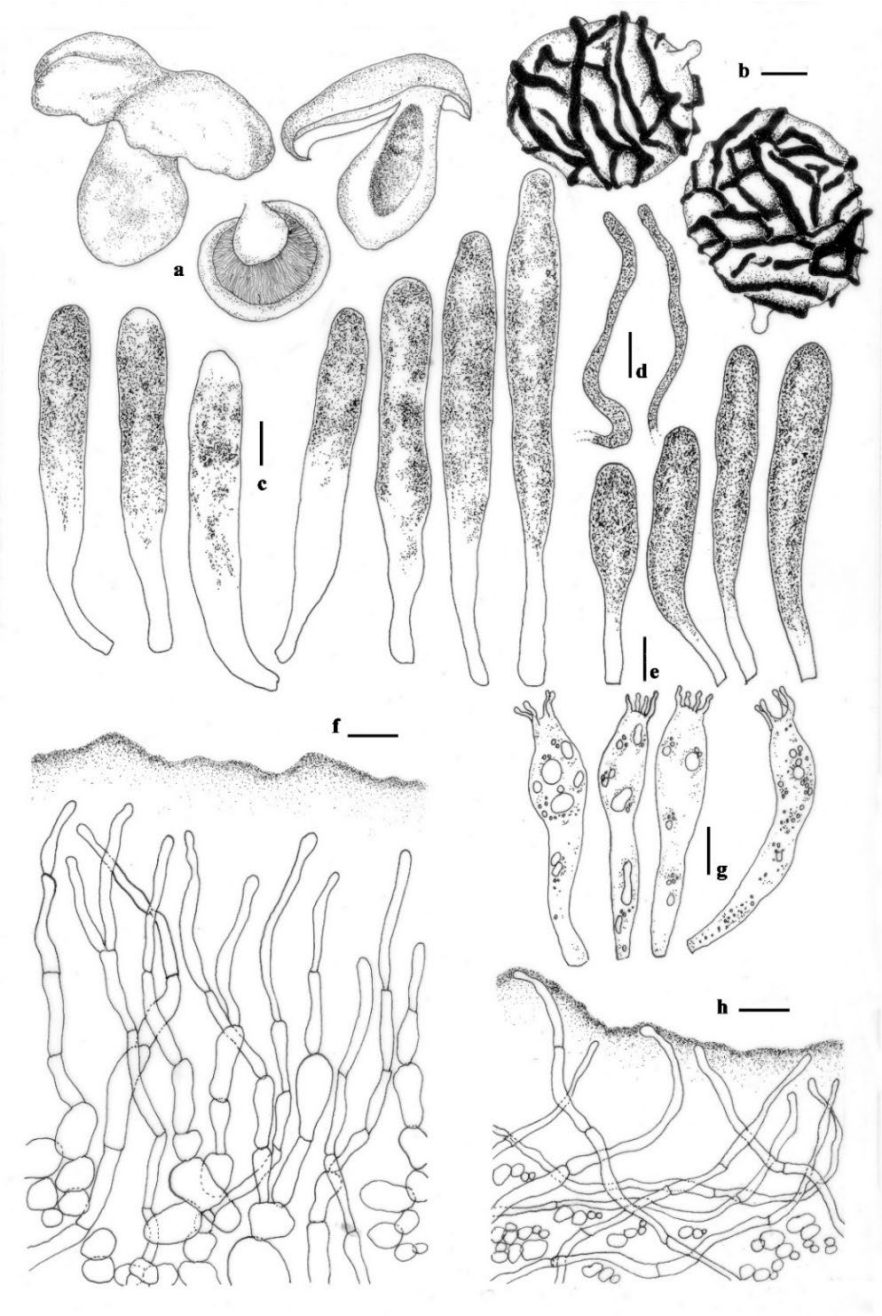

Fig. 101 – Line drawings of *Lactarius castaneus*. a Fresh basidiomata in the field and base camp. b Basidiospore. c Pleuromacrocystidia. d Pleuropseudocystidia. e Cheilomacrocystidia. f Transverse section through pileipellis. g Basidia. h Transverse section through stipitipellis. Scale bars: b = 2 µm, c–f = 10 µm.

Sebacinales M. Weiss, Selosse, Rexer, A. Urb. & Oberw, Mycological Research 108(9), 1007 (2004)
Index Fungorum number: IF 501537; Facesoffungi number: FoF 19200
Sebacinaceae K. Wells & Oberw, Mycologia 74, 329 (1982)
Index Fungorum number: IF 81612; Facesoffungi number: FoF 19182
Chaetospermum Sacc., Sylloge Fungorum 10, 706 (1892)
Index Fungorum number: IF 7593; Facesoffungi number: FoF 07151

The asexual morph fungus *Tubercularia chaetospora* was described by Patouillard (1888). Later, it was transferred to *Chaetospermum* as *C. tubercularioides* because of its morphological differences from *Tubercularia* (Saccardo 1892). Later, *C. tubercularioides* was synonymized as *C. chaetosporum* (Smith & Ramsbottom 1914). *Chaetospermum* is distributed worldwide as a saprobic fungus in terrestrial and freshwater habitats (Muntanola-Cvetkovic & Gomez-Bolea 1993, Rajeshkumar et al. 2010, Tangthirasunun et al. 2014). Species of *Chaetospermum* can be distinguished by their differences in conidiomata, which are closed while dry and become gelatinous, pulvinate, and wide open after rehydration (Sutton 1980). Hyde et al. (2024) listed 10 species in this genus, while the Index Fungorum (2025) listed 13 species. An updated phylogeny for *Chaetospermum* and closely related taxa is shown in Fig. 102.

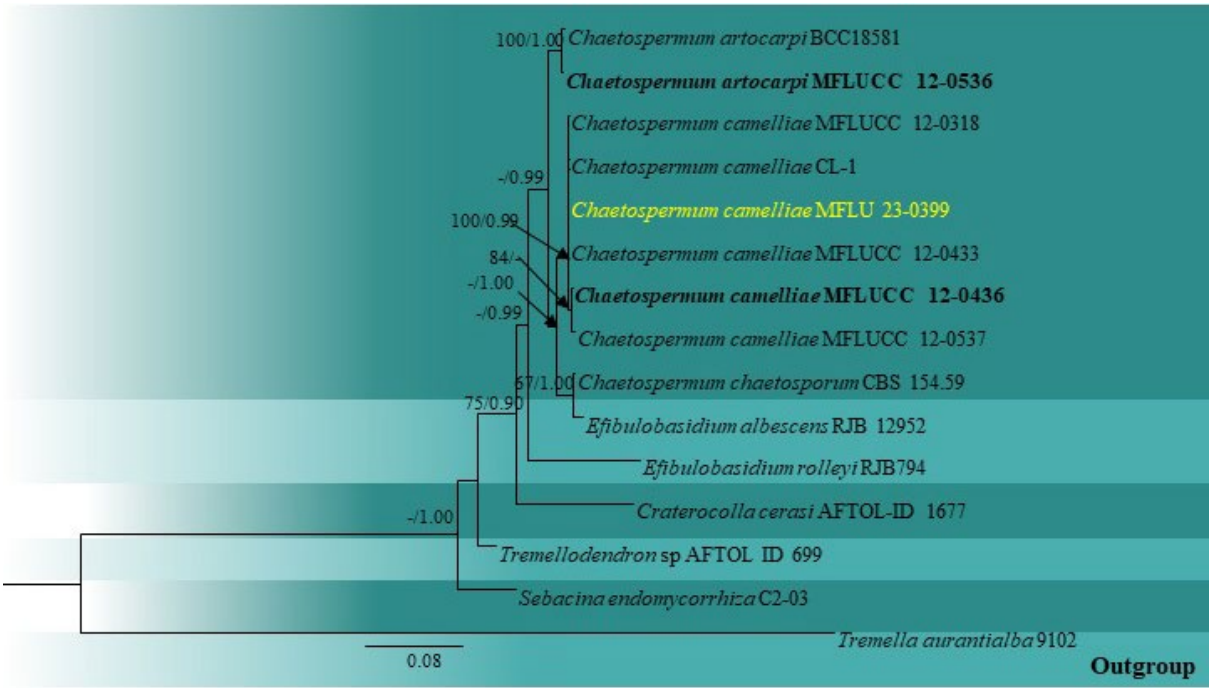

Fig. 102 – Phylogram generated from Maximum likelihood analysis based on combined LSU, SSU, and ITS sequence data. Fifteen strains were included in the combined analyses, which comprised 3,092 (634 for ITS, 1,349 for LSU, and 1,101 for SSU) after alignment. The tree topology of maximum likelihood is similar to Bayesian analysis. The best RA×ML tree with a final likelihood value of -6980.149828 is presented. Estimated base frequencies were as follows: A =0.261393, C= 0.208551, G = 0.268664, T = 0.261393; substitution rates AC = 0.764976, AG = 2.112953, AT= 0.960975, CG = 0.596594, CT = 4.629243, GT = 1.000000; gamma distribution shape parameter α = 0.247610. The evolutionary model GTRGAMMA was applied to all the gene regions. Bootstrap support values for ML ≥ 75% and Bayesian posterior probabilities ≥ 0.90 are given near nodes, respectively. The tree is rooted with *Tremella aurantialba* (9102). Ex-type strains are in bold. The newly generated sequences are indicated in yellow.

Chaetospermum camelliae Agnihothr, Mycopathologia et Mycologia Applicata 16, 115 (1962)

Index Fungorum number: IF328117; Facesoffungi number: FoF 07152 Fig. 103

Saprobic on the dead stems of *Chromolaena odorata*. *Conidiomata* 300–420 × 500–600 ($\overline{x}$ = 365.1 × 520 µm), pycnidial, superficial, solitary, gregarious, velvety, rounded, mucoid, and off-white when moist, unilocular, erumpent, raised, with gelatinized wall. *Pycnidial wall* several layers, intermixed with host cells and hyaline cells of *textura angularis*, with conidiophores arising from the innermost layer of hyaline cells from the base and sides. *Conidiophores* reduced to conidiogenous cells. *Conidiogenous*

cells discrete, sympodially arranged, holoblastic, cylindrical to subcylindrical, slightly curved, and hyaline, producing a conidium at the tip. *Conidia* 30–40 × 5–10 ($\overline{x}$ =37 × 6.8 µm), cylindrical to subcylindrical, with rounded ends, slightly curved, aseptate, hyaline, with small guttules, bearing 7–8 tubular, filiform, flexuous, polar and subpolar appendages.

Material examined – Thailand, Chiang Rai Province, Mae Chan District, 20º06'54.1"N 99º52'14.1"E, on a dried branch of *Chromonaela odorata* (*Asteraceae*), Zin Hnin Htet, 4 August 2021, MFLU 23-0399.

GenBank accession numbers – ITS: OR794170, LSU: OR794172, SSU: OR794171.

Known distribution (based on molecular data) – China (Tan et al. 2014), Estonia (unpublished), Taiwan (Kirschner et al. 2017), and Thailand (Rungjindamai et al. 2008, Tangthirasunun et al. 2014).

Known hosts (based on molecular data) – *Coelogyne leucantha* (Tan et al. 2014), *Chromolaena odorata* (this study), *Pandanus* leaf (Rungjindamai et al. 2008), *Trichilia emetica* (Crous et al. 2020), *Typha angustifolia* (Rungjindamai et al. 2008).

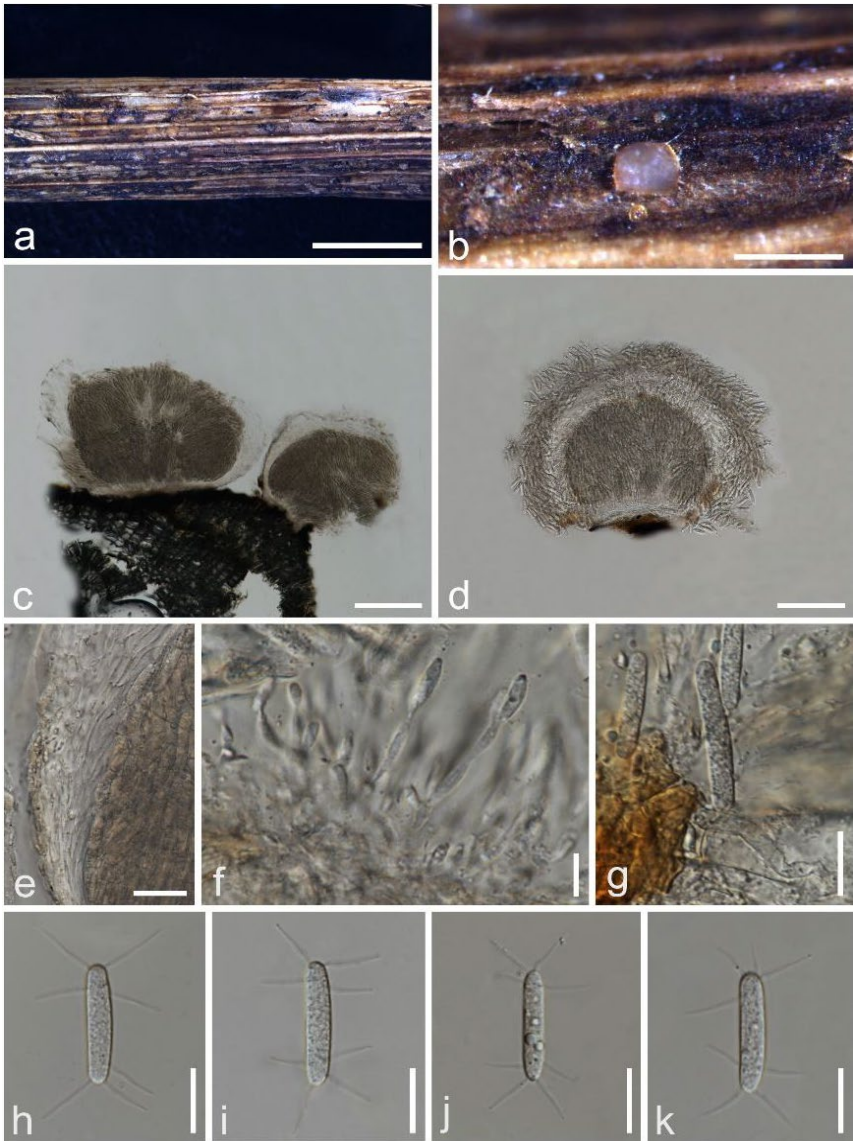

Fig. 103 – *Chaetospermum camelliae* (MFLU 23-0399, **a new host record**). a, b Fungal colonies on the host surface. c, d Section through conidiomata. e Peridium. f–g Conidia on the conidiogenous cells. h–k Conidia. Scale Bars: a, b = 500 µm, c, d = 100 µm, e = 30 µm, f–k = 20 µm.

Notes – In our phylogenetic analysis, *Chaetospermum camelliae* (MFLU 23-0399) clusters with other *C. camelliae* strains (MFLUCC 12-0536, MFLUCC 12-0318, CL-1, MFLUCC 12-0433, MFLUCC 12-0436, MFLUCC 12-0537) with Bayesian inference (BI) support (0.99) (Fig. 102). The megablast result showed that the closest match for the LSU sequence was *Chaetospermum camelliae* (MFLUCC 12-0433) with 100% similarity. The closest match for the ITS sequence was *Chaetospermum camelliae* (CPC:34736), with a similarity of 97.81%. The closest match for the SSU sequence was *Chaetospermum camelliae* (MFLUCC 12-0537), with a similarity of 99.85%. *Chaetospermum* species can be found on various hosts in the families *Meliaceae*, *Orchidaceae*, *Typhaceae*, and *Pandanaceae* (Rungjindamai et al. 2008, Tan et al. 2014, Crous et al. 2020). Tangthirasunun et al. (2014) reported *Chaetospermum camelliae* from unidentified hosts in Thailand. In this study, we collected *C. camelliae* (MFLU 23-0399) from Thailand as a new host record, associated with *Chromolaena odorata* L. (*Asteraceae*).

Acknowledgements

Thatsanee Luangharn would like to thank the Foundation Fund supported by the National Science, Research and Innovation Fund, entitled: Taxonomy, phylogeny, screening of biologically active secondary metabolite and cultivation of *Ganoderma* species (Grant no. 672A16004), the Selecting potential mushroom strains for developing leather-sustainable materials from mushroom mycelium-base (Grant no. 682A16031), the National Research Council of Thailand (NRCT) grant (Grant no. N42A650547), entitled: Total fungal diversity in a given forest area with implications towards species numbers, chemical diversity and biotechnology, thanks Mae Fah Luang University fund, entitled: Exploration and development Thai mushroom mycelium for sustainable mycelium-based material production (Grant no. 691B16034), and Dr. Roberto Farias for his valuable support in initiating the collection of data for this study. Kevin D. Hyde thanks the National Research Council of Thailand (NRCT) grant (Grant no. N42A650547), entitled: Total fungal diversity in a given forest area with implications towards species numbers, chemical diversity, and biotechnology, and was funded by the Distinguished Scientist Fellowship Program (DSFP), King Saud University, Kingdom of Saudi Arabia. Herbert Dustin Aumentado would like to thank the partial PhD scholarship from Mae Fah Luang University (GR-ST-PS-65-25) and the Department of Science and Technology – Science Education Institute, Taguig City, Philippines. Napalai Chaiwa thanks the CMU Proactive Researcher grant of Chiang Mai University (grant number EX010059) and Chiang Mai University. Naghmeh Afshari and Nethmini P. Samaradiwakara thank Chiang Mai University for providing the Presidential Scholarship 2020 and Mae Fah Luang University for the research collaboration. Further, Afshari and Samaradiwakara would like to thank Martin van de Bult, Narong Apichai, and the Doi Tung Development Project for sample collection (permission number 7700/17142 with the title "The diversity of saprobic fungi on selected hosts in forest northern Thailand"). Qi Zhao thanks the Yunnan Science and Technology Talent and Platform Plan (202405AD350054) and the Second Tibetan Plateau Scientific Expedition and Research Program (Grant No. 2024QZKK02010303). Ruifang Xu and Tianye Du thank Mae Fah Luang University for the tuition-fee scholarship. Saowaluck Tibpromma thanks the "Yunnan Revitalization Talents Support Plan" (high-End Foreign Experts Program and the Key Laboratory of Yunnan Provincial Department of Education of the Deep-Time Evolution on Biodiversity from the Origin of the Pearl River for their support. I.C. Senanayake thanks the research fund (E4614411K1) for young talent introduction program by Kunming Institute of Botany, Chinese Academy of Science and Yunnan Revitalization Talents Support Plan (High-End Foreign Experts Programs).

References

Adikaram NKB, Yakandawala DMD. 2020 – A checklist of plant pathogenic fungi and *Oomycota* in Sri Lanka. Ceylon Journal of Science 49, 93–123.

Alves A, Phillips AJL, Henriques I, Correia A. 2005 – Evaluation of amplified ribosomal DNA restriction analysis as a method for the identification of *Botryosphaeria* species. FEMS Microbiology Letters 245, 221–229.

Ariyawansa HA, Tanaka K, Thambugala KM, Phookamsak R, et al. 2014 – A molecular phylogenetic reappraisal of the *Didymosphaeriaceae* (= *Montagnulaceae*). Fungal Diversity 68, 69–104.

Ariyawansa HA, Hyde KD. 2018 – Additions to *Pestalotiopsis* in Taiwan. Mycosphere 9, 999–1013.

Ariyawansa HA, Jaklitsch WM, Voglmayr H. 2018 – Additions to Taiwan fungal flora 1: *Neomassariaceae* fam. nov. Cryptogamie Mycologie 39, 359–372.

Arx JA von. 1970 – The genera of fungi sporulating in pure culture. J. Cramer, Lehre, Germany, pp. 288.

Asif M, Saba M, Raza M, Vellinga EC. 2024 – Molecular insights into fungal diversity reveal three novel species of *Leucocoprinus* from southern Punjab, Pakistan. Mycologia 116, 1–20.

Barron GL. 1968 – The genera of hyphomycetes from soil. Williams and Wilkins, Baltimore, Md. Pp. 364.

Becker K, Wongkanoun S, Wessel AC, Bills GF, et al. 2020 – Phylogenetic and chemotaxonomic studies confirm the affinities of *Stromatoneurospora* phoenix to the coprophilous *Xylariaceae*. Journal of Fungi 6, 144.

Bensch K, Braun U, Groenewald JZ, Crous PW. 2012 – The genus *Cladosporium*. Studies in Mycology 72, 1–401.

Bensch K, Groenewald JZ, Braun U, Dijksterhuis J, et al. 2015 – Common but different: The expanding realm of *Cladosporium*. Studies in Mycology 82, 23–74.

Bensch K, Groenewald JZ, Dijksterhuis J, Starink-Willemse M, et al. 2010 – Species and ecological diversity within the *Cladosporium cladosporioides* complex (*Davidiellaceae*, *Capnodiales*). Studies in Mycology 67, 1–94.

Bensch K, Groenewald JZ, Meijer M, Dijksterhuis J, et al. 2018 – *Cladosporium* species in indoor environments. Studies in Mycology 89, 177–301.

Bezerra JDP, Machado AR, Firmino AL, Rosado AWC, et al. 2018 – Mycological diversity description I. Acta Botanica Brasilica 32, 656–666.

Bhunjun CS, Niskanen T, Suwannarach N, Wannathes N, et al. 2022 – The numbers of fungi: are the most speciose genera truly diverse?. Fungal Diversity 114, 387–462.

Birkebak JM. 2010 – The genus *Leucocoprinus* in western Washington. Mycotaxon 112, 83–102.

Boehm EW, Schoch CL, Spatafora JW. 2009 – On the evolution of the *Hysteriaceae* and *Mytilinidiaceae* (*Pleosporomycetidae*, *Dothideomycetes*, *Ascomycota*) using four nuclear genes. Mycological Research 113, 461–479.

Boerema GH, Bollen GJ. 1975 – Conidiogenesis and conidial septation as differentiating criteria between Phoma and Ascochyta. Persoonia 8, 111–144.

Boonmee S, Wanasinghe DN, Calabon MS, Huanraluek N, et al. 2021 – Fungal diversity notes 1387–1511: Taxonomic and phylogenetic contributions on genera and species of fungal taxa. Fungal Diversity 111, 1– 335.

Burgess TI, Barber PA, Mohali S, Pegg G, et al. 2006 – Three new *Lasiodiplodia* spp. from the tropics, recognised based on DNA sequence comparisons and morphology. Mycologia 98, 423–435.

Burgess TI, Tan YP, Garnas J, Edwards J, et al. 2019 – Current status of the *Botryosphaeriaceae* in Australia. Australasian Plant Pathology 48, 35–44.

Buyck B, Hofstetter V, Verbeken A, Walleyn R. 2010 – Proposals to conserve or reject names. 1919 Proposal to conserve *Lactarius* nom. cons. *Basidiomycota* with a conserved type. Taxon 59, 295–296

Cannon PF, Damm U, Johnston PR, Weir BS. 2012 – *Colletotrichum*: current status and future directions. Studies in Mycology 73, 181–213.
Cao T, Yu JR, Nguyễn TTT, Yuan HS. 2021 – Multiple-marker phylogeny and morphological evidence reveal two new species in *Steccherinaceae* (*Polyporales, Basidiomycota*) from Asia. MycoKeys 78, 169–186.
Carson ML. 2005 – Yield loss potential of *Phaeosphaeria* leaf spot of maize caused by *Phaeosphaeria maydis* in the United States. Plant Disease 89, 986–988.
Castañeda Ruíz RF, Velazquez S, Cano J, Saikawa M, et al. 2002 – *Phaeoisaria aguilerae* anam. sp. nov. from submerged wood in Cuba with notes and reflections on the genus *Phaeoisaria*. Cryptogamie Mycologie 23, 9–18.
Chandrasrikul A, Suwanarit P, Sangwanit U, Lumyong S, et al. 2011 – Checklist of mushrooms (Basidiomycetes) in Thailand. Office of Natural Resources and Environmental Policy and Planning, Bangkok, Thailand, pp. 112–113.
Chapela IH, Rehner SA, Schultz TR, Mueller UG. 1994 – Evolutionary history of the symbiosis between fungus-growing ants and their fungi. Science 266, 1691–1694.
Chen J, Zhang LC, Xing YM, Wang YQ, et al. 2013 – Diversity and taxonomy of endophytic xylariaceous fungi from medicinal plants of *Dendrobium* (*Orchidaceae*). PLoS ONE 8, 1–11.
Chen Q, Jiang JR, Zhang GZ, Cai L, et al. 2015 – Resolving the *Phoma enigma*. Studies in Mycology 82, 137–217.
Chen S, Liu XZ, Chen FJ. 2000 – *Hirsutella minnesotensis* sp. nov., a new pathogen of the soybean cyst nematode. Mycologia 92, 819–824.
Chen S, Pavlic D, Roux J, Slippers B, et al. 2011 – Characterization of *Botryosphaeriaceae* from plantation-grown Eucalyptus species in South China. Plant Pathology 60, 739–751.
Chen YJ, Wan YH, Zeng L, Meng Q, et al. 2021 – Characterization of *Pestalotiopsis chamaeropis* causing gray blight disease on tea leaves (*Camellia sinensis*) in Chongqing, China. Canadian Journal of Plant Pathology 43, 413–420.
Cheng XL, Wei L, Zhang TY. 2014 – A new species of *Phaeoisaria* from intertidal marine sediment collected in Weihai, China. Mycotaxon 127, 17–24.
Chethana KWT, Niranjan M, Dong W, Samarakoon MC, et al. 2021 – AJOM new records and collections of fungi: 101–150. Asian Journal of Mycology 4, 113–260.
Chethana KWT, Rathnayaka AR, Samarakoon BC, Wu N, et al. 2023 – AJOM new records and collections of fungi: 151–200. Asian Journal of Mycology 6, 89–243.
Chlebická M. 2014 – *Propolis rhodoleuca* (*Leotiomycetes*, inc. sed.) compared with *P. farinosa*, *P. occulta* sp. nov. and *P. strobilina*. Nova Hedwigia 98, 491–506.
Ciancio A, Colagiero M, Rosso L, Gutierrez SN, et al. 2013 – Phylogeny and morphology of *Hirsutella tunicata* sp. nov. (*Ophiocordycipitaceae*), a novel mite parasite from Peru. Mycoscience 54, 378–386.
Clements FE, Shear CL. 1931 – The genera of fungi; Hafner Publishing Co., New York, NY, USA, pp. 632.
Corda ACI. 1831 – Die Pilze Deutschlands. In: Deutschlands Flora in Abbildungen nach der Natur. Nürnberg Sturm 12, 33–64.
Corda ACI. 1838 – Iconesfungorum hucusque cognitorum. 2. Pragae, Journal of Natural History 2, 465.
Corda ACJ. 1842 – Icones fungorum hucusque cognitorum. J. Cramer, Wheldon & Wesley, Hafner, USA, pp. 1–92.
Correia KC, Câmara MPS, Barbosa MAG, Sales Jr. R, et al. 2013 – Fungal trunk pathogens associated with table grape decline in Northeastern Brazil. Phytopathologia Mediterranea 52, 380–387.
Cortez VG, da Silveira RMB. 2005 – First report of *Agrocybe retigera* (Speg.) Singer (*Bolbitiaceae*, *Agaricales*) from Brazil. Instituto de Biociências 13, 227–229.

Coutinho IBL, Freire FCO, Lima CS, Lima JS, et al. 2016 – Diversity of genus *Lasiodiplodia* associated with perennial tropical fruit plants in northeastern Brazil. Plant Pathology 66, 90–104.
Crous PW, Slippers B, Wingfield MJ, Rheeder J, et al. 2006 – Phylogenetic lineages in the *Botryosphaeriaceae*. Studies in Mycology 55, 235–253.
Crous PW, Wingfield MJ, Guarro J, Cheewangkoon R, et al. 2013 – Fungal Planet description sheets: 154–213. Persoonia: Molecular Phylogeny and Evolution of Fungi 31, 188–256.
Crous PW, Shivas RG, Quaedvlieg WV, Van der Bank M, et al. 2014 – Fungal Planet description sheets: 214–280. Persoonia-Molecular Phylogeny and Evolution of Fungi 32, 184–306.
Crous PW, Schumacher RK, Wingfield MJ, Lombard L, et al. 2015 – Fungal Systematics and Evolution. Sydowia 67, 81–118.
Crous PW, Wingfield MJ, Chooi YH, Gilchrist CL, et al. 2020a – Fungal planet description sheets: 1042–1111. Persoonia: Molecular Phylogeny and Evolution of Fungi 44, 301–459.
Crous PW, Wingfield MJ, Schumacher RK, Akulov A, et al. 2020b – New and interesting fungi. 3. Fungal Systematics and Evolution 6, 157.
Crous PW, Boers J, Holdom D, Osieck ER, et al. 2022a – Fungal Planet description sheets: 1383–1435. Persoonia: Molecular Phylogeny and Evolution of Fungi 48, 261– 371.
Crous PW, Begoude BAD, Boers J, Braun U, et al. 2022b – New and Interesting Fungi. 5. Fungal Systematics and Evolution 10, 19–90.
Cruywagen EM, Slippers B, Roux J, Wingfield MJ. 2017 – Phylogenetic species recognition and hybridisation in *Lasiodiplodia*: a case study on species from baobabs. Fungal Biology 121, 420–436.
Custódio FA, Machado AR, Soares DJ, Pereira OL. 2018 – *Lasiodiplodia hormozganensis* causing basal stem rot on *Ricinus communis* in Brazil. Australasian Plant Disease Notes 13, 1–6.
da Silva Cruz K, Cortez VG. 2015 – *Xylaria* (*Xylariaceae*, *Ascomycota*) in the Parque Estadual de São Camilo, Paraná, Brazil. Acta Biológica Paranaense 44, 1–4.
Dai YC, Cui BK, Yuan HS, Li BD. 2007 – Pathogenic wood-decaying fungi in China. Forest Pathology 37, 105–120.
Dai DQ, Bahkali AH, Ariyawansa HA, Li WJ, et al. 2016 – *Neokalmusia didymospora* (*Didymosphaeriaceae*), a new species from bamboo. Sydowia 68, 17–25.
de Silva NI, Hyde KD, Lumyong S, Phillips AJL, et al. 2022 – Morphology, phylogeny, host association and geography of fungi associated with plants of *Annonaceae*, *Apocynaceae* and *Magnoliaceae*. Mycosphere 13, 955–1076.
Deighton FC. 1974 – Four synnematous hyphomycetes. Transactions of the British Mycological Society 62, 243–252.
Dennis RWG. 1952 – *Lepiota* and allied genera in Trinidad, British West Indies. Kew Bulletin 7, 459–499.
Dickinson CH. 1968 – *Gliomastix* Gueguen. Mycological Papers 115, 1–26.
Dissanayake AJ, Phillips AJL, Li XH, Hyde KD. 2016 – *Botryosphaeriaceae*: Current status of genera and species. Mycosphere 7, 1001–1073.
Dissanayake AJ, Zhu JT, Chan YY, Maharachchikumbura SSN, et al. 2024 – A re-evaluation of Diaporthe: refining the boundaries of species and species complexes. Fungal Diversity 126, 1–125.
Doassans JE, Patouillard NT. 1892 – Une Clavariée entomogène. Revue Mycologique Toulouse 14, 67–70.
Doilom M, Dissanayake AJ, Wanasinghe DN, Boonmee S, et al. 2017 – Microfungi on *Tectona grandis* (teak) in Northern Thailand. Fungal Diversity 82, 107–182.
Dong W, Wang B, Hyde KD, McKenzie EH, et al. 2020 – Freshwater *Dothideomycetes*. Fungal Diversity 105, 319–575.

dos Santos DV, de Oliveira TGL, da Silva RMF, da Silva GA, et al. 2024 – *Neoarthrinium brasiliense*, sp. nov. (*Apiosporaceae*, *Sordariomycetes*), a new endophytic fungal species from *Lafoensia pacari* tree. Sydowia 76, 179–185.
Dou ZP, He W, Zhang Y. 2017 – Does morphology matter in taxonomy of *Lasiodiplodia*? An answer from *Lasiodiplodia hyalina* sp. nov. Mycosphere 8, 1014–1027.
Du HZ, Yang J, Liu NG, Cheewangkoon R, et al. 2022 – Morpho-phylogenetic evidence reveals new species of *Fuscosporellaceae* and *Savoryellaceae* from freshwater habitats in Guizhou Province, China. Journal of Fungi 8, 1138.
Du TY, Dai DQ, Mapook A, Lu L, et al. 2023 – Additions to *Rhytidhysteron* (*Hysteriales*, *Dothideomycetes*) in China. Journal of Fungi 9, 148.
Ekanayaka AH, Hyde KD, Gentekaki E, McKenzie EHC, et al. 2019 – Preliminary classification of *Leotiomycetes*. Mycosphere 10, 310–489.
El-Ganainy SM, Ismail AM, Iqbal Z, Elshewy ES, et al. 2022 – Diversity among *Lasiodiplodia* species causing dieback, root rot and leaf spot on fruit trees in Egypt, and a description of *Lasiodiplodia newvalleyensis* sp. nov. Journal of Fungi 8, 2–22.
Ellis JJ, Yates SG. 1971 – Mycotoxins of fungi from fescue. Economic Botany 25, 1–5.
Ellis MB. 1963 – *Dematiaceous Hyphomycetes*. Mycological Papers 93, 1–33.
Ellis MB. 1965 – Dematiaceous *Hyphomycetes* VI. Mycological Papers 103, 1–46.
Ellis MB. 1971 – *Dematiaceous Hyphomycetes*. Commonwealth Mycological Institute, Kew, Surrey, England, pp. 608.
Farr DF, Bills GF, Chamuris GP, Rossman AY. 1989 – Fungi on plants and plant products in the United States. American Phytopathological Society, APS Press, Minnesota, pp. 1252.
Farr DF, Rossman AY. 2023 – Fungal databases. U.S. National Fungus Collections, ARS, USDA. https://nt.ars-grin.gov/fungaldatabases/ (Accessed on May 1, 2025).
Fayod V. 1889 – Prodrome d'une histoire naturelle des Agaricinés. Annales des Sciences Naturelles 7, 181–411.
Ferreira AJ, Cortez VG. 2012 – *Lepiotoid Agaricaceae* (*Basidiomycota*) from São Camilo State Park, Paraná State, Brazil. Mycosphere 3, 962–976.
Fierro-Cruz JE, Jiménez P, Coy-Barrera E. 2017 – Fungal endophytes isolated from *Protium heptaphyllum* and *Trattinnickia rhoifolia* as antagonists of *Fusarium oxysporum*. Revista Argentina de Microbiologia 49, 255–263.
Flannigan MD, Wotton BM. 2001 – Climate, weather and area burned. In: Johnson EA, Miyanishi K. Forest Fires: Behavior & Ecological Effects (eds.), Academic Press, New York, pp. 335–357.
Freitas EF, Silva MD, Barros MV, Kasuya MC. 2019 – *Neopestalotiopsis hadrolaeliae* sp. nov., a new endophytic species from the roots of the endangered orchid *Hadrolaelia jongheana* in Brazil. Phytotaxa 416, 211–220.
Fries EM. 1822 – Systema mycologicum 2. Gryphiswaldiae.
Gams W. 1995 – An unusual species of *Wardomyces* (Hyphomycetes). Beihefte zur Sydowia 10, 67–72.
Ge ZW, Yang ZL. 2017 – *Pseudolepiota zangmui* gen. et sp. nov. (*Agaricaceae*, *Basidiomycota*), A new white-spored mushroom from China. Phytotaxa 312, 247–255.
Ghaderi F, Sharifnabi B, Javan-Nikkhah M. 2017 – Introduction of some species of *Parastagonospora* on poaceous plants in Iran. Rostaniha 18, 150–165.
Giraldo A, Crous PW, Schumacher RK, Cheewangkoon R, et al. 2017 – The genera of fungi–G3: *Aleurocystis*, *Blastacervulus*, *Clypeophysalospora*, *Licrostroma*, *Neohendersonia* and *Spumatoria*. Mycological Progress 16, 325–348.
Goonasekara I, Erio C, Bulgakov T, Phookamsak R, et al. 2019 – Two novel species of *Parastagonospora* (*Phaeosphaeriaceae, Pleosporales*) on grasses from Italy and Russia. Asian Journal of Mycology 2, 170–182.

Guéguen MF. 1905 – Recherches sur les homologies et l'evolution du Dictyosporium (Speira) toruloides. Bulletin de la Société Mycologique de France 21, 98–106.
Gullino ML, Gilardi G, Garibaldi A. 2017 – Evaluating severity of leaf spot of lettuce, caused by *Allophoma tropica*, under a climate change scenario. Phytopathologia Mediterranea 56, 235–241.
Hammill TM. 1981 – On *Gliomastix murorum* and *G. felina*. Mycologia 73, 229–237.
Hashemi SA, Zare R, Khodaparast SA, Elahinia SA. 2015 – A new *Xylaria* species from Iran. Mycologia Iranica 2, 1–10.
Hashimoto A, Matsumura M, Hirayama K, Tanaka K. 2017 – Revision of *Lophiotremataceae* sensu lato (*Pleosporales*, *Dothideomycetes*): establishment of *Aquasubmersaceae*, *Cryptocoryneaceae*, and *Hermatomycetaceae* fam. nov. Persoonia 39, 51–73.
Hawksworth DL, Lücking R. 2017 – Fungal diversity revisited: 2.2 to 3.8 million species. In Heitman J, Howlett BJ, Crous PW, Stukenbrock EH, et al., eds. The Fungal Kingdom. Microbiology Spectrum 5, pp. 79–95.
He MQ, Zhao RL, Hyde KD, Begerow D, et al. 2019 – Notes, outline and divergence times of *Basidiomycota*. Fungal Diversity 99, 105–367.
He J, Han X, Luo ZL, Li EX, et al. 2022 – Species diversity of *Ganoderma* (*Ganodermataceae*, *Polyporales*) with three new species and a key to *Ganoderma* in Yunnan Province, China. Frontiers in Microbiology 13, 1035434.
He X, Dong JH, Zhao CL. 2023 – Morphological and molecular identification of a new species, *Trullella yunnanensis* (*Steccherinaceae, Polyporales*) from southern China. Kew Bulletin 78, 213–221.
He MQ, Cao B, Liu F, Boekhout T, et al. 2024 – Phylogenomics, divergence times and notes of orders in *Basidiomycota*. Fungal Diversity 126, 127–406.
Heilmann-Clausen J, Verbeken A, Vesterholt J. 1998 – The genus *Lactarius*. The Danish Mycological Society, Odense, Denmark, pp. 287.
Heinemann P, Little Flower SR. 1984 – *Hymenagaricus* (*Agaricaceae*) de Kerala (Inde) et de Sri Lanka. Bulletin du Jardin Botanique National de Belgique 54, 151–182.
Heuchert B, Braun U, Schubert K. 2005 – Morphotaxonomic revision of fungicolous *Cladosporium* species (hyphomycetes). Schlechtendalia 13, 1–78.
Hibbett D, Nagy LG, Nilsson RH. 2025 – Fungal diversity, evolution, and classification. Current Biology 35, 463–469.
Hirayama K, Tanaka K. 2011 – Taxonomic revision of *Lophiostoma* and *Lophiotrema* based on re-evaluation of morphological characters and molecular analyses. Mycoscience 52, 401–412.
Hlaiem S, Zouaoui-Boutiti M, Ben Jemâa M, Della Rocca G, et al. 2018 – Identification and pathogenicity of *Pestalotiopsis chamaeropis*, causal agent of white heather (*Erica arborea*) dieback, and in vitro biocontrol with the antagonist *Trichoderma* sp. Tunisian Journal of Plant Protection 13, 49–60.
Höhnel F. 1909 – Fragmente zur Mykologie (VI. Mitteilung, Nr. 182 bis 288). Sitzungsberichten der Kaiserliche Akademie der Wissenschaften in Wien Mathematische-Naturwissenschaftliche Klasse 118, 275–452.
Höhnel F. 1919 – Fünfte vorlaüFige Mitteilungen mykologischer Ergebnisse (Nr. 399–500). Berichte der Deutschen Botanischen Gesellschaft 37, 153–161.
Hongsanan S, Hyde KD, Phookamsak R, Wanasinghe DN, et al. 2020a – Refined families of *Dothideomycetes*: orders and families incertae sedis in *Dothideomycetes*. Fungal Diversity 105, 17–318.
Hongsanan S, Hyde KD, Phookamsak R, Wanasinghe DN, et al. 2020b – Refined families of *Dothideomycetes*: *Dothideomycetidae* and *Pleosporomycetidae*. Mycosphere 11, 1553–2107.
Hosen MI, Yang ZL. 2013 – *Coniolepiota spongodes* (*Agaricaceae*, *Basidiomycota*) in Bangladesh and China. Mycotaxon 124, 341–347.

Hosen Md. I, Song ZP, Gates G, Li TH. 2018 – *Xanthagaricus caeruleus*, a new species with ink-blue lamellae from southeast China. Mycoscience 59, 188–192.
Hou YJ, Ge ZW. 2020 – New species of *Echinoderma* and *Lepiota* (*Agaricaceae*) from China. Phytotaxa 447, 221–236.
Hsieh HM, Lin CR, Fang MJ, Rogers JD, et al. 2010 – Phylogenetic status of *Xylaria* subgenus *Pseudoxylaria* among taxa of the subfamily *Xylarioideae* (*Xylariaceae*) and phylogeny of the taxa involved in the subfamily. Molecular Phylogenetics and Evolution 54, 957–969.
Hu HM, Liu LL, Zhang X, Lin Y, et al. 2022 – New species and records of *Neomassaria*, *Oxydothis* and *Roussoella* (*Pezizomycotina*, *Ascomycota*) associated with palm and bamboo from China. MycoKeys 93, 165–191.
Hu H, He M, Wu Y, Long S, et al. 2023 – Taxonomic and phylogenetic characterisations of six species of *Pleosporales* (in *Didymosphaeriaceae*, *Roussoellaceae* and *Nigrogranaceae*) from China. MycoKeys 100, 123–151.
Huanraluek N, Phunyaboon W, Jayawardena RS. 2022 – A new host record of *Diaporthe rosae* on Rambutan (*Nephelium lappaceum* L.). Phytotaxa 567, 162–172.
Huelsenbeck JP, Ronquist F. 2001 – MRBAYES: Bayesian inference of phylogenetic trees. Bioinformatics 17, 754–755.
Hughes SJ. 1958 – Revisiones hyphomycetum aliquot cum appendice de nominibus rejiciendis. Canadian Journal of Botany 36, 727–836.
Hussain S, Al-Kharousi M, Al-Maqbali D, Al-Owaisi AA, et al. 2024 – Two new species of *Hymenagaricus* (*Agaricales*, *Agaricaceae*) from Oman, based on morphology and molecular phylogeny. MycoKeys 105, 1–19.
Hussain S, Jabeen S, Khalid AN, Afshan NS, et al. 2018 – Underexplored regions of Pakistan yield five new species of *Leucoagaricus*. Mycologia 110, 387–400.
Hyde KD, Nilsson RH, Alias SA, Ariyawansa HA, et al. 2014 – One stop shop: backbones trees for important phytopathogenic genera: I. Fungal Diversity 67, 21–125.
Hyde KD, Hongsanan S, Jeewon R, Bhat DJ, et al. 2016 – Fungal diversity notes 367–490: taxonomic and phylogenetic contributions to fungal taxa. Fungal Diversity 80, 1–270.
Hyde KD, Norphanphoun C, Abreu VP, Bazzicalupo A, et al. 2017 – Fungal diversity notes 603–708: taxonomic and phylogenetic notes on genera and species. Fungal Diversity 87, 1–235.
Hyde KD, Chaiwan N, Norphanphoun C, Boonmee S, et al. 2018 – Mycosphere notes 169–224. Mycosphere 9, 271–430.
Hyde KD, Tennakoon DS, Jeewon R, Bhat DJ, et al. 2019 – Fungal diversity notes 1036–1150: taxonomic and phylogenetic contributions on genera and species of fungal taxa. Fungal Diversity 96, 1–242.
Hyde KD, de Silva NI, Jeewon R, Bhat DJ, et al. 2020a – AJOM new records and collections of fungi: 1–100. Asian Journal of Mycology 3, 22–294.
Hyde KD, Dong Y, Phookamsak R, Jeewon R, et al. 2020b – Fungal diversity notes 1151–1276: Taxonomic and phylogenetic contributions on genera and species of fungal taxa. Fungal Diversity 100, 5–277.
Hyde KD, Jeewon R, Chen YJ, Bhunjun CS, et al. 2020c – The numbers of fungi: Is the descriptive curve flattening? Fungal Diversity 103, 219–271.
Hyde KD, Norphanphoun C, Maharachchikumbura SSN, Bhat DJ, et al. 2020d – Refined families of *Sordariomycetes*. Mycosphere 11, 305–1059.
Hyde KD, Suwannarach N, Jayawardena RS, Manawasinghe IS, et al. 2021 – Mycosphere notes 325-344 – Novel species and records of fungal taxa from around the world. Mycosphere 12, 1101–1156.
Hyde KD, Abdel-Wahab MA, Abdollahzadeh J, Abeywickrama PD, et al. 2023a – Global consortium for the classification of fungi and fungus-like taxa. Mycosphere 14, 1960– 2012.

Hyde KD, Norphanphoun C, Ma J, Yang HD, et al. 2023b – Mycosphere notes 387–412 – novel species of fungal taxa from around the world. Mycosphere 14, 663–744.
Hyde KD, Noorabadi MT, Thiyagaraja V, He MQ, et al. 2024a – The 2024 Outline of Fungi and fungus-like taxa. Mycosphere 15, 5146–6239.
Hyde KD, Baldrian P, Chen Y, Chethana TKW, et al. 2024b – Current trends, limitations and future research in the fungi. Fungal Diversity 125, 1–71.
Hyde KD, Saleh A, Aumentado HDR, Boekhout T, et al. 2024c – Fungal numbers: global needs for a realistic assessment. Fungal Diversity 128, 191–225.
Index Fungorum. 2025 – http://www.indexfungorum.org/Names/Names.asp. (Accessed on May 1, 2025)
Jaklitsch W, Baral HO, Lücking R, Lumbsch HT, et al. 2016 – Book review: Syllabus of plant families – Adolf Engler's Syllabus der Pflanzenfamilien part 1/2 *Ascomycota*. Borntraeger, pp. 1–322.
Jaklitsch WM, Olariaga I, Voglmayr H. 2016 – *Teichospora* and the *Teichosporaceae.* Mycological Progress 15, 1–20.
Jayasiri S, Hyde K, Jeewon R, Bhat J, et al. 2016 – *Neoocultibambusa jonesii*, a novel taxon within *Occultibambusaceae*. Mycosphere 7, 1458–1472.
Jayawardena RS, Hyde KD, Chen YJ, Papp V, et al. 2020 – One stop shop IV: taxonomic update with molecular phylogeny for important phytopathogenic genera: 76–100. Fungal Diversity 103, 87–218.
Jayawardena RS, Bhunjun CS, Hyde KD, Gentekaki E, et al. 2021 – *Colletotrichum*: lifestyles, biology, morpho-species, species complexes and accepted species. Mycosphere 12, 519–669.
Jayawardena RS, Hyde KD, Wang S, Sun YR, et al. 2023 – Fungal diversity notes 1512–1610: taxonomic and phylogenetic contributions on genera and species of fungal taxa. Fungal Diversity 117, 1–272.
Jayawardena RS, Hyde KD, Aumentado HD, Abeywickrama PD, et al. 2025 – One stop shop V: taxonomic update with molecular phylogeny for important phytopathogenic genera: 101–125 (2024). Fungal Diversity 130, 263–429.
Jeewon R, Hyde KD. 2016 – Establishing species boundaries and new taxa among fungi: recommendations to resolve taxonomic ambiguities. Mycosphere 7, 1669–1677.
Jiang N, Dou ZP, Xue H, Piao CG, et al. 2022 – Identification of *Pestalotiopsis* species based on morphology and molecular phylogeny. Terrestrial Ecosystem and Conservation 2, 39–54.
Jiang N, Voglmayr H, Ma CY, Xue H, et al. 2022 – A new *Arthrinium*-like genus of *Amphisphaeriales* in China. MycoKeys 92, 27–43.
Jiang YL, Zhou YK, Ma KZ, Mao YL, et al. 2017 – Identification of several strains of *Pestalotiopsis*-like fungi from *Camellia oleifera*. Journal of Anhui Agricultural University 44, 609–616.
Ju YM, Rogers JD. 1996 – A revision of the genus *Hypoxylon*. Mycologia 90, 930–931.
Ju YM, Hsieh HM. 2023 – Xylaria species associated with fallen leaves and petioles. Botanical Studies 64, 19.
Kalichman J, Kirk PM, Matheny PB. 2020 – A compendium of generic names of agarics and *Agaricales*. Taxon, 69, 425–447.
Karakehian J. 2020 – A preliminary study in *Propolis* (Fungi, *Ascomycota*): *Propolis farinosa* - common, cosmopolitan and plurivorous. Master's thesis, Harvard Extension School.
Karsten P. 1881 – Enumeratio Boletinearum et Polyporearum Fennicarum, systemate novo dispositarum. Revue. Mycologigue (Toulouse) 3, 16–19.
Kendrick WB, Carmichae JW. 1973 – *Hyphomycetes*. In: Ainsworth GC, Sparrow FK, Sussman AS, eds. The fungi, an advanced treatise, Vol. IVA. A taxonomic review with keys: Ascomycetes and Fungi Imperfecti. Academic Press, New York, pp. 323–509.
Kibby G. 2019 – The genus *Leucocoprinus* in Britain with a key to species. Field Mycology 20, 129–134.

Kirschner R, Oberwinkler F, Hofmann TA. 2017 – A new species of *Globulisebacina* from Taiwan and new record of *Chaetospermum camelliae* with *Efibulobasidium teleomorph* (*Sebacinales*) from Panama. Nova Hedwigia 105, 329–340.
Kiyuna T, An KD, Kigawa R, Sano C, et al. 2011 – Molecular assessment of fungi in "black spots" that deface murals in the Takamatsuzuka and Kitora Tumuli in Japan: *Acremonium* sect. *Gliomastix* including *Acremonium tumulicola* sp. nov. and *Acremonium felinum* comb. nov. Mycoscience 52, 1–17.
Konta S, Tibpromma S, Karunarathna SC, Samarakoon MC, et al. 2023 – Morphology and multigene phylogeny reveal ten novel taxa in *Ascomycota* from terrestrial palm substrates (*Arecaceae*) in Thailand. Mycosphere 14, 107–152.
Kshirsagar AS, Rhatwal SM, Gandhe RV. 2009 – The genus *Xylaria* from Maharashtra, India. Indian Phytopathology 62, 54–63.
Kularathnage ND, Senanayake IC, Wanasinghe DN, Doilom M, et al. 2023 – Plant-associated novel *Didymellaceous* taxa in the South China Botanical Garden (Guangzhou, China). Journal of Fungi 9, 182.
Kumla J, Suwannarach N, Khuna S, Phonrob W, et al. 2023 – *Hymenagaricus siamensis* (*Agaricaceae*, *Agaricales*), a novel macrofungus from northern Thailand. Phytotaxa 585, 135–144.
Kumla J, Suwannarach N, Wannathes W. 2021 – *Hymenagaricus saisamornae* sp. nov. (*Agaricales*, *Basidiomycota*) from northern Thailand. Chiang Mai Journal of Science 48, 827–836.
Kurihara Y, Shirouzu T, Tokumasu S, Harayama S. 2009 – *Hirsutella proturicola* sp. nov. isolated from a proturan, *Baculentulus densus* (Protura, Hexapoda). Mycoscience 50, 56–62.
Lee YS, Han SS, Jeong IS. 2002 – Taxonomical characteristics of *Xylaria* spp. collected from Malaysia. Mycobiology 30, 193–196.
Li GJ, Hyde KD, Zhao RL, Hongsanan S, et al. 2016 – Fungal diversity notes 253–366: taxonomic and phylogenetic contributions to fungal taxa. Fungal Diversity 78, 1–237.
Li J, Yang W, Ren J, Cao B, et al. 2023 – A new species *Agrocybe striatipes*, also a newly commercially cultivated mushroom with highly nutritional and healthy values. Journal of Fungi 9, 383.
Li Q, Tang L, Sun W, Huang S, et al. 2019 – First report of stem canker and dieback caused by *Neofusicoccum parvum* on plum in Guangxi, Southern China. Plant Disease 103, 2952–2952.
Li WJ, Bhat DJ, Camporesi E, Tian Q, et al. 2015 – New asexual morph taxa in *Phaeosphaeriaceae*. Mycosphere 6, 681–708.
Liang JF, Yang ZL, Xu J, Ge ZW. 2010 – Two new unusual *Leucoagaricus* species (*Agaricaceae*) from tropical China with blue-green staining reactions. Mycologia 102, 1141–1152.
Liang JL, Yu F, Lu JK, Wang SK, et al. 2018 – Morphological and molecular evidence for two new species in *Lepiota* from China. Mycologia 110, 494– 501.
Liang YS, Xu YW, Ouyang M, Huang XX, et al. 2023 – *Lepiota baiyunensis* sp. nov. (*Agaricales*, *Agaricaceae*) from Baiyun Mountain, China. Phytotaxa 606, 1–15.
Link JHF. 1816 – Observationes in ordines plantarum naturales. Dissert. secunda, sistens nuperas de Mucedinum et Gastromycorum ordinibus observationes. Magazin für die Neuesten Entdeckungen in der Gesammten Naturkunde, Gesellschaft Naturforschender Freunde zu Berlin. 7, pp. 25–45.
Little Flower SR, Hosagoudar VB, Abraham TK. 1997 – *Xanthagaricus*, a new generic name in the family *Agaricaceae*. New Botanist 24, 93–100.
Liu JK, Phookamsak R, Doilom M, Wikee S, et al. 2012 – Towards a natural classification of Botryosphaeriales. Fungal Diversity 57, 149–210.
Liu JK, Hyde KD, Jones EBG, Ariyawansa HA, et al. 2015 – Fungal diversity notes 1–110: taxonomic and phylogenetic contributions to fungal species. Fungal Diversity 72, 1–197.
Liu F, Hou LW, Raza M, Cai L. 2017 – *Pestalotiopsis* and allied genera from *Camellia*, with description of 11 new species from China. Scientific Reports 7, 866.

Liu JK, Luo ZL, Liu NG, Cheewangkoon R, et al. 2018 – Two novel species of *Paradictyoarthrinium* from decaying wood. Phytotaxa 338, 285–293.
Liu QM, Song HY, Chen RX, Chen MH, et al. 2021 – Species concept of *Cyclocybe chaxingu*, an edible mushroom cultivated in China. Mycosystema 40, 981–991.
Liu SY, Liu JK, Syouphanthong P, Hyde KD, et al. 2020 – *Xanthagaricus siamensis* sp. nov. (*Agaricaceae*), A new species with dull green lamellae from northern Thailand. Phytotaxa 437, 14–22.
Liu F, Ma ZY, Hou LW, Diao YZ, et al. 2022 – Updating species diversity of *Colletotrichum*, with a phylogenomic overview. Studies in Mycology 101, 1–56.
Liu NG, Hyde KD, Sun YR, Bhat DJ, et al. 2024 – Notes, outline, taxonomy and phylogeny of brown-spored hyphomycetes. Fungal Diversity 129, 1–128.
Lodge DJ, Ammirati JF, O'Dell TE, Mueller GM. 2004 – Collecting and describing macrofungi. Biodiversity of fungi: inventory and monitoring methods. Amsterdam, Elsevier Academic Press, pp. 128–158.
Lombard L, Houbraken J, Decock C, Samson R, et al. 2016 – Generic hyper-diversity in *Stachybotriaceae*. Persoonia-Molecular Phylogeny and Evolution of Fungi 36, 156–246.
Lu L, Karunarathna SC, Hyde KD, Bhat DJ, et al. 2022 – *Crassiparies yunnanensis* sp. nov. (*Neohendersoniaceae*, *Pleosporales*) from dead twigs of *Coffea arabica* in China. Phytotaxa 543, 244–254.
Lu L, Karunarathna SC, Rajeshkumar KC, Elgorban AM, et al. 2025 – Unveiling fungal diversity associated with coffee trees in China using a polyphasic approach and a global review of coffee saprobic fungi. IMA Fungus 16, e144874.
Luangharn T, Karunarathna SC, Mortimer PE, Hyde KD, et al. 2019a – A new record of *Ganoderma tropicum* (*Basidiomycota*, *Polyporales*) for Thailand and first assessment of optimum conditions for mycelia production. MycoKeys 51, 65–83.
Luangharn T, Karunarathna SC, Mortimer PE, Hyde KD, et al. 2019b – Additions to the knowledge of *Ganoderma* in Thailand: *Ganoderma casuarinicola*, a new record; and *Ganoderma thailandicum* sp. nov. MycoKey 59, 47–65.
Luangharn T, Karunarathna SC, Mortimer PE, Hyde KD, et al. 2020 – Morphology, phylogeny and culture characteristics of *Ganoderma gibbosum* collected from Kunming, Yunnan Province, China. Phyton-International Journal of Experimental Botany 89, 743–764.
Luangharn T, Karunarathna SC, Dutta AK, Paloi S, et al. 2021 – *Ganoderma* (*Ganodermataceae*, *Basidiomycota*) Species from the Greater Mekong Subregion. Journal of Fungi 7, 819.
Luo ZL, Hyde KD, Bhat DJ, Jeewon R, et al. 2018 – Morphological and molecular taxonomy of novel species *Pleurotheciaceae* from freshwater habitats in Yunnan, China. Mycological Progress 17, 511–530.
Ma X, Chomnunti P, Doilom M, Daranagama DA, et al. 2022 – Multigene phylogeny reveals endophytic *Xylariales* novelties from *Dendrobium* species from Southwestern China and Northern Thailand. Journal of Fungi 8, 248.
Machado AR, Custódio FA, Cabral PGC, Capucho AS, et al. 2019 – *Botryosphaeriaceae* species causing dieback on *Annonaceae* in Brazil. Plant Pathology 68, 1394–1406.
Magaña-Dueñas V, Cano-Lira JF, Stchigel AM. 2022 – Novel freshwater ascomycetes from Spain. Journal of Fungi 8, 849.
Maharachchikumbura SS, Guo LD, Cai L, Chukeatirote E, et al. 2012 – A multi-locus backbone tree for *Pestalotiopsis*, with a polyphasic characterization of 14 new species. Fungal Diversity 56, 95–129.
Maharachchikumbura SS, Hyde KD, Groenewald JZ, Xu J, et al. 2014 – *Pestalotiopsis* revisited. Studies in Mycology 79, 121–186.

Malysheva E, Moreno G, Villarreal M, Malysheva V, et al. 2019 – The secotioid genus *Galeropsis* (*Agaricomycetes*, *Basidiomycota*): a real taxonomic unit or ecological phenomenon?. Mycological Progress 18, 805–831.
Manawasinghe IS, Calabon MS, Jones EBG, Zhang YX, et al. 2022 – Mycosphere notes 345–386. Mycosphere 13, 454–557.
Manawasinghe I, Hyde KD, Wanasinghe DN, Karunarathna SC, et al. 2024 – Fungal diversity notes 1818–1918: taxonomic and phylogenetic contributions on genera and species of fungi. Fungal Diversity 130, 1–261.
Marques MW, Lima NB, de Morais MA, Barbosa MAG, et al. 2013 – Species of *Lasiodiplodia* associated with mango in Brazil. Fungal Diversity 61, 181–193.
Matheny PB, Curtis JM, Hofstetter V, Aime MC, et al. 2006). Major clades of *Agaricales*: a multilocus phylogenetic overview. Mycologia 98, 982–995.
Matsushima T. 1996 – Matsushima Mycological Memoirs 9. Matsushima Mycological Memoirs 9, 1–30.
Mehl JW, Slippers B, Roux J, Wingfield MJ. 2011 – *Botryosphaeriaceae* associated with *Pterocarpus angolensis* (kiaat) in South Africa. Mycologia 103, 534–553.
Mehl JW, Slippers B, Roux J, Wingfield MJ. 2017 – Overlap of latent pathogens in the *Botryosphaeriaceae* on a native and agricultural host. Fungal Biology 121, 405–419.
Mel'nik VA. 2012 – *Phaeoisaria vietnamensis* sp. nov. and *Ph. Clematidis* (Hyphomycetes) from Vietnam. Mycosphere 3, 957–960.
Miettinen O, Ryvarden L. 2016 – Polypore genera *Antella*, *Austeria*, *Butyrea*, *Citripora*, *Metuloidea* and *Trulla* (*Steccherinaceae*, *Polyporales*). In Annales Botanici Fennici 53, 157–172.
Moncalvo JM, Ryvarden L. 1997 – A nomenclatural study of the *Ganodermataceae* Donk. Fungi Flora, 10, 1–114.
Mortimer PE, Jeewon R, Xu JC, Lumyong S, et al. 2021 – Morpho-phylo taxonomy of novel *Dothideomycetous* fungi associated with dead woody twigs in Yunnan Province. China. Front Microbiology 12, 582.
Moslemi A, Taylor PWJ. 2015 – *Pestalotiopsis chamaeropis* causing leaf spot disease of round leaf mint-bush (*Prostanthera rotundifolia*) in Australia. Australasian Plant Disease Notes 10, 29.
Muntanola-Cvetkovic M, Gomez-Bolea A. 1993 – *Chaetospermum chaetosporum* (coelomycetes) first record from the Iberian Peninsula. Mycotaxon 47, 59–65.
Nagarjun N, Suryanarayana V, Improvement T. 2016 – Documentation, characterization and management of leaf spot of *Syzygium cumini* (L.) Skeels. Journal of Pharmaceutical Sciences 29, 381–385.
Naranjo-Ortiz MA, Gabaldón T. 2019 – Fungal evolution: major ecological adaptations and evolutionary transitions. Biological reviews of the Cambridge Philosophical Society 94, 1443–1476.
Niveiro N, Popoff O, Albertó E. 2013 – Presence of *Leucocoprinus cretaceus* and *L. fragilissimus* in Argentina. Mycotaxon 121(1), 265–273.
Niveiro N, Uhart M, Albertó E. 2020 – Revision of the genera *Agrocybe* and *Cyclocybe* (*Strophariaceae*, *Agaricales*, *Basidiomycota*) in Argentina. Rodriguésia 71, 1–26.
Noordeloos ME. 2011 – *Strophariaceae* s.l. Fungi Europeai no. 13. Canduso Edizione, Saronno.
Norphanphoun C, Gentekaki E, Hongsanan S, Jayawardena R, et al. 2022 – *Diaporthe*: formalizing the species-group concept. Mycosphere 13, 752–819.
Nozawa S, Seto Y, Watanabe K. 2019 – First report of leaf blight caused by *Pestalotiopsis chamaeropis* and *Neopestalotiopsis* sp. in Japanese andromeda. Journal of General Plant Pathology 85, 449–452.
Okane I, Srikitikulchai P, Tabuchi Y, Sivichai S, et al. 2012 – Recognition and characterization of four Thai *xylariaceous* fungi inhabiting various tropical foliages as endophytes by DNA sequences and host plant preference. Mycoscience 53, 122–132.

Park H, Shim JS, Kim JS, Choi HS, et al. 2017 – Five previously unreported endophytic fungi isolated from the leaves of woody plants in Korea. Korean Society of Mycology 45, 345–354.
Patouillard MN. 1888 – Note sur une Tubercullariée graminicole. Bulletin de la Société Mycologique de France 4, 29–40.
Peng C, Crous PW, Jiang N, Fan XL, et al. 2022 – Diversity of *Sporocadaceae* (pestalotioid fungi) from Rosa in China. Persoonia 49, 201–260.
Pennycook SR, Samuels GJ. 1985 – *Botryosphaeria* and *Fusicoccum* species associated with ripe fruit rot of *Actinidia deliciosa* (kiwifruit) in New Zealand. Mycotaxon 24, 445–458.
Perera RH, Hyde KD, Peršoh D, Jones EB, et al. 2018 – Additions to wild seed and fruit fungi 1: The sexual morph of *Diaporthe rosae* on *Magnolia champaca* and *Senna siamea* fruits in Thailand. Mycosphere 9, 256–270.
Pérez CA, Wingfield MJ, Slippers B, Altier NA, et al. 2010 – Endophytic and canker-associated *Botryosphaeriaceae* occurring on non-native *Eucalyptus* and native *Myrtaceae* trees in Uruguay. Fungal Diversity 41, 53–69.
Peršoh D, Melcher M, Graf K, Fournier J, et al. 2009 – Molecular and morphological evidence for the delimitation of *Xylaria hypoxylon*. Mycologia 101, 256–268.
Persoon CH. 1797 – Tentamen dispositionis methodicae fungorum in classes, ordines, genera et familias, cum supplement adjecto. Petrum Philippum Wolf, Leipzig.
Phillips AJL, Alves A, Abdollahzadeh J, Slippers B, et al. 2013 – The *Botryosphaeriaceae*: genera and species known from culture. Studies in Mycology 76, 51–167.
Phillips AJL, Alves A, Pennycook SR, Johnston PR, et al. 2008 – Resolving the phylogenetic and taxonomic status of dark-spored teleomorph genera in the *Botryosphaeriaceae*. Persoonia 21, 29–55.
Phillips AJL, Alves A, Pennycook SR, Johnston PR, et al. 2008 – Resolving the phylogenetic and taxonomic status of dark-spored teleomorph genera in the *Botryosphaeriaceae*. Persoonia 21, 29–55.
Phillips AJL, Hyde KD, Alves A, Liu JK. 2019 – Families in *Botryosphaeriales*: a phylogenetic, morphological and evolutionary perspective. Fungal Diversity 94,1–22.
Phookamsak R, Hyde KD, Jeewon R, Bhat DJ, et al. 2019 – Fungal diversity notes 929–1035: taxonomic and phylogenetic contributions on genera and species of fungi. Fungal Diversity 95, 1–273.
Phookamsak R, Liu JK, McKenzie EHC, Manamgoda DS, et al. 2014 – Revision of *Phaeosphaeriaceae*. Fungal Diversity 68, 159–238.
Phukhamsakda C, McKenzie EHC, Phillips AJ, Jones EBG, et al. 2020 – Microfungi associated with *Clematis* (*Ranunculaceae*) with an integrated approach to delimiting species boundaries. Fungal Diversity 102, 1–203.
Qiu L, Liu JW, Kuang WG, Zhang K, et al. 2022 – First report of *Pestalotiopsis chamaeropis* causing leaf spot on *Eurya nitida* in China. Plant Disease 106, 329.
Qu J, Zou X, Cao W, Xu Z, et al. 2021 – Two new species of *Hirsutella* (*Ophiocordycipitaceae*, *Sordariomycetes*) that are parasitic on lepidopteran insects from China. MycoKeys 82, 81–96.
Quaedvlieg W, Verkley GJ, Shin HD, Barreto RW, et al. 2013– Sizing up *Septoria*. Studies of Mycology 75, 307–390.
Rajeshkumar KC, Paras NS, Yadav LS, Swami SV, et al. 2010 – *Chaetospermum setosum* sp. nov. from the Western Ghats, India. Mycotaxon 113, 397–404.
Ramírez-Cruz V, da Silva PS, Villalobos-Arámbula AR, Matheny PB, et al. 2020 – Two new species of *Deconica* (*Agaricales*, *Basidiomycota*) from Australia and Mexico. Mycological Progress 19, 1317–1328.
Ramírez-Cruz V, Guzmán G, Guzmán-Dávalos L. 2012 – New combinations in the genus *Deconica* (Fungi, *Basidiomycota*, *Agaricales*). Sydow 64, 217–219.

Rangel-Montoya EA, Paolinelli M, Rolshausen PE, Valenzuela-Solano C, et al. 2021 – Characterisation of *Lasiodiplodia* species associated with grapevines in Mexico. Phytopathologia Mediterranea 60, 237–251.

Rathnayaka AR, Chethana KWT, Manawasinghe IS, Wijesinghe SN, et al. 2023 – *Lasiodiplodia*: Generic revision by providing molecular markers, geographical distribution and haplotype diversity. Mycosphere 14, 1254–1339.

Réblová M, Seifert KA, Fournier J, Štěpánek V. 2012 – Phylogenetic classification of *Pleurothecium* and *Pleurotheciella* gen. nov. and its dactylaria-like anamorph (sordariomycetes) based on nuclear ribosomal and protein-coding genes. Mycologia 104, 1299–1314.

Réblová M, Seifert KA, Fournier J, Štěpánek V. 2016 – Newly recognised lineages of perithecial ascomycetes: the new orders *Conioscyphales* and *Pleurotheciales*. Persoonia Molecular Phylogeny and Evolution of Fungi 37, 57– 81.

Redhead SA. 2023 – Nomenclatural novelties. Index Fungorum. 551, 1.

Ren GC, Wanasinghe DN, Jeewon R, Monkai J, et al. 2022 – Taxonomy and phylogeny of the novel *Rhytidhysteron*-like collections in the Greater Mekong Subregion. MycoKeys 86, 65.

Rosado AW, Custodio FA, Pinho DB, Ferreira AP, et al. 2019 – *Cladosporium* species associated with disease symptoms on *Passiflora edulis* and other crops in Brazil, with descriptions of two new species. Phytotaxa 409, 239–60.

Rungjindamai N, Sakayaroj J, Plaingam N, Somrithipol S, et al. 2008 – Putative basidiomycete teleomorphs and phylogenetic placement of the coelomycete genera: *Chaetospermum*, *Giulia* and *Mycotribulus* based on nu-rDNA sequences. Mycological Research 112, 802–810.

Russell JR, Huang J, Anand P, Kucera K, et al. 2011 – Biodegradation of polyester polyurethane by endophytic fungi. Applied and Environmental Microbiology 77, 6076–6084.

Saccardo PA. 1878 – Fungi Veneti novi vel critici vel mycologiae Venetae addendi. Ser. IX. Michelia 1, 407.

Saccardo PA. 1892 – Supplementum universale, Pars II. Discomyceteae-hyphomyceteae. Sylloge Fungorum 10, 1–964.

Saccardo PA. 1913 – Notae mycologicae. Series XVII. Annales Mycologici 11, 546–568.

Sakalidis ML, Hardy GES, Burgess TI. 2011 – Use of the genealogical sorting index (GSI) to delineate species boundaries in the *Neofusicoccum parvum- Neofusicoccum ribis* species complex. Molecular Phylogenetics and Evolution 60, 333–344.

Salvatore MM, Alves A, Andolfi A. 2021 – Secondary metabolites produced by *Neofusicoccum* species associated with plants: A review. Agriculture 11, 149.

Samaradiwakara NP, de Farias ARG, Tennakoon DS, Bhunjun CS, et al. 2023 – Sexual morph of *Allophoma tropica* and *Didymella coffeae-arabicae* (*Didymellaceae*, *Pleosporales*, *Dothidiomycetes*) including novel host records from leaf litter in Thailand. New Zealand Journal of Botany, 192–215.

Samarakoon MC, Persoh D, Hyde KD, Bulgakov TS, et al. 2018 – *Colletotrichum acidae* sp. nov. from northern Thailand and a new record of *C. dematium* on *Iris* sp. Mycosphere 9, 583–597.

Samuels GJ, Müller E. 1979 – Life-history studies of Brazilian *Ascomycetes*. 7. *Rhytidhysteron rufulum and* the genus *Eutryblidiella*. Sydowia 32, 277–292.

Sandoval-Denis M, Gené J, Sutton DA, Wiederhold NP, et al. 2016 – New species of *Cladosporium* associated with human and animal infections. Persoonia 36, 281–298.

Santos J, Hilário S, Pinto G, Alves A. 2022 – Diversity and pathogenicity of pestalotioid fungi associated with blueberry plants in Portugal, with description of three novel species of *Neopestalotiopsis*. European Journal of Plant Pathology 162, 539–555.

Schneider R, Boerema GH. 1975 – *Phoma tropica* n. sp., ein a Gewächshauspflanzen häuFig vorkommender, nicht pathogener Pilz. Journal of Phytopathology 83, 239–243.

Schoch CL, Shoemaker RA, Seifert KA, Hambleton S, et al. 2006 – A multigene phylogeny of the *Dothideomycetes* using four nuclear loci. Mycologia 98, 1041–1052.
Schubert K, Greslebin A, Groenewald JZ, Crous PW. 2009 – New foliicolous species of *Cladosporium* from South America. Persoonia-Molecular Phylogeny and Evolution of Fungi 22, 111–122.
Seifert K, Morgan-Jones G, Gams W, Kendrick B. 2011 –The genera of Hyphomycetes–2011 update. Persoonia-Molecular Phylogeny and Evolution of Fungi 27, 119–129.
Senanayake IC, Rathnayaka AR, Marasinghe DS, Calabon MS, et al. 2020 – Morphological approaches in studying fungi: collection, examination, isolation, sporulation and preservation. Mycosphere 11, 2678–2754.
Senwanna C, Mapook A, Samarakoon MC, Karunarathna A, et al. 2021 – Ascomycetes on Para rubber (*Hevea brasiliensis*). Mycosphere 12, 1230–1408.
Shu C, Jiang X, Cheng X, Wang N, et al. 2015 – Genetic structure and parasitization-related ability divergence of a nematode fungal pathogen *Hirsutella minnesotensis* following founder effect in China. Fungal Genetics and Biology 81, 212–220.
Simmons DR, Kepler RM, Rehner SA, Groden E. 2015 – Phylogeny of *Hirsutella* species (*Ophiocordycipitaceae*) from the USA: Remedying the paucity of *Hirsutella* sequence data. IMA Fungus 6, 345–356.
Singer R. 1950 – Type studies on Basidiomycetes IV. Lilloa 23, 147–246.
Singer R. 1986 – The *Agaricales* in modern taxonomy, 4th ed. Koenigstein, Germany, Koeltz Scientific Books, pp. 981.
Slippers B, Boissin E, Phillips AJL, Groenewald JZ, et al. 2013 – Phylogenetic lineages in the Botryosphaeriales: a systematic and evolutionary framework. Studies in Mycology 76, 31–49.
Smith AL, Ramsbottom J. 1914 – New or rare fungi. Transactions of the British Mycological Society 4, 318–330.
Smith WG. 1870 – *Clavis agaricinorum*; an analytical key to the British agaricini, with characters of the genera and subgenera. The London Journal of Botany 8, 213–233.
Song W, Yu JF, Zhang TY. 2008 – Notes on soil dematiaceous hyphomycetes from Mount Taibai and its surrounding area I. Mycosystema 27, 16–28.
Song Y, Tangthirasunun N, Maharachchikumbura SSN, Jiang YL, et al. 2014 – Novel *Pestalotiopsis* species from Thailand point to the rich undiscovered diversity of this chemically creative genus. Cryptogamie Mycologie 35, 139–149.
Species Fungorum 2025 – https://www.speciesfungorum.org/Names/Names.asp (Accessed on May 1, 2025).
Spegazzini C. 1881 – Fungi argentini additis nonnullis brasiliensibus montevideensibusque. *Pugillus quartus* (Continuacion). Anales de la Sociedad Científica Argentina 12, 174–189.
Spegazzini C. 1922 – *Cryptogamae nonnullae* Fuegianae. Anales de la Sociedad Cientifica Argentina 94, 59–85.
Stadler M, Kuhnert E, Persŏh D, Fournier J. 2013 – The *Xylariaceae* as model example for a unified nomenclature following the ‘‘One fungus-one name’’ (1F1N) concept. Mycology: An International Journal on Fungal Biology 4, 5–21.
Stallman J. 2019 – Taxonomy of Hawaii island’s lepiotaceous (*Agaricaceae*) Fungi: *Chlorophyllum*, *Cystolepiota*, *Lepiota*, *Leucoagaricus*, *Leucocoprinus* (Master’s thesis). University of Hawaii at Hilo, Hilo, HI, United States.
Stallman JK, Hemmes DE, Hynson NA, Shintaku MH. 2020 – *Lepiota punaensis* sp. nov. from Hawaii Island, and a discussion of *L. elaiophylla*. Mycotaxon 135, 471–489.
Steyaert RL. 1949 – Contribution à l'étude monographique de Pestalotia de Not. et Monochaetia Sacc. (*Truncatella* gen. nov. et *Pestalotiopsis* gen. nov.). Bulletin du Jardin botanique de l'Etat, Bruxelles, Botanic Garden Meise, Brussel, Belgium, pp. 285–354.

Summerbell RC, Gueidan C, Schroers HJ, De Hoog GS, et al. 2011 – *Acremonium* phylogenetic overview and revision of *Gliomastix*, *Sarocladium*, and *Trichothecium*. Studies in Mycology 68, 139–162.
Sun YR, Jayawardena RS, Sun JE, Wang Y. 2023 – Pestalotioid species associated with medicinal plants in southwest China and Thailand. Microbiology Spectrum 11, e0398722.
Sun YF, Xing JH, He XL, Wu DM, et al. 2022 – Species diversity, systematic revision and molecular phylogeny of *Ganodermataceae* (*Polyporales*, *Basidiomycota*) with an emphasis on Chinese collections. Studies in Mycology 101, 287–415.
Sundararaj R, Swetha P, Mondal S, Reddy MK, et al. 2023 – Incidence and effect of heart rot in Marayur Sandalwood (*Santalum album* L.) Reserve, Kerala, and its natural durability against fungi. Forest Science 69, 133–142.
Sutton BC. 1973 – *Hyphomycetes* from Manitoba and Saskatchewan, Canada. Mycological Papers 132, 1–143.
Sutton BC. 1980 – The coelomycetes: fungi imperfecti with pycnidia, acervuli and stromata. Commonwealth Mycological Institute, Slough, England, pp. 696.
Sysouphanthong P, Thongklang N, Liu JK, Vellinga EC. 2021 – Description of lepiotaceous fungal species of the genera *Chlorophyllum*, *Clarkeinda*, *Macrolepiota*, *Pseudolepiota*, and *Xanthagaricus*, from Laos and Thailand. Diversity 13, 666.
Takahashi H. 2001 – Notes on new *Agaricales* of Japan 3. Mycoscience 42, 355–360.
Talhinhas P, Baroncelli R. 2021 – *Colletotrichum* species and complexes: geographic distribution, host range and conservation status. Fungal Diversity 110, 109–198.
Talhinhas P, Baroncelli R. 2023 – Hosts of *Colletotrichum*. Mycosphere 14, 158–261.
Tanaka K, Endo M, Hirayama K, Okane I, et al. 2011 – Phylogeny of *Discosia* and *Seimatosporium*, and introduction of *Adisciso* and *Immersidiscosia* genera nova. Persoonia 26, 85–98.
Tanaka K, Harada Y. 2003 – *Pleosporales* in Japan (2): *Lophiotrema*. Mycoscience 44, 115–121.
Tanaka K, Hashimoto A, Matsumura M, Sato T. 2017 – *Brevicollum*, a new genus in *Neohendersoniaceae*, Pleosporales. Mycologia 109, 608–619.
Tanaka K, Hirayama K, Yonezawa H, Sato G, et al. 2015 – Revision of the *Massarineae* (*Pleosporales*, *Dothideomycetes*). Studies in Mycology 82, 75–136.
Tangthirasunun N, Silar P, Bhat DJ, Chukeatirote E, et al. 2014 – Morphology and phylogeny of Chaetospermum (asexual coelomycetous *Basidiomycota*). Phytotaxa 175, 61–72.
Tanney JB, Seifert KA. 2019 – *Tryblidiopsis magnesii* sp. nov. from *Picea glauca* in Eastern Canada. Fungal Systematics and Evolution 4, 13–20.
Tennakoon DS, Jeewon R, Thambugala KM, Gentekaki E, et al. 2021 – Biphasic taxonomic approaches for generic relatedness and phylogenetic relationships of *Teichosporaceae*. Fungal Diversity 110, 199–241.
Tennakoon DS, Kuo CH, Maharachchikumbura SS, Thambugala KM, et al. 2021 –Taxonomic and phylogenetic contributions to *Celtis formosana*, *Ficus ampelas*, *F. septica*, *Macaranga tanarius* and *Morus australis* leaf litter inhabiting microfungi. Fungal Diversity 108, 1–215.
Thambugala KM, Hyde KD, Tanaka K, Tian Q, et al. 2015 – Towards a natural classification and backbone tree for *Lophiostomataceae*, *Floricolaceae*, and *Amorosiaceae* fam. nov. Fungal Diversity 74, 199–266.
Thambugala KM, Daranagama DA, Phillips AJL, Bulgakov TS, et al. 2016 – Microfungi on Tamarix. Fungal Diversity 82, 239–306.
Thambugala KM, Wanasinghe DN, Phillips AJL, Camporesi E, et al. 2017 – Mycosphere notes 1–50: Grass (*Poaceae*) inhabiting *Dothideomycetes*. Mycosphere 8, 697–796.
Tibpromma S, Hyde KD, McKenzie EHC, Bhat DJ, et al. 2018 – Fungal diversity notes 840–928: micro-fungi associated with *Pandanaceae*. Fungal Diversity 93, 1–160.

Torres-Cortés G, Ghignone S, Bonfante P, Schüßler A. 2015 – Mosaic genome of endobacteria in arbuscular mycorrhizal fungi: transkingdom gene transfer in an ancient mycoplasma-fungus association. Proceedings of the National Academy of Sciences 112, 7785–7790.
Tóth A, Hausknecht A, Krisai-Greilhuber I, Papp T, et al. 2013 – Iteratively refined guide trees help improving alignment and phylogenetic inference in the mushroom family *Bolbitiaceae*. PLoS One 8, e56143.
Trakunyingcharoen T, Lombard L, Groenewald JZ, Cheewangkoon R, et al. 2015 – *Caulicolous* Botryosphaeriales from Thailand. Persoonia 34, 87–99.
Tulloss RE. 2005 – Amaniteae: *Amanita*, *Limacella* & *Torrendia*. By Pierre Neville & Serge Poumarat, etc. Mycotaxon 92, 474–484.
Ul Haq I, Ijaz S, Khan NA. 2021 – Genealogical concordance of phylogenetic species recognition-based delimitation of *Neopestalotiopsis* species associated with leaf spots and fruit canker disease affected guava plants. Pakistan Journal of Agricultural Sciences 58, 1301–1313.
Úrbez-Torres JR, Peduto F, Gubler WD. 2010 – First report of grapevine cankers caused by *Lasiodiplodia crassispora* and *Neofusicoccum mediterraneum* in California. Plant Disease 94, 785–785.
Úrbez-Torres JR, Gubler WD. 2011 – Susceptibility of grapevine pruning wounds to infection by *Lasiodiplodia theobromae* and *Neofusicoccum parvum*. Plant Pathology 60, 261–270.
Valenzuela-Lopez N, Sutton DA, Cano-Lira JF, Paredes K, et al. 2017 – *Coelomycetous* fungi in the clinical setting: morphological convergence and cryptic diversity. Journal of Clinical Microbiology 55, 552–567.
Van Niekerk JM, Bester W, Halleen F, Crous PW, et al. 2010 – First report of *Lasiodiplodia crassispora* as a pathogen of grapevine trunks in South Africa. Plant Disease 94, 1063.
Van Niekerk JM, Crous PW, Groenewald JZ, Fourie PH, et al. 2004 – DNA phylogeny, morphology and pathogenicity of *Botryosphaeria* species on grapevines. Mycologia 96, 781–798.
Vellinga, E. 2001a – *Leucocoprinus*. In: Noordeloos ME, Kuyper TW, Vellinga EC, eds. Flora Agaricina Neerlandica vol. 5. Balkema.
Vellinga EC. 2001a – *Agaricaceae*. In: Noordeloos ME, Kuyper TW, Vellinga EC. (eds.) Flora Agaricina Neerlandica 5. Rotterdam: A.A. Balkema Publishers, Netherlands, pp. 220.
Vellinga EC. 2001b – Glossary. In: Noordeloos ME, Kuyper ThW, Vellinga EC (eds). Flora Agaricina Neerlandica 5, 6–11.
Vellinga EC. 2001c – *Lepiota* (Pers.: Fr.) S.F. Gray. In: Noordeloos ME, Kuyper TW, Vellinga EC (eds.). Flora Agaricina Neerlandica 5. Lisse: A.A. Balkema Publishers, pp. 109–151.
Vellinga EC, Noordeloos ME. 2001 – Glossary. In: Noordeloos ME, Kuyper ThW, Vellinga EC (Eds) Flora Agaricina Neerlandica 5. Aa Balkema Publishers, Tokyo, pp. 6–11.
Vellinga EC. 2003 – Phylogeny of *Lepiota* (*Agaricaceae*) – evidence from nrITS and nrLSU sequences. Mycological Progress 2, 305–322.
Vellinga EC, Sysouphanthong P, Hyde KD. 2011 – The family *Agaricaceae*: phylogenies and two new white-spored genera. Mycologia 103, 494–509.
Vellinga EC, Kuyper TW, Ammirati J, Desjardin DE, et al. 2015 – Six simple guidelines for introducing new genera of fungi. IMA Fungus 6, 66–68.
Vu D, Groenewald M, De Vries M, Gehrmann T, et al. 2019 – Large-scale generation and analysis of filamentous fungal DNA barcodes boosts coverage for kingdom fungi and reveals thresholds for fungal species and higher taxon delimitation. Studies in Mycology 92, 135–154.
Wanasinghe DN, Mortimer PE. 2022 – Taxonomic and phylogenetic insights into novel *Ascomycota* from forest woody litter. Biology 11, 889.
Wanasinghe DN, Phukhamsakda C, Hyde KD, Jeewon R, et al. 2018 – Fungal diversity notes 709–839: taxonomic and phylogenetic contributions to fungal taxa with an emphasis on fungi on *Rosaceae*. Fungal Diversity 89, 1–236.

Wang S, Cannon P, Li ZJ, Hou CL. 2014 – Multigene phylogenetic analysis detects cryptic species of *Tryblidiopsis* in China. Mycologia 106, 95–104.
Wang XH. 2007 – Type studies of *Lactarius* species published from China. Mycologia 99, 253–268.
Wang YB, Yu H, Dai YD, Chen ZH, et al. 2015 – *Polycephalomyces yunnanensis* (*Hypocreales*), a new species of *Polycephalomyces* parasitising *Ophiocordyceps nutans* and stink bugs (hemipteran adults). Phytotaxa 208, 34–44.
Wang YH, Ban S, Wang WJ, Li Y, et al. 2021 – *Pleurocordyceps* gen. nov. for a clade of fungi previously included in *Polycephalomyces* based on molecular phylogeny and morphology. Journal of Systematics and Evolution 59, 1065–1080.
Wartchow F, Putzke J, Cavalcanti MAQ. 2008 – *Agaricaceae* Fr. (*Agaricales*, *Basidiomycota*) from areas of Atlantic forest in Pernambuco, Brazil. Acta Botanica Brasilica 22, 287–299.
Watling R, Abraham SP. 1986 – Observations on the *Bolbitiaceae* 26. *Bolbitiaceae* of Kashmir with particular reference to the genus *Agrocybe*. Nova Hedwigia 42, 387–415.
Watling R. 1998 – *Heinemannomyces*: a new lazuline-spored agaric genus from South East Asia. Belgian Journal of Botany 131, 133–138.
Wells K, Oberwinkler F. 1982 – *Tremelloscypha gelatinosa*, a species of a new family *Sebacinaceae*. Mycologia 74, 325–331.
Whalley AJ, Suwannasai N, Ruchikachorn N, Sangvichien E, et al. 2015 – Endophytic *Xylariaceae* from Thai plants: a research review. Suan Sunandha Science and Technology Journal 2, 11–17.
Wijayawardene NN, Hyde KD, Lumbsch HT, Liu JK, et al. 2018 – Outline of *Ascomycota*: 2017. Fungal Diversity 88, 167–263.
Wijayawardene NN, Dissanayake LS, Li QR, Dai DQ, et al. 2021 – Yunnan–Guizhou Plateau: a mycological hotspot. Phytotaxa 523, 1–31.
Wijayawardene NN, Hyde KD, Dai D, Sánchez-García M, et al. 2022a – Outline of Fungi and fungus-like taxa – 2021. Mycosphere 11, 1060–1456.
Wijayawardene NN, Hyde KD, Dai DQ, Sánchez-García M, et al. 2022b – Outline of Fungi and fungus-like taxa-2021. Mycosphere 13, 53–453.
Willis K. 2018 – State of the World's fungi 2018 report. Royal Botanic Gardens, Kew Royal Botanical Gardens.
Wu B, Hussain M, Zhang W, Stadler M, Liu X, Xiang M, et al. 2019 – Current insights into fungal species diversity and perspective on naming the environmental DNA sequences of fungi. Mycology 10, 127–140.
Xiao YP, Hongsanan S, Hyde KD, Brooks S, et al. 2019 – Two new entomopathogenic species of *Ophiocordyceps* in Thailand. MycoKeys 47, 53–74.
Xiao YP, Wang YB, Hyde KD, Elini G, et al. 2023 – *Polycephalomycetaceae*, a new family of clavicipitoid fungi segregates from *Ophiocordycipitaceae*. Fungal Diversity 120, 1–76.
Xu D, Xi P, Xu J, Lin Z, et al. 2022– Association of *Neofusicoccum parvum* with leaf scorch on *Cinnamomum cassia* in China. Forest Pathology 52, e12726.
Xu J, Yang XB, Lin Q. 2014 – Chemistry and biology of *Pestalotiopsis*-derived natural products. Fungal Diversity 66, 37–68.
Xu MF, Jia OY, Wang SJ, Zhu Q. 2016 – A new bioactive diterpenoid from *Pestalotiopsis adusta*, an endophytic fungus from *Clerodendrum canescens*. Natural Product Research 30, 2642–2647.
Xu XL, Wang FH, Liu C, Yang HB, et al. 2022 – Morphology and phylogeny of *Ascomycetes* associated with walnut trees (*Juglans regia*) in Sichuan province, China. Frontiers in Microbiology 13, 1016548.
Yan H, Jiang N, Liang LY, Yang Q, et al. 2019 – *Arthrinium trachycarpum* sp. nov. from *Trachycarpus fortuneii* in China. Phytotaxa 400, 203–210.
Yan JY, Xie Y, Zhang W, Wang Y, et al. 2013 – Species of *Botryosphaeriaceae* involved in grapevine dieback in China. Fungal Diversity 61, 221–236.

Yang EF, Tibpromma S, Karunarathna SC, Phookamsak R, et al. 2022 – Taxonomy and phylogeny of novel and extant taxa in *Pleosporales* associated with *Mangifera indica* from Yunnan, China. Journal of Fungi 8, 152.
Yang J, Liu JK, Hyde KD, Jones EBG, et al. 2017 – Two new species in *Fuscosporellaceae* from freshwater habitats in Thailand. Mycosphere 8, 1893–1903.
Yang J, Maharachchikumbura SS, Bhat DJ, Hyde KD, et al. 2016 – *Fuscosporellales*, a new order of aquatic and terrestrial *Hypocreomycetidae* (Sordariomycetes). Cryptogamie, Mycologie 37, 449–475.
Yang Y, Luo W, Zhang W, Mridha MA, et al. 2023 – *Cladosporium* Species associated with fruit trees in Guizhou Province, China. Journal of Fungi 9, 250.
Yang YH, Liao CF, Manawasinghe IS, de Farias ARG, et al. 2023 – *Neomassaria khayae* sp. nov., a novel PIleosporalean species on *Khaya senegalensis* from Guangdong Province, China. Phytotaxa 599, 65–77.
Yu XD, Zhang SN, Cheewangkoon R, Liu JK. 2021 – Additions to *Occultibambusaceae* (*Pleosporales*, *Dothideomycetes*): Unrevealing Palmicolous Fungi in China. Diversity 13, 516.
Yuan HS, Lu X, Dai YC, Hyde KD, et al. 2020 – Fungal diversity notes 1277–1386: taxonomic and phylogenetic contributions to fungal taxa. Fungal Diversity 104, 1–266.
Yuan M, Jiang Z, Bi G, Nomura K, et al. 2021 – Pattern-recognition receptors are required for NLR-mediated plant immunity. Nature 592, 105–109.
Zalar PD, De Hoog GS, Schroers HJ, Crous PW, et al. 2007 – Phylogeny and ecology of the ubiquitous saprobe *Cladosporium sphaerospermum*, with descriptions of seven new species from hypersaline environments. Studies in Mycology 58, 157–183.
Zhai L, Zhang M. 2019 – First report of *Neofusicoccum parvum* causing fruit rot on *Eriobotrya japonica* in China. Plant Disease 103, 2125–2125.
Zhang Y, Jeewon R, Fournier J, Hyde KD, et al. 2008 – Multi-gene phylogeny and morphotaxonomy of *Amniculicola lignicola*: a novel freshwater fungus from France and its relationships to the *Pleosporales*. Mycological Research 112, 1186–1194.
Zhang Y, Fournier J, Crous PW, Pointing SB, et al. 2009a – Phylogenetic and morphological assessment of two new species of *Amniculicola* and their allies (*Pleosporales*). Persoonia-Molecular Phylogeny and Evolution of Fungi 23, 48–54.
Zhang Y, Schoch CL, Fournier J, Crous PW, et al. 2009b – Multi-locus phylogeny of *Pleosporales*: a taxonomic, ecological and evolutionary re-evaluation. Studies in Mycology 64, 85–102.
Zhang JF, Liu JK, Jeewon R, Wanasinghe DN, et al. 2019 – Fungi from Asian Karst formations III. Molecular and morphological characterization reveal new taxa in *Phaeosphaeriaceae*. Mycosphere 10, 202–220.
Zhao LL, Zhang L, Jiao N, Li M, et al. 2025 – Branch blight and dieback of walnut (*Juglans regia* L.) caused by *Rhytidhysteron juglandis* sp. nov. and its endophytic biocontrol agent *Granulobasidium vellereum*. Phytotaxa 705, 19–34.
Zheng XJ, Liu X, Li XP, Quan CT, et al. 2023 – *Pestalotiopsis* species associated with blueberry leaf spots and stem cankers in Sichuan Province of China. Plant Disease 107, 149–156.